

TAP Recommendations

No.	TAP Recommendation	SFPW and SFPUC Comment	Oct 31, 2019 Phase 1 Horizontal Geotechnical Report Reference	Required Actions	How Resolved	Response by Langan and MRP, and TAP follow-up Langan responses in black , updates in blue MRP (S. Minden) responses in red , updates in purple	Referenced language from Langan Report dated 31 October 2019
1	Applicable Codes	SFPW: Applicable code to be determined based on time of permit submittal. Note that the 2019 model codes will reference ASCE 7-16 which requires site specific ground motion analysis that could change the design spectra required by ASCE 7-10.	Section 6.2	MRP to expand the response.	Reference Port Building Code for areas under its jurisdiction; Applicable Code determined upon application, not frozen to the 2016 Codes	11-6-19 Langan Response: 2016 California Building Code (ASCE 7-10) 12-10-19 Langan Response: Understood. We understand this project will be permitted now under the 2016 San Francisco Building Code. 12-10-19 MRP Response: Note, the above Code is the basis of Seismic design. SF Public Works (SFPW), Public Utilities (SFPUC) and Transportation Authority (SFMTA) Codes and Standards are also being used as applicable for different features of the horizontal infrastructure. 2-7-20 The applicable code for future phases will be updated with the current code at the time the phase is designed. 2-18-20 TAP Response: TAP concerns with this comment resolved 2-5-2020. SFPW and SFPUC have not necessarily concluded their own reviews.	*Value obtained from United States Geological Survey (USGS) website for liquefaction analysis per ASCE 7-10 and 2016 California Building Code (CBC) ** Site specific rotated maximum PGA = 0.46g. Analyses was performed using 0.47g consistent with the ASCE 7-10.
2	Long Term Settlement in Building Area	SFPW: The geotechnical report states typical over consolidation ratio (OCR) is about 1 to 1.6. Provide Pp (maximum past pressure) or OCR profile to demonstrate the site has OCR of 1.6 and at what depth the Young Bay Mud is normally consolidated. Provide the published coefficients (C _{αε}) used for estimating secondary compression.	Section 7.2	TAP to review 10/31 Geotechnical Investigation (Horizontal Development) Section 7.2 for secondary	City considers recommendation from the TAP	See reference Section of Geotechnical Report 2-18-20 TAP Response: TAP concerns with this comment resolved 2-5-2020. SFPW and SFPUC have not necessarily concluded their own reviews.	Section 7.2 "The results of consolidation testing in the Phase 1 Development site indicate the Bay Mud is generally slightly overconsolidated, but may be normally consolidated in some areas. Accordingly, we judge consolidation is complete under the existing fill loads that were placed in the late 1800s to early 1900s. These results are consistent with the thickness of the Bay Mud, the length of time the fill has been in place, and the history of site use. Based on consolidation theory, after primary consolidation is complete, soils that are subjected to a sustained load at their maximum past pressure (i.e. normally consolidated) will undergo strain-related movements associated with clay particle deformation (a phenomenon called secondary compression), leading to a small amount of future settlement over time. If secondary compression were ongoing at the site, we would calculate about ¼ to ½ inch of settlement in the last 8 years using published coefficients (C _{αε}) for estimating secondary compression. However, thigation measures will be taken to offset the potential stress increase associated with the planned dewatering. We understand the contractor plans to limit dewatering to no more than 2 feet below the planned LCC excavation. As indicated on the onsite street improvement plans prepared for the project, the majority of the planned excavat

TAP Recommendations

No.	TAP Recommendation	SFPW and SFPUC Comment	Oct 31, 2019 Phase 1 Horizontal Geotechnical Report Reference	Required Actions	How Resolved	Response by Langan and MRP, and TAP follow-up Langan responses in black , updates in blue MRP (S. Minden) responses in red , updates in purple	Referenced language from Langan Report dated 31 October 2019
3	Construction Dewatering	SFPW: The Pilot program shows there are 15 inclined wellpoints at the crest of open cut on three sides of the pilot area. The 29-ft-wide pilot roadway section in the pilot represents about half of the future roadway section (total width of 60 ft.). The limit of open cut, if used as excavation technique for future roadway construction, will be much wider than the pilot (the pilot is dimensioned at 81.3 ft.). A dewatering program that is representative to future dewatering plan is needed to assess the groundwater profile during dewatering. In addition, Langan's Vertical Development geotechnical report stated that "Excavations for the below-grade structures will generally extend below the existing groundwater level; therefore, groundwater will need to be lowered to below excavation during construction. The rate of groundwater flow through the fill is anticipated to be high... In addition to dewatering wells, localized sumps and pumps	Section 7.2	Specifications developed by MRP for "safe envelope"	Langan monitoring and assessing of the Pilot will provide guidance for them to develop controlling allowable limits for dewatering	11-6-19 Langan Response: That section discusses dewatering during construction and that the dewatering will be assessed during the LCC pilot test program. Monitoring is discussed in Section 8.4 of the 31 October 2019 report. 12-10-19 Langan Response: The LCC Pilot Section required the groundwater be drawn down to Elevation 88 feet at the test section. This was performed using dewatering wells as outlined in the LCC Pilot Program Submittal. As of 9 December 2019, groundwater at a distance of about 35 feet from the LCC Pilot only lowered about 6 to 9 inches following initiating dewatering as compared with the baseline elevation. Although dewatering continues, the groundwater levels are currently at or above the baseline elevations. 12-10-19 MRP Response: (See also Mission Rock Geotechnical Investigation for Phase 1 Horizontal Development, 31 October 2019, (the Geotech Report) Section 8.4 for Dewatering Recommendations) 2-18-20 TAP Response: TAP concerns with this comment resolved 2-5-2020. SFPW and SFPUC have not necessarily concluded their own reviews.	Section 7.2 "During construction, localized dewatering will be required. Because of the likely relatively high permeability of the on-site fill, the dewatering required for the LCC excavations may lower the groundwater beyond the excavation areas. The depth of dewatering, permeability of the soil, and duration of the planned dewatering in any given portion of the site will influence the amount of groundwater is lowered. Stresses in the soil will increase as soil within the zone of lowered groundwater is no longer buoyant. Since placement of the historic fill, the compressible Bay Mud has been subjected to repeated cycles of groundwater fluctuation over more than 100 years, and is overconsolidated. However, care should be taken not to add excessive stress to the Bay Mud, in order to reduce the potential for initiating new primary consolidation or additional secondary compression. Therefore, where groundwater will be required to be lowered below the average typical low groundwater level (Elevation 90 feet), mitigation measures will be taken to offset the potential stress increase associated with the planned dewatering. We understand the contractor plans to limit dewatering to no more than 2 feet below the planned LCC excavation. As indicated on the onsite street improvement plans prepared for the project, the majority of the planned excavations for the placement of the LCC will bottom above Elevation 92 feet; therefore lowering the water 2 feet below the excavation depth will not lower the groundwater in the surrounding areas more than Elevation 90 feet. However, near the intersection of Shared Public Way and Channel Street, the excavation for the LCC will likely range from Elevation 90 to 92 feet, and the required dewatering will extend 0 to 2 feet below the average typical
4	Backfilling for Future Utilities and Emergency Repair	SFPW: Defer to result of pilot testing program. Appendix G of geotechnical report, Specification for Permeable/Open Cell Lightweight Cellular Concrete (P-LCC), Section 3.5 Placement, "Place P-LCC in lifts not to exceed 36 inches in thickness, unless otherwise recommended by the P-LCC manufacturer and approved by the GEOR." The 36" maximum lifts in the specification is acceptable as normal industry-practice. This is thinner than the Cellular Concrete Proposed Maintenance Policy and Procedures (dated 12/18/2018) that "for trenches with deeper backfill, LCC can be placed in single lifts of up to 6-7' with skilled crews" or "possible to place two lifts of 5' in a day with a 4 hour interval between the lifts." If thicker lift is used for emergency repair, the developer should demonstrate the recommended thickness is achievable.	Not addressed in Geotechnical Report	MRP to provide a detailed procedure; City to review	Defer Final Map condition until best practices developed during the construction phase	MRP: A proposed Excavation and Backfill Procedure for LCC in Mission Rock Streets" is provided in Exhibit F. The procedure recommends 3' lifts for LCC backfill. Higher lifts may be approved on a case-by-case basis. When multiple backfill lifts are required, the trench would be covered with road plates between lifts as is the case for conventional soil backfill. MRP is still willing to accept responsibility for backfill of any public utility trenches in LCC in Mission Rock as an MOU condition. MRP: 2-10-20 Filter fabric to be provided between LCC and adjacent native soil, pipe bedding and cover, structural soil and other materials to prevent fines from migrating into the LCC List of Approved LCC Contractors has been added to Exhibit F 2-18-20 TAP Response: TAP concerns with this comment resolved 2-5-2020. SFPW and SFPUC have not necessarily concluded their own reviews.	

TAP Recommendations

No.	TAP Recommendation	SFPW and SFPUC Comment	Oct 31, 2019 Phase 1 Horizontal Geotechnical Report Reference	Required Actions	How Resolved	Response by Langan and MRP, and TAP follow-up Langan responses in black , updates in blue MRP (S. Minden) responses in red , updates in purple	Referenced language from Langan Report dated 31 October 2019
4	Backfilling for Future Utilities and Emergency Repair (continued)					MRP 02-24-20 LCC Repair and Backfill Procedure has been revised to allow non-permeable LCC backfill in limited areas. This would allow LCC to be made with foaming agents from different manufactures rather than just Aerix, which has the sole patent for permeable foaming agent. In these repairs non-preamble LCC can be placed above Elevation 95 feet or in localized trenches that with a volume less than 10 cubic yards.	
5	Stone Column Design and Installation	SFPW: SFPW defers to recommendations from the TAP on the disturbance of Young Bay Mud due to Stone Column/RIC. We understand that the TAP is also concerned that the installation of wick drain may disturb Young Bay Mud.	Sections 7.4 and	Specifications must be developed to mitigate potential impacts (disturbance and stress) to the Bay Mud layer:	Post ground improvement test panel project will gather data to determine the location of Bay Mud or lower limit of liquefiable soils	11-6-19 Langan response: Section 7.4 provides a discussion on stone columns and that the disturbance of Bay Mud will be assessed during the test project. Section 8.1 provides detailed recommendations on ground improvement and the acceptance criteria. 12-10-19 Langan Response: No response required at this time. 2-10-20 MRP: In response to verbal comment from Port, we confirm that filter fabric (Mirafi fabric) will be placed between LCC and all adjacent soil, pipe bedding and cover, structural soil and any other material with fines to prevent migration of fines into LCC 2-18-20 TAP Response: TAP concerns with this comment are conditionally resolved 2-18-2020. Developer to provide supporting material for final review. SFPW and SFPUC have not necessarily concluded their own reviews. 2-19-20 Langan Response: Additional language will be added to the stone column specification stating that wick drains shall be installed prior to stone column installation. The wick drains will be installed through the fill into the underlying Bay Mud. Detailed records of the wick drain depths will be kept by the contractor and relayed to the geotechnical engineer, who will in turn recommend the final depths of the required stone columns. Based on the work performed during stone column test sections this method is achievable and works well in the field.	Section 7.4: "Ground improvement in the fill may cause some disturbance of the underlying Bay Mud, which could result in some settlement. This condition will be evaluated during the ground improvement test program, and measures will be implemented to minimize the potential disturbance to the Bay Mud" Section 8.1: "To minimize the disturbance in the underlying Bay Mud, we recommend stone columns terminate at the bottom of the liquefiable fill, or one to two feet above the underlying Bay Mud, whichever is shallower. "
6a	Earthquake Considerations for LCC		Section 6.2	Include a discussion of the design basis earthquake and expected site/soil amplification effects, the design peak ground acceleration, and the expected level of ground motion within the LCC backfill. This information is needed by the TAP and others (e.g., utility and pipeline designers) to complete their engineering evaluations	Provide requested discussion and supporting documentation for the analysis and evaluations.	11-6-19 Langan Response: Section 6.2 provides discussion of the ground motions. 12-10-19 Lagan Response: The fundamental performance of the LCC under seismic loading is discussed in the Horizontal Geotechnical report dated 31 October 2019. However, as requested we have evaluated the seismic performance of the LCC compared to the demands expected during an MCEr Earthquake. To evaluate the potential for breakage of the LCC under the stresses of vertically propagating shear waves, we first evaluated the magnitude of the shear stress ratio (shear stress/effective stress) from our linear and non-linear evaluation of the site response analyses under MCEr loading at the site. The maximum shear stress ratio in the fill at the site is about 0.6 to 0.66. Therefore, the maximum anticipated shear stresses imposed on the LCC from an MCEr earthquake are on the order of 200 to 265 psf, which 10 percent of the target minimum LCC strength (2,880 psf), see Exhibit A. If there is an existing crack or cold-joint in the LCC and the residual strength at this interface is equivalent to a friction ratio of 35 degrees, the LCC still has sufficient strength to resist further degradation.	*Value obtained from United States Geological Survey (USGS) website for liquefaction analysis per ASCE 7-10 and 2016 California Building Code (CBC) ** Site specific rotated maximum PGA = 0.46g. Analyses was performed using 0.47g consistent with the ASCE 7-10.

TAP Recommendations

No.	TAP Recommendation	SFPW and SFPUC Comment	Oct 31, 2019 Phase 1 Horizontal Geotechnical Report Reference	Required Actions	How Resolved	Response by Langan and MRP, and TAP follow-up Langan responses in black , updates in blue MRP (S. Minden) responses in red , updates in purple	Referenced language from Langan Report dated 31 October 2019
6a Cont.						<p>In addition, considering these are linear elements, we evaluated the potential for LCC breakage from a horizontally propagation Rayleigh wave. Our analyses indicates the unit shear stress in the LCC is on the order of 1/4 to 1/2 of the minimum target strength of the LCC, See Exhibit A</p> <p>2-18-20 TAP Response: TAP concerns with this comment are conditionally resolved 2-18-2020. Developer to provide supporting material for final review. SFPW and SFPUC have not necessarily concluded their own reviews.</p> <p>2-19-20 Langan Response: See Revised Exhibit A for updated LCC calculation and narrative about the potential consequences of LCC cracking.</p>	
6b	Earthquake Considerations for LCC	SFPW: Section 7.3 of the geotechnical report stated that "We have checked that during a seismic event, the shear strength of the LCC is greater than the anticipated peak cyclic shear stress generated by an earthquake. We therefore conclude the LCC should perform adequately under a seismic event. In addition, even if the LCC cracks it will still provide vertical support for the streets and improvements." Please elaborate on methodology and what earthquake ground motions were used to develop peak cyclic shear stress. Please provide dynamic properties of P-LCC.	Section 7.3	What is the magnitude of seismic demand placed on the LCC backfill in terms of the peak cyclic shear stress caused by the earthquake?	Same as above	<p>11-6-19 Langan Response: Section 7.3 provides discussion on peak cyclic shear stress vs LCC shear strength.</p> <p>12-10-19 Langan Response: see above.</p> <p>2-18-20 TAP Response: TAP concerns with this comment are conditionally resolved 2-18-2020. Developer to provide supporting material for final review. SFPW and SFPUC have not necessarily concluded their own reviews.</p> <p>2-19-20 Langan Response: See Revised Exhibit A for updated LCC calculation and its resistance to cyclic shear stress.</p>	Section 7.3: "We have checked that during a seismic event, the shear strength of the LCC is greater than the anticipated peak cyclic shear stress generated by an earthquake. We therefore conclude the LCC should perform adequately under a seismic event. In addition, even if the LCC cracks it will still provide vertical support for the streets and improvements."
6c	Earthquake Considerations for LCC			Evaluate whether or not the stiffness of the LCC would be sufficiently degraded so as to impact its long-term function and performance	Same as above	<p>12-10-19 Langan Response: Based on our calculations the shear strength is greater than the anticipated peak shear stress. However, if the LCC does crack, it will still perform as intended.</p> <p>2-18-20 TAP Response: TAP concerns with this comment are conditionally resolved 2-18-2020. Developer to provide supporting material for final review. SFPW and SFPUC have not necessarily concluded their own reviews.</p> <p>2-19-20 Langan Response: See Revised Exhibit A for updated LCC calculation and its resistance to cyclic shear stress.</p>	
6d	Earthquake Considerations for LCC	SFPW: The vertical geotechnical report states, "At least six inches compressible material such as EPS14 geofoam should be placed between the LCC and below-grade elements; accordingly, passive resistance in the LCC should be ignored." Please confirm excavation method for LCC construction. Will formwork be constructed similar to LCC pilot and LCC will be poured within the roadway limits? How are the EPS14 geofoam and filter fabric installed against LCC roadway section without formwork?	Section 8.2	Consequences of cracking of the LCC apron should also be evaluated	Traffic signal poles, light poles, and full height trees should be evaluated with mitigating details provided no later than the next SIP	<p>11-6-19 Langan Response: Agreed. 6 inches of compressible material is discussed in Section 8.2.</p> <p>12-10-19 MRP Response: Next SIP will include structural calculations of light poles and any other structural elements embedded or found in LCC.</p> <p>2-18-20 TAP Response: TAP concerns with this comment resolved 2-5-2020. SFPW and SFPUC have not necessarily concluded their own reviews.</p>	Section 8.2: "To prevent application of high shear loads from adjacent buildings, 6 inches of compressible material should be provided between buildings and LCC."

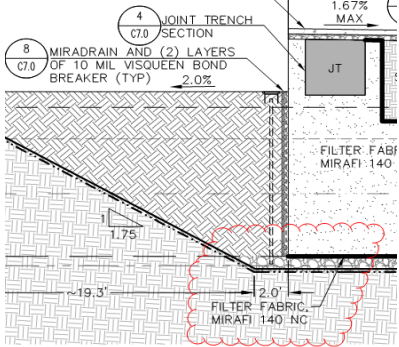
TAP Recommendations

No.	TAP Recommendation	SFPW and SFPUC Comment	Oct 31, 2019 Phase 1 Horizontal Geotechnical Report Reference	Required Actions	How Resolved	Response by Langan and MRP, and TAP follow-up Langan responses in black , updates in blue MRP (S. Minden) responses in red , updates in purple	Referenced language from Langan Report dated 31 October 2019
6e	Earthquake Considerations for LCC			The planned bedding or wrapping materials placed around utilities placed in the LCC should be clearly identified in all project drawings and documents. Furthermore, their interface properties (i.e., material stiffness, coefficient of interface friction, adhesion, cohesion, etc.) are often required by utilities to complete their seismic and other pipeline evaluations.	PG&E gas and proposed telecom companies must provide a letter approving of the proposed trench backfill (currently proposed as LCC).	12-10-19 MRP Response: We will provide standard sand bedding and shading in joint trench. This should not require any variances from current standards by PG&E, ATT, Comcast or others. 2-18-20 TAP Response: TAP concerns with this comment resolved 2-5-2020. SFPW and SFPUC have not necessarily concluded their own reviews.	
7	Buoyancy During Construction	SFPW: The intent of the TAP recommendation is during construction, not for the completed work. Note that there is still a potential issue with buoyancy for the completed work at the transition from the elevated supported streets to unsupported streets. See recommendation 13 below.	Section 7.3	The buoyancy calculations performed by the design team need revisions in light of the recent testing done by Castle Rock Consulting. In addition, these calculations need to evaluate the potential for buoyancy uplift for temporary/interim conditions where dewatering may have been discontinued or interrupted.	Langan has used 79 pcf as the basis of design. Saturated tests interpolates 27 pcf permeable LCC to be around 59 pcf and thus continue to have uplift. Langan must evaluate the data and provide justification for it's selected input.	11-6-19 Langan Response: Section 7.3 discusses the hydrostatic uplift checks based on no saturation. However, based on tests the permeable LCC will become partially saturated, which reduces the hydrostatic uplift pressures on the LCC section. Therefore, our evaluation is conservative. 12-10-19 Langan Response: We take no exception to the data showing the permeability may be on the order of 59 pcf, this value lies within the range of evaluated conditions. Langan's calculations that check for uplift are based on no infiltration (full hydrostatic pressures acting act the bottom of the LCC). Because the infiltration will increase density of the LCC, it will improve the factor of safety against uplift over time. If the project team wishes to value engineer the necessary section thickness based on site-specific data, this can be discussed with the team. 2-18-20 TAP Response: TAP concerns with this comment resolved 2-5-2020. SFPW and SFPUC have not necessarily concluded their own reviews.	Section 7.3: "To prevent significant hydrostatic uplift, open cell (porous) LCC will be used. The open cell LCC will allow water to flow through the material, preventing hydrostatic pressure from building up at the bottom of the LCC section. However, we have also checked the resistance to uplift of the LCC if the LCC is subjected to full hydrostatic pressures (i.e. acts impermeable) as an added check."

TAP Recommendations

No.	TAP Recommendation	SFPW and SFPUC Comment	Oct 31, 2019 Phase 1 Horizontal Geotechnical Report Reference	Required Actions	How Resolved	Response by Langan and MRP, and TAP follow-up Langan responses in black , updates in blue MRP (S. Minden) responses in red , updates in purple	Referenced language from Langan Report dated 31 October 2019
8	Long-Term Durability in Brackish Water	SFPW: SFPW defers to the response from	Not addressed in Geotechnical Report	Some testing should be performed to determine what the compressive strength losses will be when saturated with the brackish water on-site, at least through 28 days.	Developer transmitted 15 gallons of bay water to Colorado for testing. Initial tests show a 25% decrease in strength (same as regular water).	11-6-19 MRP Response: MRP is working with General Contractor Granite and LCC subcontractor, Cell-Crete Aerix and Castle Rock Consultants to perform long term test on LCC samples cured in air, fresh water and groundwater from site. Samples of groundwater from the site were sent to Aerix’s Lab in Colorado. Below is a description of the test, On October 18th, Aerix Industries molded forty (40) 3” x 6” cylinders from the same batch to test them for compressive strength under 3 different curing scenarios. The first scenario is a baseline where curing takes place as normal, with no exposure to saturation. In the second circumstance, a dozen cylinders are demolded at 7 days of age, placed in 4” x 8” PVC cylinder molds filled with fresh water and sealed. In the third scenario, a dozen cylinders are demolded at 7 days of age and placed in the 4” x 8” PVC molds but the molds are filled with brackish or salty groundwater and sealed. Samples cured the three different ways will tested for compressive strength at specific ages 28 days, 56 days, 3 months, 6 months, 9 months and 1 year. 12-10-19 Langan Response: No response required at this time.	
8	Long-Term Durability in Brackish Water (Continued)					1-24-20 MRP: Exhibit G shows test results through the 90 day breaks on 16 Jan 2020. From this data we note the following: 1. Observations: a. The compressive strength of the fresh and brackish water-cured samples are 78% and 80% of the normal cured samples, (or a 22% and 20% reduction compared to normal curing), respectively. b. All sets showed steady increase of compressive strength over time. Between the 28 and 90 day breaks, the water cured samples increased roughly 10psi/month or 25% and the normal cured sample increased roughly 15% 2. Preliminary Conclusions/Remarks a. Although the strength of the water cured samples are lower than the normal dry cured samples, they are well above the minimum compressive strength specified b. There is no significant difference in the effect of fresh water from brackish water curing. The brackish water cured samples are actually slightly stronger. c. There is a small increase in compressive strength over time after the initial 28 day cure time. This increase appears to be slightly more for the water cured samples. So far, the compressive strength is well below the 200 psi maximum specified for excavatability.	
8 Cont.	Long-Term Durability in Brackish Water (Continued)					We expect this increase to flatten out well below 200psi over the next nine months. This will be confirmed over the remaining test period. 2-18-20 TAP Response: TAP concerns with this comment resolved 2-5-2020. SFPW and SFPUC have not necessarily concluded their own reviews.	

TAP Recommendations

No.	TAP Recommendation	SFPW and SFPUC Comment	Oct 31, 2019 Phase 1 Horizontal Geotechnical Report Reference	Required Actions	How Resolved	Response by Langan and MRP, and TAP follow-up Langan responses in black , updates in blue MRP (S. Minden) responses in red , updates in purple	Referenced language from Langan Report dated 31 October 2019
9	Protection of the Pervious LCC from Fines Infiltration	SFPW: Developer to confirm if silt-barrier geotextile fabric will be installed during production for protection of the pervious LCC from fines infiltration. The response only shows a filter fabric in the pilot detail, but did not confirm it will be included in production LCC. Will formwork be constructed similar to LCC pilot and LCC will be poured within the roadway limits?	Not addressed in Geotechnical Report but this is shown in LCC Pilot Plans Sheet C6.0	A suitable silt-barrier geotextile filter fabric should be installed before placing pervious LCC in any excavation, to prevent migration of clay fines and clogging the pores.	Developer details tree planters with an internal filter fabric between soil and LCC in the 2nd SIP submittal.	<p>11-6-19 MRP Response:</p>  <p>12-10-19 Langan Response: No response required at this time. 2-18-20 TAP Response: TAP concerns with this comment resolved 2-5-2020. SFPW and SFPUC have not necessarily concluded their own reviews.</p>	
10	Waterline Leak Detection	SFPW: SFPUC to respond. SFPUC response 12/17/19: By not objecting to Recommendation 10 of the LCC Pilot Project Program, the SFPUC is not necessarily approving of this leak detection methodology. Close coordination with SFPUC operators during the leak detection test along with internal coordination after the test will be required and the SFPUC reserves the right to employ a different technology or method to detect water line leaks in the LCC.	Not addressed in Geotechnical Report, but is described in LCC Pilot Narrative (see excerpts in response)	The developer team should propose a method to identify and locate leaks in pipes that are embedded in LCC since the porosity of the LCC will prevent water from rising to the surface where it is visible.	A Developer method detailed in the LCC Pilot Project will be tested	<p>11-6-19 MRP Response: 2.10.19.2 Place 8 mil Polyethylene (PE) cover at bottom and sides of trench. Leave selvage to cover top and ends for trench. Note PE is proposed to be used in lieu of filter fabric in order to contain any leak in pipe. Water from leak will travel through pea gravel and through modified valve box and cover—see marked-up detail CDD-LP-250 as end of annotated plans. 3.3Simulate pipe leak in LPW line 3.3.33.3.1 Open gate valve in mock-up. Connect 4” fire hose to test rig end of pipe, close valve on test rig, connect other end of fire hose to hydrant or water truck pump. 3.3.2Turn water supply on. Gradually open valve on test rig. 3.3.4Observe water, verify water comes up through gate valve box and cover. 3.3.53.3.4vClose gate valve in mock-up. Water leak should stop. 3.3.6Turn off water supply, close valve on test rig.</p> <p>12-10-19 Langan Response: No response required at this time. 01-24-20 MRP Response: The Pilot demonstrated a leak detection method using a polyethylene wrap around pea gravel cover (shading) which conducted a simulated leak to the street through a valve riser.</p>	
10 Cont.	Waterline Leak Detection (Continued)					<p>Subsequently, representatives from CCD requested that the polyethylene wrap would be replaced with permeable filter fabric and the sand cover be provided for the full depth of trench to the top of subgrade/bottom of pavement base. This will be reflected in the third SIP submission. Note that this only applies to LPW.</p> <p>2-18-20 TAP Response: TAP concerns with this comment resolved 2-5-2020. SFPW and SFPUC have not necessarily concluded their own reviews.</p>	

No.	TAP Recommendation	SFPW and SFPUC Comment	Oct 31, 2019 Phase 1 Horizontal Geotechnical Report Reference	Required Actions	How Resolved	Response by Langan and MRP, and TAP follow-up Langan responses in black , updates in blue MRP (S. Minden) responses in red , updates in purple	Referenced language from Langan Report dated 31 October 2019
11a	Pavement Design	SFPW: SFPW defers to the response from	Sections 8.2 and	CBR value, modulus of subgrade reaction, or resilient modulus for the LCC materials and subjected to low-strain repetitive loading	Developer has not addressed how long term performance (dependent upon LCC stiffness)	<p>11-6-19 Langan Response: Sections 8.2 and 8.8 discuss the use of LCC as subgrade below the pavement section. We agree with this comment, but the pavement is not being designed to any CBR value or modulus. Therefore, this has not been provided.</p> <p>12-10-19 Langan Response: See Exhibit B showing that the resilient modulus for subgrade in pavement design is an estimate of the elastic modulus of a material. See Exhibit C showing the elastic modulus for LCC from Cell-Crete. For the requested pavement design calculations, we have used a resilient modulus of 95 ksi. This is at the lower bound of the reported modulus for similar materials. See Exhibit B, C, and E.</p> <p>01-24-20 MRP Response: See also Thesis on Use of LCC as a Subbase Material by S Averyanov, University of Waterloo, Ontario, Canada, 2018. Refer to Exhibit E attached.</p> <p>02-10-20 MRP: Response to verbal comment given by Port to MRP on thickness and type of base under pavement: The SIP Plans 3rd submittal show 4" of aggregate base material between the bottom of concrete pavement (sidewalks and PCC in streets) and the top of LCC. We believe that aggregate base, not sand is the most appropriate material for this application. Sand is generally not used as a bas or subbase material.</p>	<p>Section 8.2: "We understand that the San Francisco standard pavement section will be used for the streets, consisting of 4 inches of asphalt concrete over 8 inches of concrete. The San Francisco standard pavement section does not take into account the subgrade below the concrete and many streets in Mission Bay are supported on heterogeneous fill with varying strengths and quality. The LCC is stronger than the pavement subgrade in Mission Bay and we judge the LCC is adequate for pavement subgrade."</p> <p>Section 8.8: "We understand that the San Francisco standard pavement section will be used for the streets within the Horizontal Development at Mission Rock, which consists of 4 inches of asphalt concrete over 8 inches of concrete. The San Francisco standard pavement section does not take into account the subgrade below the concrete and many streets in Mission Bay are supported on heterogeneous fill with varying strengths and quality. The LCC is stronger than the pavement subgrade in Mission Bay and we judge the LCC is adequate for pavement subgrade. We recommend the four-inch-thick subgrade material consist of some type of strong granular fill material."</p> <p>See Exhibit B, C, and E</p>
11a Cont.	Pavement Design					<p>We believe that 4" is adequate separation thickness to prevent damage to LCC during pavement removal for future repairs. From a pavement design standpoint, we have demonstrated the PCC alone on LCC subgrade is more than adequate, no base is needed. Increasing the thickness of base would only add unnecessary weight and require more excavation, LCC and cost with no added value.</p> <p>2-18-20 TAP Response: TAP concerns with this comment are conditionally resolved 2-18-2020. Developer to provide supporting material for final review. SFPW and SFPUC have not necessarily concluded their own reviews.</p>	

TAP Recommendations

No.	TAP Recommendation	SFPW and SFPUC Comment	Oct 31, 2019 Phase 1 Horizontal Geotechnical Report Reference	Required Actions	How Resolved	Response by Langan and MRP, and TAP follow-up Langan responses in black , updates in blue MRP (S. Minden) responses in red , updates in purple	Referenced language from Langan Report dated 31 October 2019
11b	Pavement Design			Assumed properties of LCC, the pavement support, and design life calculations for the LCC should be provided for review	Provide the calculations	12-10-19 Langan Response: as described in the geotechnical report for the project, the City and County of San Francisco have specified a pavement type for this project. This pavement section consists of 4 inches of Asphalt Concrete over 8 inches of Portland Cement Concrete (PCC) with an unconfined compressive strength of 4,500psi. In addition, a 4-inch layer of aggregate base is provided beneath the PCC layer. This composite section is not consistent with either rigid or flexible pavement design methodologies. However, the calculation in Exhibit D shows the assumed properties for a rigid pavement design consistent with AASHTO 1993 for the concrete section alone, ignoring the Asphalt Concrete and the underlying Aggregate Base cushion. This design calculation indicates the concrete section over the LCC is capable of supporting more than 11 million equivalent 18 kips axle loads (ESAL's). This ESAL value suggest that for a typical 20-year pavement design life the pavement could support either 395 trucks per day (three axles, max legal weight at rear, with a combined weight of 54,000 pounds, examples include dump, trash, fire, or full concrete trucks) or 500,000 light trucks per day (two axles with a combined weight of 8,500 pounds, examples include Box Vans, Utility Trucks, or a Pick-up with a Trailer).	See Exhibit D
11b Cont.	Pavement Design Continued					The TAP or SFDPW should assess if this loading and timeframe match their assumed design intent. See Exhibit D for example calculations. 2-18-20 TAP Response: TAP concerns with this comment are conditionally resolved 2-18-2020. Developer to provide supporting material for final review. SFPW and SFPUC have not necessarily concluded their own reviews.	

TAP Recommendations

No.	TAP Recommendation	SFPW and SFPUC Comment	Oct 31, 2019 Phase 1 Horizontal Geotechnical Report Reference	Required Actions	How Resolved	Response by Langan and MRP, and TAP follow-up Langan responses in black , updates in blue MRP (S. Minden) responses in red , updates in purple	Referenced language from Langan Report dated 31 October 2019
11c	Pavement Design			Recommend that the pavement designer evaluate this extreme loading case to see if potential cracking might occur from the truck loading. Also, it is recommended that plate load tests be conducted prior and after the vehicle loading to evaluate potential changes in vertical stiffness. Lastly, careful documentation should be made of any deflection or distress caused by the loading. It may be possible for the planned pilot LCC testing to incorporate these	Provide the evaluations and tests and consider incorporating into the LCC Pilot Project.	11-6-19 Langan Response: Loading test being performed as part of the LCC pile testing. 12-10-19 Langan Response: This can be incorporated into the LCC Pilot if the modulus testing described in Exhibit E are not satisfactory to the TAP. 2-18-20 TAP Response: TAP concerns with this comment are conditionally resolved 2-18-2020. Developer to provide supporting material for final review. SFPW and SFPUC have not necessarily concluded their own reviews.	
12	Compressive Strength of Saturated LCC	SFPW: Not yet received to review.		The developer should perform testing of compressive strength of LCC cylinders when saturated with both brackish (saltwater) and on site ground water	Continue working with Aerix Industries and provide results to the City.	11-6-19 Langan Response: Currently being performed. 12-10-19 Langan Response: We understand there are ongoing tests regarding the compressive strength of the LCC in a saturated condition, and understand that there could be a 20 to 25 percent reduction of compressive strength. Based on this reduction, our analysis shows that the section still has a factor of safety against crushing greater than 2. 12-10-19 MRP Response: See also response to issue 8 above. 2-18-20 TAP Response: TAP concerns with this comment resolved 2-5-2020. SFPW and SFPUC have not necessarily concluded their own reviews.	

TAP Recommendations

No.	TAP Recommendation	SFPW and SFPUC Comment	Oct 31, 2019 Phase 1 Horizontal Geotechnical Report Reference	Required Actions	How Resolved	Response by Langan and MRP, and TAP follow-up Langan responses in black , updates in blue MRP (S. Minden) responses in red , updates in purple	Referenced language from Langan Report dated 31 October 2019
13	Tapered LCC Transitions	SFPW: MRP has indicated that they will design the tapered LCC transition zones from the elevated supported streets to unsupported streets to account for buoyancy effects. However, this has yet to be provided to us for review.		The developer team should evaluate the proposed tapered LCC transitions to confirm their effectiveness.	Transitions are not evident in SIP	<p>11-6-19 Langan Response: The LCC section will become thinner when approaching 3rd Street, but the LCC section will still be designed to unload the effective stress of the Bay Mud by 10 percent.</p> <p>12-10-19 The overall engineering design approach is to unload the Bay Mud by 10 percent at locations beneath the LCC. Therefore, once the weight of the pavement thickness, improvements are accounted for, in addition to unloading by 10%, the tapered section of LCC is still on the order of 5 to 7 feet thick. Therefore it may not look significantly tapered at locations where the LCC meets the adjacent roadways.</p> <p>2-6-20 Additionally, the LCC section includes unloading of the underlying Bay Mud. The stress decrease from the LCC decreases stress in the area beyond the footprint of the LCC. Therefore, if there is ongoing settlement in 3rd Street, the use of LCC will allow for a more gradual differential settlement from this unloading.</p> <p>2-18-20 TAP Response: TAP concerns with this comment are conditionally resolved 2-18-2020. Developer to provide supporting material for final review. SFPW and SFPUC have not necessarily concluded their own reviews.</p> <p>2-19-20 Langan Response: As discussed 12-10-20, all of the street sections, including the portions adjacent to 3rd Street, will be designed to unload the Bay Mud by 10 percent. These sections are thinner that areas where grades will be raised within Mission Rock, but still extend 5 to 6 feet below the ground surface. This is because the new street section includes the weight of a new pavement section, structural soil, and surface loads associated with trees, light poles, and other elements that will need to be offset to prevent additional consolidation settlement. As discussed 2-6-20, unloading these areas by 10 percent will allow for more gradual transitions and not abrupt changes due to differential settlement at the project limits.</p>	
14	Placement of LCC Fill	SFPW: The specification in Appendix G is different from the specification in LCC Pilot submittal, Permeable/Open Cell lightweight Cellular Concrete (P-LCC) specification, dated 10/29/2019. Per Article 4.3.2 of the 10/29/19 specification, Field Falling Head Permeability test is part of the quality control testing. Field permeability testing should be demonstrated in the pilot testing. Core of the LCC used in the Pilot (in situ sample, cured in water after 28 days) shall be lab tested for permeability. This should be compared to the specified permeability (0.10 to 0.65 cm/s) to make sure water can freely move around within LCC.	See Appendix G for specification	QA/QC procedures	Consider suggestions from Castle Rock Consulting and develop QA/QC procedures	<p>11-6-19 Langan Response: See specification.</p> <p>12-10-19 Langan Response: No response required at this time.</p> <p>12-10-19 MRP Response: Stan Peter's of the TAP has developed recommendations for testing and inspection that will be incorporated in the final LCC Specification including field tests for cast density, sampling and testing frequency and procedures, lab tests for compressive strength, permeability and saturated density.</p> <p>01-24-20 Proposed Draft of the final Spec , including testing and inspection schedule is in Exhibit H</p> <p>2-18-20 TAP Response: TAP concerns with this comment resolved 2-5-2020. SFPW and SFPUC have not necessarily concluded their own reviews.</p>	

TAP Recommendations

No.	TAP Recommendation	SFPW and SFPUC Comment	Oct 31, 2019 Phase 1 Horizontal Geotechnical Report Reference	Required Actions	How Resolved	Response by Langan and MRP, and TAP follow-up Langan responses in black , updates in blue MRP (S. Minden) responses in red , updates in purple	Referenced language from Langan Report dated 31 October 2019
15	Future Sourcing of LCC		Not addressed in Geotechnical Report	A separate specification should be provided for small batch LCC for emergency repairs.	The specification is for the City to impress upon third party applicants of LCC post acceptance of the project.	<p>11-6-19 MRP Response: See response to recommendation 4 above</p> <p>12-10-19 Langan Response: No response required at this time.</p> <p>2-10-20 MRP Response: A list of approved LCC contractors was added in Appendix B of the Exhibit F Proposed Excavation and Backfill Procedures. Three local LCC contactor/vendors are listed: Cell-Crete, Throop and Confoam.</p> <p>2-18-20 (TAP Comment): The Proposed Excavation and Backfill procedures given in Exhibit F refer to the LCC Specification for the main project in terms of material to be used for backfill during repairs. There are concerns that this exact material may not be available in the future. For example, Aerix is currently a sole source provider of permeable LCC foaming agents that are used by all LCC suppliers in the Bay Area. If they were to cease operations the specified material would no longer be available for future repairs. A more generic specification should be provided for backfill material for future repairs that includes other lightweight materials that are acceptable if LCC per the project spec cannot be obtained.</p> <p>MRP 02-24-20 LCC Repair and Backfill Procedure has been revised to allow non-permeable LCC backfill in limited areas. This would allow LCC to be made with foaming agents from different manufactures rather than just Aerix, which has the sole patent for permeable foaming agent. In these repairs non-preamble LCC can be placed above Elevation 95 feet or in localized trenches that with a volume less than 10 cubic yards.</p>	
16a	Pilot Test			The Developer should submit a written narrative description of the Pilot Test including objectives, construction sequence, and testing methodology.	This has been completed.	<p>11-6-19 Langan Response: See Pilot Test plan and Narrative</p> <p>12-10-19 Langan Response: No response required at this time.</p> <p>2-18-20 TAP Response: TAP concerns with this comment resolved 2-18-2020. SFPW and SFPUC have not necessarily concluded their own reviews.</p>	

TAP Recommendations

No.	TAP Recommendation	SFPW and SFPUC Comment	Oct 31, 2019 Phase 1 Horizontal Geotechnical Report Reference	Required Actions	How Resolved	Response by Langan and MRP, and TAP follow-up Langan responses in black , updates in blue MRP (S. Minden) responses in red , updates in purple	Referenced language from Langan Report dated 31 October 2019
16b	Pilot Test			Demonstrate that the isolation joint can accommodate the anticipated differential settlements.	Consider testing as part of the LCC Pilot Project.	<p>12-10-19 Langan Response: Comment is unclear. There will be six inches of compressible foam between the buildings and the LCC to accommodate differential settlement. If a different question is being asked, please let us know.</p> <p>12-10-19 MRP Response: If desired separate mock-ups can be made for these joints as part of Vertical design and construction.</p> <p>If the question is referring to differential settlement between the LCC and existing streets such as 3rd St. and Mission Rock St. This is not contemplated in the scope of the LCC Pilot, but has been addressed extensively in the BOD and SIP.</p> <p>Note that the horizontal and vertical geotechnical recommendations have been coordinated so that no lateral resistance or forces at the below grade are transferred between the LCC and buildings.</p>	
16b Cont.	Pilot Test Continued					<p>2-10-20 MRP: We have added an new Exhibit I: Typical Sections at LCC Interfaces showing details of LCC, Pavement and utilities. Please also refer to the recent SIP 3rd Submittal Plan Sheet Series C6: plans and profiles of grading & LCC , C 7 Series: plans, sections and profiles of utilities in streets, C8 Series: typical street cross sections and C9 Series: Details</p> <p>2-18-20 TAP Response: TAP concerns with this comment resolved 2-18-2020. SFPW and SFPUC have not necessarily concluded their own reviews.</p>	
16c	Pilot Test			Test the LCC surface for damage prior to protecting it. Determine and note the depth of damage. This will inform any future repairs that must be made due to damage that may occur during construction.	Test the bare unprotected LCC by driving a typical maintenance vehicle over it and also while parked.	<p>12-10-19 Langan Response: Damaged LCC should be removed and replaced with new LCC as part of the routine repairs during the life of the roadway. This test therefore does not provide meaningful data and we do not recommend performing this test.</p> <p>12-10-19 MRP Response: Note that a temporary wearing surface such as AC grindings and or AC will be provided to protect the LCC during vertical construction. Any damage to the LCC from construction will be repaired with fresh LCC prior to permanent paving.</p> <p>2-18-20 TAP Response: TAP concerns with this comment resolved 2-18-2020. SFPW and SFPUC have not necessarily concluded their own reviews.</p>	

Project Title - Mission Rock Project Phase 1

Mission Rock LCC Pilot Construction and Testing Procedure Submittal

CDD Reviewed for water items only - forward to other agencies as appropriate

Mission Rock Partners (MRP) Responses in Blue Langan. Responses in Black

- Notes to Reviewers
1. Please complete your review and return comments to TBD.
 2. Please be as specific as possible and propose corrections or solutions to the problem identified.
 3. Please consolidate the comments for all reviewers in your division and make sure the reviewer is identified for each comment.
 4. Let us know if there is anything that we can do or any additional information that we can provide to assist in your review!

Please provide the following information for your agency:

Agency:	SFPUC
Division/Unit:	CDD
Primary Contact Name:	Brandy Batelaan
Primary Contact Email:	bbatelaan@sfwater.org
Primary Contact Phone:	

Color key:

Red = consider incorporating **ASAP** for current pilot test

Yellow = MRP to provide **written response**. Possible action if response is not adequate.

Green = **defer** to maintenance/repair demonstration or training session at future date.

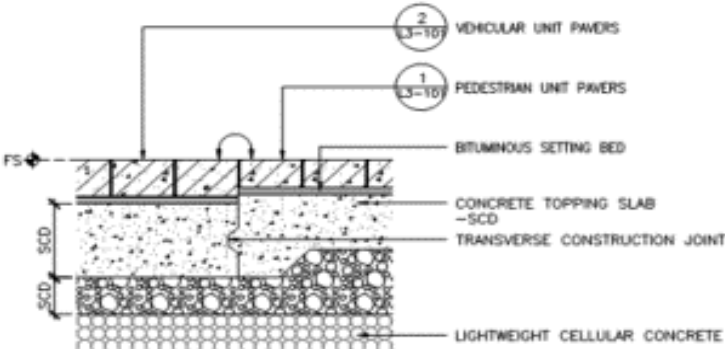
Comment #	Reviewer Name	Comment Date	Application Page #	Text, Figure or Other Document Reference	Comment / Issue	Proposed Revision or Solution (proposed by Fan Lau 12/18/19)	Response	Response Date
1				General	Forward to Fire Department for review	ASAP. Procedural action.	2-10-20 MRP: Fire Truck Test was coordinated with SFFD and performed on Thursday 1/16/20	
2				General	Add another test using the same conditions listed below, but with no valve or air valve riser.	ASAP. Change to design and installation of water main to include a control scenario for main break test.	2-10-20 MRP: Comment was received too late to make this change	
3				General	Part of the Testing Procedure shall include CDD Operations simulating a response to a main break. At a minimum, the CDD leak detection crew, CDD Operations, CDD Engineering, will need to detect and excavate for the main, and the pavement shall be subjected to H-20 loading after the main break has finished (to determine areas of undermining). The backfill material shall be fully cured at the time of this excavation. Excavation may include heavy machinery and hand-digging. the footprint of the excavation may be 6' wide x 5' deep, so that proper clearances can be provided to remove the main. Coordinate this simulation with CDD.	ASAP. Coordinate with CDD leading up to and during main break test.	2-10-20 MRP: Several on site meetings were held with Brian Barry, PE of CDD as well as other CDD representatives to coordinate the test and demonstration. Mr. Barry and other representatives also witnessed the leak repair demonstration on Friday, 1/17/20. As an outcome of this coordination and feedback after the test we have revised the trench details for Low Pressure Water (LPW) lines--see response to TAP Recommendation #10.	
4				General, C5.0	The test shall occur at 72 psi for 1 hour. The size of the hole can be between 1/4" and 1" diameter.	ASAP. Change to installation of water main and operation of main break test.	2-10-20 MRP: Leak simulation was performed at residual pressure from nearest fire hydrant on 3rd St. which was about 60-70psi. Leak hole was approximately 3/4" round	
5				General	it appears the steel plates may be a bottleneck for the water to escape the trench. Describe how water is anticipated to exit the valve risers and what will happen to the valve covers. Are the valve covers expected to become airborne?	Written response. If written response is inadequate, possible change to design and installation of water main.	2-10-20 MRP: The demonstrations showed that the water leak flowed past the plate and up the riser. Water gently bubbled up through the Valve Box riser and cover. The cover did not become airborne.	
6				General	The proposed test footprint appears to be too small. CDD requests that the test includes two sticks of pipe (40' length).	ASAP. This may not be possible.	2-10-20 MRP: Comment was received too late to make this change. The truck was accommodated by the addition of temporary ramps/berms on either end of the Pilot as shown in the Pilot Narrative Annotated Plans. The Pilot itself was subject to the full axel loads and outrigger loads of the truck tractor with latter fully extended and rotated.	
7				General	Confirm the pipe will not shift during the test. Provide pipe anchors and supports if appropriate.	Written response. If response is inadequate, possible change to design and installation of water main.	2-10-20 MRP: Confirmed, temporary thrust blocks and pipe restraints were provided and no pipe movement occurred	

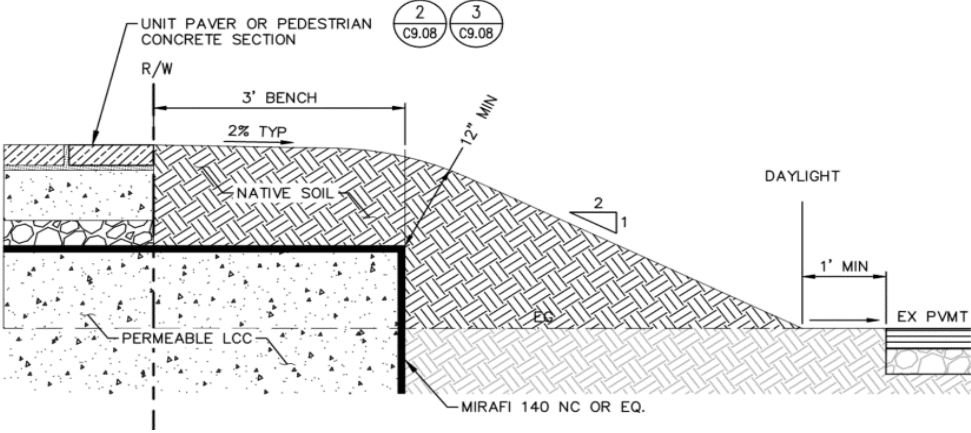
Comment #	Reviewer Name	Comment Date	Application Page #	Text, Figure or Other Document Reference	Comment / Issue	Proposed Revision or Solution (proposed by Fan Lau 12/18/19)	Response	Response Date
8				C5.0	what is the intent of the callout that begins "3'x3'x1" spectacle flange..." ? This configuration needs further clarification. What is preventing these flanges from being be washed away?	Written response. If response is inadequate, possible change to design and installation of water main.	2-10-20 MRP: This was proved to contain the pea gravel surrounding the pipe. Flanges were held in position by positive connection to pipe at either end of the pipe at the face of the LCC mockup.	
9				C6.0	30PCF LCC is typically not allowed in SFWD trenches for trench backfill. Trench backfill, bedding, and pipe zone immediate backfill should be sand. CDD will need to access the main in a main break in a timely manner. LCC may not allow for this. Additionally, after the main is repaired, CDD will likely restore with sand.	ASAP. Comment regarding sand affects installation of water main.	2-10-20 MRP: Trench detail was modified to provide sand, not pea gravel for the full depth of the LPW trench to top of subgrade/bottom of pavement. See response to TAP Recommendation 10	
						Defer. Comment regarding repair to be deferred to maintenance/repair demonstration.	2-10-20 MRP: Repair demonstration took approximately 3 hours from start of pavement removal to backfill. Removal of LCC fill was done within approximately 30 minutes with a combination of excavator and hand digging.	
10				C5.0, modified CDD-LP-250	pipe shall be wrapped in v-bio for test. Add to plans and add callout	ASAP. Change to design and installation of water main.	2-10-20 MRP: Comment receive too late to implement.	
11				modified CDD-LP-250	bedding and pipe zone immediate backfill shall be sand, not pea gravel	ASAP. Change to design and installation of water main.	2-10-20 MRP: See above, sand will be used in SIP.	
12				modified CDD-LP-250	submit product for fiberglass screen. Why fiberglass? Why not steel mesh?	Written response. If response is inadequate, possible change to design and installation of water main.	2-10-20 MRP: This is a moot point since leak detection concept demonstrated in Pilot has been changed in favor of standard sand cover and backfill with filter fabric between trench sides and sand. Fiberglass screen was to prevent pea gravel from clogging riser box. Fiberglass was called out because it is non-corrosive. However this is irrelevant now	
13				C6.0, modified CDD-LP-250	2' clear (Horizontal) and 1' clear (vertical) is needed between outside edge of pipe and the edge of the trench for CDD to remove and replace the main in-kind. The above clearance dimensions assume shoring will be provided and that it can be provided in a way to meet these clearances. The Engineer of Record shall demonstrate that the walls will not cave in without shoring. Also, the EOR shall demonstrate that shoring can be installed while maintaining these clearances.	ASAP. Change to design and installation of water main.	2-10-20 MRP: Stated clearances were maintained in Pilot and are followed in SIP. Repair demonstrated that walls did not cave without shoring.	
14				General	Upon completion of the water main break simulation, the pavement shall be subjected to vehicular loads to determine where road base has been undermined.	ASAP. Change to operation of main break test.	2-10-20 MRP: Pavement has not been restored in case further investigation is desired, however basecourse can be clearly seen at exposed edge of pavement cut. If desired pavement can be patched following CDD standard "T" patch detail. A vehicle can be driven on patch however it will be hard to actually run traffic because of small size of Pilot.	
15				C7.0	Detail 1 / C7.0 indicates LCC is permeable. How will surrounding trenches and structural soil be protected from undermining? Is water expected wash away the structural soil? what is the trench backfill of the SD? Is water expected to wash away the SD backfill? How about Joint Trench?	Written response. If response is inadequate, possible change to design and installation of water main.	2-10-20 MRP: The LCC is permeable, but cohesive. Unlike soil, flowing water will not erode it at pressure < 2000psi. This is one of the advantages of LCC over conventions soil fill. The structural soil will be separated from LCC with filer fabric to prevent any fines in the structural soil from migrating into LCC-- see response to TAP Recommendations 5 and 16b	
TAP Panel Comments on Pilot Project								

Comment #	Reviewer Name	Comment Date	Application Page #	Text, Figure or Other Document Reference	Comment / Issue	Proposed Revision or Solution (proposed by Fan Lau 12/18/19)	Response	Response Date
Comment #	Reviewer Name	Comment Date	Application Page #	Text, Figure or Other Document Reference	Comment / Issue	Proposed Revision or Solution	Response	Response Date
1				Narrative Section 1.3	In 1.3, are they just going to survey elevations of sidewalks and manhole rims, or will they also install TBMs (temporary bench marks) to monitor ground heave at various locations on and around the pilot surface?		2-10-20 MRP: Yes ground heave during hydrostatic uplift tests was measured at corners of the surrounding fill just beyond LCC during hydrostatic uplift tests 2-18-20 TAP Response: TAP concerns with this comment resolved 2-18-2020. SFPW and SFPUC have not necessarily concluded their own reviews.	
2				Sheet C2.0	the “Referenced Documents” section appears to have older version of the GTECH report (the one we have is dated 31 October 2019 but the note says December 18, 2018 and Revised March 1, 2019). and older version of the POSF Building Code is referenced (Note says 2010 but it should be 2016).		1-2-2020 Langan Response: Understood, the project will be permitted under the 2016 SF Building Code. 2-18-20 TAP Response: TAP concerns with this comment resolved 2-18-2020. SFPW and SFPUC have not necessarily concluded their own reviews.	
3					As requested, Field testing procedures for both Falling-Head Permeability and Natural Saturation Density have been developed, that can be performed on-site at three days. See Appendix L.		2-10-20 MRP: See Exhibit H: LCC Specification and TQA/QC Procedures, at the end of the Consolidated Comment Log 2-18-20 TAP Response: TAP concerns with this comment resolved 2-18-2020. SFPW and SFPUC have not necessarily concluded their own reviews.	
4					A QC-QA Testing Schedule has been developed for the Pilot Project, and final construction. See Appendix L.		2-10-20 MRP: See comment above 2-18-20 TAP Response: TAP concerns with this comment resolved 2-18-2020. SFPW and SFPUC have not necessarily concluded their own reviews.	
5					The Long-Term Durability Study is underway. The 28day results show approximately a 25% strength loss over the control dry samples, with no real difference whether submerged in fresh or on-site saltwater. The 56day results will be available on December 13 th . Verification by Langan that the loss of strength of the LCC when saturated, will still be acceptable.		2-10-20 MRP: The 90 day test results are included in Appendix G: Long Term Test of LCC Cured in Water at the end of this Log. 2-18-20 TAP Response: TAP concerns with this comment resolved 2-18-2020. SFPW and SFPUC have not necessarily concluded their own reviews.	
6					<ul style="list-style-type: none">Discussion of the current permeability specs (0.65 to 0.1 cm/sec) will occur. A minimum of E-2 cm/sec has been proposed for the permeable LCC. Discussion with Langan should occur.		1-2-2020 Langan Response: A minimum permeability of E-2 cm/sec is acceptable from a geotechnical standpoint. This can be revised in the final version of the spec after the LCC Pilot Program is completed. 2-18-20 TAP Comment: E-2 cm/sec is not consistent with the most recent specification. Please edit this response to be consistent with Section 2.2 of the specifications, including markups from TAP panel dated 2-17-20. 2-19-20 Langan Response: The specification has been updated to state a minimum permeability is 5E-3 cm/sec.	

Comment #	Reviewer Name	Comment Date	Application Page #	Text, Figure or Other Document Reference	Comment / Issue	Proposed Revision or Solution (proposed by Fan Lau 12/18/19)	Response	Response Date
7					A change to the LCC specifications should include placement when rain is anticipated; Cell Crete uses a criteria of postpone placement if rain of 0.25” within 10-12 hours is forecast.		1-2-2020 Langan Response: This can be added to the final version of the spec after the LCC Pilot Program is completed. 2-18-20 TAP Comment: Please add language to the specification that requires the contractor to address rain and surface water runoff that might enter the excavation. Detailed requirements that are properly left to the contractor's means and methods are not needed; however, a basic requirement that the contractor address the issue is necessary as shown by the LCC placement during rain on the pilot project. 2-20-20 Langan Response: Rain and Surface water entering the excavation are covered in Section 3.5.3 and 3.5.4 in the updated specification.	
8					<ul style="list-style-type: none">A field specification for Field Saturation Density of 50pcf or greater has been discussed. This is deemed acceptable for making decisions regarding de-watering terminations. This value has been achieved whenever the permeability is acceptable as well.		2-10-20 MRP: the 50pcf saturated density target has been incorporated in the LCC Specification--see Exhibit H: LCC Specification and TQA/QC Procedures, at the end of the Consolidated Comment Log 2-18-20 TAP Comment: 50 pcf target is not consistent with the TAP markups of the most recent specification. Please edit this response to be consistent with Section 2.2 of the specifications, including markups from TAP panel dated 2-17-20. 2-20-20 Langan Response: We have updated the specification to target the 55 pcf. See updated specification.	
9					2-18-20 TAP Comment: With regard to Appendix 6 – Geotechnical Observations, prepared by Langan, dated 12 February 2020, (on page 3, second paragraph) it is not clear in the discussion how they conclude that the permeability of the LCC is similar to or higher than the rate at which water was pumped into the test section. Please elaborate or provide calculation. On the same page in the third paragraph please provide the referenced calculations for estimating the permeability of LCC in-situ to provide the basis for the conclusions.		2-20-20 Langan Response: Based on the recorded water levels measured in the piezometers bottoming in the drain rock below the LCC section and the piezometers located in the LCC, the water levels rose at approximately the same time. This means that as the water is being added to the gravel and the water head measured in the gravel piezometers rise at about the same rate - therefore the permeability of the LCC must be high. We've performed a calculation based on the lag time in one portion of the flood test, see attached Exhibit J.	

Comment #	Reviewer Name	Comment Date	Application Page #	Text, Figure or Other Document Reference	Comment / Issue	Proposed Revision or Solution (proposed by Fan Lau 12/18/19)	Response	Response Date
10					<p>2/18/2020 TAP Comment: With regard to the Mission Rock Approval Criteria, dated 2-13-20:</p> <p>The LCC strength table in Section II (Crushing Resistance). Should say “28-day compressive strength”. This entry also says "at least 20 psi", which conflicts with the minimum value in P-LCC specs, which says 50 psi (TAP markups suggest revising that further to 80 psi and 100 psi, for 26 pcf and 30 pcf densities, respectively). Please revise Section II to match specifications.</p> <p>The LCC strength table in Section III (LCC Excavatability). Should say “28-day strength”. Uses at least 300 psi, which conflicts with the maximum value in P-LCC specs, which says 200 psi (TAP markups suggest revising that further to 200 psi and 300 psi, for 26 pcf and 30 pcf densities, respectively). Please revise Section III to match specifications.</p>		<p>2-20-20 Langan Response: We think that the minimum specified 28-day compressive strength of 50 psi for both the 26 pcf and 30 pcf density LCC, is appropriate and provides a large factor of safety for the intended use but is still sufficiently permeable.</p> <p>The 20 psi (which is not shown in the specifications or Performance Goals and Design Criteria letter) would represent a minimum strength; this strength of LCC is still strong enough to support traffic loads with an adequate factor of safety.</p> <p>The specified compressive strengths in the specification and are intended to be values that the contractor must achieve, but not the absolutely minimum strength that LCC could be to still support the traffic loads.</p> <p>See the attached updated specification regarding the minimum 28-day compressive strength of 50 psi for 26 pcf and 30 pcf density LCC, and the maximum 28-day compressive strength of 200 psi, which should provide a factor of safety on being excavatable. These documents are now in agreement.</p>	
11					<p>2-18-2020 TAP Comment: The Developer Team is currently revising the Project Criteria Document dated 1-24-20. As part of those revisions please add a new section before the "Design Criteria" Section that addresses Performance Goals. Please include a performance goal that corresponds to each bullet point in the Design Criteria Section per previous discussions.</p>		<p>2-26-2020 Langan Response: We have updated the Design Criteria Document.</p>	

No.	Comment	Response
1	Construction details of interfaces of LCC, soils, buildings and how to connect utilities to the buildings:	<p>MRP: See Exhibit I: Typical Interface Sections and Details at the end of this Log</p> <p>Langan Response: From a geotechnical standpoint, there is no need for a special construction detail at the interfaces of LCC and neighboring streets. As currently envisioned, there is a layer of filter fabric (Mirafi 140 NC or similar) at what is presumably a near vertical interface. The LCC section on Mission Rock includes unloading of the underlying Bay Mud. This unloading decreases the stress in the Bay Mud beyond the footprint of the LCC. Therefore, if there is some small ongoing settlement in 3rd Street, the use of LCC will allow for a more gradual differential settlement near the interface from this unloading. As currently designed, the vertical development parcels are also designing for up to 1.5 inches of heave or settlement at the building interfaces, including utility connections. Utilities will be designed to accommodate this differential movement through flexible connections.</p>
2	Construction details for interface of raised streets to existing streets	MRP: See Exhibit I: Typical Interface Sections and Details at the end of this Log and Langan Response above
3	Construction details for pavers	<p>MRP: Generally the paver details will be the same as any normal City street. Pavers will be set on aon a bituminous setting bed on a 4" either a concrete slab for sidewalks or an 8" PCC slab in vehicle travel ways. See Exhibit I: Typical Interface Sections and Details at the end of this Log. Paver details can also also be found on the SIP drawings C10 Series: Details; and L3 Series Pavement Details. Below is an example Detail 1/L3-103</p>  <p>The diagram illustrates a cross-section of a pavement structure. At the top, there are two types of pavers: 'VEHICULAR UNIT PAVERS' (labeled 2) and 'PEDESTRIAN UNIT PAVERS' (labeled 1). These pavers are supported by a 'BITUMINOUS SETTING BED'. Below the setting bed is a 'CONCRETE TOPPING SLAB'. A 'TRANSVERSE CONSTRUCTION JOINT' is shown as a vertical line separating the concrete slab from the underlying 'LIGHTWEIGHT CELLULAR CONCRETE'. The LCC layer is shown with a grid pattern. Dimensions are indicated: 'FS' for the total thickness of the pavers and setting bed, and 'SCD' for the thickness of the concrete topping slab and the LCC layer.</p>

4	How to construct and maintain LCC roads and sidewalks until and after buildings are built, including how maintain virtually vertical walls of LCC unloaded, loaded by construction or other vehicles, and under vibratory loads like pile driving	<p>MRP: horizontal LCC subgrade will be protected during constuction with 6-8" of AC grindings and/or temporary AC pavement. Vertical faces of LCC at Phase 1 parcels will be protected by the vertical contractors until gradebeams and kneewalls are poured. Construction loads will be kept back from the edges of LCC base on a 1:1 slope back from the base of the exposed LCC-- e.g. for a 4' face of exposed wall, no construction loads would be allowed < 4' back from the edge. If loads were required to be placed closer than that distance, temporary shoring or embankment designed by a qualified shoring engineer would be placed against the face of the LCC to stabilize it. Vertical faces of LCC at future Phase development parcels (e.g. Parcel K and J) will be protected with a temporary earth and LCC berm-- see detail 5/C9.09 on SIP plasn and thumbnail below.</p> <p>Langan Response: Once cured, the LCC can maintain vertical edges, but if any damage occurs during construction, the damaged section of LCC will be replaced</p> 
5	How to perform new installations and repairs, including procedures and specifications (routine and emergency work	MRP: This is covered in response to TAP Recommendation 4 and Exhibit F of the comment log
6	Stone columns final design and construction plans	Langan Response: After the ground improvement test program is complete, we will recommend a spacing of the stone columns to be used for the remainder of the site

MISSION ROCK LIGHTWEIGHT CELLULAR CONCRETE (LCC) TECHNICAL ADVISORY PANEL (TAP) COMMENT AND RESPONSE EXHIBITS

Rev. 02
27 February 2020

Exhibit A: LCC Shear Strength vs. Stress

Exhibit B: Resilient Modulus Definition

Exhibit C: LCC Modulus

Exhibit D: Pavement Design Calculations

Exhibit E: LCC as Subbase Material Thesis

Exhibit F: LCC Excavation and Backfill Procedure

Exhibit G: Long Term Testing of LCC Cured in Water

Exhibit H: LCC Specification (DRAFT)

Exhibit I: Typical Sections at LCC Interfaces

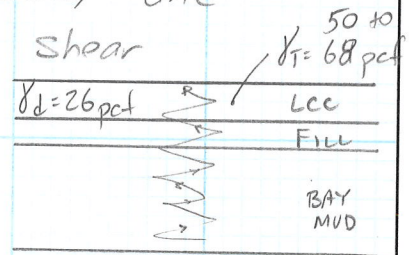
- Interface with Existing Street
- Interface with Vertical Parcel

Exhibit J: Permeability Based on Lag Time

EXHIBIT A
LCC Shear Strength vs Stress
Calculation

Mission Rock: Resistance of LCC to Cyclic Shear.

Goal: Estimate the Peak Cyclic Shear during the Design Earthquake in Light Weight Cellular Concrete (LCC) and compare this to the expected shear strength of the LCC.



Strength of LCC:

Unconfined compressive Strength - Target Min. = 50 psi

Assume a 20% degradation potential if saturated

∴ Design minimum uncompressive strength = 40 psi

Shear strength (S_u) = $\frac{1}{2}$ Unconfined compressive strength.

∴ $S_u = 20 \text{ psi} = \underline{2,880 \text{ psf}}$

Estimated Shear Forces in LCC - Method 1 - Simple Calc

Cyclic shear forces from vertically propagating horizontal shear waves can be estimated from the Peak Ground Acceleration (PGA) on site.

↳ Using the DE level of shaking and the response spectra from our report the $PGA_{DE} \approx 0.31g$ ($\frac{2}{3}$ of MCE value per code)

Cyclic Shear (τ) = $T_v \cdot g$ - for simplified analyses
 $g = PGA$

$T_{v \max}$ occurs @ the base of the LCC - Assume Water @ El. 95'

From Elevation 104.5' down to ~90' the section is:

: 12" AC/PCC + 4" AB + 2' of LCC @ 30 pcf + 6.2' of LCC @ 26 pcf + 5' of LCC @ 68 pcf + Surface loads (assume 150 psf to be conservative)

$T_v = 1' \cdot 150 \text{ pcf} + 0.33' \cdot 133 \text{ pcf} + 2' \cdot 30 \text{ pcf} + 6.2' \cdot 26 \text{ pcf} + 5' \cdot 68 \text{ pcf} + 150 \text{ psf}$

$T_{v \max} \approx 905 \text{ psf.}$

Mission Rock Horizontal

Simple LCC Shear Check

BY SAW DATE 2/13/2020

CKD JAS DATE 2/19/2020

PROJ. NO. 750604203

SHEET 1 OF 5

LANGAN

MR- Resistance of LCC to Cyclic Shear - continued.

Cyclic Shear stress (τ) = $\tau_{V_{max}} \cdot PGA$

$$\tau_{DE} = 905 \text{ psf} \cdot 0.31g$$

$$\tau_{DE} = \underline{281 \text{ psf.}}$$

$$\text{if @ MCE } \tau_{MCE} = 905 \text{ psf} \cdot 0.46g$$
$$\tau_{MCE} = 416 \text{ psf}$$

\therefore Max likely shear stress @ DE $\approx 281 \text{ psf}$

Anticipated minimum strength = 2,880 psf.

\therefore Factor of safety against crushing from horizontal shear waves @ DE =

$$F.S._{DE} = \frac{2880 \text{ psf}}{281 \text{ psf}} = \underline{10.2}$$

FOR MCE

$$F.S._{MCE} = \frac{2880 \text{ psf}}{416 \text{ psf}}$$

$$F.S._{MCE} \approx \underline{6.9}$$

Conclusion (From Method 1)

The anticipated minimum strength of LCC is sufficiently strong to resist the anticipated shear forces from horizontal shear generated by earthquakes. Therefore we do not expect significant degradation or damage from these types of forces.

However - other types of earthquake waves could subject the LCC to bending or tensile forces. These types of movement may cause the LCC to locally crack. See discussion on Page 5 regarding likely performance of cracked LCC to support the roadway, utilities, & traffic.

Mission Rock

Simple LCC Shear Check - con't.

BY SAW

DATE 2/13/2020

CKD.

DATE

PROJ. NO. 750604203

SHEET 2 OF 5

LANGAN

Estimated Shear Stress in LCC - Method 2 - enhanced calc.

Cyclic shear stresses from vertically propagating horizontal shear waves can also be estimated from existing evaluations used to develop the design spectra for the project.

Site specific design spectra for Mission Rock utilized the program Deep Soil to evaluate the anticipated linear and non-linear behavior of the soils during an MCE event. \therefore Use Deep Soil to extract these estimated forces.

Step 1: Add the LCC material to the existing Deep Soil model. - Typical LCC thickness is 8 to 13' - Use 10'

Dynamic Soil Parameters needed:

$\gamma_d = 26$ pcf G/G_{max} = degradation curve of shear modulus

G_{max} = Max Shear Modulus @ strain, V_s = shear wave velocity

G/G_{max} curve from Tiwari (2018) - see attached
- "mean" curve used in the analyses

$G_{max} = 29.48 \gamma_v' + 8,110.76$ (kPa) - from Tiwari (2018)
- See attached paper.

Within the LCC γ_v' is very low

$$\therefore G_{max} \approx 8,111 \text{ kPa} \approx 168 \text{ ksf}$$

To estimate V_s - use $G_{max} = \frac{\gamma V_s^2}{g}$ -

$$\therefore V_s = \sqrt{\frac{G_{max} \cdot g}{\gamma_d}} = \sqrt{\frac{168,000 \text{ psf} \cdot 32.2 \text{ ft/s}^2}{26 \text{ pcf}}}$$

$$V_s \approx 450 \text{ ft/s}$$

Step 2: Run Deep Soil. - See Attached Appendix from our report for details.

From Deep Soil we extracted the maximum shear stress ratio from our linear & non-linear evaluations within the LCC layers.

Max Shear stress ratio (τ/σ_v) = 0.47 - see attached plots.

Max Shear strain $\approx 0.07\%$

MR - Horizontal

Enhanced LCC Shear Check

BY SAW DATE 2/13/2020

CHKD. _____ DATE _____

PROJ. NO. 750604203

SHEET 3 OF 5

LANGAN

MR- Enhanced calc for estimated shear stress in LCC -continued.

$$\text{Max Shear Stress} = 0.47 \cdot \tau_v$$

$$\tau_v \approx 905 \text{ psf @ base of LCC (see Page 1)}$$

$$\text{Max Shear Stress } (\tau) = 0.47 \cdot \text{psf} = \underline{425 \text{ psf}}$$

$$\text{Anticipated minimum Shear Strength } (S_{\text{min}}) = \underline{2,880 \text{ psf}} - \text{see page 1}$$

\therefore Factor of safety against crushing for horizontal shear waves from an MCE earthquake event =

$$F.S. = \frac{S_{\text{min}}}{\tau} = \frac{2,880 \text{ psf}}{425 \text{ psf}} \approx \underline{6.8}$$

Conclusion From Method 2 - enhanced.

- 1) The minimum anticipated strength of LCC is sufficient to resist shear stresses generated by vertically propagating shear waves. We therefore do not expect significant degradation or damage from these stresses.
- 2) The simplified method (method 1) is adequate to evaluate this condition on future evaluations.
- 3) The LCC may still crack as a result of being exposed to surface waves, body waves, and differential ground deformation. However, LCC cracking will have a different potential effects on the performance of the overlying roadway and sidewalks or underground utilities. See Discussion on Page 5.

MR- Horizontal

Enhanced LCC Shear Check.

BY SAW

DATE 2/13/2020

PROJ. NO. 750604/203

CKD.

DATE

SHEET 4 OF 5

LANGAN

From: Scott A. Walker, GE

Date: 19 February 2020

Re: Performance of LCC During a Major Seismic Event
Mission Rock Phase 1 Horizontal Improvements
San Francisco, California
Langan Project No.: 750604203

This discussion presents the predicted performance of lightweight cellular concrete (LCC) during a major seismic event at Mission Rock. We previously performed a geotechnical investigation for the Phase 1 Horizontal Improvements project for Mission Rock and presented the results in a report dated 31 October 2019.

In general, as currently planned, within the 60- to 70-foot-wide public right of way (ROW), there will be new streets, sidewalks, and tree planting areas between the parcels to be developed. These street improvements will be underlain by LCC as detailed in our report. The LCC section will be about 6 to 13 feet thick and overlain by either structural soil in planter areas or a layer of aggregate base and vehicular or sidewalk pavement sections.

During a seismic event, the LCC will be subjected to several types of earthquake-induced loading, including (1) vertically-propagating shear waves, (2) surface waves (e.g. Rayleigh waves), and (3) potentially differential ground movements due to variation in depth to bedrock, thickness of Old Bay Clay, and thickness of Young Bay Mud. One of the potential sources of damage to the integrity of LCC would be the horizontal cyclic shear stresses induced within LCC from vertically propagating horizontal shear waves. We have analyzed this condition and our calculations show the LCC has sufficient strength to resist the shear stresses from these types of waves (see previous pages of this package).

Considering that the LCC section is long (several hundred feet long) compared to its thickness (6 to 13 feet thick), analyses of the LCCs resistance to cracking when subjected to surface waves and differential ground deformation is complex; the LCC will be subjected to compression, tension, and shear under these cases. Therefore, it seems prudent to discuss the likely performance of the horizontal improvements at Mission Rock if the LCC is cracked by these waves or differential horizontal / vertical movement.

The LCC material is a relatively brittle material once cured; it will remain relatively linear-elastic until its tensile or shear capacity has been reached and will then crack. Beyond the point of breakage, stress within blocks of LCC will be released through differential movements occurring between blocks along the breakage planes. This cracking will essentially act to dampen the stresses in the surrounding blocks as the energy is dissipated through friction along the breakage surfaces. As such, LCC within each block will retain its original strength and stiffness and still provide support of improvements; however, there may be an overall reduction in stiffness of the LCC and differential movement may occur between blocks during shaking. The effects of a possible reduction in stiffness and potential for differential movement of the blocks of LCC is discussed below.

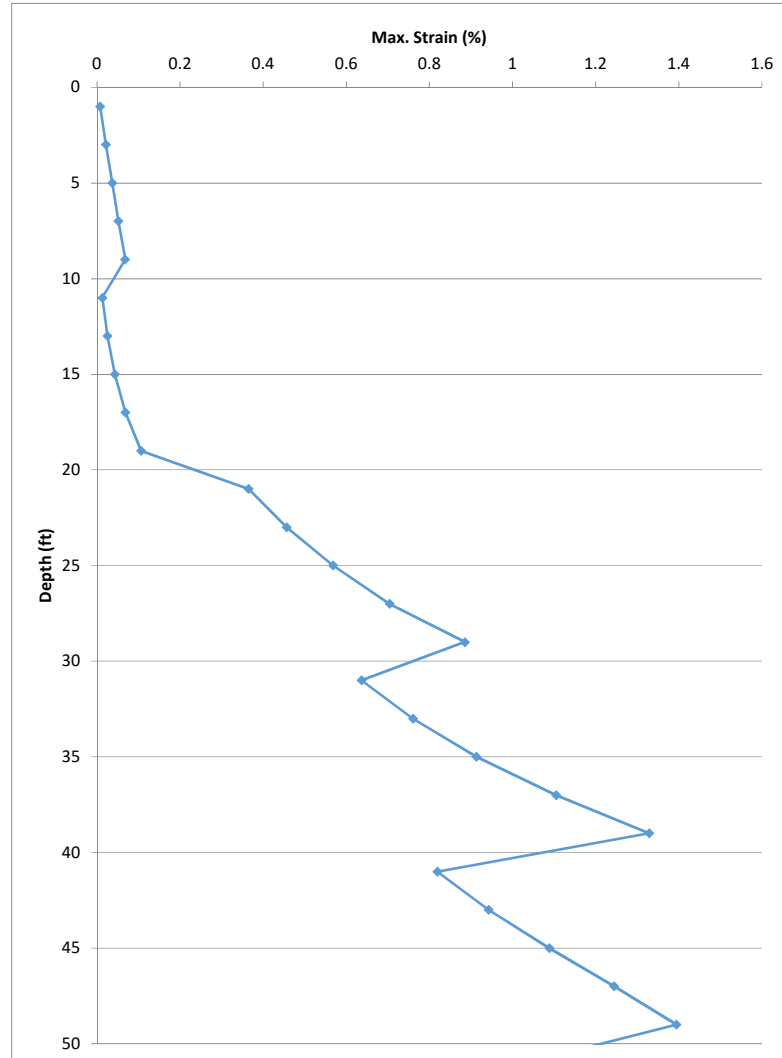
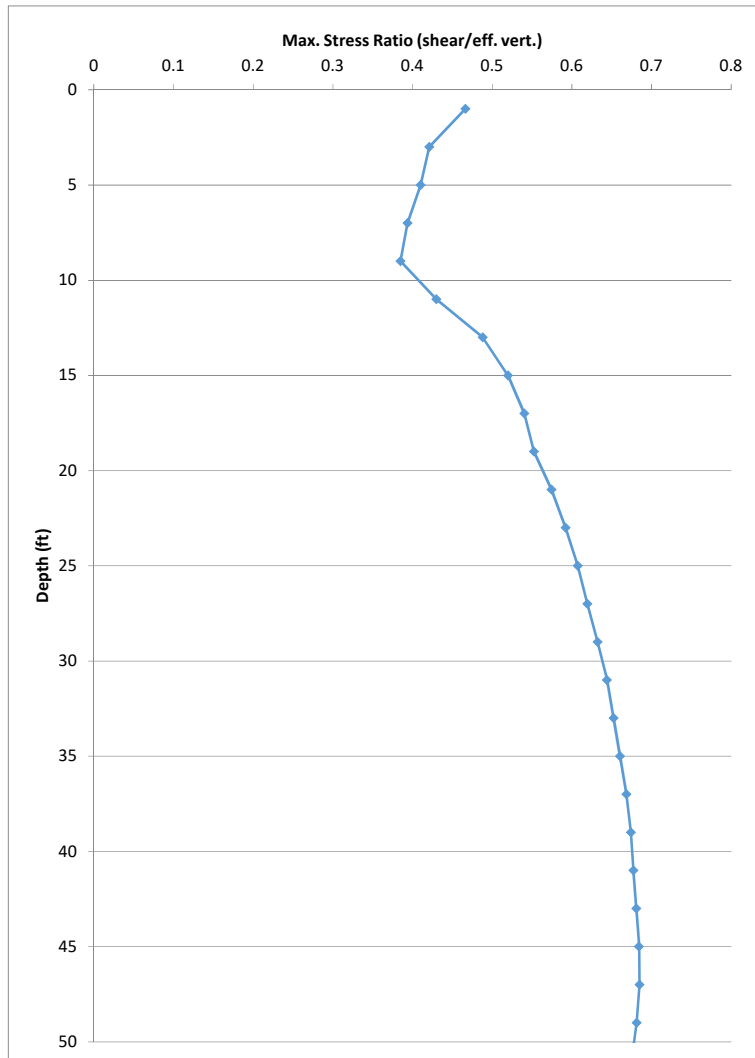
To evaluate the long-term performance of the pavement that is underlain by blocks of cracked LCC, we performed supplemental calculations assuming some strength loss within areas of heavy LCC cracking. The exact amount of strength loss (and corresponding loss of shear modulus) is difficult to assess for this condition. Langan has estimated that in areas that are heavily cracked, the modulus could degrade by 30 percent compared to intact LCC. We analyzed the planned pavement section assuming this degraded modulus value. The resulting calculations show no reduction in the amount of Equivalent Single Axle Loads (ESALs) necessary, as the stiffness of the LCC is still off the chart for the combined spring values. In fact, the modulus of the LCC can be reduced by as much as 40 percent with no reduction to the ESALS for the planned pavement section.

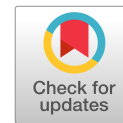
In areas where differential movement potentially occurs at LCC cracks, the overlying pavement or sidewalks may crack and need repair following a major seismic event. The level of cracking expected in the pavement or sidewalks cast above the LCC will likely be similar to or less severe than the cracking or distress to pavements or sidewalks nearby soil sites.

For underground utilities within the LCC at locations where cracking may occur, there are mechanisms in place that will reduce the likelihood of damage to the utilities. All underground utilities except district energy system (DES) piping are surrounded by bedding and cover sand or gravel. The bedding and cover materials are not compacted in place, and moderate differential movement along LCC cracks is expected to be accommodated in the bedding and cover material. The DES pipes consist of highly ductile HDPE piping which will be encased directly in the LCC because of the insulating value of the LCC. However, considering the strength and ductility of the HDPE piping, we would not expect appreciable damage at locations where the LCC cracks. In general, we would expect better performance in the utilities within the LCC than at nearby soil sites; however, repairs may be necessary following a major seismic event.

We judge that, to perform as intended on the project, it is not necessary that the LCC be free of cracking, but rather that the effects of cracking be taken into account in the design of the horizontal improvements at Mission Rock. We conclude that during a major earthquake, it is likely that the LCC will crack when subjected to the combined forces of surface waves and differential ground deformation. However, the likely consequences of LCC cracking due to a major earthquake do not jeopardize the ability of the LCC to perform as intended to support the proposed roadway and underground utilities, and that the cracking should be able to be addressed with post-earthquake maintenance.

DeepSoil Results from upper 50 feet of Profile.
LCC thickness = 9 feet.





Dynamic Properties of Lightweight Cellular Concrete for Geotechnical Applications

Binod Tiwari, M.ASCE¹; Beena Ajmera, A.M.ASCE²; and Diego Villegas³

Abstract: Lightweight cellular concrete (LCC) materials have been used in various civil engineering applications for several decades. In this study, the dynamic behavior of LCC materials was evaluated for possible geotechnical applications, such as mechanically stabilized earth (MSE) retaining walls. Lightweight cellular concrete materials having four different unit weights were subjected to various amplitudes of sinusoidal waves at effective normal stresses ranging from 25 to 350 kPa. Results from this study show that the effective normal stress influenced the shear strength and stiffness more than the unit weight of the LCC materials. The backbone curves could be represented with a hyperbolic function, which can be developed for a known effective normal stress using the equations proposed in this paper. The maximum shear moduli of the LCC materials increased with a decrease in the unit weight and an increase in the effective normal stress. Likewise, the rate of reduction in normalized shear modulus (G/G_{\max}) with strain also decreased with an increase in effective normal stress applied during seismic loading. Moreover, the damping ratio decreased with an increase in shear strain up to certain shear strain, which ranged from 0.25 to 0.35% for effective normal stresses of 25 and 350 kPa, respectively, and increased with shear strain after that transitional shear strain. The damping ratio of each type of LCC material tested was similar at the highest shear strain, i.e., 0.5% at a given effective normal stress. The results from this study can be used to evaluate the shear strength and deformation of the LCC materials in various geotechnical projects, such as in the backfill of MSE walls. DOI: 10.1061/(ASCE)MT.1943-5533.0002155. This work is made available under the terms of the Creative Commons Attribution 4.0 International license, <http://creativecommons.org/licenses/by/4.0/>.

Background

Construction on soft soils can pose a number of challenges for geotechnical engineers, including dealing with high amounts of consolidation settlement and low shear strengths, and bearing capacities. When these soft soils are located in seismic regions around the world, additional challenges arise, such as the amplification of seismic ground motions and, hence, an increased structural demand on the infrastructure (Pradel and Tiwari 2015). Traditionally, these poor ground conditions are improved with the implementation of costly ground modification techniques. However, the recent use of lightweight cellular concrete (LCC) in place of the existing weak soils is becoming more widespread. Particularly, LCC has been implemented as backfill for retaining walls and to absorb shocks around tunnels and pipelines in earthquake zones (LaVallee 1999). Mechanically stabilized earth (MSE) retaining walls with LCC backfills are found at several locations in California. A few examples are the Silicon Valley Berryessa Extension in San Jose, Colton Crossing for the Union Pacific–Burlington Northern Santa Fe (BNSF) railroad in Colton, and the San Bruno Railroad Grade Separation in San Bruno (Teig and Anderson 2012; Pradel and Tiwari 2015).

Lightweight cellular concrete is composed of a mixture of the traditional components of concrete (water, aggregates, and cement) and air voids. These air voids are established in the material via the introduction of either a protein-based or synthetic-based foaming agent that reacts mechanically and chemically with the other components to entrap the air (Maruyama and Camarini 2015; Panesar 2013; Tian 2011; Albayrak et al. 2007; LaVallee 1999). Because these materials can have between 10 and 70% air voids (Panesar 2013) depending on the amount of foaming agent introduced in the mixture, the materials can have unit weights as low as 3.1 kN/m³ (The Aberdeen Group 1963).

Because LCC can provide several benefits, such as being lightweight, durable, noncorrosive, permanent, and stable, and have high freeze-thaw resistance, high insulating capacities, low water absorption, and low permeability, this material can be used in a number of geotechnical engineering applications (Maruyama and Camarini 2015; Tikalsky et al. 2004; LaVallee 1999; The Aberdeen Group 1963). Thus, it is important to understand how this material will behave under static and dynamic loading conditions. Several researchers have presented results related to a number of properties of this material under static conditions, including its thermal conductivity (Neville 2002; Narayanan and Ramamurthy 2000; Loudon 1979; The Aberdeen Group 1963), unconfined compressive strength (Zaidi et al. 2008; Narayanan and Ramamurthy 2000; LaVallee 1999), bearing capacity (LaVallee 1999), drying shrinkage (The Aberdeen Group 1963), thermal expansion (The Aberdeen Group 1963), water absorption capacities (Maruyama and Camarini 2015), and modulus of elasticity (Narayanan and Ramamurthy 2000). However, the dynamic properties of LCC has not been extensively studied and characterized.

In this paper, results obtained from the cyclic simple shear tests that were conducted on LCC specimens representing four different unit weight materials are presented. Specifically, the behavior of these materials pertinent to the maximum shear modulus, modulus reduction curves, and damping ratios is discussed in detail.

¹Professor, Dept. of Civil and Environmental Engineering, California State Univ., Fullerton, 800 N. State College Blvd., E-419, Fullerton, CA 92834. E-mail: btiwari@fullerton.edu

²Assistant Professor, Dept. of Civil and Environmental Engineering, California State Univ., Fullerton, 800 N. State College Blvd., E-318, Fullerton, CA 92834 (corresponding author). E-mail: bajmera@fullerton.edu

³Engineer, Cell-Crete Corporation, 135 E. Railroad Ave., Monrovia, CA 91016. E-mail: dvillegas@cell-crete.com

Note. This manuscript was submitted on March 20, 2016; approved on August 2, 2017; published online on November 22, 2017. Discussion period open until April 22, 2018; separate discussions must be submitted for individual papers. This paper is part of the *Journal of Materials in Civil Engineering*, © ASCE, ISSN 0899-1561.

Moreover, a discussion on the use of these properties in geotechnical engineering applications also is included.

Materials and Methods

Casting Procedures

The LCC materials used in this study were provided by the Cell-Crete Corporation (Monrovia, California). Two concurrent processes are used by the Cell-Crete Corporation to cast the LCC samples tested in this study. First, one part of a specific biodegradable protein-based surfactant (a by-product of the food industry) and 40 parts of water were mechanically agitated through a small nozzle to produce a foam, and subjected to compressed air action at a high air pressure. The use of different protein-based surfactants will produce LCC materials with varying unit weights. Second, on the basis of a specific mix design, cement and water were blended together to produce a neat cement slurry. This mixing process took place in a customized concrete mixer, which was coupled with a progressing cavity pump. Then, the neat cement slurry was used to produce an air-filled cellular concrete in a proprietary blending system with the addition of the preformed foam. The unit weight of the LCC was determined on the basis of the quantity of the preformed foam added to the neat cement slurry, and ranged from 3.14 to 18.9 kN/m³. The LCC mixture then was poured into Styrofoam molds with the required dimensions to begin the curing process. In this study, five sets of samples were cast to a height of approximately 38.1 mm and a diameter of approximately 66.0 mm. Samples representing four different unit weights were cast. The details of the samples will be discussed subsequently.

Curing Process

After the LCC mixture was poured into the Styrofoam molds, the samples were allowed to set for 4 days. Between the 5th and 7th

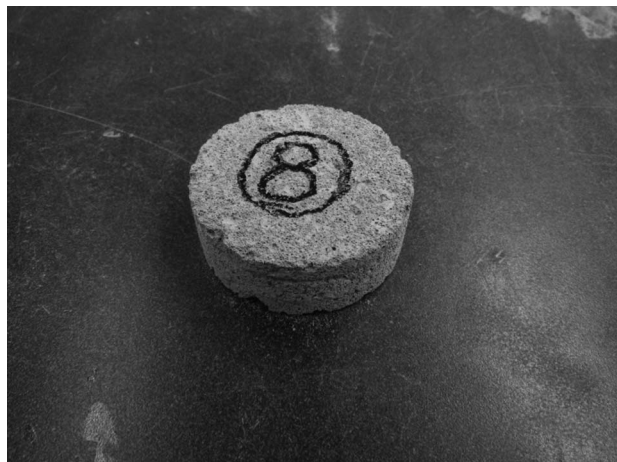


Fig. 1. Typical trimmed LCC sample prior to testing

day after the pour date, the Styrofoam molds were cut carefully and the cast samples were removed. During this process, careful attention was paid to ensure that the samples were not accidentally broken or cut. Each removed sample was wrapped in wet towels. These towels were soaked in deionized water for approximately 30 min prior to use. The wrapped LCC samples then were placed in an air-tight container, in which they were stored for 25 days after the pour date. The towels were moistened on a daily basis during this curing period. The wet towels and the lid to the air-tight container were removed on the 26th day after the pour date. For the next 3 days, that is, until the 28th day after the pour date, the LCC samples were allowed to air dry and continue curing. The trimming and testing of the samples took place on the 29th and 30th day after the pour date.

Sample Trimming

For each cured sample, the height, weight, and diameter of the sample first were recorded. Using a Vernier Caliper (Aerospace, South El Monte, California), height measurements were taken at three different locations approximately 120° apart. A total of nine (three each at the top, middle, and bottom of the sample) diameter measurements were taken. Each sample also was weighed three times. These measurements were used to determine the moist unit weight of the specimen prior to trimming. After obtaining all of these measurements, the samples were carefully twisted into a ring with an inside diameter of 63.5 mm, such that the 25.4-mm tall ring was located at central 25.4 mm of the specimen. This twisting process trimmed the LCC sample to the required diameter. The portion of the specimen extruding outside the ring was carefully trimmed, on either side, using a frosted knife to obtain a specimen with a height of 25.4 mm. A typical trimmed LCC sample prior to testing is presented in Fig. 1. The height, weight, and diameter of the specimen was measured again following the procedure outlined previously. These measurements were used to compute the test unit weight of the specimen following the trimming procedures. The measured unit weights are outlined in the next section. The dry unit weight for each specimen was computed after the completion of cyclic simple shear testing using the weight measurements obtained after the specimen was placed in an oven for at least 24 h at a constant temperature of 110°C.

Unit Weight

Although the same the LCC batch mixture was used to cast each set of specimens, some differences in the unit weights of the specimens was expected. In this study, the unit weight of each specimen was determined prior to trimming, after trimming just prior to testing (or the test unit weight), and after 24 h of oven drying following the cyclic simple shear testing (or the dry unit weight). The range and average unit weights for each set of samples tested in this study are presented in Table 1. Table 1 shows that the average unit weight of the specimen prior to and after the trimming process was nearly the same; hence, it is safe to assume that the results

Table 1. Ranges of and Average Unit Weights for Tested Specimens

Batch description	Unit weight prior to trimming (kN/m ³)	Test unit weight (kN/m ³)	Dry unit weight (kN/m ³)
Class II–Batch 1	3.03–3.35 (average = 3.17)		Not measured
Class II–Batch 2	3.32–4.18 (average = 3.80)	3.52–4.12 (average = 3.91)	2.94–3.38 (average = 3.16)
Class IV	4.45–4.76 (average = 4.61)	4.62–4.79 (average = 4.71)	3.80–3.98 (average = 3.91)
7.1 kN/m ³ cast unit weight	5.55–6.68 (average = 6.24)	4.95–6.68 (average = 6.10)	4.20–5.74 (average = 5.06)
8.6 kN/m ³ cast unit weight	5.03–6.93 (average = 5.66)	5.03–7.37 (average = 5.64)	4.48–6.41 (average = 5.17)

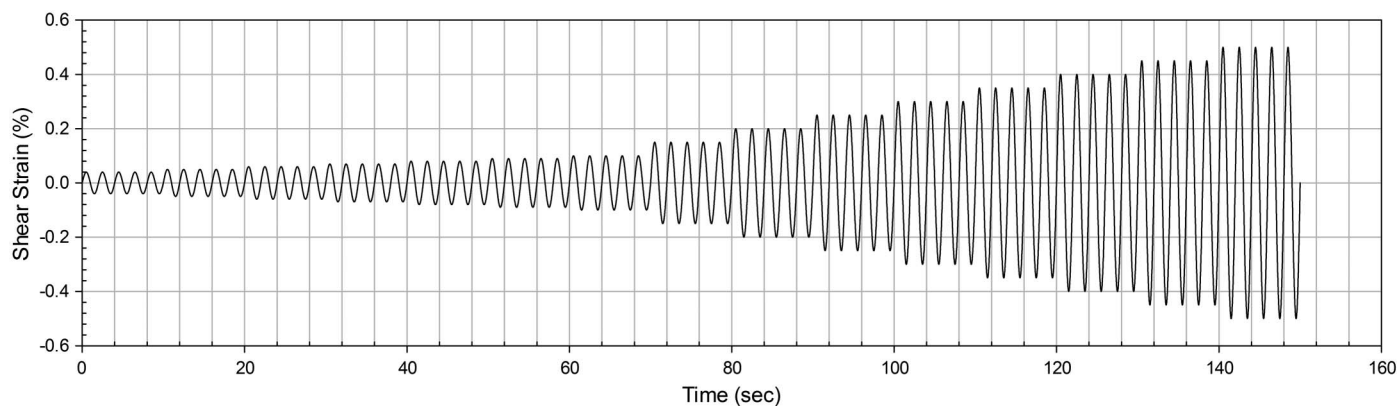


Fig. 2. Applied strain-controlled cyclic loading function

obtained in this study were not affected by the trimming procedures followed.

Cyclic Direct Simple Shear Testing

In this study, a Norwegian Geotechnical Institute (NGI)-type CDSS device, manufactured by GeoComp (Acton, Massachusetts), was used to conduct the cyclic direct simple shear (CDSS) testing (Dyvik et al. 1987; Bjerrum and Landva 1966). This automated, computer controlled apparatus uses a stack of 31 Teflon rings to confine the specimen laterally. Each Teflon ring is 0.94-mm thick. The horizontal loads were applied via a servo-motor; whereas, a microstepper motor was used to apply the vertical loads on the specimen. The CDSS device has both horizontal and vertical load capacities of 4,448 kN. In the horizontal direction, ± 12.5 mm displacement was permitted. Similarly, 12.5 mm of deformation was permitted in the vertical direction. Both the horizontal and vertical displacement readings were resolved to 0.0013 mm.

The trimmed LCC specimens were placed in a rubber membrane, confined by the stack of Teflon rings and secured in the cyclic simple shear apparatus. Then, the specimen was subjected to the desired consolidation pressure. At the end of the primary consolidation, determined from a real-time logarithm of time versus vertical deformation curve, the cyclic loading phase began. In this study, cyclic loading consisted of a series of different strain-controlled sinusoidal waves applied to the sample in undrained conditions. Each specimen was subjected to five cycles, each of 0.5-Hz frequency, of sinusoidal waves with strain amplitudes of 0.04, 0.05, 0.06, 0.07, 0.08, 0.09, 0.10, 0.15, 0.20, 0.25, 0.30, 0.35, 0.40, 0.45, and 0.50%. The test progressed through each of these amplitudes with no pauses between each step. The loading function applied is presented in Fig. 2. At the end of the cyclic loading phase, the specimen was removed from the cyclic simple shear device and placed into an oven for at least 24 h to determine its moisture content and dry unit weight. A total of 11 specimens were tested for each batch of LCC under four different consolidation pressures, i.e., 25 kPa (three specimens), 50 kPa (three specimens), 100 kPa (three specimens), and 350 kPa (two specimens).

A limitation of this study was the use of specimens that were 25.4 mm in height in all of the testing conducted. In the case of soft rock, surface fracture depends on the size of the specimen. These tests were conducted with the sample size specific to the testing equipment; larger size samples may yield slightly different results than those presented in the subsequent sections. A separate study is needed to evaluate the influence of the sample size on the dynamic behavior of the LCC materials.

Material Testing Results and Analysis

Although mechanical properties of the LCC materials also were measured with different static soil testing procedures, the details of those tests are not presented in this paper. Please refer to Tiwari et al. (2017), Tiwari and Ajmera (2015), and Maw and Cole (2015) for the testing methodology and study results pertinent to static soil tests. However, a summary of the mechanical properties of the LCC materials is presented in Table 2. For the purpose of comparison with other geomaterials, the friction angle of saturated loose sands typically ranges between 30° and 36° , whereas the friction angle for saturated dense sands is typically between 36° and 41° . Soft clays tend to have unconfined compressive strengths between 12.5 and 25 kPa, whereas stiff clays typically have unconfined compressive strengths between 50 and 100 kPa. The static properties of the materials will help to understand the dynamic behavior of the LCC materials. This paper primarily focuses on the dynamic properties of the LCC materials.

Stress-Strain Hysteresis Loops

A typical set of stress-strain hysteresis loops obtained from the CDSS test is presented in Fig. 3. The results in Fig. 3 are for a Class II–Batch 1 specimen under a consolidation pressure of 25 kPa. However, all of the specimens exhibited behavior similar to that shown in Fig. 2. The area of the hysteresis loop increased as the amplitude of the cyclic loading increased. The samples tested at higher consolidation pressures also exhibited similar behavior, but the area enclosed by the hysteresis loop at the same strain amplitude decreased. None of the hysteresis loops for any sample became open or banana-shaped.

Backbone Curves

The results obtained from the hysteresis loops were used to develop backbone curves for the LCC materials, as provided in Fig. 4, which represents a Class II–Batch 1 specimen tested at a consolidation stress of 25 kPa. In Fig. 4, the data points represent the peaks and troughs, corresponding to the points of stress reversal in the stress-strain hysteresis loops from Fig. 3. Also presented in Fig. 4, is a hyperbolic function as expressed in Eq. (1), which was fitted to these data points. In Eq. (1), τ is the shear stress, γ is the shear strain, whereas a and b are curve-fitting parameters. The CDSS apparatus is limited in measuring the cyclic shear stresses for shear strains less than 0.02%. However, as presented in Fig. 4, the hyperbolic function fitted well into the results provided by the CDSS for all samples. The maximum shear modulus (G_{\max}) value was

Table 2. Mechanical Properties of the LCC Materials Used in This Study

Material	Unconfined compressive strength (kPa)	Friction angle for partially saturated conditions (degrees)	Cohesion for partially saturated conditions (kPa)	Friction angle for saturated conditions (degrees)	Cohesion for saturated conditions (kPa)	Undrained strength ratio	Hydraulic conductivity (cm/s)	At-rest earth pressure coefficient	Poisson's ratio
Class II-Batch 1	265–1,657	19	408	35	36	0.36–1.82	Not measured	Not measured	Not measured
Class II-Batch 2		20	187	35	36	0.28–1.54	1.7×10^{-4} to 7.7×10^{-4}	0.4–0.5	0.2–0.3
Class IV	628–2,765	21	615	35	36	0.48–1.80	1.2×10^{-3} to 9.5×10^{-4}	0.2–0.3	0.2–0.3
7.1 kN/m ³	8,979–10,845	22	820	35	36	0.50–3.53	Not measured	Not measured	Not measured
cast unit weight									
8.6 kN/m ³	10,729–13,406	21	1,174	35	36	0.54–1.89	Not measured	Not measured	Not measured
cast unit weight									

calculated by measuring the slope of the curve at axial strain of 0% by first calculating the derivative of the hyperbolic function and substituting γ as 0%. The shear wave velocities obtained from the CDSS for five samples was calculated on the basis of the value of G_{\max} , obtained with the process outlined previously, one for each type of LCC material at 25-kPa consolidation pressure, matched well with the shear wave velocities obtained through bender element tests (Tiwari and Ajmera 2015). Fig. 5 contains several backbone curves for Class II–Batch 1 specimens tested with different consolidation stresses. This figure shows that the backbone curves shift upward as the consolidation pressure increased. Fig. 6 depicts the backbone curves for all types of LCC materials used in this study, in which upper and lower bounds referred to the Class II and 7.1-kN/m³ cast unit weight LCC material, respectively, measured at the consolidation stress of 50 kPa. Close observation of all test data showed that the unit weight of the LCC had a very small influence on the backbone curves. Therefore, the results presented in Fig. 6 can be considered as the maximum and minimum ranges, and as average backbone curves for the LCC materials

$$\tau = \frac{a\gamma}{b + \gamma} \quad (1)$$

The values of parameters a and b in Eq. (1) can quantitatively provide additional insight into the behavior of the backbone curves. Eq. (1) shows that the parameter a scales the hyperbolic function such that an increase in a corresponds to an upward shift in the position of backbone curve. In this study, an increase in a would imply that a larger stress was required to cause the same amount of deformation in the LCC specimen. In contrast, slope of the hyperbolic function at a strain value of zero; thus, the curvature of the hyperbolic function is controlled by the parameter b . Specifically, an increase in the value of b implies that the curvature decreases. A higher value of b will imply that a lower shear stress is required to cause the same shear deformation.

Because Figs. 5 and 6 showed that there was a significant influence of the consolidation pressure and very small effect of the LCC unit weight on the backbone curves, the variation in the parameters a and b with the consolidation pressure was calculated and presented in Figs. 7 and 8, respectively. The bars in these figures represent the range of values for the parameters a and b across all specimens tested at any particular consolidation pressure. It shows that an increase in the consolidation pressure (σ'_v) resulted in an increase in the value of a , which can be modeled by Eq. (2). Similarly, an increase in the consolidation pressure also resulted in an increase in the value of the parameter b . The best-fit regression line for the values of the parameter b with respect to the consolidation pressure is provided in Eq. (3). In Eqs. (2) and (3), the consolidation pressure should be expressed in kPa. Figs. 7 and 8 with Eqs. (2) and (3), respectively, suggest that as the consolidation pressure increased, the backbone curves for the LCC specimens shifted upward and tended to become less curved. Vertical solid lines presented in both Figs. 7 and 8, and in all subsequent figures, are the ranges of data and the solid circles are the average values

$$a = 0.4593\sigma'_v \quad (2)$$

$$b = 0.0027\sigma'_v + 0.0502 \quad (3)$$

Maximum Shear Modulus (G_{\max})

The maximum shear modulus was calculated as the maximum slope of the backbone curve, which occurred at zero shear strain. The variation in the maximum shear modulus with the consolidation

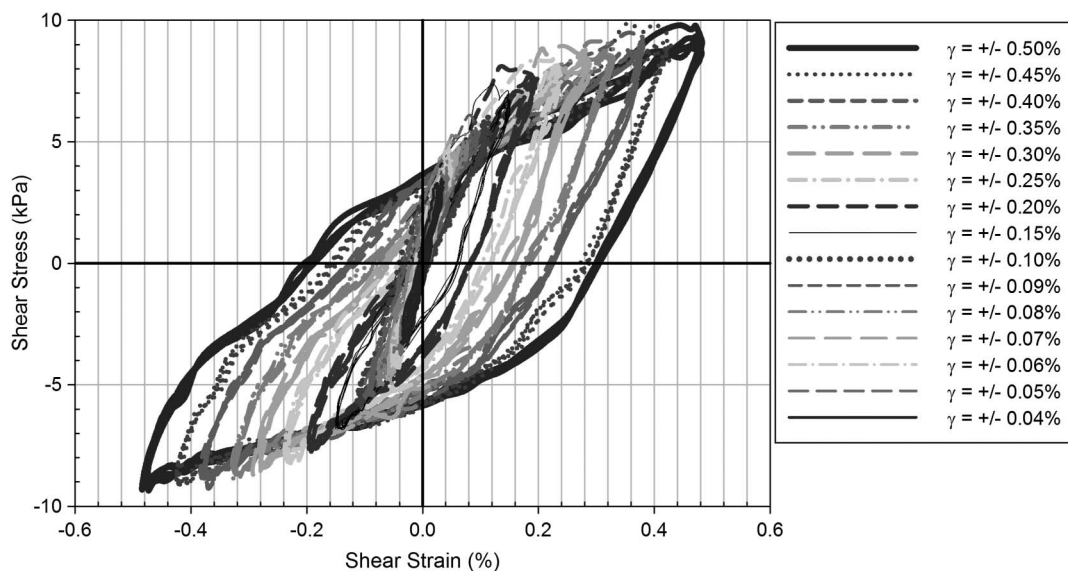


Fig. 3. Typical stress-strain hysteresis loops (a Class II–Batch 1 specimen with consolidation stress of 25 kPa)

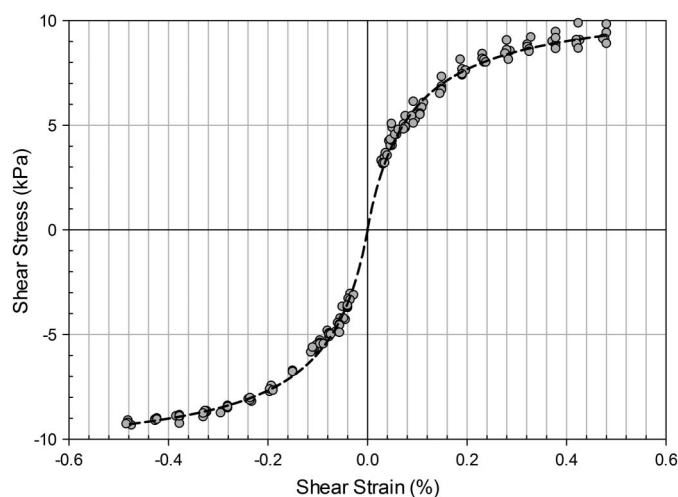


Fig. 4. Backbone curve for a Class II–Batch 1 specimen with consolidation stress of 25 kPa; data points represent the peaks and troughs of the stress-strain hysteresis loops presented in Fig. 3, whereas the line is the best fit hyperbolic function from Eq. (1) representing those data points

pressure is presented in Fig. 9. To compare the values of G_{\max} for LCC materials with those for other geomaterials, AASTHO (1996) suggested that G_{\max} range from 69 to 345 MPa for dense sands and gravels, from 27.6 to 138 MPa for silty sands, from 6.9 to 34.5 MPa for medium stiff clays, and from 27.5 to 137.5 MPa for soft clays. For all types of the LCC materials tested, the maximum shear modulus increased as the consolidation pressure increased. The increase in the maximum shear modulus with consolidation pressure was constant regardless of the unit weight of the material. The maximum shear modulus was highly dependent on the unit weight of the LCC materials and nearly independent of the consolidation stress, as presented in Fig. 10. The regression equations obtained from Figs. 9 and 10 are presented in Eqs. (4) and (5), respectively. The values of G_{\max} and σ'_v are in kPa, and γ is in kN/m^3

$$G_{\max} = 29.48\sigma'_v + 8,110.76 \quad (4)$$

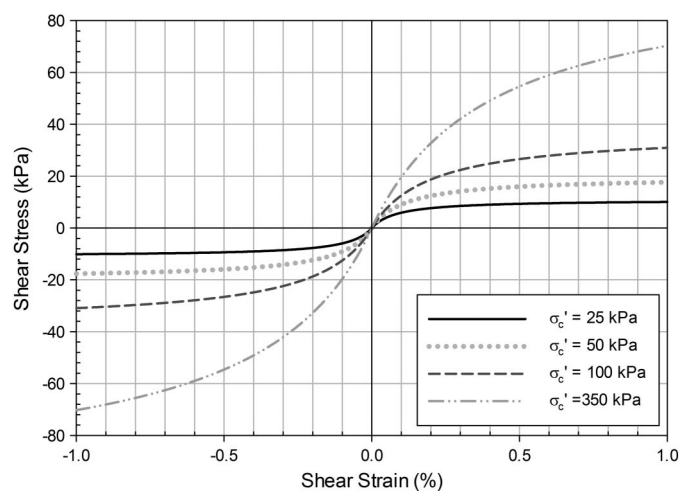


Fig. 5. Backbone curves for a Class II–Batch 1 specimens with different consolidation pressures

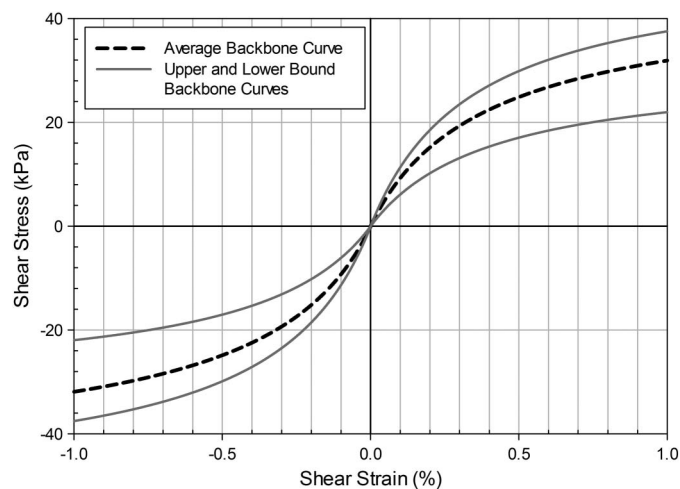


Fig. 6. Upper and lower ranges, and average backbone curves for all LCC specimens tested at a consolidation pressure of 50 kPa

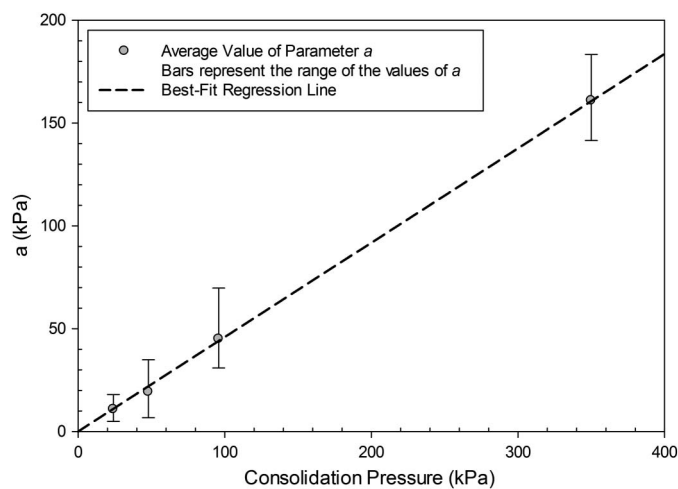


Fig. 7. Variation in parameter a of the hyperbolic function for backbone curves with consolidation pressure

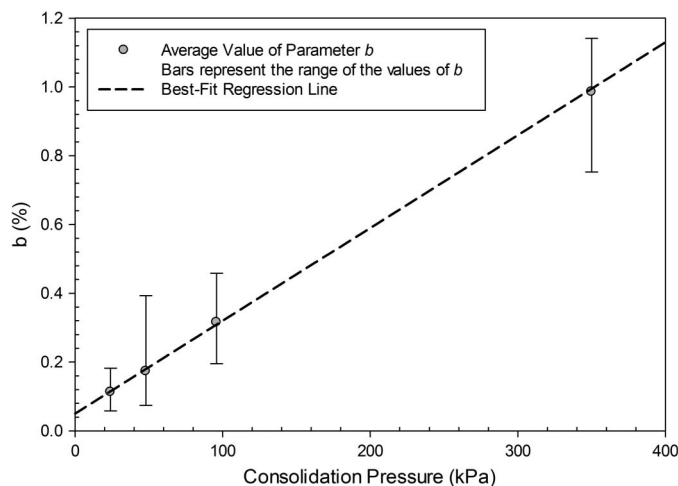


Fig. 8. Variation in parameter b of hyperbolic function for backbone curves with consolidation pressure

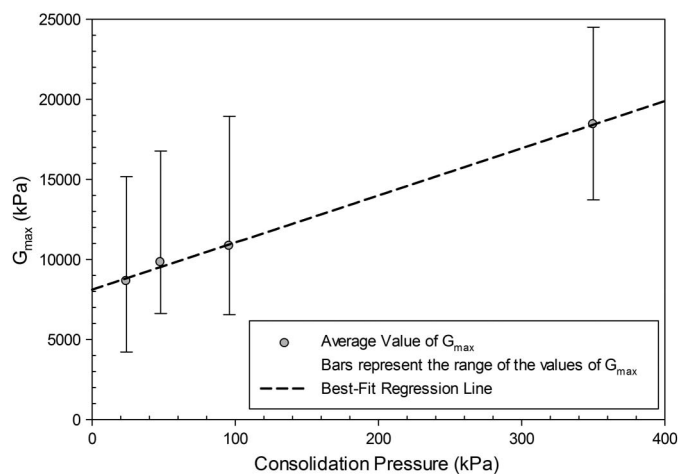


Fig. 9. Variation in the maximum shear modulus with the consolidation pressure

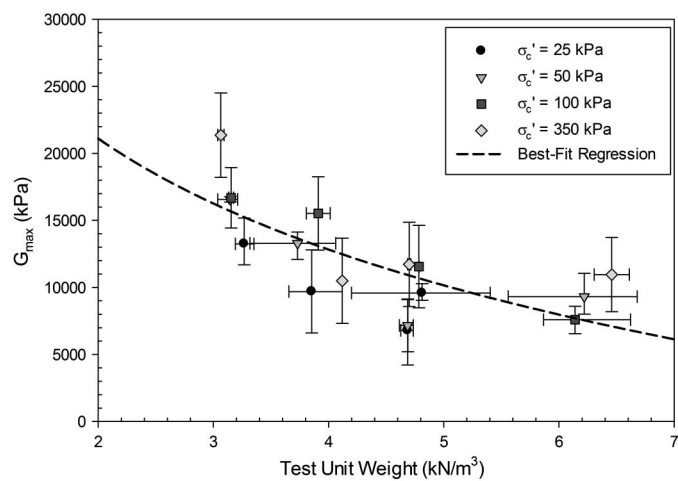


Fig. 10. Average reduction in maximum shear modulus for LCC materials having different unit weights tested at different consolidation pressures

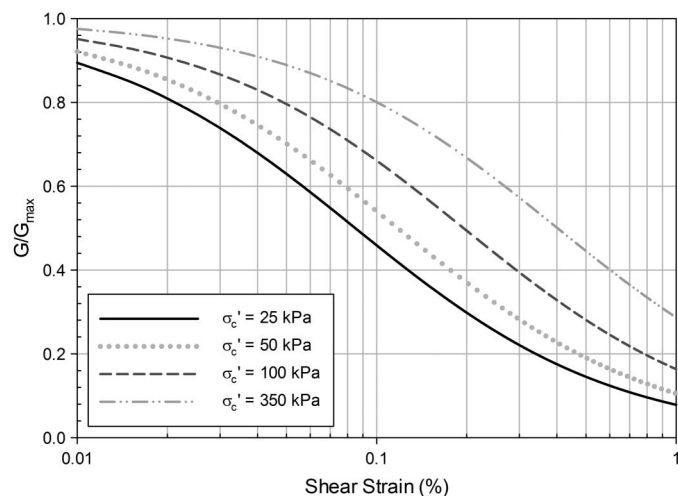


Fig. 11. Modulus degradation curves for Class II-Batch 1 samples at different consolidation pressures

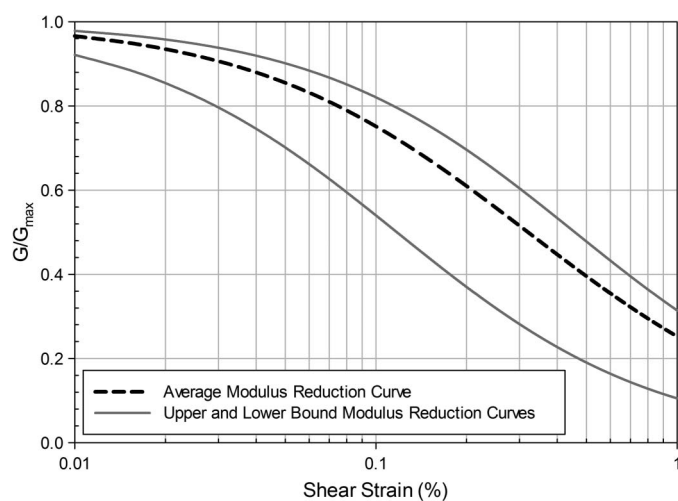


Fig. 12. Ranges and average modulus reduction curves for all light-weight cellular concrete specimens tested at a consolidation pressure of 100 kPa

$$G_{\max} = 11,955 \gamma + 29,400 \quad (5)$$

Modulus Reduction Curves

Fig. 11 contains a typical set of modulus reduction curves for LCC samples from Class II–Batch 1 at different consolidation pressures.

At a constant shear strain, the ratio of the shear modulus to the maximum shear modulus (G/G_{\max}) decreased as the consolidation pressure increased. Samples from different unit weights behaved in a manner similar to that shown in Fig. 11, although the results are not presented in this paper, but are available in Tiwari and Ajmera (2015). Similar to the behavior observed in the backbone curves,

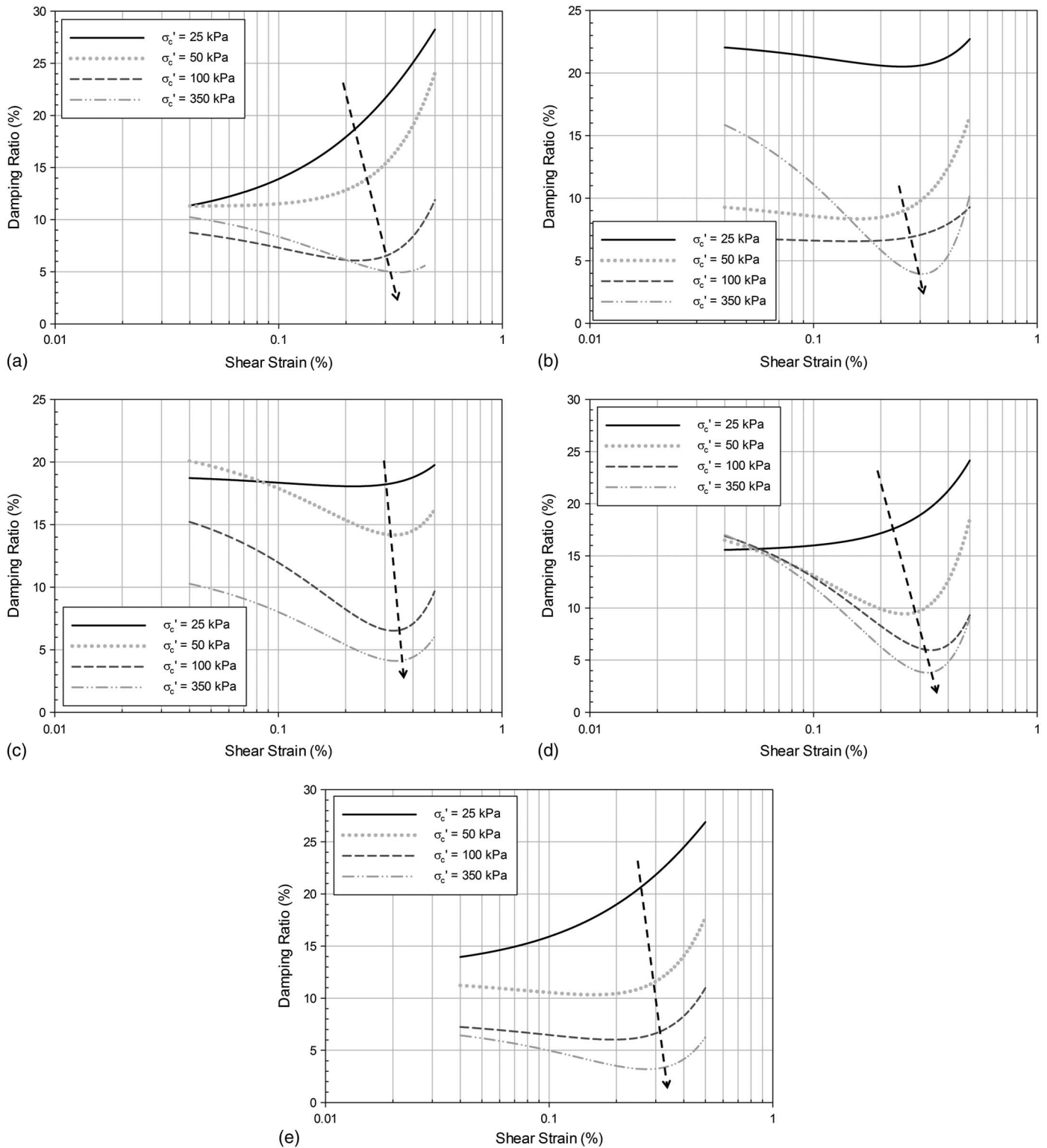


Fig. 13. Damping ratio versus shear strain for (a) Class II–Batch 1; (b) Class II–Batch 2; (c) Class IV; (d) 7.1 kN/m³ pour unit weight; (e) 8.6 kN/m³ pour unit weight LCC materials

close observation of the data showed that the unit weight of the LCC materials appeared to have little influence on the reduction in the shear modulus with respect to the shear strain experienced by the material. The ranges of modulus reduction curves for all the specimens tested at a consolidation pressure of 100 kPa and the curve for average values are presented in Fig. 12.

Damping Ratio

The results obtained from the CDSS test also were used to compute the damping ratios for the LCC specimens. Figs. 13(a–e) contains the variation in the damping ratio with shear strain separated on the basis of the consolidation pressure for each of the five sets of LCC specimens tested. Broken lines with arrows in Fig. 13 show the points of maximum curvature in each curve. The damping ratio was dependent on both the consolidation pressure and the shear strain. Fig. 13 shows that except for the samples consolidated at the effective stress of 25 kPa, there was a slight decrease in the damping ratio with an increase in the shear strain up to certain shear strains, generally between the shear strains of 0.25 and 0.35%, beyond which there was a significant increase in damping ratio with an increase in shear strain. The shear strain values corresponding to when the change in the mode of damping occurred was dependent on the consolidation pressure. Fig. 14 shows the variation of

damping ratio with shear strain for all types of LCC materials tested at the consolidation stress of 50, 100, and 350 kPa. Samples behaved in a similar manner at other consolidation pressures as well. Broken lines with arrows in Fig. 14 show the points of maximum curvatures. These locations exhibited the strain in which the mode of damping ratio-shear strain relationship changed. Fig. 14 shows that except for one sample, the damping ratios of all samples at shear strain of 0.5% were similar, despite the unit weight of the LCC material. The cause for the difference in behavior in the Class II–Batch 2 sample was not obvious. Moreover, Fig. 14 shows that the majority of the samples exhibited a similar range of shear strains in which the damping ratio changed the mode, i.e., from a slight reduction in damping ratio to a significant increase in damping ratio with shear strain.

Discussion on the Dynamic Properties of LCC Materials

Figs. 5 and 7 illustrate that although the unit weight had a small influence, the effective vertical stress had a substantially larger effect on the dynamic shear strength of the LCC materials. On the contrary, the unit weight of the LCC materials played a significant role in the small strain stiffness of the LCC materials when compared with the effective vertical stress (Figs. 9 and 10). Moreover,

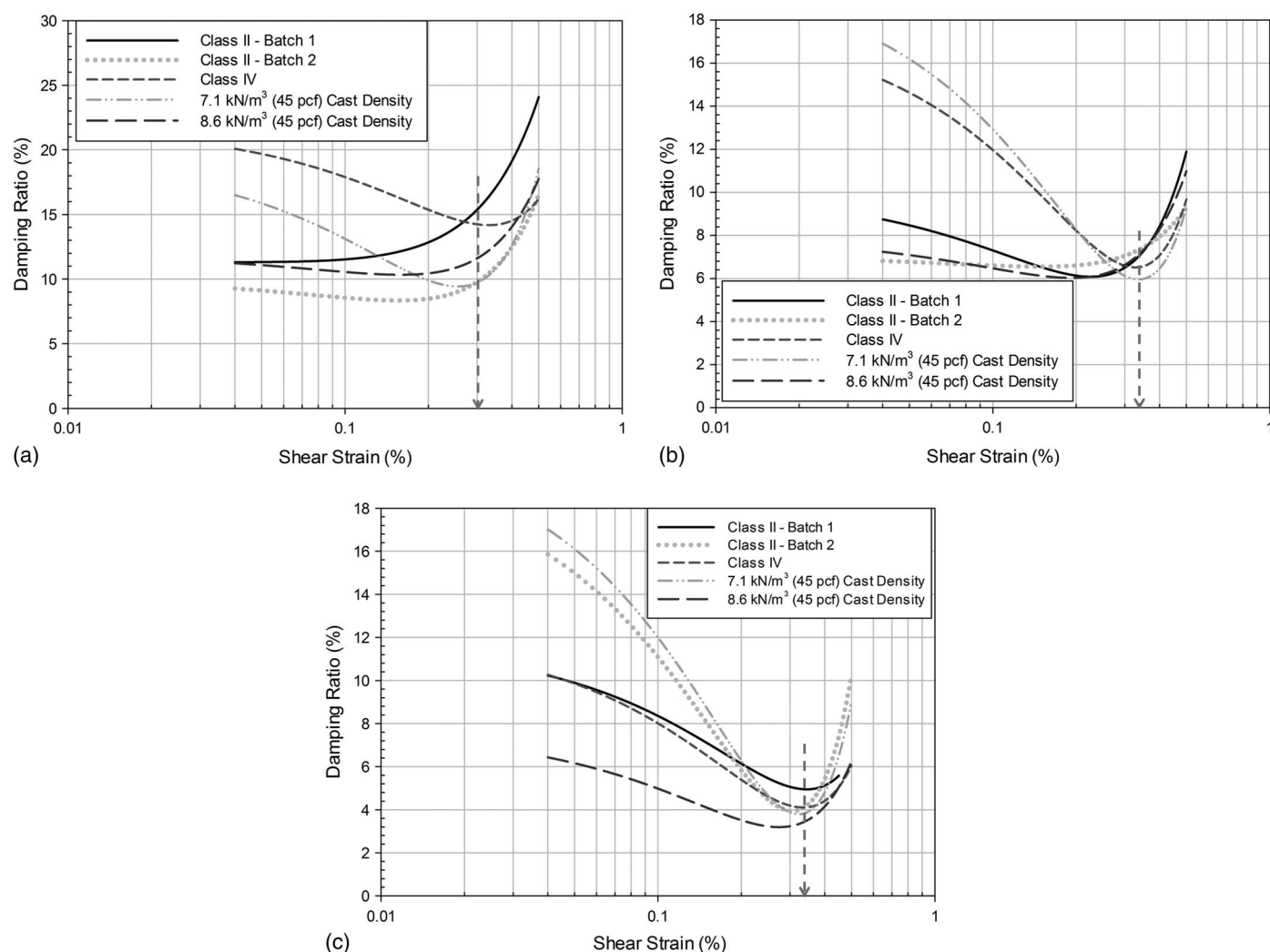


Fig. 14. Damping ratio versus shear strain for all types of LCC materials tested at consolidation pressure of (a) 50 kPa; (b) 100 kPa; (c) 350 kPa

significantly higher maximum shear moduli of LCC materials with lower unit weights in comparison with the higher unit weight materials implied that the low unit weight LCC materials were more advantageous in reducing the deformation during seismic events. Likewise, Figs. 11 and 12 show that the reduction in shear modulus with shear strain slightly decreased with an increase in effective vertical stress. This further supports the beneficial use of low unit weight LCC materials in various geotechnical applications, such as in the backfill of MSE walls.

As presented in Figs. 13 and 14, the damping ratio decreased with the shear strain up to certain values of shear strain, and then increased with shear strain. The shear strain at which such a transition occurred increases with the effective normal stress applied in the LCC materials, and ranged from 0.25 to 0.35% for the materials tested in this study. Trandafir and Erickson (2012) presented similar results for three different types of expanded polystyrene (EPS) materials. Although they discussed in the literature that the values of damping ratio decreased with an increase in axial strain, close observation of the data presented by Trandafir and Erickson (2012) shows that the damping ratio values increased with an increase in axial strain for axial strain values higher than 0.1–0.2%. The similarity in the unit weights of both of these materials can be attributed to the cause of the similarity in behavior between the EPS and LCC materials. The result obtained from this study for the LCC materials showed that for the shear strain that provided such transition for one specific effective normal stress, did not change significantly with the unit weight of the LCC material. Moreover, at the higher shear strains, the damping ratios remained similar for different unit weight LCC materials consolidated at the same effective vertical stress.

Summary and Conclusion

Lightweight cellular concrete materials have been used advantageously in civil engineering application for the past few decades. In this study, the dynamic properties of LCC materials with four different unit weights were measured using a fully automated CDSS device for the shear strains up to 0.5%. Specific attention was paid to evaluate the dynamic shear strength, stiffness, and damping of the materials at different effective vertical stresses, unit weights, and amplitudes of loading. The data analysis and results presented previously was helpful in arriving at the following conclusions:

1. The backbone curves representing the stress-strain relationship fit well with hyperbolic function presented in Eq. (1) for the strain range used in this study.
2. Shearing resistance with cyclic loading depended significantly on the effective normal stress applied. Larger shearing resistance was observed in the LCC materials consolidated and subjected to cyclic loading at higher normal stresses.
3. Although the dynamic shearing resistance increased slightly with unit weight, the effect of unit weight on the dynamic shearing resistance was very small compared with the influence of the effective normal stress on the dynamic shearing resistance.
4. The shape of the backbone curve depended significantly on effective normal stress. Using the relationships presented in Eqs. (2) and (3), the backbone curves can be developed for LCC materials at different effective normal stresses.
5. The maximum shear modulus increased with a decrease in unit weight of the LCC material and an increase in the effective normal stress. The values of maximum shear modulus can be estimated using Eqs. (4) and (5) for known unit weight and effective normal stress values.

6. Reduction in the shear modulus with the shear strain also was dependent on the effective normal stress.
7. Lightweight cellular concrete materials exhibited unique damping behavior with an increase in shear strain. Up to certain transitional shear strain, which in this study ranged from 0.25 to 0.35%, the damping ratio decreased with an increase in shear strain. Beyond this transitional shear strain, the damping ratio increased with shear strain. Such a transitional strain depended on the effective normal stress during dynamic loading and was found to increase with an increase in the effective normal stress.
8. The variation in the damping ratio with the shear strain was different for LCC materials with different unit weights at low values of shear strain. However, at shear strains of 0.5%, the damping ratios for all materials at any effective normal stress did not vary significantly with the unit weight of LCC materials.

Acknowledgments

Many individuals and organizations contributed to this project, and the authors would like to acknowledge their insight and assistance. In addition, several graduate students at California State University, Fullerton, including Miss Sneha Upadhyaya, Mr. Duc Tran, Mr. Janak Koirala, Mr. Prakash Khanal, and Miss Smriti Dhital, assisted in conducting the laboratory tests and in analyzing the data. Lab technician, Mr. Hector Zazueta, is thanked for his help in preparing and setting up the laboratory tests.

References

- AASHTO. (1996). *Standard specification for highway bridges*, Washington, DC.
- Albayrak, M., Yorukoglu, A., Karahan, S., Atlihan, S., Aruntas, H. Y., and Girgin, I. (2007). "Influence of zeolite additive on properties of autoclaved aerated concrete." *Build. Environ.*, 42(9), 3161–3165.
- Bjerrum, L., and Landva, A. (1966). "Direct simple shear tests on a Norwegian quick clay." *Géotechnique*, 16(1), 1–20.
- Dyvik, R., Berre, T., Lacasse, S., and Raadim, B. (1987). "Comparison of truly undrained and constant volume direct simple shear tests." *Géotechnique*, 37(1), 3–10.
- LaVallee, S. (1999). "Cellular concrete to the rescue." *The Aberdeen Group Publication No. C99A039*, Hanley-Wood, Inc., Washington, DC.
- Loudon, A. G. (1979). "The thermal properties of lightweight cellular concretes." *Int. J. Lightweight Concr.*, 1(2), 71–85.
- Maruyama, R. C., and Camarini, G. (2015). "Properties of cellular concrete for filters." *Int. J. Eng. Technol.*, 7(3), 223–228.
- Maw, R., and Cole, R. (2015). *Technical memorandum on laboratory testing of cellular concrete samples*, Gerhart Cole, Inc., Draper, UT.
- Narayanan, N., and Ramamurthy, K. (2000). "Structure and properties of aerated concrete: A review." *Cem. Concr. Compos.*, 22(5), 321–329.
- Neville, A. M. (2002). *Properties of concrete*, Pearson Education Limited, Harlow, U.K.
- Panesar, D. K. (2013). "Cellular concrete properties and the effect of synthetic and protein foaming agents." *Constr. Build. Mater.*, 44, 575–584.
- Pradel, D., and Tiwari, B. (2015). "The use of MSE walls backfilled with lightweight cellular concrete in soft ground seismic areas." *Proc., 3rd Int. Conf. on Deep Foundations*, Mexican Society for Geotechnical Engineering, Mexico.
- Teig, J., and Anderson, J. (2012). "Innovative design for colton flyover grade separation of IPRR and BNSF, Colton, CA." *AREMA Annual Conf. and Exposition*, American Railway Engineering and Maintenance-of-Way Association, Lanham, MD.
- The Aberdeen Group. (1963). *Cellular concrete*, Boston.
- Tian, Y. (2011). "Experimental study on aerated concrete produced by iron tailings." *Adv. Mater. Res.*, 250, 853–856.
- Tikalisky, P. J., Pospisil, J., and MacDonald, W. (2004). "A method for assessment of the freeze-thaw resistance of preformed foam cellular concrete." *Cem. Concr. Res.*, 34(5), 889–893.

- Tiwari, B., and Ajmera, B. (2015). "Geotechnical properties of lightweight cellular concrete." *Research Rep. in Civil and Environmental Engineering Department*, California State Univ., Fullerton, CA.
- Tiwari, B., Ajmera, B., Maw, R., Cole, R., Villegas, D., and Palmerson, P. (2017). "Mechanical properties of lightweight cellular concrete for geotechnical applications." *J. Mater. Civ. Eng.*, [10.1061/\(ASCE\)MT.1943-5533.0001885](#), 06017007.
- Trandafir, A. C., and Erickson, B. A. (2012). "Stiffness degradation and yielding of EPS geofoam under cyclic loading." *J. Mater. Civ. Eng.*, [10.1061/\(ASCE\)MT.1943-5533.0000362](#), 119–124.
- Zaidi, A. A. M., Rahman, A. I., and Zaidi, N. H. A. (2008). "Behavior of fiber reinforced foamed concrete: Indentation test analysis." *Proc., Seminar on Geotechnical Engineering*, Univ. Tun Hussein Onn Malaysia, Johore, Malaysia, 92–101.

APPENDIX E

SITE-SPECIFIC RESPONSE SPECTRA

This appendix presents the details of our estimation of the level of ground shaking at the Phase 1 Vertical Development sites during future earthquakes. Specifically, we developed site-specific response spectra for three representative subsurface profiles for 1) for Parcel A, 2) for Parcels B and G, and 3) for Parcel F. These profiles assume that the fill has been improved and will not liquefy in the event of a major earthquake.

We expect this site will experience strong ground shaking during a major earthquake on any of the nearby faults. To develop site-specific response spectra in accordance with 2016 San Francisco Building Code (SFBC) criteria, and by reference ASCE 7-10, we performed probabilistic seismic hazard analysis (PSHA) and deterministic seismic hazard analysis to develop smooth, site-specific horizontal rock spectra for two levels of shaking, namely:

- Risk-Targeted Maximum Considered Earthquake (MCE_R), which corresponds to the lesser of two percent probability of exceedance in 50 years (2,475-year return period) or 84th percentile of the controlling deterministic event both considering the maximum direction as described in ASCE 7-10
- Design Earthquake (DE) which corresponds to 2/3 of the MCE_R .

Because of the presence of soft clay, we performed ground response analysis to develop site-specific design response spectra for the project. Specifically, we performed the following:

- time domain spectral matching of five recorded time series to the MCE_R for use as input motions in ground response analyses
- ground response analyses to compute response spectra at the ground surface for the MCE_R and DE levels of shaking
- development of recommended spectra.

E1.0 PROBABILISTIC SEISMIC HAZARD ANALYSIS

Because the location, recurrence interval, and magnitude of future earthquakes are uncertain, we performed a PSHA, which systematically accounts for these uncertainties. The results of a PSHA define a uniform hazard for a site in terms of a probability that a particular level of shaking will be exceeded during the given life of the structure.

To perform a PSHA, information regarding the seismicity, location, and geometry of each source, along with empirical relationships that describe the rate of attenuation of strong ground motion with increasing distance from the source, are needed. The assumptions necessary to perform the PSHA are that:

- the geology and seismic tectonic history of the region are sufficiently known, such that the rate of occurrence of earthquakes can be modeled by historic or geologic data;
- the level of ground motion at a particular site can be expressed by an attenuation relationship that is primarily dependent upon earthquake magnitude and distance from the source of the earthquake; and
- the earthquake occurrence can be modeled as a Poisson process with a constant mean occurrence rate.

As part of the development of the site-specific spectra, we performed a PSHA to develop site-specific response spectra for 2 percent probability of exceedance in 50 years. The ground surface spectra were developed using the computer code EZFRISK 7.65 (Risk Engineering 2015). The approach used in EZFRISK is based on the probabilistic seismic hazard model developed by Cornell (1968) and McGuire (1976). Our analysis modeled the faults in the Bay Area as linear sources, and earthquake activities were assigned to the faults based on historical and geologic data. The levels of shaking were estimated using Next Generation Attenuation for the Western United States, NGA-West 2, relationships that are primarily dependent upon the magnitude of the earthquake, the distance from the site to the fault, and the shear wave velocity in the top 30 meters of the profile.

E1.1 Probabilistic Model

In probabilistic models, the occurrence of earthquake epicenters on a given fault is assumed to be uniformly distributed along the fault. This model considers ground motions arising from the portion of the fault rupture closest to the site rather than from the epicenter. Fault rupture lengths were modeled using fault rupture length-magnitude relationships given by Wells and Coppersmith (1994).

The probability of exceedance, $P_e(Z)$, at a given ground-motion, Z , at the site within a specified time period, T , is given as:

$$P_e(Z) = 1 - e^{-V(z)T}$$

where $V(z)$ is the mean annual rate of exceedance of ground motion level Z . $V(z)$ can be calculated using the total-probability theorem.

$$V(z) = \sum_i v_i \iint P[Z > z | m, r] f_{M_i}(m) f_{R|M_i}(r; m) dr dm$$

where:

v_i = the annual rate of earthquakes with magnitudes greater than a threshold M_{oi} in source i

$P[Z > z | m, r]$ = probability that an earthquake of magnitude m at distance r produces ground motion amplitude Z higher than z

$f_{M_i}(m)$ and $f_{R|M_i}(r; m)$ = probability density functions for magnitude and distance

Z represents peak ground acceleration, or spectral acceleration values for a given frequency of vibration. The peak accelerations are assumed to be log-normally distributed about the mean with a standard error that is dependent upon the magnitude and attenuation relationship used.

E1.2 Source Modeling and Characterization

The segmentation of faults, mean characteristic magnitudes, and recurrence rates were modeled using the data presented in the WGCEP (2008) and Cao et al. (2003) reports. We also included the combination of fault segments and their associated magnitudes and recurrence rates as described in the WGCEP (2008) in our seismic hazard model. Table E-1 presents the distance and direction from the site to the fault, mean characteristic magnitude, mean slip rate, and fault length for individual fault segments. We used the California fault database identified as "USGS08" in EZFRISK 7.65. We understand EZFRISK obtained this database directly from USGS and models the faults with multiple segments. Each segment is characterized with multiple magnitudes, occurrence or slip rates and weights. This approach takes into account the epistemic uncertainty associated with the various seismic sources in our model.

TABLE E-1
Source Zone Parameters

Fault Segment	Approx. Distance from fault (km)	Direction from Site	Mean Characteristic Moment Magnitude	Mean Slip Rate (mm/yr)	Approx. Fault Length (km)
N. San Andreas; SAN+SAP	13	West	7.73	22	274
N. San Andreas; SAN+SAP+SAS	13	West	7.87	21	336
N. San Andreas; SAO+SAN+SAP	13	West	7.95	22	410
N. San Andreas; SAO+SAN+SAP+SAS	13	West	8.05	22	472
N. San Andreas; SAP	13	West	7.23	17	85
N. San Andreas; SAP+SAS	13	West	7.48	17	147
Hayward-Rodgers Creek; HN	16	East	6.60	9	35
Hayward-Rodgers Creek; HN+HS	16	East	7.00	9	87
Hayward-Rodgers Creek; RC+HN	16	East	7.19	9	97
Hayward-Rodgers Creek; RC+HN+HS	16	East	7.33	9	150
N. San Andreas; SAN	16	West	7.51	24	189
N. San Andreas; SAO+SAN	16	West	8.00	24	326
Hayward-Rodgers Creek; HS	17	East	6.78	9	52
San Gregorio Connected	19	West	7.50	5.5	176
Mount Diablo Thrust	33	East	6.70	2	25
Calaveras; CN	34	East	6.87	6	45
Calaveras; CN+CC	34	East	7.00	11	104
Calaveras; CN+CC+CS	34	East	7.03	12	123
Hayward-Rodgers Creek; RC	35	North	7.07	9	62
Green Valley Connected	38	East	6.80	4.7	56
Monte Vista-Shannon	40	Southeast	6.50	0.4	45
Point Reyes	43	West	6.90	0.3	47
West Napa	45	Northeast	6.70	1	30
Greenville Connected	50	East	7.00	2	50
Great Valley 5, Pittsburg Kirby Hills	55	East	6.70	1	32
Calaveras; CC	63	Southeast	6.39	15	59
Calaveras; CC+CS	63	Southeast	6.50	15	78
Great Valley 4b, Gordon Valley	69	Northeast	6.80	1.3	28
N. San Andreas; SAS	75	Southeast	7.12	17	62
Great Valley 7	76	East	6.90	1.5	45
Hunting Creek-Berryessa	77	North	7.10	6	60
Zayante-Vergeles	85	Southeast	7.00	0.1	58
Great Valley 4a, Trout Creek	91	Northeast	6.60	1.3	19
Maacama-Garberville	93	North	7.40	9	221
Monterey Bay-Tularcitos	98	South	7.30	0.5	83

E1.3 Attenuation Relationships

To develop site-specific rock spectra, we assigned an average shear wave velocity of the upper 30 meters (100 ft), V_{s30} , of the rock surface of approximately 760 meters per second (mps), corresponding to 2,500 feet per second (fps).

Pacific Earthquake Engineering Research Center (PEER) embarked on the NGA-West 2 project to update the previously developed ground motion prediction equations (attenuation relationships), which were mostly published in 2008. We used the relationships by Abrahamson et al. (2014), Boore et al. (2014), Campbell and Bozorgnia (2014) and Chiou and Youngs (2014). These attenuation relationships include the average shear wave velocity in the upper 100 feet. Furthermore, these relationships were developed using the subset of the same earthquake databases at the discretion of the different developer teams, therefore, the average of the relationships was used to develop the recommended spectra

The NGA-West 2 relationships were developed for the orientation-independent geometric mean of the data. Geometric mean is defined as the square root of the product of the two recorded components.

E2.0 PSHA RESULTS

Figure E-1 presents results of the PSHA for rock for 2 percent probability of exceedance in 50 years (2,475 return period) using the four relationships discussed above. The average of these relationships is also presented on Figure E-1.

ASCE 7-10 specifies the development of MCE_R site-specific response spectra in the maximum direction. Shahi and Baker (2013) provide scaling factors that modify the geometric mean spectra to provide spectral values for the maximum response (maximum direction). We used the scaling factors presented on Figure 3.1 of Shahi and Baker (2013) ratios $Sa_{RotD100}/Sa_{GMRot150}$ to modify the average of the PSHA results. The maximum direction spectrum is also shown on Figure E-1.

Figure E-2 presents the deaggregation plots of the PSHA results for the 2 percent probability of exceedance in 50 years hazard level. From the examination of these results, it can be seen that the San Andreas fault dominates the hazard at the project site at different periods of interest.

E3.0 DETERMINISTIC ANALYSIS

We performed a deterministic analysis to develop the MCE_R spectrum at the site. In a deterministic analysis, a given magnitude earthquake occurring at a certain distance from the source is considered as input into an appropriate ground motion attenuation relationship. The

MCE_R was defined as an event having a Moment Magnitude of 8.0, consistent with the mean magnitude assigned by WGCEP (2008) for a repeat of the 1906 earthquake on the San Andreas fault at a distance of about 13 kilometers from the site.

The same attenuation relationships as discussed in Section E1.3 were used in our deterministic analysis. Figure E-3 presents the 84th percentile deterministic results and the average of the four relationships for the rock. The average results are presented for geometric mean; similar to Section E2.0, we developed the deterministic spectrum in the maximum direction using the Shahi and Baker (2013) factors.

E4.0 RECOMMENDED ROCK SPECTRA

The MCE_R is defined in ASCE 7-10 as the lesser of the maximum direction PSHA spectrum having a two percent probability of exceedance in 50 years (2,475-year return period) or the maximum direction 84th percentile deterministic spectrum of the governing earthquake scenario and the DE spectrum is defined as 2/3 times the MCE_R spectrum. Additionally, the MCE_R spectrum is defined as a risk-targeted response spectrum, which corresponds to a targeted collapse probability of one percent in 50 years. According to USGS website, the risk coefficients for the PSHA spectra for short and long periods are, 1.074 and 1.018, respectively. We used these risk coefficients to develop the risk-targeted PSHA response spectra.

Furthermore, we followed the procedures outlined in Chapter 21 of ASCE 7-10 to develop the site-specific spectra for MCE_R and DE. Chapter 21 of ASCE 7-10 requires the following checks:

- the deterministic spectrum used to develop the MCE_R shall not fall below the Deterministic Lower Limit spectrum as shown on Figure 21.2-1 of ASCE 7-10;
- the DE spectrum shall not fall below 80 percent of general design spectrum (Section 21.3 of Chapter 21 ASCE 7-10).

Figure E-4 and Table E-2 present a comparison of the site-specific spectra for the PSHA 2,475 year return period (max. direction), the 84th percentile deterministic (max. direction), and the Deterministic Lower Limit spectra for Site Class B per ASCE 7-10 (SFBC 2016). We included the risk coefficients as discussed above for the PSHA spectrum. The deterministic 84th percentile

spectrum is less than the Deterministic Lower Limit spectrum for periods between 0.08 and 1 second; hence for periods between 0.08 and 1 second, the MCE_R is defined as the lower of the Deterministic Lower Limit and the PSHA spectrum for 2,475-year return period. For a period of 0.01 second and periods greater than or equal to 1.5 seconds the deterministic 84th percentile spectrum is greater than the Deterministic Lower Limit spectrum and the MCE_R spectrum is defined as the lower of the 84th percentile and the PSHA spectrum for 2,475-year return period. The recommended MCE_R spectrum is also presented on Figure E-4 and in Table E-2.

TABLE E-2
Comparison of Site-specific and Code Spectra for Development of MCE_R Rock Spectrum
per ASCE 7-10
 S_a (g) for 5 percent damping

Period (seconds)	Risk Targeted PSHA – 2,475-Year Return Period – Maximum Direction	Deterministic 84th percentile – Maximum Direction	ASCE 7-10 (SFBC 2016) Deterministic Lower Limit Site Class B	Recommended Rock MCE_R
0.01	0.937	0.643	0.604	0.643
0.08	1.876	1.212	1.500	1.500
0.10	2.092	1.332	1.500	1.500
0.20	2.273	1.492	1.500	1.500
0.30	1.885	1.288	1.500	1.500
0.40	1.632	1.133	1.500	1.500
0.50	1.449	1.002	1.200	1.200
0.60	1.273	0.879	1.000	1.000
0.75	1.080	0.748	0.800	0.800
1.00	0.796	0.590	0.600	0.600
1.50	0.528	0.407	0.400	0.407
2.00	0.394	0.313	0.300	0.313
3.00	0.263	0.222	0.200	0.222
4.00	0.201	0.178	0.150	0.178
5.00	0.161	0.147	0.120	0.147
6.00	0.130	0.121	0.100	0.121

Table E-3 presents the recommended DE spectrum for development of following the procedures outlined in Chapter 21 of ASCE 7-10. The DE is defined as 2/3 of the MCE_R per ASCE 7-10; however, the recommended DE may not be below 80 percent of the general spectrum at any period (ASCE 7-10 Section 21.3). Figure E-4 and Table E-3 presents a comparison of 2/3 of the MCE_R spectrum and 80 percent of the general spectrum for Site Class B. As shown in Table E-3 and Figure E-5, 80 percent of the general spectrum is lower than 2/3 of the MCE_R spectrum.

Therefore, we recommend that 2/3 of the MCE_R spectrum be used to develop the DE spectrum. The recommended DE spectrum is also shown on Figure E-4.

TABLE E-3
Comparison of Site-specific and Code Spectra for Development of DE Rock Spectrum
per ASCE 7-10
 S_a (g) for 5 percent damping

Period (seconds)	Recommended Rock MCE_R	2/3 times MCE_R	80% of General Design Spectrum	Recommended Rock DE
0.01	0.643	0.429	0.320	0.429
0.08	1.500	1.000	0.800	1.000
0.10	1.500	1.000	0.800	1.000
0.20	1.500	1.000	0.800	1.000
0.30	1.500	1.000	0.800	1.000
0.40	1.500	1.000	0.800	1.000
0.50	1.200	0.800	0.640	0.800
0.60	1.000	0.667	0.533	0.667
0.75	0.800	0.533	0.427	0.533
1.00	0.600	0.400	0.320	0.400
1.50	0.407	0.271	0.213	0.271
2.00	0.313	0.209	0.160	0.209
3.00	0.222	0.148	0.107	0.148
4.00	0.178	0.119	0.080	0.119
5.00	0.147	0.098	0.064	0.098
6.00	0.121	0.080	0.053	0.080

The recommended rock spectra and the 2016 SFBC spectra are shown on Figure E-5.

E5.0 MATCHED ROCK TIME SERIES

To develop time series that are compatible with the recommended MCE_R rock spectrum, we performed time domain spectral matching using the matching routine in the computer program EZFRISK (7.65). The selection of a recorded time series is an important step in developing the ground motion. The intent in this selection process is to choose time series that have a similar magnitude, distance and fault mechanism as that of the controlling target spectrum. The records were obtained from the NGA-West 2 PEER data base website. Table E-4 presents the five selected time series used in spectral matching for this evaluation.

TABLE E-4
Earthquake Time Series Used
for Matching to the Recommended MCE_R Rock Spectrum

No.	Earthquake and Year	NGA-West 2 Sequence RSN No.	Rupture Mechanism	Magnitude	Time History	Preferred Vs30* (mps), Site Classification	Epicentral Distance* (km)	Closest Distance to Rupture* (km)	Component	PGA (g)	PGV (cm/sec)	PGD (cm)
1	Loma Prieta, 1989	741	Reverse, oblique	6.9	Bran	376, C	9	11	0 deg	0.481	55.7	11.7
2	Kocaeli, 1999	1161	Strike-slip	7.5	Gebze	792, B	47	11	0 deg	0.244	50.3	42.8
3	Imperial Valley, 1940	6	Strike-slip	7.0	El Centro	213, D	13	6	270 deg	0.215	29.7	22.1
4	Chi-Chi, 1999	1529	Reverse, oblique	7.6	TCU 102	714, C	46	<2	E	0.298	112.5	89.2
5	Chi-Chi, 1999	1549	Reverse, oblique	7.6	TCU 129	664, C	14	<2	E	1.010	34.7	50.1

* From NGA-West 2 West

Figures E-6 through E-10 present the acceleration, velocity, and displacement of the matched time series and comparison between the initial, target and the matched spectra for the MCE_R ground motion level. Because the DE rock spectrum is $2/3$ times MCE_R , we used a scalar of $2/3$ on the matched MCE_R time series to perform the analyses for the DE level of shaking.

E6.0 DESIGN RESPONSE SPECTRA

To provide site-specific response spectra, the ground motion should be modified to take into account the soil conditions at the site. Three idealized soil profiles designated as "Parcel A", "Parcels B and G", and "Parcel F" were developed based on data from our investigations at and adjacent to the site.

The soil column for Parcel A consists of 13 feet of improved fill underlain by 55 feet of soft to medium stiff Bay Mud clay. It is in turn underlain by 20 feet of dense to very dense sand of the Colma Formation. The Colma Formation is underlain by 74 feet of stiff to very stiff Old Bay Clay. Beneath the Old Bay Clay is 68 feet of dense to very dense sands and gravels and very stiff to hard clays over bedrock, which is 220 feet below the ground surface.

The soil column for Parcels B and G consists of 20 feet of improved fill underlain by 42 feet of soft to medium stiff Bay Mud clay. It is in turn underlain by 21 feet of dense to very dense sand of the Colma Formation. The Colma Formation is underlain by 72 feet of stiff to very stiff Old Bay Clay. Beneath the Old Bay Clay is 83 feet of dense to very dense sands and gravels and very stiff to hard clays over bedrock, which is 238 feet below the ground surface.

The soil column for Parcel F consists of 20 feet of improved fill underlain by 50 feet of soft to medium stiff Bay Mud clay. It is in turn underlain by 24 feet of dense to very dense sand of the Colma Formation. The Colma Formation is underlain by 73 feet of stiff to very stiff Old Bay Clay. Beneath the Old Bay Clay is 86 feet of dense to very dense sands and gravels and very stiff to hard clays over bedrock, which is 253 feet below the ground surface. Table E-5 presents a summary of inputs for the DEEPSOIL model.

TABLE E-5
DEEPSOIL Inputs

Profile	Strain Reduction Modulus / Percent Damping Curves Used	Inputs			
		Unit Weight (pcf)	Discretized Layer Thickness (ft)	Shear Wave Velocity (ft/sec)	PI
Fill	Seed and Idriss (1971), Sand(Mean)	130	1 to 2	Based on Shear Wave Velocity Profiles	N/A
Bay Mud	Vucetic and Dobry (1991), Clay	100	1 to 2		40
Colma	Seed and Idriss Sand 1971 (Upper Limit)	130	1 to 2		N/A
Old Bay Clay	Vucetic and Dobry (1991) Clay	110	1 to 2		40
Alluvium / Colluvium	Seed and Idriss (1971), Sand (Upper Limit)	135	1 to 2		N/A

The site-specific effects of the overburden soil were evaluated using the ground response program DEEPSOIL (Hashash et al. 2016). DEEPSOIL is a one-dimensional, site response analysis based on vertically propagating, horizontal shear waves. The program mathematically transmits input motions vertically through an idealized soil column to the ground surface. To account for the non-linear characteristics of soil, this program uses equivalent-linear and non-linear procedures with strain compatible shear moduli and damping ratios. The rock time series described above were used as input motion for the ground response analyses.

The fill at the site may liquefy during a major earthquake. We understand the team has decided to improve the fill to mitigate the potential for liquefaction. Therefore, our analysis assumed the fill will be improved and mitigated against liquefaction.

The MCE_R results of the DEEPSOIL analyses for Parcel A, Parcels B and G, and Parcel F are shown on Figures E-11, E-13, and E-15, respectively. The recommended MCE_R is presented in Table E-6 and Figures E-12, E-14, and E-16 for Parcel A, Parcels B and G, and Parcel F, respectively. The recommended MCE_R spectra were developed such that they do not fall below 80 percent of the mapped code MCE_R spectrum per 2016 SFBC for site class E.

TABLE E-6

**Recommended MCE_R Surface Spectra
Spectral Acceleration (g's) for Damping Ratio 5%**

Period (seconds)	PARCEL A	PARCELS B & G	PARCEL F
0.01	0.462	0.462	0.462
0.10	0.736	0.736	0.736
0.20	1.040	1.040	1.040
0.21	1.080	1.080	1.080
0.30	1.080	1.080	1.080
0.40	1.080	1.080	1.080
0.50	1.080	1.080	1.080
0.75	1.200	1.080	1.080
1.00	1.220	1.080	1.080
1.07	1.200	1.080	1.080
1.25	1.100	0.980	0.980
1.50	1.000	0.900	0.897
2.00	0.889	0.840	0.830
3.00	0.423	0.449	0.495
4.00	0.288	0.288	0.293
5.00	0.230	0.230	0.230
6.00	0.192	0.192	0.192

The DE results of the DEEPSOIL analyses for Parcel A, Parcels B and G, and Parcel F are shown on Figures E-17, E-19 and E-21, respectively. The recommended DE is presented in Table E-7 and Figures E-18, E-20, and E-22 for Parcel A, Parcels B and G, and Parcel F, respectively. The recommended DE spectra were developed such that they do not fall below 80 percent of the mapped code DE spectrum per 2016 SFBC for site class E.

TABLE E-7

**Recommended DE Surface Spectra
Spectral Acceleration (g's) for Damping Ratio 5%**

Period (seconds)	PARCEL A	PARCELS B & G	PARCEL F
0.01	0.385	0.385	0.385
0.10	0.491	0.491	0.491
0.20	0.693	0.693	0.693
0.21	0.720	0.720	0.720
0.30	0.850	0.720	0.720
0.40	0.928	0.720	0.731
0.50	0.990	0.810	0.793
0.75	1.052	0.938	0.901
1.00	0.940	0.866	0.873
1.07	0.918	0.840	0.850
1.25	0.890	0.790	0.790
1.50	0.840	0.750	0.740
2.00	0.577	0.593	0.604
3.00	0.256	0.260	0.280
4.00	0.192	0.192	0.192
5.00	0.154	0.154	0.154
6.00	0.128	0.128	0.128

Because site-specific procedure was used to determine the recommended response spectra, the corresponding values of S_{MS} , S_{M1} , S_{DS} and S_{D1} per Section 21.4 of ASCE 7-10 should be used as shown in Table E-8.

TABLE E-8
Design Spectral Acceleration Values

Parameter	PARCEL A	PARCELS B & G	PARCEL F
S_{MS}	1.098	1.040	1.040
S_{M1}	1.778	1.680	1.660
S_{DS}	0.947	0.844	0.811
S_{D1}	1.154	1.186	1.208

* S_{MS} and S_{DS} are the spectral accelerations at 0.2 seconds, but they cannot be less than 90% of the peak spectral value.

** S_{M1} and S_{D1} are based on the site-specific response spectra and are governed by the spectral acceleration at a period of two seconds.

EXHIBIT B
Resilient Modulus Definition

Resilient Modulus

The Resilient Modulus (M_R) is a measure of subgrade material stiffness. **A material's resilient modulus is actually an estimate of its modulus of elasticity (E).** While the modulus of elasticity is stress divided by strain for a slowly applied load, resilient modulus is stress divided by strain for rapidly applied loads – like those experienced by pavements.

Resilient modulus is determined using the [triaxial test](#). The test applies a repeated axial cyclic stress of fixed magnitude, load duration and cycle duration to a cylindrical test specimen. While the specimen is subjected to this dynamic cyclic stress, it is also subjected to a static confining stress provided by a triaxial pressure chamber. It is essentially a cyclic version of a triaxial compression test; the cyclic load application is thought to more accurately simulate actual traffic loading.

<https://www.pavementinteractive.org/reference-desk/design/design-parameters/resilient-modulus/>

EXHIBIT C
LCC Modulus

Min Modulus for LCC with similar densities as the LCC for Mission Rock project. 655 MPa = 95ksi

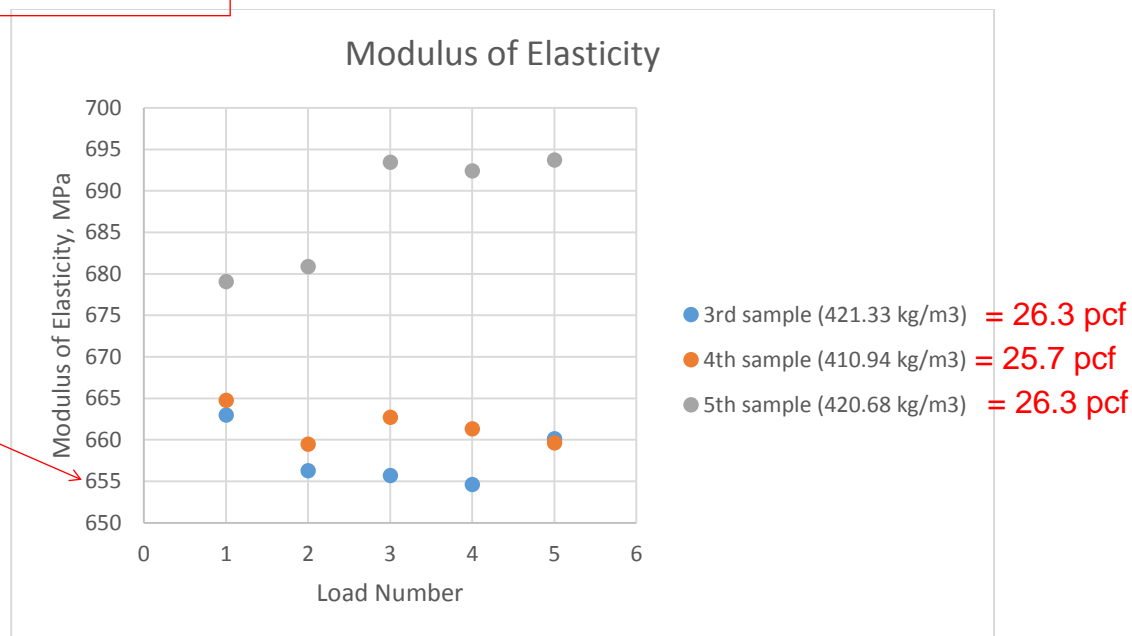


Figure 5-9: Modulus of Elasticity Test Results for 28 Days Samples

The average modulus of elasticity was determined as 657, 661 and 687 MPa for the 3rd, 4th, and 5th samples respectively. The result for modulus of elasticity for the 5th sample was obtained to be the highest, corresponding to the 420.68 kg/m³ density, whereas for the 3rd sample modulus of elasticity was determined as the lowest with the sample density at 421.33 kg/m³ (Figure 5-9). During the testing of the 5th sample, it was found that the reading increased from 680 to 693 MPa after the second cycle. This may be explained due to the fact that the test frame had some noise during testing and several adjustments were made to the longitudinal extensometer. According to Table 5-1, the lower limit for modulus of elasticity of the 400 kg/m³ density is approximately 800 MPa, whereas laboratory results observed it to be in the range of 657 to 687 MPa.

The Poisson's ratio was observed in the range of 0.24 to 0.30 (Appendix III), which is consistent to the past literature (BCA, 1994).

5.4.3 Relationship between Properties

Correlation between compressive strength and density is shown in Figure 5-10. The trend for 7 days samples was not typical because the lower density was observed, the higher compressive strength was, though 7 days samples had a good R^2 value of 0.96. For the 14 and 21 days samples with hardened state density of 404 to 414 kg/m³ the range of the compressive strength was relatively different, laying in the range of 1.2 to 1.69 MPa. For the 28 days samples, despite the expectations, compressive strength was observed to be at approximately same level as for other days samples (1.52 to 1.55MPa).

EXHIBIT D
Rigid Pavement Design
Calculation

Goal: Estimate the equivalent 18 kips axle loads (ESAL's) for the Mission Rock street section consisting of 4 inches of asphalt concrete (AC), over 8 inches of portland cement concrete (PCC), over 4 inches of aggregate base (AB), and supported on lightweight cellular concrete (LCC) that has a modulus degraded by 30 percent to evaluate areas that may have cracked during a major seismic event.

Assumed Pavement Section

4" AC (ignored)
8" PCC (f'c = 4,500 psi)
4" AB (ignored)
LCC (Mr = 66.5 ksi, 30% max Mr)

CALCULATION PER MGPEC PAVEMENT DESIGN STANDARDS - 2019

Parameters			
ZR (%)	0.9	Log(W18)	= 7.05
So	0.34	W18 - (ESALs)	= 11,273,391.52
D (in)	8		
delta PSI	0.8		
Po	4.5		
k (pci)	1000		
S'c (psi)	629		
Ec (psi)	3400000		
Jt	3.6		
Cd	1		
Pt	3.7		

Equation 5.2B-1 Rigid Pavement Design Equation
from AASHTO Guide for Design of Pavement Structures (1993)

$$\log_{10} W_{18} = Z_R \times S_0 + 7.35 \times \log_{10}(D + 1) - 0.06 + \frac{\log_{10} \left[\frac{\Delta PSI}{4.5 - 1.5} \right]}{1 + \frac{1.624 \times 10^7}{(D + 1)^{8.46}}}$$
$$+ (4.22 - 0.32 \times p_t) \times \log_{10} \left[\frac{S'_c \times c_d [D^{0.75} - 1.132]}{215.63 \times Jt \left[D^{0.75} - \frac{18.42}{\left(\frac{E_c}{k} \right)^{0.25}} \right]} \right]$$

Where:

W18 = 18-kip equivalent single axle loads (ESALs) over design life

ZR = Standard normal deviate (function of the design reliability level)

S0 = Overall standard deviation (function of overall design uncertainty)

ΔPSI = Serviceability loss at end of design life (p0- p1)

P0 = Initial serviceability; P1 = Terminal serviceability

k = Modulus of subgrade reaction (pci)

S'c = PCC modulus of rupture (psi)

Ec = PCC modulus of elasticity (psi)

Jt = Joint load transfer coefficient

Cd = Drainage coefficient

D = PCC slab thickness (inches)

Table 5.2B-2
Rigid Pavement Design Inputs

Parameter	Input Values
Design Life, Years	20 is normal. Other as Agency requires.
18k ESAL, ESAL20 or other	See Section 4.1
Reliability Level (%), Refer to 1993 AASHTO for needed Zr value	<ul style="list-style-type: none">90% - Arterial, all Collector, Industrial Streets:85% - Residential Street
Overall Standard Deviation, So	0.34
Initial Serviceability, Po	4.5
Terminal Serviceability, P1	<ul style="list-style-type: none">2.5 - Arterial, all Collector, Industrial Streets2.0 - Residential Streets
Modulus of Subgrade Reaction, k	Use ACPA "k-value" Calculator: http://www.apps.acpa.org/apps/kValue.aspx Moisture Treated Subgrade without any Intermediate Stiff Layers (ISL) shall be k =60, for R-value of 1, or justify higher value.
Composite Modulus of Subgrade Reaction (k-value) using Intermediate Stiff Layer*. All materials to meet Section 4.2D requirements.	See below for Intermediate Stiff Layers use*: <ul style="list-style-type: none">Unbound Granular Base (UGB): Mr = 20,000 psi.Chemically Treated Subgrade (CTS): use ACPA default minimum Mr = 20,000 or by test.Mechanically Stabilized Base (MSB): Mr = 37,000 psi.
Modulus of Rupture, S'c	650 psi
Modulus of Elasticity, Ec	3,400,000 psi
Load Transfer Coefficient, Jt	See Table 5.2C-3: <i>Dowels are recommended for all Arterial, Industrial & Collector roads.</i>
Drainage Coefficient, Cd	1.0 _ Assumes subgrade has been considered as outlined in Section 4.2 and a drainage layer is provided)

Note: * Intermediate Stiff Layer (ISL) is required for all pavement designs where there is subgrade mitigation for swell or where the design subgrade resilient modulus is less than 5,000 psi. The Intermediate Stiff Layer provides long term stability for the pavement foundation in situations where the subgrade may experience elevated water content during the design life.

Conclusion: This design calculation indicates that the concrete section over the LCC that has lost 30 percent the strength, is capable of supporting more than 11 million ESALs. This is the same value if the LCC does not degrade because the material is still sufficiently strong to be off the conventional charts for subgrade materials. This ESAL value suggest that for a typical 20-year pavement design life the pavement could support either 395 trucks per day (three axles, max legal weight at rear, with a combined weight of 54,000 pounds, examples include dump, trash, fire, or full concrete trucks) or 500,000 light trucks per day (two axles with a combined weight of 8,500 pounds, examples include Box Vans, Utility Trucks, or a Pick-up with a Trailer).

MISSION ROCK PHASE 1 HORIZONTAL DEVELOPMENT
LCC RIGID PAVEMENT CALCULATION

750604203
LANGAN
PDB/SAW
19 FEBRUARY 2020

F. Calculate Design ESALs

When designing for Arterial, Non-residential Collector and Industrial streets, this section presents the most involved generation of design ESALs. Residential streets and Residential collectors can be estimated with Default equations. Various inputs are needed and discussed below and used to determine the Design ESALs. ESALs calculated for 20 years (expressed as ESAL₂₀) is the minimum recommended time for permanent pavements, and is shown in accordance with Equation 1:

Equation 1 (=> ESAL calculation for 20 or 30 years)

$$ESAL_{years} = \sum \left(LEF \text{ (flexible or rigid) class \#} \times VPD \times \frac{\text{days}}{\text{week}} \times \frac{\text{weeks}}{\text{year}} \times \text{Grown Years} \right) + \text{Defaults}$$

Where:

LEF = Load Equivalency Factor for each vehicle type (Class) on flexible or rigid pavement material type, Table 4.1G-1;

VPD = Vehicle per day in Design Lane, per each Vehicle Class Number (FHWA Classification system) in Table 4.1G-1. Lane distribution is assumed per Section 4.1D,

Years = Minimum 20 years for all permanent pavements. Less years may be used for temporary or short-term designs. More years such as 30 years for critical designs.

Grown Years = Use when yearly Growth Factors may apply. See Section 4.1E;

Defaults – See Section 4.1H. for default ESAL equations for special situations. The Designer may need to generate other add-on ESALs for specialized traffic loading sources for each project.

G. LEFs (Load Equivalency Factors)

This section presents vehicle LEFs (load equivalency factors) taken from the 1993 AASHTO, Appendix MM for vehicles loaded near the maximum axle load limits, provided by Colorado regulated legal load limits or GVWR (Gross Vehicle Weight Rating) for un-regulated buses.

The LEF variables according to FHWA vehicle classification below and modified with descriptions, are based on the axle weights and configurations shown for flexible or rigid pavements as defined in Table 4.1G-1 below. Refer to Appendix A of this PDS for a description of the FHWA classification vehicles.

TABLE 4.1G-1

LEF (Load Equivalency Factor) VARIABLES for EQUATION 1

LEF from 1993 AASHTO Appendix MM, at equal traffic capacity for Flexible and Rigid pavement

Vehicle Class Number (FHWA), type	Vehicle Description	Axle Type and Loads pounds, front to rear, [average total = pounds] S = single, t = tandem	LEF - (Load Equivalency Factor)		LEF Ratio Rigid / Flexible (for information only)
			<u>Flexible</u> [SN = 4, approx..9 inch]	<u>Rigid</u> [D =8 inches]	
1	Motorcycles	1,000 single each end [2,000]	0.0002	0.0002	100%
2	Automobiles & Sport Utility	Average of 2,000 single, 3,000 single, with or not: 1,000 single trailer [5,500]	0.0018	0.0013	72%
3	Pickup with trailer -or- Utility & Box Vans (average)	2,000 single, 3,000 single, 6,000 2-axle trailer -or- 2,000 single, 4,000 single. [8,500]	0.0030	0.0028	92%
4 School Type A	<u>Bus</u> , 2 axles (10+ passenger)	5,000 single, 10,000 single. [15,000]	0.110	0.090	82%
4 School Type C or D [half loaded]	Bus, 2 axles (63-71 passenger)	10,000 single, 16,000 single. [26,000] Curb weight plus driver+ 40 passengers	0.747	0.694	93%
4 School Type C or D [GVWR]	Bus, 2 axles (63-71 passenger)	13,000 single, 23,000 single. [36,000] GVWR	2.791	3.014	108%
4 Bus, City, single unit	Bus, 2 axles, [RTD], 93% of GVWR	14,000 single, 25,000 single. (93% of 14.6k single, 27k single). [38,000]	3.701	4.084	110%
4 Bus, City Transit, articulated,	Bus, 3 axles, [RTD], Average: empty, GVWR	15,000 single, 24,000 single, 28,000 single full loaded. (10k,11k ,21k empty). [54,500]	5.328	5.875	110%
5 _SUT	<u>Single Unit Truck</u> , Two axles	8,000 single, 17,000 single. [25,000]	0.864	0.838	97%
6 _SUT	Three axles, max legal at front & total	20,000 single, 34,000 tandem. [54,000] (ex: full concrete)	2.580	3.420	133%
6 _SUT	Three axles, max legal at rear & total	14,000 single, 40,000 tandem. [54,000] (ex: dump, trash, small fire)	2.418	3.897	161%
6 _SUT <i>*unweighted average</i>	See above	See above	2.499	3.659	146%
7 _SUT	Four axles, max legal at rear & total maximum legal.	10,000 single, 34,000 tandem, 10,000 single pusher or tag. [54,000] (ex: concrete truck).	1.314	2.038	155%

7 _SUT	Four axles, maximum legal.	12,000 single, 3 x 14,000 single. [54,000]	1.377	1.222	89%
7 _SUT <i>unweighted average</i>	<i>See above</i>	<i>See above</i>	1.346	1.630	121%
5+6+7 _SUT <i>*unweighted average</i>	See 5, 6, 7	See 5, 6, 7	1.036	1.523	147%
8 _MUT-1	Multi-Unit Truck, One Trailer , Three or Four axles,	12,000 single, 20,000 single, 34,000 tandem. [66,000] ** less than max legal.	2.793	3.601	129%
9 _MUT-1	Five axles, one trailer, less than max. legal.	10,000 single, 2 x 34,000 tandem [78,000]	2.322	3.824	165%
9 _MUT-1 [Curb weight only]	Five axles, one trailer, less than max. legal.	8,000 single, 16,000 & 8,000 & tandem [36,000] curb weight = fueled, no cargo	0.102	0.123	129%
10 _MUT-1	Six or more axles, one trailer with tridem. Max. legal	9,000 single, 26,000 tandem, 45,000 tridem [80,000]	1.313	2.551	194%
8+9+10 _MUT <i>One Trailer</i> <i>*unweighted average</i>	See 8, 9, 10	See 8, 9, 10	2.143	3.325	155%
11 _MUT-2	Multi-Unit Truck, Multi-Trailers Five or less axles.	10,000 single, 3x 18,000 single, 1x 16,000 single [80,000]	3.747	3.694	99%
12 MUT-2	Six axles, multi-trailers.	12,000 single, 34,000 tandem, 1 x 10,000 + 2 x 12,000 single. [80,000]	1.851	2.497	135%
13 _MUT-2	Seven or more axles, multi-trailers	12,000 single, 22,000 & 24,000 tandem, 10,000 & 12,000 single . [80,000]	1.027	1.209	118%
11+12+13 _MUT <i>Multi Trailer</i> <i>*unweighted average</i>	See 11,12,13	See 11,12,13	2.208	2.467	112%

Notes: *SUT = Single Unit Truck, *MUT-# = Multi Unit Truck (Combination of tractor and # of trailers), *Any axle may have single or dual wheels. GVWR =gross vehicle weight rating

EXHIBIT E
LCC as a Subbase Material
Thesis

**Analysis of construction experience of using lightweight
cellular concrete as a subbase material**

by

Sergey Averyanov

A thesis

presented to the University Of Waterloo

in fulfilment of the

thesis requirement for the degree of

Master of Applied Science

in

Civil Engineering

Waterloo, Ontario, Canada

© Sergey Averyanov 2018

AUTHOR'S DECLARATION

I hereby declare that I am the sole author of this thesis. This is a true copy of the thesis, including any required final revisions, as accepted by my examiners.

I understand that my thesis may be made electronically available to the public.

ABSTRACT

Canada has the second largest territory in the world and its pavement network has over 1,000,000 km of roads spread over regions with various existing soil types. One of the challenges for engineers is to determine the soil type for a particular road project and to develop a pavement design accordingly. It is very important to identify weak or frost-susceptible soils, as they are influenced greatly by weather conditions which may lead to settlement issues and may affect the overall pavement performance. One viable option to overcome the consequences of settlement problems is the usage of lightweight materials, such as Lightweight Cellular Concrete (LCC), which reduces the effective stress on the underlying soil. This material has a number of advantages including: it is lightweight; exhibits superior thermal properties; is freeze-thaw resistant; has good flowability; is cost-effective; and sustainable.

This study aims to assess LCC in terms of performance in past projects, mechanical properties of LCC from the ongoing project as well as prediction of its field performance in the future. Already existing road sections with the installed LCC as a subbase were studied. The available information from those road sections was compiled and analyzed to establish similarities and differences in the cases as well as challenges and recommendations for LCC installation. All projects were aiming to solve the settlement problem. It is observed that settlement usually occurs on localized parts of the road and not on its whole length. After visual inspection, some of the studied sections, such as Winston Churchill Boulevard and Highway 9 were found to have no severe rutting or fatigue cracking, however, longitudinal and transverse cracking were observed at Dixie Road, particularly at the adjacent section to the Granular base pavement.

The samples from the ongoing site were collected for laboratory testing. Results from the laboratory determined the density of the LCC in the hardened stage as approximately 40 kg/m^3 lower than its plastic density. The similar information was found in the literature. However, compressive strength of the in-situ cast material was determined to be higher than for the similar densities in the previous findings. Modulus of elasticity also differs from the typical values, whereas it was found to be lower. Poisson's ratio values were found to be in the typical range.

To predict the ability of the road sections to bear the designed traffic loads and to predict in-service performance, the case studies with settlement issues were considered. Failure criteria analysis has been conducted. The results of the failure criteria analysis indicated that the usage of LCC as a subbase material is more durable than the conventional granular material with similar thickness. This also shows that using LCC as a subbase layer material could be potentially effective.

ACKNOWLEDGEMENTS

I would first like to thank my supervisor Dr. S.L. Tighe from the Civil and Environmental Engineering Department at the University of Waterloo, for her support and guidance over the course of this research.

I would also like to express my gratitude to my thesis readers Dr. W.C. Xie, from the Department of Civil and Environmental Engineering at The University of Waterloo and Dr. V. Henderson – an adjunct professor from the Department of Civil and Environmental Engineering at the University of Waterloo. Thanks also to the Civil Engineering Department lab technicians, Richard Morrison, Douglas Hirst, Peter Volcic, Ya Ting Yang, and Azka Aqib.

Appreciation is also extended to CEMATRIX and National Sciences and Engineering Research Council (NSERC) for the supply of research materials and funding this project. Special thanks to Dan Hanley, Brad Dolton, Dr. J. Li, Steve Bent, and Cameron Nerland from CEMATRIX for sharing their knowledge during my research.

In addition, I would like to thank my colleagues at the University of Waterloo who contributed their time and effort during my project. Namely, Dr. H. Baaj, Frank Mi-Way Ni, Abimbola Grace Oyeyi, Eskedil Melese, Daniel Pickel, Dahlia Malek, Drew Dutton, Seyedata Nahidi, Frank Liu, Qingfan Liu, Taha Younes, Yashar Azimi Alamdary, Zaid Alyami, Luke Zhao, Taher Baghaee Moghaddam, Jessica Rossi, Beverly Seibel. This work would not have been possible without your help.

DEDICATION

*This thesis is dedicated to my family, whose support and love
have made this a possibility.*

TABLE OF CONTENTS

AUTHOR'S DECLARATION.....	ii
ABSTRACT.....	iii
ACKNOWLEDGEMENTS.....	iv
DEDICATION.....	v
Table of Contents	vi
List of Figures	ix
List of Tables.....	xi
List of Abbreviations.....	xiii
1 Introduction.....	1
1.1 Background	2
1.2 Research Hypotheses.....	3
1.3 Research Scope and Objectives.....	3
1.4 Thesis Organization.....	3
2 Literature Review	5
2.1 Lightweight Cellular Concrete (LCC).....	5
2.2 Composition of LCC	7
2.3 Properties of LCC.....	8
2.3.1 Fresh State.....	8
2.3.2 Hardened State	10
2.4 Challenges	15
2.5 Sustainability	16
2.6 Applications.....	17
2.7 Applications in Pavement Engineering	18
2.8 Summary of Literature Review and Research Gaps.....	19
3 Field Performance Review.....	20
3.1 Methodology	20
3.2 Case Studies	21

3.2.1	Dixie Road. Region of Peel, Caledon, Ontario, Canada	22
3.2.2	Brentwood Light Rail Transit (LRT) Bus-Lane. Calgary, Alberta, Canada	31
3.2.3	Winston Churchill Boulevard. Brampton, Ontario, Canada	34
3.2.4	Highway 9. Holland Marsh, Ontario, Canada	36
3.2.5	View and Vancouver Streets, City of Victoria, British Columbia, Canada	40
3.3	Summary of Case Studies	44
3.4	Discussions and Recommendations	45
4	Pavement Design and Analysis	48
4.1	Introduction into Pavement Design	48
4.2	Pavement Design with Lightweight Cellular Concrete (LCC)	48
4.3	Analysis Method	49
4.4	Failure Criteria Analysis	50
4.4.1	First Approach	51
4.4.2	Second Approach	55
4.4.3	Third Approach	59
4.5	Summary	65
5	Toronto Project	66
5.1	Site Description	66
5.2	Approach	67
5.3	Production and Placement	67
5.4	Laboratory Tests	69
5.4.1	Unconfined Compressive Strength	70
5.4.2	Modulus of Elasticity and Poisson's Ratio	74
5.4.3	Relationship between Properties	76
5.5	Summary	77
6	Conclusions and Future Recommendations	78
6.1	Conclusions	78
6.2	Future Recommendations	79
	References	81

Appendix I.....	86
Appendix II.....	89
Appendix III.....	91

LIST OF FIGURES

Figure 1-1: Typical Cross Section of a Rural Conventional Asphalt Concrete Pavement (TAC, 2013)	1
Figure 2-1: Texture of Wet LCC (Maher and Hagan, 2016)	6
Figure 2-2: "Wet" Mix Equipment (Dolton et al., 2016)	6
Figure 2-3: "Dry" Mix Equipment (Dolton et al., 2016)	7
Figure 2-4: Instability Issues with Ultra-Low Density LCC (Field Performance)	9
Figure 2-5: Lightweight Cellular Concrete being Placed with a Flexible Hose (Taylor et al., 2016)	10
Figure 2-6: Splitting Tensile Strength Test Setup.....	12
Figure 2-7: Global Use of Cellular Concrete (Oginni, 2015)	17
Figure 3-1: Overview of Research Methodology.....	21
Figure 3-2: Road Section Location (Google maps, 2018)	22
Figure 3-3: Typical Cellular Cross Section (Griffiths and Popik, 2013)	23
Figure 3-4: Construction Process of Dixie Road, Region of Peel, Caledon, Ontario, Canada (CEMATRIX)	24
Figure 3-5: Condition of Dixie Road, Region of Peel, Caledon, Ontario, Canada.....	25
Figure 3-6: Ground Penetrating Radar Equipment	26
Figure 3-7: GPR Longitudinal Image of Southbound Lane, L10 (Griffiths and Popik, 2013)	27
Figure 3-8: GPR Transverse Images at Longitudinal Crack Locations, L4, and L5 (Griffiths and Popik, 2013)	28
Figure 3-9: FWD Truck and Trailer (Griffiths and Popik, 2013)	28
Figure 3-10: Structural Number Comparison Plot (Griffiths and Popik, 2013)	29
Figure 3-11: Site Location (Google Maps, 2018)	31
Figure 3-12: Bus Lane. (a) Reconstruction Process. Placing the LCC (CEMATRIX) (b) After Installing the LCC Layer (CEMATRIX)	32
Figure 3-13: Pavement Distresses on the non-LCC section - 1(CEMATRIX, 2018).....	33
Figure 3-14: Pavement Distresses on the non-LCC section - 2(CEMATRIX, 2018).....	33
Figure 3-15: Location of the Road Section (Google Maps, 2018).....	34

Figure 3-16: Pavement Structure. Winston Churchill Boulevard (CEMATRIX).....	35
Figure 3-17: Condition of Winston Churchill Boulevard, August 2017	35
Figure 3-18: Highway 9 Site Location (Google Maps, 2018)	36
Figure 3-19: Highway 9 Site Location with the Local Landscape (Google Maps, 2018)	36
Figure 3-20: Highway 9 Construction Process (CEMATRIX).....	38
Figure 3-21: Condition of Highway 9, Three Years after Construction	39
Figure 3-22: Condition of Highway 9, Three Years after Construction	39
Figure 3-23: Site location. (Google maps, 2018).....	40
Figure 3-24: View Street and Vancouver Street Construction Process. Wet Mix Equipment (CEMATRIX)	41
Figure 3-25: Benkelman Beam Deflection Testing	42
Figure 4-1: Pavement Structure with LCC.....	49
Figure 4-2: Vertical and Tensile Stresses. Comparison for Dixie Road, Highway 9 and Winston Churchill Blvd (WESLEA software, 2018)	54
Figure 4-3: Allowable Number of Load Repetition. Fatigue Cracking and Rutting for Dixie Road, Highway 9 and Winston Churchill Blvd (WESLEA software, 2018).....	58
Figure 4-4: Predicted Damage. Fatigue Cracking and Rutting for Dixie Road, Highway 9 and Winston Churchill Blvd (WESLEA Software, 2018).....	64
Figure 5-1: Site Location (Google Maps, 2018)	67
Figure 5-2: Construction Process. Toronto, May 2018.....	68
Figure 5-3: Samples, Collected on Site.....	69
Figure 5-4: Weather Forecast during Construction and Casting the Samples	70
Figure 5-5: Unconfined Compressive Strength.....	71
Figure 5-6: UCS Test Results	72
Figure 5-7: Average UCS Test Results.....	73
Figure 5-8: Modulus of Elasticity and Poisson's Ratio Test Setup	75
Figure 5-9: Modulus of Elasticity Test Results for 28 Days Samples	76
Figure 5-10: Correlation of Compressive Strength and Density.....	77

LIST OF TABLES

Table 2-1: Typical Properties of LCC Based on British Concrete Association (BCA, 1994).	11
Table 2-2: Empirical Model for Cellular Concrete Modulus of Elasticity Determination (Amran, Farzadnia and Ali, 2015)	13
Table 2-3: Summary of Cellular Concrete Applications Based on Density (Sari and Sani, 2017)	18
Table 3-1: Comparison of Pavement Structures	27
Table 3-2: Project Specifications and QC Results (Maher and Hagan, 2016).....	38
Table 3-3: Benkelman Beam Results (Golder Associates Ltd. Report, 2008).....	42
Table 3-4: FWD Test Data.....	43
Table 3-5: Summary of the Available Cases of Using LCC as a Subbase Material in Pavement Construction in Canada.....	44
Table 4-1: WESLEA Settings for Dixie Road, Highway 9 and Winston Churchill Boulevard (Material Properties of the Pavement)	50
Table 4-2: ESALs for Three Road Sections in Ontario	51
Table 4-3: Vertical and Tensile Stresses. Dixie Road.....	51
Table 4-4: Vertical and Tensile Stresses. Highway 9	52
Table 4-5: Vertical and Tensile Stresses. Winston Churchill Blvd	52
Table 4-6: Allowable Number of Load Repetition. Fatigue Cracking and Rutting for Dixie Road	55
Table 4-7: Allowable Number of Load Repetition. Fatigue Cracking and Rutting for Highway 9.....	56
Table 4-8: Allowable Number of Load Repetition. Fatigue Cracking and Rutting for Winston Churchill Boulevard.....	56
Table 4-9: Predicted Damage (Fatigue Cracking and Rutting) of Pavement with Granular B Subbase. Dixie Road (WESLEA, 2018)	60
Table 4-10: Predicted Damage (Fatigue Cracking and Rutting) of Pavement with LCC Subbase. Dixie Road (WESLEA, 2018).....	60
Table 4-11: Predicted Damage (Fatigue Cracking and Rutting) of Pavement with Granular Subbase. Highway 9 (WESLEA, 2018).....	61

Table 4-12: Predicted Damage (Fatigue Cracking and Rutting) of Pavement with LCC Subbase. Highway 9 (WESLEA, 2018)	61
Table 4-13: Predicted Damage (Fatigue Cracking and Rutting) of Pavement with Granular Subbase. Winston Churchill Boulevard (WESLEA, 2018)	62
Table 4-14: Predicted Damage (Fatigue Cracking and Rutting) of Pavement with LCC Subbase. Winston Churchill Boulevard (WESLEA, 2018)	62
Table 5-1: Typical Properties of Cellular Concrete Based on British Concrete Association (BCA 1994)	73

LIST OF ABBREVIATIONS

AADT	Average Annual Daily Traffic
AASHTO	American Association of State Highway and Transportation Officials
ACD	Activity Cycle Diagram
ARA	Applied Research Associates
ASTM	American Standards Tests and Methods
BCA	British Concrete Association
CBR	California Bearing Ratio
CPATT	Centre for Pavement and Transportation Technology
ESAL	Equivalent Axle Single Load
FWD	Falling Weight Deflectometer
GPR	Ground Penetrating Radar
HMA	Hot Mix Asphalt
PC	Portland Cement
LCC	Lightweight Cellular Concrete
LCCA	Life-Cycle Cost Analysis
LVDT	Linear Variable Displacement Transducers
LRT	Light Rail Transit
MEPDG	Mechanistic-Empirical Pavement Design Guide
MTO	Ministry of Transportation Ontario
RAP	Recycled Asphalt Pavement
RCA	Recycled Concrete Aggregate
SCC	Self Consolidating Concrete
TAC	Transportation Association of Canada
QA	Quality Assurance
QC	Quality Control
UCS	Unconfined Compressive Strength

CHAPTER 1

1 INTRODUCTION

Canada has the second largest territory in the world and its pavement network has over 1,000,000 km of roads (TAC, 2013). The typical pavement structure in Canada consists of a surface layer, which can be made up of bituminous layers or rigid concrete layers, a granular base and a subbase overlying the subgrade (Figure 1-1). The main purpose of the layers is to support the wheel loads from traffic and distribute it to the underlying subgrade. When designing pavement, it is very important to take into consideration: thickness of each layer; volume and composition of traffic; climate; range of construction materials available; desired serviceable life; and subgrade type and strength (TAC, 2013).

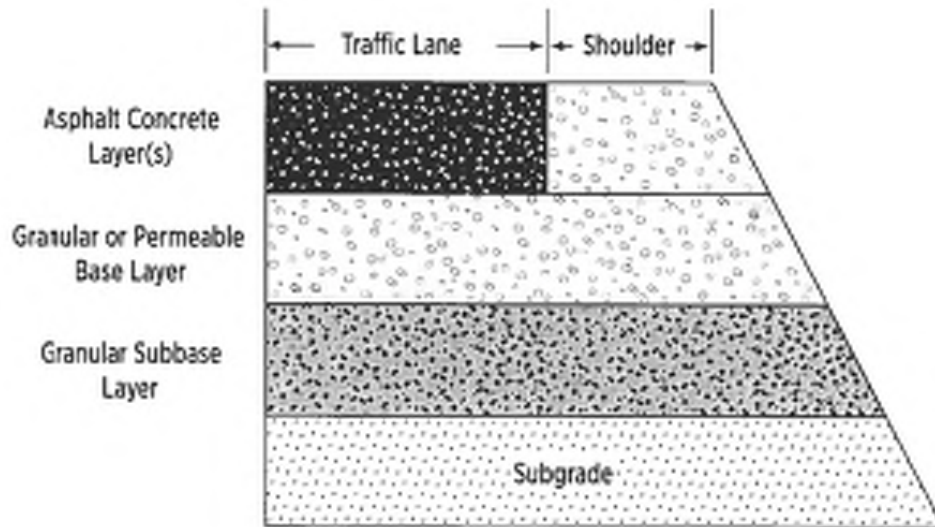


Figure 1-1: Typical Cross Section of a Rural Conventional Asphalt Concrete Pavement (TAC, 2013)

The subgrade type is a very significant factor because Canada's road network is spread over regions with various existing soil types. Some of these soil types, such as weak or frost-susceptible soils are referred to as difficult geotechnical conditions. In addition to the type of soil, serious temperature fluctuations in winter months, as well as thawing during spring months, play a significant role in pavement performance with respect to the subgrade. Frost heave in winter months as well as thawing during spring months influences the settlement of pavements and reduces bearing capacity of the pavement layers. Materials that are commonly used in the subbase layer include unbound granular materials, which have low insulation

properties and may lead to penetration of frost through the pavement structure straight to the subgrade (Hoff et al., 2002).

As a result of having unbound granular materials in a subbase, water can easily penetrate through the pavement structure into the subgrade and saturate the underlying soils. Thus, during the freeze-thaw cycles, those soils may become unstable, leading to settlement and causing distresses to the whole pavement structure (Hoff et al., 2002). To address this problem, it is recommended to remove weak organic soils from exposed subgrade areas prior to placement of embankment materials. In some cases, it is time-consuming and not economically beneficial, to replace these weak soils with stiff and stable materials or pavement structure. Another feasible solution may be using geosynthetics, including geotextiles, geofabrics, and geogrids, to provide “bridge” embankments over thick deposits of these organic-rich soils (TAC, 2013).

In order to overcome settlement issues due to excessive weight of pavement, the following materials may be utilized: (TAC, 2013)

- Expanded polystyrene
- Expanded lightweight clay
- Air cooled blast furnace slag
- Recycled Concrete Aggregates (RCA)
- Reclaimed Asphalt Pavement (RAP)
- Waste glass and ceramic

To address the problem of weak soils, and to mitigate settlement and fast deterioration of the pavements, Lightweight Cellular Concrete (LCC) is considered as another potential solution. For a better understanding of the benefits and drawbacks of using LCC, as well as performance evaluation of the pavement structure, analysis of construction experience of using LCC as a subbase material has been performed in this research.

1.1 Background

LCC, sometimes referred to as "foamed concrete" or "aerated concrete", is a useful construction material with many applications. It differs from conventional concrete in that it does not contain any coarse aggregate. Instead, it is made from a mixture of cement and water that is mixed with a foaming compound to generate a matrix of small air bubbles, which makes the concrete extremely lightweight. Apart from being lightweight, LCC is a cost-effective and sustainable material and has superior thermal properties, freeze-thaw resistance, and good flowability. LCC technology was originally developed in Sweden in the early 1900s, but was not put into commercial use until after World War 2. More recently, technological advances in LCC have led to its use for various applications. Today, LCC is used in areas that require strong, yet lightweight and inexpensive materials. Commonly, LCC is used as a lightweight fill material

in embankments and beneath roads, or as an energy-absorbing material. Though many of its properties are still not thoroughly studied, the usage of LCC is becoming more popular in construction projects in North America and abroad.

For the most part, lightweight fill materials are progressively utilized in civil engineering purposes such as backfilling, slope stabilization, embankment fills, and pipe bedding (Horpibulsuk et al., 2014). The main intent of lightweight fill materials is to be used as an alternative construction material that significantly reduce the weight of fills, thereby mitigating excessive settlements and bearing failures. This can subsequently result in more economic designs for structures such as retaining walls and base layers of roadways.

1.2 Research Hypotheses

The primary hypotheses of this research are as follows:

- Pavement structures with already installed LCC as a subbase can exhibit result in good pavement performance
- Pavement performance of LCC pavement can be predicted using WESLEA analysis
- Mechanical properties of LCC samples cast in-situ are different from the typical values in the literature

1.3 Research Scope and Objectives

The scope of this project is to review the condition and performance of existing road sections that were constructed using LCC as well as to evaluate the mechanical properties of this material during the construction. This methodology will enable the prediction of future performance. To achieve this goal, the specific objectives are as follows:

1. Assess the condition of existing pavement sections with LCC as a subbase material
2. Conduct an analysis of the LCC performance of the existing roads
3. Determine structural properties of in-situ LCC

1.4 Thesis Organization

The components of the thesis include outline of scope and objectives, literature review, review of case studies, performance evaluation of LCC in past and current projects and prediction of the future performance (failure criteria analysis). At the end of the thesis, conclusions and recommendations will be provided.

This thesis is organized into six Chapters.

Chapter 1 explains the scope and objectives of the research project and provides the thesis organization.

Chapter 2 provides an extensive review of the literature related to Lightweight Cellular Concrete, its composition and properties. Fresh and hardened states of LCC are presented by various mechanical properties of the material. This Chapter covers methods of producing LCC and presents benefits and drawbacks of this material. In addition, potential sustainable benefits from using LCC are presented in this Chapter. Number of applications of LCC are presented in Chapter 1, as well as applications in pavement engineering. Research gaps are also described in this Chapter.

Chapter 3 presents case studies of using LCC as a subbase material in pavement engineering across Canada. This Chapter describes each of the cases separately by discussing the location of the site, problem, possible solutions to the issue, construction process, results and tests that were done after construction. At the end of the Chapter, a table summarizing all of the case studies is presented. The most crucial issues that future contractors could potentially face, as well as recommendations, are discussed in Chapter 3.

Chapter 4 describes performance prediction analysis by introducing failure criteria. Three case studies from the previous Chapter were taken as the examples of pavement structure and were analyzed on bearing capacity of the layer, ability of the pavement to resist fatigue cracking and rutting issues, and potential number of ESALs that the pavement could potentially preserve without any maintenance.

Chapter 5 provides the results of the laboratory testing of the samples collected from the ongoing Toronto project. Site and project details are described in this Chapter. The tests were conducted at the Centre for Pavement and Transportation Technology (CPATT). The laboratory results were analyzed and correlation between the properties was made. Values, obtained from the laboratory work were compared to the typical values for LCC in the literature.

Chapter 6 contains the conclusions and recommendations based on the research conducted for the thesis.

CHAPTER 2

2 LITERATURE REVIEW

This Chapter provides a summary of the relevant literature related to this thesis. It describes composition, methods of production, mechanical properties and applications of Lightweight Cellular Concrete (LCC).

2.1 Lightweight Cellular Concrete (LCC)

ASTM C796 (2012) defines LCC as:

“A lightweight product consisting of Portland Cement, cement-silica, cement-pozzolan, lime-pozzolan, or lime-silica pastes, or pastes containing blends of these ingredients and having a homogeneous void or cell structure, attained with gas-forming chemicals or foaming agents (for cellular concretes containing binder ingredients other than, or in addition to Portland Cement, autoclave curing is usually employed)”.

Cellular concrete is relatively homogeneous compared to conventional concrete, as it does not contain coarse aggregate, so there is limited variation in its properties. The properties of Lightweight Cellular Concrete (LCC) depend on its microstructure and composition, methods of pore-formation and curing. LCC is lightweight, easy to construct, and economical in terms of transportation. LCC is comprised of cement or lime mortar matrix, in which air-voids are entrapped by a suitable aerating agent (Ramamurthy, Nambiar and Ranjani, 2009). Traditional concrete mix components densities may vary between 1000 kg/m^3 (water) and 3200 kg/m^3 (cement) (Darshan, 2016). By appropriate method of production, LCC densities are considerably lower, ranging from 250 kg/m^3 to 1800 kg/m^3 , but typically between 400 kg/m^3 and 600 kg/m^3 (Dolton et al., 2016). This makes LCC desirable as a very low-density material. The cellular pore network of LCC also provides a high degree of thermal insulation, as well as considerable savings in material. Figure 2-1 shows the texture of wet LCC as it is being placed from a pipe.



Figure 2-1: Texture of Wet LCC (Maher and Hagan, 2016)

LCC can be produced in two different ways: “dry” mix or “wet” mix. Figure 2-2 shows “wet” mix process, where cement, water, and admixtures are pre-batched into a slurry and sent to site in trucks. Once on site, the temperature, density, and viscosity of the slurry is measured to confirm compliance with the requirements to make LCC. After quality is verified, the slurry is delivered into the LCC equipment, which then injects foam into the slurry and pumps the LCC into place (CEMATRIX, 2018). The “dry” mix process is better for high-volume projects (Figure 2-3). All the components are blended on site to form the slurry, then foam is injected and the concrete is pumped into place (Dolton et al., 2016). With a skilled and experienced construction team, installation is usually quick and inexpensive. Those two factors usually come as a significant part of the overall project cost (Loewen, Baril, and Eric, 2012).



Figure 2-2: "Wet" Mix Equipment (Dolton et al., 2016)



Figure 2-3: “Dry” Mix Equipment (Dolton et al., 2016)

2.2 Composition of LCC

LCC is typically composed of Portland Cement, water, pre-formed foaming agent, with no coarse aggregate. Sometimes pozzolan materials such as fly ash, silica fume, slag, or various chemical admixtures are also included (Ozlutas, 2015).

Portland Cement

The main cementitious component of LCC is Portland Cement. The content is approximately $300\text{--}400\text{ kg/m}^3$ in the lightweight cellular concrete mix and it can vary depending on the desired density and strength of the final product (Jones, 2001).

Pozzolan Materials

Pozzolans are a broad class of siliceous or siliceous and aluminous materials, which, in themselves, possess little or no cementitious value. In order to improve compressive and flexural strength, reduce cost, heat of hydration, drying shrinkage, thermal conductivity and sustainability, fly ash, blast furnace slag or silica fume may be added to PC (Dolton et al., 2016; Kearsley and Wainwright 2001; 2002). Jones et al. (2017) stated that replacing Portland Cement with fly ash up to 40% could significantly reduce the embodied carbon dioxide by 65% compared to the 100% Portland Cement mix while has a similar 28-day compressive strength (0.25 MPa compared to 0.31 MPa). However, the drawbacks of using fly ash are the slow rate of strength gain, and it might cause foam instability as the water demand may increase (Ozlutas, 2015).

Fine Aggregates

Fine sand typically is composed of 2mm maximum size aggregates for use in LCC with dry densities equal to or greater than 600kg/m^3 . In lower density LCC, fillers like fly ash can be used instead (BCA, 1994; Dransfield, 2000). Carbon nanotubes (CNTs) have also been incorporated to LCC mix as fillers for support. They are found to develop more homogenous cell structure with closed cell bubbles (Yakovlev et al., 2006). However, CNTs can form clumps and ultimately cause foam instability, this will require dispersion in water which might not prove effective (Ozlutas, 2015).

Water

The cement to water ratio used for LCC ranges from 0.4 to 1.25 (Kearsley, 1996). It must be noted that the quantity of water required is dependent on the composition and use of the material which relies on consistency and stability (Ramamurthy, Nambiar and Ranjani, 2009). Excess water in the mix leads to segregation while insufficient water content may collapse the mix (Nambiar and Ramamurthy, 2006).

Foam

A foaming agent is usually added to the base mix (cement slurry) to produce the bubble structure in the LCC material. Foaming agents can either be blended with the base mix after they have been produced separately or mixed along with the ingredients for the base mix (Byun, Song and Park, 1998). The former is being used more often. The main requirement is that the foaming agent be stable and firm in order to resist mortar pressure (Koudriashoff, 1949). Foam can either be wet or dry. Studies have reported stability issues with the wet foam producing bubble sizes of between 2 mm to 5 mm. However, dry foam is reported to have more reliability in terms of stability with bubble sizes of 1mm (Aldridge, 2005). Examples of foaming agents include detergents, resin soap, hydrolized protein, saponin, and neopar (Ramamurthy, Nambiar and Ranjani, 2009; Valore, 1954a).

2.3 Properties of LCC

2.3.1 Fresh State

Fresh state of cellular concrete is described as free-flowing, self-leveling and self-compacting. The higher the air volume in the LCC is, the easier it is to place it. In addition, it does not need further consolidation during placement (Ozlutas, 2015). However, in some mixes with the increased volume of the air, cohesion of the mix increases and self-weight of the mix reduces, thus, resulting in reducing of the self-leveling properties of the cellular concrete (Nambiar and Ramamurthy, 2006). There are two main properties that describe fresh state of the LCC: stability and consistency.

2.3.1.1 Stability

Khayat and Assaad (2002) defined stability as a state that is required to ensure the presence of an adequate air void system and maintain it in a stable state until the time of hardening in Self-Consolidating Concrete (SCC).

Factors affecting mix stability are the following: (Brady, Jones, and Watts, 2001; Jones, Ozlutas and Zheng, 2016)

- Environmental conditions (wind, evaporation, temperature, vibration)
- Materials used (quality and volume of foam)
- Quality of production (mixing and placing processes)

It was stated by a number of researchers (McGovern, 2000; Aldridge, 2005; Jones and McCarthy, 2005b, 2006; Mohammad, 2011) that instability of LCC was a result of poor foam quality as well as the type of constituents used. However, in the case of instability at ultra-low densities (600 kg/m^3 and less), the stability of the mix has been observed to occur even in the absence of the above-mentioned factors (Ozlutas, 2015). The nature of stability or instability depends on the size of the bubbles in the bubble structure. The draining properties of LCC allow water to penetrate inside the material and if stays there, causing the increase in the bubbles inside the structure; thus, collapsing the foam. Meanwhile, the strength of bubbles decreases and cannot support the pressures. Figure 2-4 demonstrates typical instability issue.



Figure 2-4: Instability Issues with Ultra-Low Density LCC (Field Performance)

2.3.1.2 Consistency and Workability

Consistency and workability of cellular concrete are usually characterized by its flowability. The presence of air-voids in the fresh mix due to the addition of stable foam agents allows LCC to be placed easily. The lightweight concrete can be pumped through flexible hoses over a distance of 200 m. Furthermore, its flowability allows it to easily spread into complex forms. It settles into place without the use of compaction equipment as it is self-consolidating material. This makes it an excellent candidate for pipe bedding, and for fill around utilities or not easily accessible areas. Since it flows so easily, forms usually have to be lined with plastic to prevent seepage. Also, the surface of LCC pours cannot be sloped greater than 1 degree due to its low viscosity (Taylor et al., 2016). Figure 2-5 shows a typical placement of LCC by flexible hose.



Figure 2-5: Lightweight Cellular Concrete being Placed with a Flexible Hose (Taylor et al., 2016)

2.3.1.3 Compatibility

According to Amran, Farzadnia, and Ali (2015), the compatibility of LCC is referred to as a condition of strong interaction between the mix design and its constituent parts, in particular between chemical admixtures and the foam agent. Thus, at the areas where the mixture constituents fail to interact, the compatibility of foam mortar decreases. In addition, segregation challenges may occur when there is no interaction between the surfactant and plasticizers (Brady, Jones and Watts, 2001).

2.3.2 Hardened State

Hardened state is characterized by mechanical, physical, durability and functional properties of the cellular concrete. These properties include compressive, flexural and tensile strength,

modulus of elasticity, porosity and permeability, drying shrinkage, freeze-thaw resistance, and Poisson's ratio.

2.3.2.1 Compressive Strength

The compressive strength represents the capacity of a material to resist loads due to compression. LCC has considerably lower range of densities (from 250 kg/m³ to 1800 kg/m³) than conventional concrete, thus lower compressive strength (Table 2-1). In general, compressive strength depends not only on density, but also on number of parameters such as rate of foam agent, w/c ratio, sand particle type, the curing method, cement/sand ratio, and characteristics of additional ingredients and their distribution (Valore, 1954b; Deijk, 1919; Valore, 1954a).

Table 2-1: Typical Properties of LCC Based on British Concrete Association (BCA, 1994)

Dry Density (kg/m ³)	Compressive Strength (MPa)	Modulus of Elasticity (MPa)	Thermal Conductivity (3% moisture) (W/mK)	Drying Shrinkage (%)
400	0.5-1.0	800-1000	0.10	0.30-0.35
600	1.0-1.5	1000-1500	0.11	0.22-0.25
800	2.0-2.5	2000-2500	0.17-0.23	0.2-0.22
1000	2.5-3.0	2500-3000	0.23-0.30	0.15-0.18
1200	4.5-5.5	3500-4000	0.38-0.42	0.09-0.11
1400	6.0-8.0	5000-6000	0.5-0.55	0.07-0.09
1600	7.5-10	10 000-12	0.62-0.66	0.06-0.07

2.3.2.2 Split Tensile Strength

Tensile strength is typically used as a concrete performance measure for pavements because it best simulates tensile stresses at the bottom of the concrete surface course as it is subjected to loading. These stresses are typically important in controlling structural design stresses (Pavement Interactive, 2018). A diametric compressive load is applied along the length of the cylinder until it fails. The test setup is shown in Figure 2-6. Because concrete is much weaker in tension than compression, the cylinder will typically fail due to horizontal tension and not vertical compression. The splitting tension test on regular concrete shows the value of 10% of its compressive strength (Raphael, 1984). For cellular concrete, it is still to be determined, but according to Amran, Farzadnia, and Ali (2015), the tensile strength is in the range between 20% and 40% of its compressive strength.

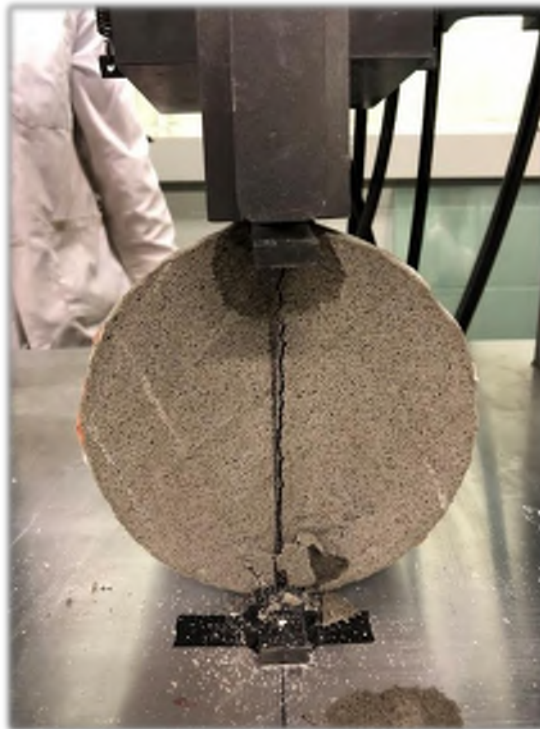


Figure 2-6: Splitting Tensile Strength Test Setup

2.3.2.3 Modulus of Elasticity

The modulus of elasticity in pavement design represents how much the concrete will compress under load (TAC, 2013). The modulus of elasticity generally correlates with compressive strength of LCC. Conventional concrete has a modulus of elasticity of 14,000 to 41,000 MPa, depending on compressive strength and aggregate type. It is reported that E-value of LCC is four times lower than conventional concrete (Jones and McCarthy, 2005b). In cellular concrete, the modulus of elasticity is more related to its density. According to the studies, for range of dry density from 500 to 1600 kg/m³, the modulus of elasticity typically falls between 1.0 and

12 kN/m² respectively (Brad, Jones and Watts, 2001). In addition, it was stated by Jones and McCarthy (2005b) that E-value is dependent on the composition of the mix, and may be altered by fly ash or sand addition. Table 2-2 presents the relationship between compressive strength, modulus of elasticity and density.

Table 2-2: Empirical Model for Cellular Concrete Modulus of Elasticity Determination (Amran, Farzadnia and Ali, 2015)

Equations	Annotations
$E = 33W^{1.5}(fc)^{0.5}$	Pauw's equation
$E = 0.99 (fc)^{0.67}$	Fly ash utilized as fine aggregate
$E = 0.42 (fc)^{1.18}$	Sand is utilized as fine aggregate
$E = 5.31 \times W - 853$	Density ranges from 200 to 800 kg/m ³
$E = 6326(\gamma_{con})^{1.5} (fc)^{0.5}$	γ_{con} = unit weight of concrete fc = compressive strength of concrete where average Poisson's ratio=0.2, and using polymer foam agent
$E = 57,000 (fc)^{0.5}$	Density of conventional concrete limited between 2200 and 2400 kg/m ³ substituting with 80 kg/m ³ for steel
$E = 9.10 (fc)^{0.33}$	fc = compressive strength of concrete
$E = 1.70 \times 10^{-6} p^2 (fc)^{0.33}$	p = plastic density (kg/m ³)

2.3.2.4 Drying Shrinkage

Drying shrinkage is a damaging process to concrete that is caused by the loss of absorbed water from the material. Due to high total porosity (40-80%) drying shrinkage is of high significance in lightweight cellular concrete. The main reasons that intensify shrinkage include pore size decrease as well as a growing number of small-sized pores. Drying shrinkage of LCC where cement is the only binder is notably higher than the one manufactured with lime or lime and cement. Air-cured specimens have very high drying shrinkage potential. On the contrary, moist-cured cement and sand mixes demonstrate drying shrinkage values ranging from 0.06% to over 3.0% when dried at normal temperature, the lowest numbers are correlated with higher densities and higher percentage of sand. The time dependence of shrinkage is inclined by the properties of material, size of specimen and shrinkage climate. In addition to these factors, shrinkage value varies according to the initial moisture content. In the range of higher moisture content (>20% by volume), comparatively insignificant shrinkage takes place accompanied by loss of

moisture, which, in its turn, can be explained by the presence of a large amount of big pores which do not facilitate shrinkage (Darshan, 2016).

2.3.2.5 Poisson's Ratio

Poisson's ratio shows the lateral to axial strain relationship for a material under the load. Its value is obtained using the strains resulting from uniaxial stress only. Poisson's ratio is one of the input parameters for MEPDG (TAC, 2013). The typical range of Poisson's ratio for cellular concrete with densities of 1000 kg/m³ to 1400 kg/m³ is 0.13 to 0.16 and 0.18 to 0.19 respectively (Lee et al., 2009). Neville (2011) reported that the Poisson ratio for normal weight concrete is 0.15 to 0.22. Study by Tiwari et al., (2017) found Poisson ratio for LCC to range between 0.2 to 0.3 for LCC densities between 230 kg/m³ to 800 kg/m³.

2.3.2.6 Porosity and Permeability

Porosity is a measure of the voids in cellular concrete in comparison to the total volume. Porosity can affect the other material properties such as compressive strength, flexural strength, and durability (Amran, Farzadnia and Ali, 2015). However, Amran, Farzadnia, and Ali (2015) are reporting that the permeability and the degree of fluid flow through the concrete matrix were not significantly related to the total porosity, but to larger capillary pores. The porosity of LCC concrete allows the aggressive fluids to penetrate inside the matrix of the concrete in the hardened stage. Porosity of the hardened concrete may be affected by mix design compositions, foam agents, w/c ratio and the curing type. The porosity depends on degree of infusion characteristics such as water absorption, sorption, and permeability.

According to Sabir, Wild and O'Farrell (1997), permeability is defined as a measure of the water flow under pressure in a saturated porous medium. Permeability of the cellular concrete has a significant correlation with the water absorption of the material. Water absorption of the cellular concrete is twice conventional concrete at similar water to binder ratio. Moreover, permeability may be affected by the inclusion of aggregates or mineral admixtures and entrained air in the cement paste (Amran, Farzadnia and Ali, 2015).

2.3.2.7 Freeze-Thaw Resistance

Lower density LCC has been observed to have good freeze-thaw resistance due to the voids restraining the expansion forces from frozen water (Brady, Jones and Watts, 2001). Freeze-thaw characteristic of LCC is dependent on its initial depth of penetration, absorption and absorption rate (Jones, 2001).

2.3.2.8 Thermal Insulation and Conductivity

Another benefit of LCC which stands out against the other materials is its thermal properties. The air entrapped within the concrete acts as an insulator, so heat does not easily transfer

through. This makes LCC desirable as an insulation in buildings, or in tank bases to prevent heat damage to liners (Taylor et al., 2016). Moisture content, density and components of the material account for its thermal conductivity. Density is the key factor in thermal conductivity, as the way of curing the product (moist-curing or autoclaving) is of no importance here. The number of pores and their arrangement are essential for thermal insulation as well. Smaller pores have been found to facilitate better insulation (Darshan, 2016). Concrete is inert and fireproof and does not easily conduct sound, which further suggests it would be a good material for insulation.

A drawback for LCC of being a good insulator is frost heave. Because of that, there can be differential heating and cooling between the cellular concrete and the surrounding materials. If the LCC is used in pavement subgrade, water can seep through the highly porous matrix and pool in areas. Differential cooling in the wintertime can cause ice to form, which expands and causes upheaval that can damage overlying pavements and structures. To mitigate this risk, LCC forms should be sloped downward to the sides and extended out past the overlying road or structure so water cannot pool at the base of the concrete (Maher and Hagan, 2016).

2.3.2.9 Buoyancy Forces

Density of LCC can be less than half the density of water, so if the concrete is submerged there will be buoyancy forces. For an application such as a river embankment fill material, this could be a major problem: if river banks rise, buoyancy forces can push the concrete upwards causing upheaval and failure of the overlying pavements and structures (Friesen et al., 2012).

2.4 Challenges

Number of advantages and disadvantages were discussed in this Chapter. Challenges, associated with LCC are summarized as follows:

- LCC has high potential of drying shrinkage because of the significant amount of cement in its composition (up to 80 % of cement). According to Ramamurthy (2009), LCC can be 10 times more susceptible to drying shrinkage than conventional concrete.
- Instability issues could be a significant problem, especially at the ultra-low densities of LCC during construction process.
- Initial cost might be higher than for similar lightweight materials or for Granular materials, if measuring them m^3 to m^3 . However, in most projects less m^3 of LCC is needed to obtain the same performance.
- Since LCC has good flowability, it may be challenging to place it on the slope surfaces. The technique of “lifts” may be used, when LCC is being placed by levels in steps. Although, this method requires additional framework.

- Another issue with LCC material can be its seepage through the underlying layers when it is placed over the open graded layers. Additional protective layers such as polyethylene sheets may be used to prevent this problem.
- Groundwater seepage control of the excavations, where LCC will be placed, is required. This needs to be done to prevent floating of the material, as LCC density for the case studies was 475 kg/m^3 , which is less than water density (1000 kg/m^3).

2.5 Sustainability

Sustainable development according to the World Commission on Environment and Development (WCED, 1987) is defined as: “Development that meets the needs of the present without compromising the ability of future generations to meet their own needs”.

The potential sustainability benefits of using LCC are outlined below:

- At low densities, it can contain 80 -90% voids which means less virgin material usage and waste produced (Ozlutas, 2015).
- Reduction in the use of non – renewable natural resource by eliminating coarse aggregates, and fine aggregates at densities below 600 kg/m^3 (BCA, 1994).
- It makes use of industry by-product such as slag and fly ash thereby reducing the amount of waste disposed (Dolton et al., 2016; Jones et al., 2012; Awang et al., 2014). Fly ash can also be used to replace Portland Cement up to 75% in lower density LCC, this has the advantage of reducing embodied CO₂ (eCO₂).
- No need for compaction as it flows freely, therefore noise pollution reduction during construction and less energy consumed as compaction is eliminated (Jones and McCarthy, 2005a).
- Not only has it great constructability as the material can be installed very quickly, but also can be placed during winter time with some protective measures and during the light rain (Maher and Hagan, 2016).
- LCC can be easily excavated and removed as it has low strength.
- It can be recycled and used for producing more cellular concrete (Jones et al., 2012).
- LCC has been shown to have good freeze-thaw resistance (Ramamurthy, Nambiar and Ranjani, 2009), fire resistance, sound absorption, and superior thermal insulating properties which improve with lower plastic densities (Wei et al., 2013; Jones and McCarthy, 2005a).
- Due to its high strength-to-weight ratio, there is typically less material required for fill operations, which means less machinery is required during manufacturing and construction, leading to less energy use, less greenhouse gas emissions, and less noise pollution (Dolton et al., 2016).

2.6 Applications

Lightweight fill materials are increasingly being used in civil engineering applications such as roadway base layers, embankment fill material, grout for tunnels and pipes, soil stabilization, fill for abandoned mines or other types of void fill, landslide repair, arrestor material at the end of airport runways, sound-dampening walls, fireproof insulation, and retaining wall backfill (Maher and Hagan, 2016; Horpibulsuk et al., 2014). The air bubble structure of LCC is exceptional at absorbing energy, so there have been successful uses of this material in military ranges, as rockfall protection, and in airports as the safety barrier in order to safely slow down planes and jets if they were to overshoot their runways (Taylor et al., 2016). Amran, Farzadnai, and Ali (2015) report a significant interest in LCC in North America, and in Canada in particular, not only because this material has a wide range of applications but also because of the increased prices for the other lightweight building materials. The annual market size of cellular concrete is estimated to be about 250,000 – 300,000 m³ in United Kingdom including massive mine stabilization project. In Western Canada, the market size of LCC is about 50,000 m³ and it is actively growing. North Koreans mostly use cellular concrete in floor heating systems with the total market for this country as 250,000 m³. In order to reduce the effect of earthquakes and to mitigate the effect from temperature changes, cellular concrete is being used in the Middle East. It can be used as a great thermal insulator for those cases (Amran, Farzadnia and Ali, 2015).

LCC has been used in more than 50 countries. Oginni (2015) presented Figure 2-7, indicating use of cellular concrete technology globally. Asia and Europe alone accounted for 83% of the use of cellular concrete technology economy worldwide.

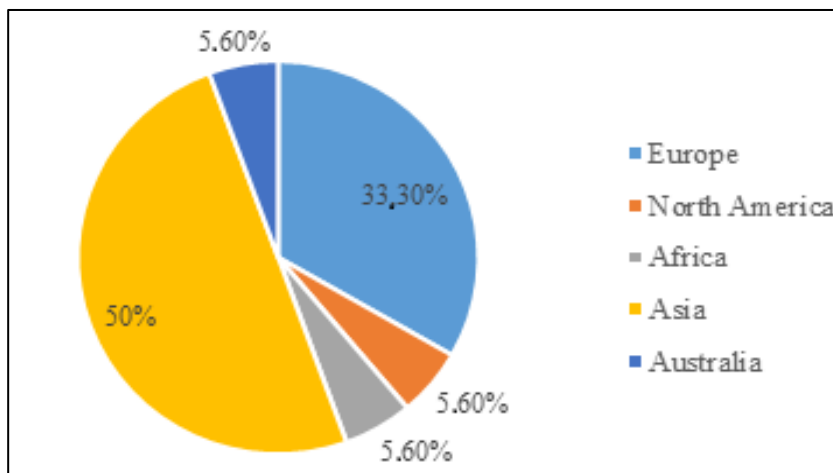


Figure 2-7: Global Use of Cellular Concrete (Oginni, 2015)

The main intent of lightweight fill materials is an alternative construction material to significantly reduce the weight of fills, thereby mitigating excessive settlements and bearing failures. This can subsequently result in more economic designs for structures such as retaining walls and base layer of roadways. The summary of the typical usage of the cellular concrete based on its density is studied and presented in Table 2-3. Moreover, density is potentially easier to control than compressive strength while placing the LCC.

Table 2-3: Summary of Cellular Concrete Applications Based on Density (Sari and Sani, 2017)

Density (kg/m³)	Application
300-600	Replacement of existing soil, soil stabilization, raft foundation.
500-600	Currently being used to stabilize a redundant, geotechnical rehabilitation and soil settlement. Road construction.
600-800	Widely used in void filling, as an alternative to granular fill. Some such applications include filling of old sewer pipes, wells, basement, and subways.
800-900	Primarily used in production of blocks and other non-load bearing building element such as balcony railing, partitions, parapets, etc.
1100-1400	Used in prefabrication and cast-in-place wall, either load bearing or non-load bearing and floor screeds.
1100-1500	Housing applications.
1600-1800	Recommended for slabs and other load-bearing building element where higher strength required.

2.7 Applications in Pavement Engineering

Various lightweight fill materials including LCC have been developed in recent years for usage in various civil engineering applications (Arulrajah et al., 2015). It has potential success in being used as a material for structural purposes, stabilization of weak soils, base layer of sandwich solutions for foundation slabs, industrial floor and highway as well as subway engineering applications (Kadela, Kozlowski and Kukielka, 2017).

Maher and Hagan (2016) state that the biggest issue in constructing the highways and roads over peat, organics or soft soil deposits is continual and long-term settlements that are hard to address. Full depth reconstruction requires long-term closures of the damaged pavement section. Moreover, it is usually expensive and not an efficient way of solving the problem. According to Kadela, Kozlowski, and Kukielka (2017), areas with difficult geotechnical conditions are characterized as weak soils, including grounds containing layers of organic layers. Factors, influencing decision-making processes of choosing the proper method for

dealing with those issues include geological substrate system, size of loads acting on subsoil, excessive moisture of soil, technological capabilities and costs of using the technology. Kadela, Kozlowski, and Kukiela (2017) introduced several methods of dealing with those weak soils and LCC as a potential solution to this issue was studied.

Maher and Hagan (2016) stated that using cellular concrete in the areas with weak soils allows pavement to be “floated” over the subgrade as the density of this material is a quarter of that of conventional granular fill and it is a less expensive solution than traditional lightweight materials such as polystyrene. In terms of ability of the lightweight cellular concrete to bear the loads, Kadela, Kozlowski, and Kukiela have presented the results of numerical simulations that proves that using cellular concrete as a subbase layer is potentially possible in terms of bearing the loads. The same study has shown that the tensile stress in the lower zone of the subbase layer is lower than the flexural strength of LCC that was tested.

2.8 Summary of Literature Review and Research Gaps

Lightweight Cellular Concrete offers potential construction, performance, sustainable and cost benefits when used in a pavement structure. As an alternative roadbed support over weak soils, LCC has been installed as pavement subbase material to provide more stable and stronger foundations. It has been placed in a few pavement sections across Canada and preliminary information shows that it can improve pavement performance. However, there is a lack of integrated field and laboratory evaluation, adequate information, and practices of using LCC as pavement subbase layer. There is a need to investigate the in-situ performance as a material incorporated into the pavement structure.

The overall purpose of this project is to summarize the information about the performance of the pavement sections with LCC in its structure. The laboratory tests are concentrated on mechanical properties and the possible correlation between parameters, characterizing cellular concrete in terms of density, UCS, and modulus of elasticity.

Another aim of this research is to predict the LCC performance for a given sections and compare it to the typical pavement structures in terms of failure criteria.

CHAPTER 3

3 FIELD PERFORMANCE REVIEW

This Chapter describes five road sections with installed Lightweight Cellular Concrete (LCC) layer as a subbase. All the available information was compiled in a table and analyzed at the end of the Chapter. Similar features of the road sections, as well as challenges during construction and recommendations for the future construction of similar pavement, are discussed in this Chapter. In addition, methodology for the thesis is described in this Chapter (Figure 3-1).

3.1 Methodology

For analyzing the construction experience of using LCC as a subbase material, past projects (case studies) were studied. As a first step of collecting the data, published papers on the past projects where LCC was installed as a subbase layer were studied. After that, technical reports were analyzed and visual inspections on the road sections were completed. All of the available information from the road sections was compiled and analyzed concluding in similarities and/or differences in the performance.

After analyzing the data from the past projects, the next step was to predict performance of the installed LCC sections in the future. Chapter 4 aimed to predict the performance of the road sections located in Ontario in terms of fatigue cracking and rutting resistance. In addition, bearing capacity of the road sections was determined. These parameters were discussed under the failure criteria analysis. Furthermore, the comparison between LCC and Granular B subbase materials that were installed on the same road sections was completed and discussed.

Knowing the current condition of the LCC road sections that were reconstructed in the past as well as having an idea of the predicted performance of the sections in the future, it is crucial to understand the mechanical properties of LCC that are currently being used in construction. In Chapter 5, mechanical properties of the in-situ cast samples will be determined and compared to the typical values in literature. In addition, the relationship between the mechanical properties of LCC will be discussed.

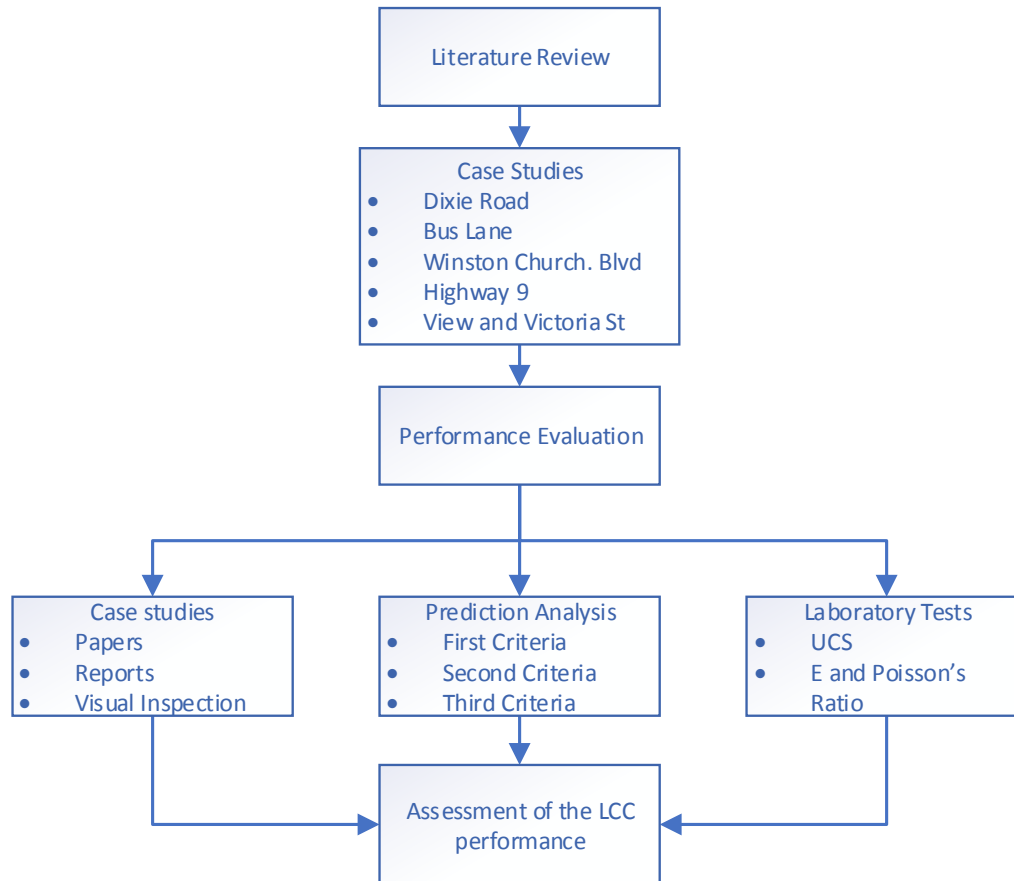


Figure 3-1: Overview of Research Methodology

3.2 Case Studies

LCC may be used in many applications in infrastructure projects. Currently, there are not many companies who produce and provide cellular concrete solutions. There are several cases when LCC was installed into roadway sections and infrastructure applications in Canada. The scope of this project is to study the LCC as a subbase layer.

Five road sections that were constructed using LCC as a subbase layer were investigated, including Dixie Road, Winston Churchill Boulevard, Highway 9, Brentwood Light Rail Transit (LRT) Bus-Lane and View and Vancouver Streets. All five sections have similar pavement structures, including an asphalt concrete surface layer, an unbound granular base layer, a lightweight cellular concrete subbase layer, and subgrade soil. The pavement surface distresses were determined by following ASTM D6433, which classifies nineteen types of pavement distresses. These distresses such as alligator cracking, bleeding, corrugation, longitudinal and transverse cracking, and rutting were inspected. The inspections were conducted manually

instead of using automated data collection vehicles. The results of the field inspections are described in the following sections.

3.2.1 Dixie Road. Region of Peel, Caledon, Ontario, Canada

3.2.1.1 Background

The Region of Peel reconstructed a 120-metre section of rural highway in 2009. The main issue, within the section, was ongoing settlement for a number of years. The proposed solution was required to be environmentally friendly and to minimize the impact on the adjoining wetlands. Instead of removing and replacing the existing embankment with granular material, the Region chose to use lightweight cellular concrete as an alternative. Traditional reconstruction would have required considerable dewatering, extensive peat removal, the erection of sheet piling and then replacing peat with granular materials. Figure 3-2 demonstrates the location of the road.



Figure 3-2: Road Section Location (Google maps, 2018)

A geotechnical investigation was completed before reconstruction of the road in 2009. This investigation included pavement cores and boreholes throughout the settlement area, resulting in the following conclusions:

- Thickness of the asphalt layer ranged from 150 mm to 280 mm
- Granular base/subbase was at the depth from 1.4 to 1.8 m
- Peat/marl deposits were located from the depth of 2.1 m up to 5.4 m. with $M_r = 17$ MPa

After the geotechnical investigation was done by a contractor. Full excavation of the weak soils, followed by backfilling with granular material was suggested. The pavement structure to support 500,000 cumulative ESALs was recommended as follows:

- Removal of existing material - 5.2 m
- Hot Mix Asphalt - 140 mm
- Granular A Base Course - 150 mm
- Granular B Type I Subbase - 400 mm

Instead of removing and replacing the embankment to a depth of 5.2 m, the Region chose the following pavement structure:

- Hot Mix Asphalt - 140 mm
- Granular A Base Course - 150 mm
- LCC CEMATRIX CMEF-475 (CEMATRIX Manufactured Engineering Fill) - 650 mm

The typical cross section for the cellular concrete section is presented in Figure 3-3.

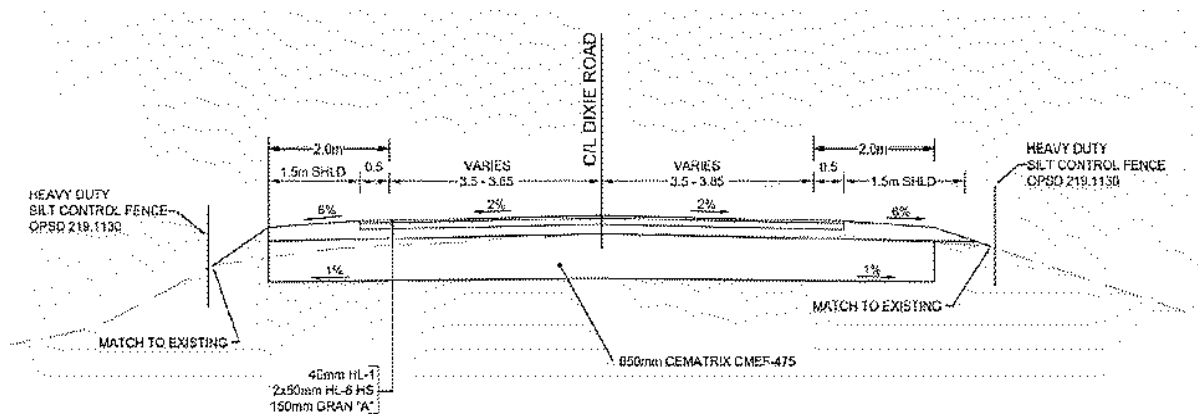


Figure 3-3: Typical Cellular Cross Section (Griffiths and Popik, 2013)

Cellular concrete was produced and placed on site by CEMATRIX Company with the dry-mix production units. The construction process is shown in Figure 3-4.



Figure 3-4: Construction Process of Dixie Road, Region of Peel, Caledon, Ontario, Canada (CEMATRIX)

3.2.1.2 Field Investigation

Griffiths and Popik (2013) investigated the in-place performance in 2013. The evaluation of the section included the following:

- Visual condition survey of the existing pavement surface
- Ground Penetrating Radar (GPR) survey with various transverse scans to provide layer thicknesses and subsurface images of the pavement utilizing the CEMATRIx LCC
- Falling Weight Deflectometer (FWD) testing to determine the structural capacity of the lightweight cellular concrete section in comparison with the adjacent pavement

Visual Condition Survey

The visual pavement condition survey of the site was completed on June 4, 2013, and concluded that pavement section was in good condition. In total, three slight longitudinal cracks and one moderate pavement distortion/heave were observed in the area. Figure 3-5 shows the cracks. The longitudinal cracks were located in the northbound lane, approximately at the midpoint of the site.



Longitudinal Cracking (centreline)



Transverse Cracking



Minor crack



Transverse Cracking

Figure 3-5: Condition of Dixie Road, Region of Peel, Caledon, Ontario, Canada

All three cracks were found to be close to the centreline, with a slight meander into the outer wheel-path. The pavement distortion/heave at the north transition extended for approximately 25 m and appeared to be worse in the southbound lane, than in the northbound direction. The distress appeared to be caused by a heave in the area marked at the end of the LCC material. The adjacent pavement sections were also investigated, and it appears to be in excellent condition without any distresses. In general, the condition of the section is performing adequately after three years of construction.

It was also observed that LCC material was exposed at the SB shoulder rounding. It was observed that part of the gravel, which was intended to cover and protect the LCC from weather, was eroded into the ditch. Thus, the LCC layer was easily broken from the exposed edge.

A. Ground Penetrating Radar

As part of this evaluation, a Ground Penetrating Radar (GPR) survey was completed. GPR is a non-destructive device that uses a radar pulse to produce subsurface images. Ground Penetrating Radar equipment is shown in Figure 3-6.

The GPR survey was completed in order to identify the thicknesses of the pavement layers and the border with the adjacent road sections. More comprehensive GPR surveying was completed at the areas containing longitudinal cracking. The GPR data was collected by summarizing results obtained from 3 cycles of measurement for each line:

1. Using SmartCart, equipped with a NOGGIN 250 MHz GPR sensor
2. Using SmartCart, equipped with a NOGGIN 500 MHz GPR sensor
3. Using SmartCart, equipped with a NOGGIN 1000 MHz GPR sensor



Figure 3-6: Ground Penetrating Radar Equipment

Griffiths and Popik (2013) reported that thicknesses of the pavement layers varied (some of which were within the normal range and some were not). For example, Table 3-1 shows a part of the report for lane №10 (L10):

Table 3-1: Comparison of Pavement Structures

Layers	Designed, mm	GPR reading (range), mm
Asphalt	140	126-178
Granular Base	150	68-235
LCC	650	Vary because of the not flat underlying subgrade

Longitudinal and transverse images of the lanes were also obtained (Figures 3-7, 3-8).

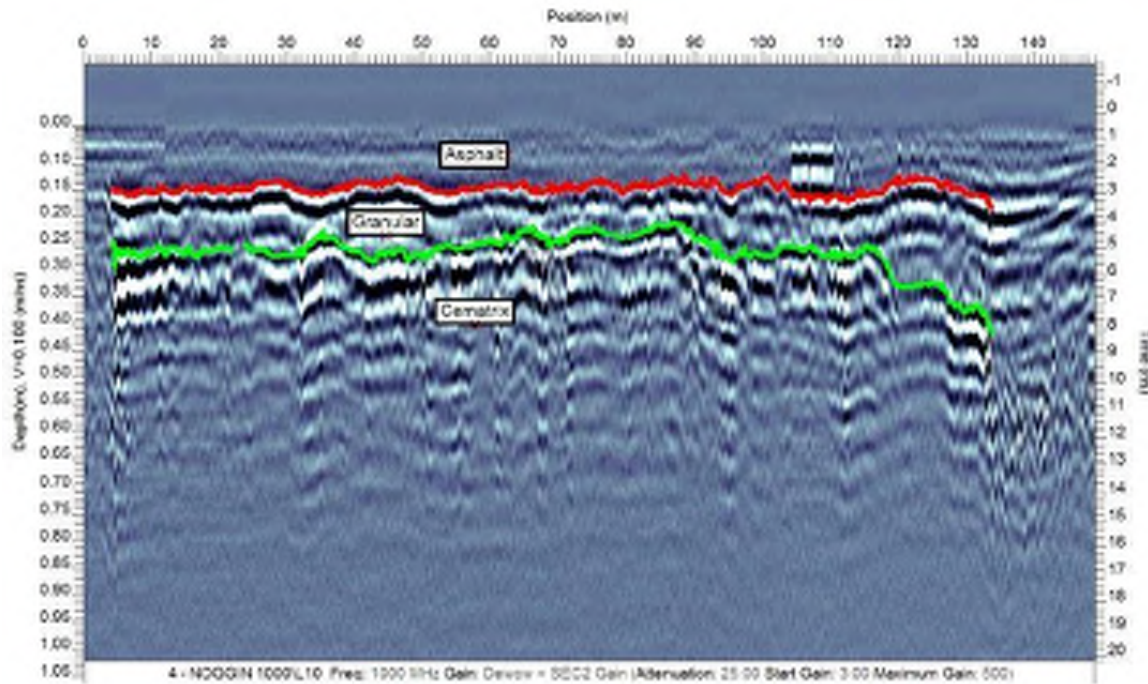


Figure 3-7: GPR Longitudinal Image of Southbound Lane, L10 (Griffiths and Popik, 2013)

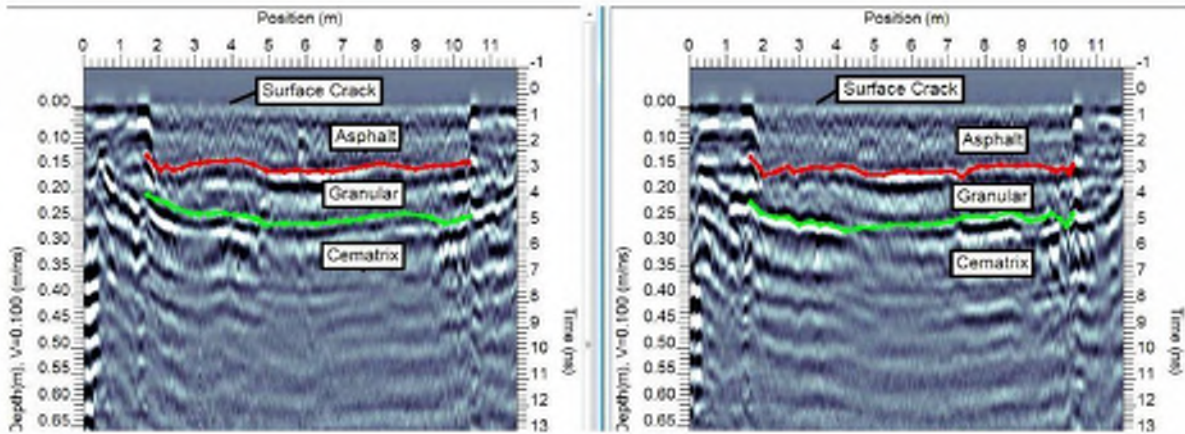


Figure 3-8: GPR Transverse Images at Longitudinal Crack Locations, L4, and L5 (Griffiths and Popik, 2013)

B. Falling Weight Deflectometer

Pavement load/deflection testing was completed on July 30, 2013, and included 54 tests. The Dynatest Falling Weight Deflectometer (FWD) was used for the structural evaluation of this pavement section. On the traditional road section, from the both sides of the LCC section, FWD testing was completed every 5 m in southbound and northbound directions. For the transition areas, between LCC and traditional section, FWD testing was completed on 2 m intervals for a length of 10 m. Each test included 4 drops, with the first drop being a seating load, and the following three loads at roughly 30, 40 and 75 kN. The testing equipment is shown in Figure 3-9. Full FWD report is presented in Appendix I.



Figure 3-9: FWD Truck and Trailer (Griffiths and Popik, 2013)

The collected FWD data was analyzed based on the pavement thickness measured by the GPR survey. For the purposes of the FWD analysis within the Lightweight Cellular Concrete section, the LCC layer was assumed to be part of the pavement structure. Two parameters were determined: the composite elastic pavement modulus and the structural coefficient. The composite elastic pavement modulus of LCC section ranged from 714 to 737 MPa, which is higher than the adjacent section (514 to 670 MPa). This resulted in increasing of the composite pavement structural number of LCC section, which ranges from 175 to 224 mm while the adjacent section range from 128 to 154 mm.

The structural coefficient of the LCC material was determined by the analysis of FWD data. The structural coefficients of the asphalt and Granular base layers used in the analysis were 0.38 and 0.12 respectively (Griffiths and Popik, 2013). In comparing the overall strength of the LCC section, the composite elastic pavement modulus of the pavement structure incorporating the LCC material was found to be stronger, than the adjacent conventional pavement structures (Figure 3-10).

The calculated structural number (SN) for each layer was added together and subtracted from the SNEff at each FWD test location. The resulting SN for the LCC layer was divided by the layer thickness of 650 mm to obtain the equivalent AASHTO structural coefficient for the LCC material. The averaged back-calculated structural coefficient for the LCC material used on this site is approximately 0.2, after removing outliers that were more than one standard deviation of the average. In conclusion, following the AASHTO flexible pavement design methodology for designing a flexible pavement utilizing the CEMATRIX LCC-475 (with a density of 475 kg/m³), a structural coefficient of 0.2 should be used. Structural coefficient was obtained after the road had been in use for four years, thus, some adjustments may be applied to the structural coefficient. Similar tests may be conducted in the future on the newly constructed pavements in order to determine structural coefficient soon after construction.

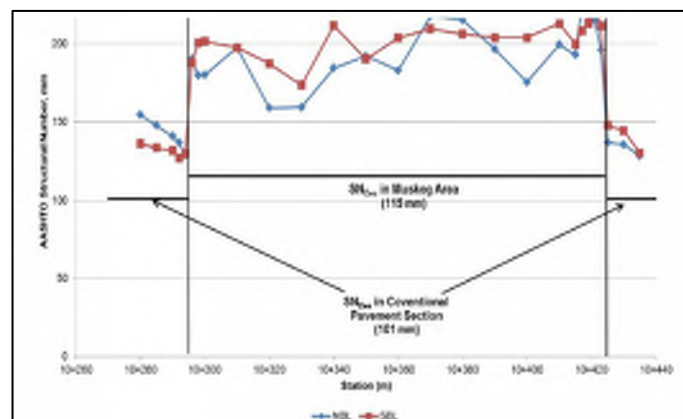


Figure 3-10: Structural Number Comparison Plot (Griffiths and Popik, 2013)

3.2.1.3 Findings and Discussion

1. In general, the pavement structure on Dixie Road appeared to be in good condition, with few distresses. With the LCC section in service for roughly three years, it is encouraging to see that the condition of the roadway in this section continued to perform similarly to the pavements adjacent on either side of the LCC section.
2. The overall average asphalt thickness along the whole road section is close to the designed number – 148 mm vs 140 mm. The thickness of the Granular base is not consistent and in some places, it is thinner than the design requirement of 150 mm. The lowest thickness of the Granular base is 68 mm which was found in the place where longitudinal cracks were observed by visual survey.
3. It was also observed that the top of the LCC layer was not flat at the border with the adjacent road section. It was observed on the longitudinal image of the GPR survey. Because of that, the granular layer was detected as thick as 235 mm instead of designed 150 mm. Griffiths and Popik (2013) linked this information with the fact that some distortions on the pavement surface in this area were observed as consequences of some ground movement continued after construction.
4. In order to access those distresses and its cause, a detailed forensic investigation was recommended.
5. It can be noticed that on the GPR transverse images that pavement layers were shown as a bowl shape, with the sides of the layers going up. Griffiths and Popik (2013) reported that this is a result of the top surface, which was constructed with a crossfall but was shown on the image as a flat line. If these images were adjusted to include the surface crossfall of the pavement and shoulders, then the top of LCC layer would have shown a relative flat surface.
6. The construction of the LCC embankment should be completed in lifts, with suitable layer thicknesses to optimize strength of the material, with the practical construction of the embankment. It is recommended that the individual lift thickness do not exceed 300 mm. Furthermore, the design of each lift should be such that the edges of the upper lift are offset by a minimum of 500 mm inward from the edge of the lower lift. The LCC layer should be constructed with a pyramid shape, with the top lift constructed 0.5 m beyond the edge of the travel lane. The staggering of the various lifts of the LCC embankment will allow for easier grading of the embankment slopes while maintaining adequate coverage of the LCC material at all times.
7. The top lift should also be constructed with a minimum 1 percent cross-fall, so that subsurface drainage is maintained at the top of the LCC material toward the outside ditches. Any imperfections in the transverse profile of this layer could create a ‘bath-tub’ situation, which would trap water at this layer interface. This could affect the performance in the Granular base material placed on top of the LCC layer. The embankment slopes should be covered using Granular base type material, with the

embankment slope designed to minimize erosion of the material that could potentially expose the LCC. Transitions at each end of the LCC embankment should also be carefully designed to provide a smooth transition and minimize any abrupt heaves with the adjacent earth embankments. It is critical that frost susceptible material is not used to construct the transition areas. Furthermore, the design of these transitions will need to ensure that they are constructible while meeting the foundation requirements for embankment stability.

3.2.2 Brentwood Light Rail Transit (LRT) Bus-Lane. Calgary, Alberta, Canada

The Brentwood bus-lane in Calgary was experiencing heavy loading due to the single rear axles of city buses. The bus lane had traffic volumes of up to 100 buses per hour and had frost-heaved substantially and became virtually impossible to drive on. The subbase of the road was composed of saturated silty deposits, over 30 m in depth. The subgrade soil had a California Bearing Ratio (CBR) of 0.8%. In 2000, the road was completely reconstructed with the following structure:

- 125 mm of asphalt
- 150 mm of Granular base course
- 200 mm of CEMATRIX CMRI-475 Insulating Road Base
- 50 mm of drainage rock (with subdrains beneath the curb & gutter)
- Geotextile fabric

The location of the road section is presented in Figure 3-11.

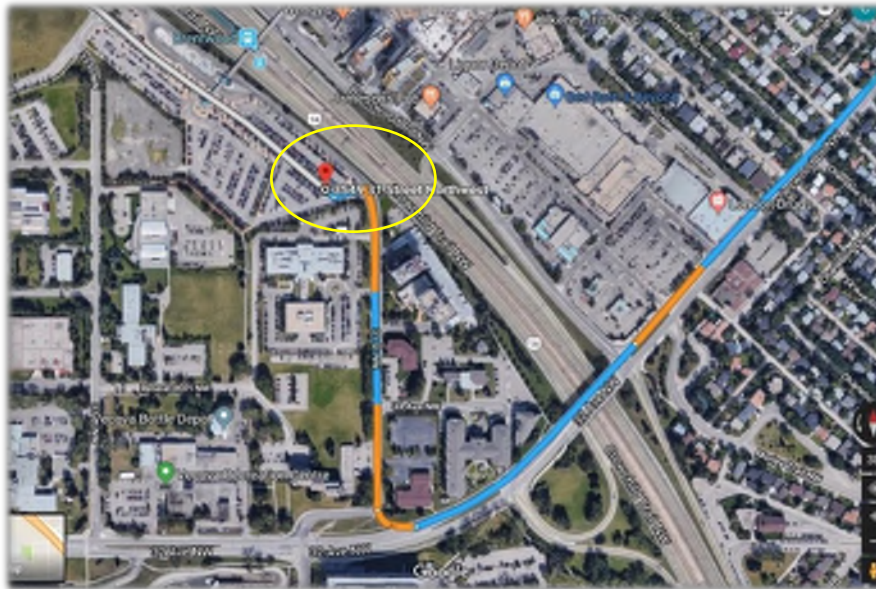


Figure 3-11: Site Location (Google Maps, 2018)

Figure 3-12 presents the reconstruction process of the bus-lane before and after pouring the LCC material.



Figure 3-12: Bus Lane. (a) Reconstruction Process. Placing the LCC (CEMATRIX) (b) After Installing the LCC Layer (CEMATRIX)

Since construction, the road has experienced no frost heaving and required no additional remediation between 2000 and April 2018. A Benkelman Beam Deflection Test resulted in 0.012 inches (0.30 mm) of deflection, much less than the 0.035 inches (0.89 mm) allowed for such a road.

The performance of the LCC section in comparison to the adjacent conventional pavement structure is shown in Figures 3-13 and 3-14. The transition area between the LCC and non-LCC section is obvious and distresses at the conventional section were observed after the visual inspection in April 2018. The Lightweight Cellular Concrete section performed for a significant period of time (18 years) without any potholes and severe cracks. No maintenance was conducted to this section of the road during its service life.



Figure 3-13: Pavement Distresses on the non-LCC section - 1(CEMATRIX, 2018)

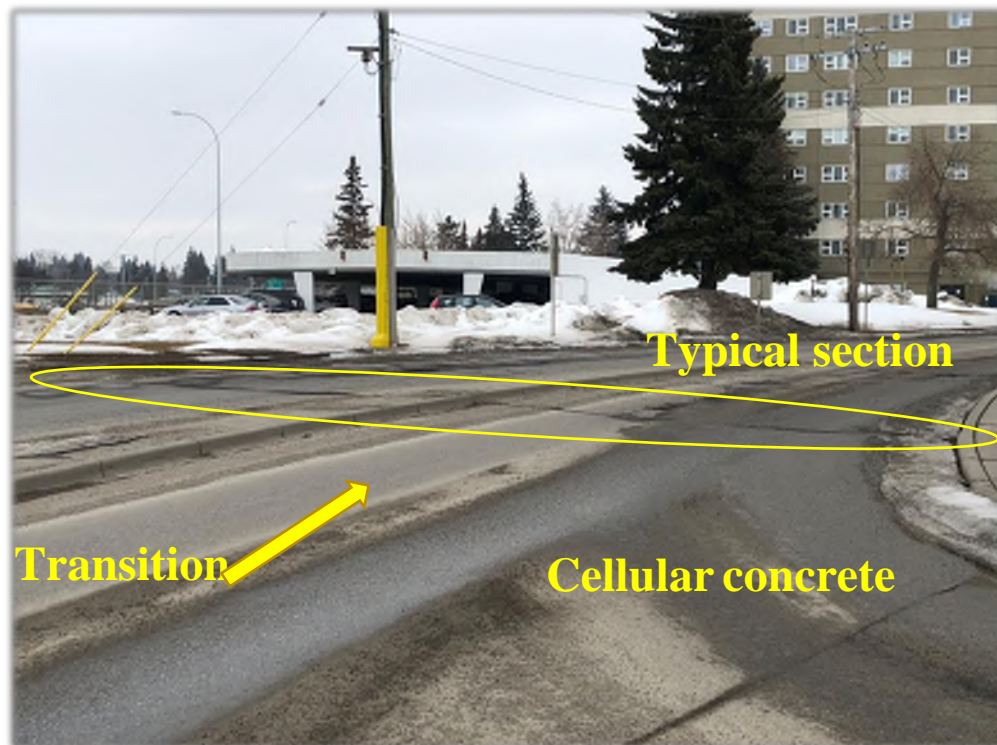


Figure 3-14: Pavement Distresses on the non-LCC section – 2 (CEMATRIX, 2018)

3.2.3 Winston Churchill Boulevard. Brampton, Ontario, Canada

The reconstruction of Winston Churchill Boulevard is similar to the Dixie Road project. It is a two-lane rural road. The project was completed in 2016. The location of the road section is presented in Figure 3-15.



Figure 3-15: Location of the Road Section (Google Maps, 2018)

The pavement structure consists of the following layers:

- Asphalt concrete layer - 120 mm
- Granular A base layer - 240 mm
- Lightweight Cellular Concrete at the density of 475 kg/m^3 – 550 mm
- Existing subgrade – peat

The pavement structure that was installed on Winston Churchill Boulevard is shown in Figure 3-16.

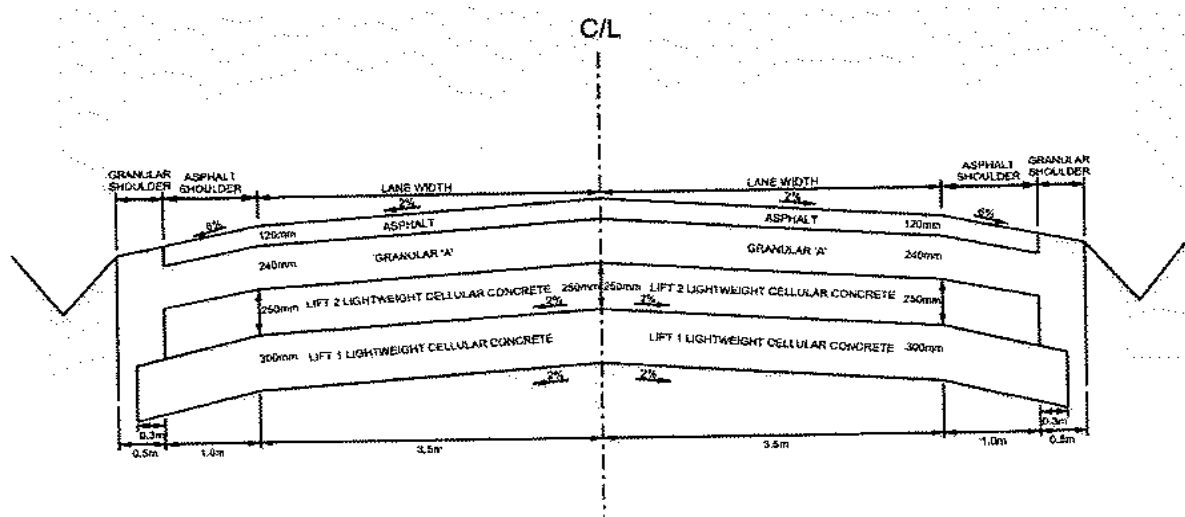


Figure 3-16: Pavement Structure. Winston Churchill Boulevard (CEMATRIX)

The field inspection found that the pavement remains in good condition after one year of construction. No severe cracks or rutting were found during the inspection (Figures 3-17 a, 3-17 b).



(a)



(b)

**Figure 3-17: Condition of Winston Churchill Boulevard, August 2017 (one year after construction).
(a), (b) – Overall Condition of the Road**

3.2.4 Highway 9. Holland Marsh, Ontario, Canada

The Highway 9 site is located north of Toronto. It is 1.5 km meters west from Highway 400. The location of the problematic area on Highway 9 is presented in Figure 3-18.



Figure 3-18: Highway 9 Site Location (Google Maps, 2018)

The construction project on Highway 9 aimed to overcome a weak soil problem. The soil in this area included thick organic deposits, which are challenging for pavement design. According to the geotechnical investigation, completed by Stantec in 2014, pavement structure was underlain by organic material ranging from 3.7 to 7.0 m. The site is located directly adjacent to the Pottageville Swamp Conservation Area wherein organic soil materials such as peat can be found at the surface (Figure 3-19). Inorganic soil was also observed, consisting of soft to firm clayey silt to silty clay and compact silt and sand. The groundwater level ranged from 1.5 m to 2.3 m below the surface of the existing pavement.



Figure 3-19: Highway 9 Site Location with the Local Landscape (Google Maps, 2018)

Settlement was observed on a portion of Highway 9 in 2014. Asphalt padding and other temporary repairs were considered as possible solutions to this issue, but it would only add additional weight to the current pavement structure, thus leading to potential further settlement. The potential for future repairs was a deterrent. LCC was chosen as an economical and sustainable remediation treatment to address the continued settlement, reduce safety concerns and minimize future maintenance costs. The use of LCC reduced the need of deep excavation, thus, reducing a considerable amount of excess material requiring disposal, construction time, amount of backfill material, and reducing the impact on the environment (Maher and Hagan, 2016).

The section was reconstructed in 2014. The settlement problem was observed only at the eastbound lanes, so traffic was temporarily moved to the westbound lanes. The settlement remediation treatment included excavation of a length of 100 m to a depth of 1.5 m to provide the pavement structure of:

- Asphalt concrete layer – 200 mm
- Granular “O” base layer – 200 mm
- Lightweight Cellular Concrete at the density of 475 kg/m^3 – 1100 mm
- Existing subbase

The permeability of the subgrade fill material was relatively low, so no polyethylene sheet was used to mitigate the loss of LCC material. A biaxial geogrid with a minimum tensile strength of 0.8 kN/m was installed in a LCC layer at a depth of 0.3 m below the top of the LCC.

The placement of the LCC was completed in three days. In total, 905 m^3 of LCC material was placed. Figure 3-20 demonstrates the construction process of installing the LCC layer. During the placement of cellular concrete, Quality Control (QC) testing including casting unconfined compressive strength cylinders, wet cast density, and air temperature. A list of the QC specifications is presented in Table 3-2.



Figure 3-20: Highway 9 Construction Process (CEMATRIX)

In order to mitigate the presence of water below the LCC layer, a drainage system was developed, including 1% slope of the bottom of LCC layer to the existing subgrade, a transversely installed subdrain at the end of LCC, and a longitudinally installed subdrain on the highway centerline. All these measures were done to capture water that could pond below the LCC. In addition, transition sections were arranged from both ends of the LCC section. Those transitions were critical in mitigating differential performance of LCC and adjacent sections.

Table 3-2: Project Specifications and QC Results (Maher and Hagan, 2016)

Item	Project Specification Requirements	QC Results	Average of QC Results
Minimum Unconfined Compressive Strength	1.0 MPa @ 28 days	0.9 to 1.7 MPa	1.3 MPa
Wet Cast Density	523 to 578 kg/m ³	525 to 580 kg/m ³	550 kg/m ³
Air Temperature	Protection required for sub-zero temperatures	10 to 17 ⁰ C	14 ⁰ C
Cellular Concrete Temperature	-	22 to 26 ⁰ C	24 ⁰ C
Max. Lift Thickness	500 to 600 mm	300 to 500 mm	N/A

Field visual inspection was completed in 2015, one year after construction. It was observed that the pavement was performing well. Figures 3-21 and 3-22 show that no severe distresses were found on the pavement surface. One negligible imperfection was noted in the transition area.

Another field visual inspection was completed in 2017, three years after construction. The field inspection stated that the pavement remained in good condition after three years of service. No severe cracks or rutting were observed during the inspection.



Figure 3-21: Condition of Highway 9, Three Years after Construction



Figure 3-22: Condition of Highway 9, Three Years after Construction

3.2.5 View and Vancouver Streets, City of Victoria, British Columbia, Canada

The City of Victoria was experiencing several settlements in the area around the intersection of Vancouver Street and View Street (Figure 3-23). The intersection had been reconstructed several times previously, but the major settlement issue continued to occur. Settlement was a major issue in this area because of the excessive decay and consolidation of the underlying peat. The option of removing and replacing the weak soils was proposed, but because it was an expensive and impractical procedure, finding a different solution was a priority. Moreover, since this intersection is located in the downtown area, the time of the closures played a big role in selecting a construction approach.



Figure 3-23: Site location. (Google maps, 2018)

Dolton et al. (2016) reported that due to excessive total differential settlement in the area, the roadways and sidewalk experienced surface distresses and damage had occurred to underlying utilities. These roadways were originally built over a peat layer that extends up to 5.3 m below the existing ground surface. Below the peat is a thick layer of soft silty clay overlying bedrock at a depth of 30 – 40 m. Use of Lightweight Cellular Concrete was chosen for this project with the following pavement structure design:

- Asphalt concrete – 75 mm
- Crush Granular base course - 150 mm of 20 mm

- LCC with wet density of 475 kg/m^3 – 500 mm
- Existing subgrade

The construction at View Street and Vancouver Street in the City of Victoria, British Columbia was completed from September 2007 to April 2008 in several stages. The LCC was produced on site, and as it is shown in Figure 3-24, using the “wet” process of production (Dolton et al., 2016). LCC with wet density of 475 kg/m^3 was used as subbase in this project. Quality Assurance/Quality Control (QA/QC) testing was carried out during construction and found that cast density ranged between 435 kg/m^3 to 486 kg/m^3 with an average of 462 kg/m^3 . Cylinders were also cast according to ASTM C495 for Compressive strength of LCC and results revealed an average of 1.0 MPa (range 0.8 to 1.1 MPa) at 28 days.



Figure 3-24: View Street and Vancouver Street Construction Process. Wet Mix Equipment (CEMATRIX)

Total length of the sections that were reconstructed was 430 m on View Street and 137 m on Vancouver Street with a total of $2,246 \text{ m}^3$ of LCC. It was placed over fourteen pour days of construction. Gravel backfill compacted with no vibration was placed on the cellular concrete before traffic was allowed on the roadway.

Golder Associates Ltd. carried out Benkelman Beam and Falling Weight Deflectometer (FWD) testing at about 20 m intervals in February 2008. The intention of the test was to carry out the test within the outer wheel paths, however, due to different obstacles, some inner wheel paths were tested as well. The weather conditions during the testing were cloudy, with an air temperature of 13° C and pavement temperature of 10° C .

The Benkelman Beam test is a method for measuring pavement deflections under static wheel loads. As presented in Figure 3-25, a 3.65 m beam is placed between the dual tires of a truck (80 kN axle load) and height measurement gauge on the end of the beam measure the vertical

rebound of the pavement after the truck is driven away (TAC, 2016). The testing was following the ASTM D 4695 “Standard Guide for General Pavement Deflection Measurements” procedure. The Benkelman Beam deflection data analysis was carried out in accordance with the Asphalt Institute MS-17 method: “Asphalt Overlays for Highway and Street Rehabilitation, Manual Series № 17”. No seasonal correction factor was applied for Maximum Pavement Spring Rebound (MPSR) due to winter conditions. The average rebound was 0.63 mm on View Street and 0.65 mm on Vancouver Street (Table 3-3).

Table 3-3: Benkelman Beam Results (Golder Associates Ltd. Report, 2008)

Section	Average Rebound Reading (mm)	Temperature Corrected Rebound (mm)	Standard Deviation	Mean plus 2 STDV	MRSR (mm)
View St. New Pavement	0.63	0.73	0.15	1.03	1.03
Vancouver St. New Pavement	0.65	0.75	0.23	1.21	1.21
View St. Old Pavement	0.53	0.57	0.41	1.40	1.40



Figure 3-25: Benkelman Beam Deflection Testing

Falling Weight Deflectometer (FWD) testing was also conducted. This involves evaluating the dynamic response to the fall of the weight from a recorded height. Seven sensors were installed and spaced out at known distances from the load plate to measure deflection. FWD testing was following ASTM D 4694 “Standard Test Method for Deflections with a Falling-Weight-Type Impulse Load Device”. Three load levels were used to determine the deflection response (40, 50, and 75 kN approximately) at each test point.

The measured FWD dynamic deflections were normalized to represent the equivalent deflection for a standard wheel load of 40 kN at an asphalt pavement temperature of 21⁰ C. The pavement surface modulus, which indicates the overall strength of the pavement, was also determined. A summary of the FWD testing data is shown in Table 3-4. Spring correction factor was not applied. Results reflected consistent static deflection for the LCC sections, and that the deflection of the non-LCC section was 111% times higher than that of the LCC section. The elastic moduli of the LCC was also reported to be 445 MPa (Standard deviation 146 MPa) and 341 MPa (Standard deviation 99 MPa) which are higher than the typical values for gravel (University of Waterloo, 2011). The elastic moduli of various layers were estimated using ELMOD software (Dynatest 2006). The mean elastic modulus derived from LCC layer was inferred to be 341 MPa on View Street and 445 MPa on Vancouver Street.

Table 3-4: FWD Test Data

Street Name	Normalized Deflection (mm)				Pavement Surface Modulus (MPa)	
	Mean	Standard Deviation	Mean+ 2 STDV	Static Deflection	Mean	Standard Deviation
View St. New Pavement	0.49	0.08	0.64	1.0	361	60
Vancouver St. New	0.43	0.05	0.55	0.85	402	53
View St. Old Pavement	0.51	0.41	1.36	2.11	488	238

3.3 Summary of Case Studies

Table 3-5: Summary of the Available Cases of Using LCC as a Subbase Material in Pavement Construction in Canada

	Dixie Road, Region of Peel, Ontario	Highway 9, Holland Marsh, Ontario	View and Vancouver Streets, City of Victoria, British Columbia	Brentwood Light Rail Transit (LRT) Bus-Lane. Calgary, Alberta	Winston Churchill Boulevard, Brampton. Ontario
Location	Ontario 43°80'49.24" N 79°84'98.97" W	Ontario 44°02'52.65"N 79°61'25.19"W	British Columbia 48°42'45.48"N 123°35'67.65" W	Alberta 51°08'51.72"N 114°12'95.76" W	Ontario 43°69'87. 0"N 79°92'11. 0"W
Cause of Reconstruction	Settlement. Length-120m Peat/marl deposits were located from the depth of 2.1 m to 5.4 m below the existing pavement surface	Settlement. Length-100m Underlain with organic materials (peat) and inorganic (soft to firm clayey silt to silty clay or compact silt and sand)	Settlement. Length- 430m on View Street and 137m on Vancouver Street. Excessive decay and consolidation of the underlying peat	Length-60m. Severe frost heave and subsequent spring thaw weakening of the frost susceptible soils.	Settlement. Length- 300m. Underlain with peat.
Date of Construction	August- November 2009	October 2014	November- February 2007	Summer (July- August) 2000	Summer 2016
Road Type	Rural highway	Highway	Urban	Urban	Rural
Structure	AC-140mm; Granular 'A'- 150mm; LCC-650mm	AC-200mm; Granular "O" base layer-200mm; LCC-1100mm; Biaxial geogrid (300m from the top of LCC layer)	AC-75mm; Crushed Granular base course- 150mm; LCC-500mm; (Tensar BX1100 geogrid was placed between the LCC layers)	AC-125mm; Granular base course-150mm; LCC-200mm; drainage rock- 50mm; Geotextile fabric (at the bottom of LCC layer)	AC-120mm; Granular base course- 240mm; LCC- 550mm; geogrid reinforce fiber glass

Material Composition	CEMATRIX CMEF-475. "Dry" mix	CEMATRIX-475. "Wet" mix	CEMATRIX-475. "Wet" mix	CEMATRIX CMRI-475.	CEMATRI X-475. "Dry" mix
Performance Evaluation	Visual inspection, FWD, Benkelman Beam test	Visual inspection	FWD, Benkelman Beam test	Visual inspection, Benkelman Beam test	Visual inspection
Construction Challenges	Water, stability issues, transition areas	Transition areas, drainage, stability issues	Underlying utilities, Stability issues	Heavy traffic, stability issues	Crossfall, wet soils, stability issues

3.4 Discussions and Recommendations

Summarizing the available case studies of using LCC as a subbase in pavement construction, it is worth saying that LCC can be successfully used in rural and in urban conditions. The ages of the sections reviewed varied from two years up to 18 years, which gives an approximate understanding of pavement performances up-to-date. The oldest of the presented section is Brentwood Light Rail Transit (LRT) Bus-Lane in Calgary (18 years) and is performing well, especially in comparison to the adjacent road sections without LCC installation. The younger cases such as Winston Churchill Boulevard (Ontario), Highway 9 (Ontario) and Dixie Road (Ontario) are also performing well, with no severe cracks. The minor cracks that were observed on Dixie Road by visual survey seven years after construction are, most likely, the result of construction defects of the upper layers (GPR and FWD results confirm this theory). The road sections in the City of Victoria, British Columbia performed well up to 2010 when the last inspection was made. Unfortunately, no further performance data for this section was found.

Three out of five considered road sections are located in Ontario, approximately in one area, with similar weather conditions, one section is in Calgary, and one section is located in British Columbia.

All projects were aiming to solve a settlement problem. It is observed that settlement usually occurs on localized parts of the road and not on the whole length of the road. In four projects, the length of the reconstructions was less than 150 meters and only in one project was a longer section (the City of Victoria) needed. Moreover, this section consisted of two intersecting roads, which formed a bigger area of settlement.

The common time for construction was summer-fall time as the soil is more stable and no freeze-thaw cycles are occurring and the subgrade is thawed. Most of the projects were done in July-November and none in the spring.

In terms of the structure of the sections, they all follow the same pattern: LCC layer at the bottom (usually with the geogrid or geotextile reinforcement), followed by Granular base material and asphalt concrete layer at the top. The thicknesses of the layers are different, depending on the purpose of the road and underlying soil.

FWD and Benkelman Beam tests are the most commonly used methods for evaluating the performance of the LCC sections to date.

Some projects were using “dry” mix process and some “wet”. It is common to use “dry” mix process of producing the material for the projects, where relatively high volumes of LCC were needed. However, in the City of Victoria, the installation process happened in three stages and in different months because of the specific road closures and downtown location of the road. In that project, “wet” mix process was used.

In order to use LCC in a pavement structure as a subbase, certain activities have to be taken into consideration and implemented into the construction process. A number of general observations that are applicable to most LCC projects have been made from studying the road sections across Canada. These observations are presented in the following paragraphs.

Soils

Generally, the main issue that using LCC is intended to address is a process of settlement of road sections. In most of the case studies, settlement is happening because of weak subgrade soils. It can be either organic material (peat) or inorganic soils (soft to firm clayey silt to silty clay or compacted silt and sand). Placing a thick layer of unbound granular material on top of those subgrade types, to solve the settlement issue, may lead to more settlements in the future due to the excessive weight of the whole structure. In addition to that, a lot of excavation is often needed to remove the weak soil before placing the unbound Granular material.

Water

Placement of the LCC during light rain is possible but should be avoided in heavy rain. Water is a significant factor, influencing the construction of pavements using LCC. Groundwater seepage control of the excavations, where LCC will be placed, is required. This needs to be done to prevent floating of the material, as the target density of LCC in the case studies was 475 kg/m^3 , which is less than water density (1000 kg/m^3). Ignoring water presence in the excavations may lead to buoyancy forces affecting the pouring and restarting the production and placement from the very beginning may be required.

Drainage

It is very important to prevent moisture from weakening the pavement structure once it is in-service. Usually, pavements require a slope of 2% in order to let the stormwater from the surface of the pavement, and subsurface water to drain by the gravity force. For achieving the 2% slope, LCC must be placed in steps, using formwork.

Transitions

Constructing the quality and proper transition areas between pavement sections with LCC and conventional granular pavement is crucial. Those two different pavement structures have different thermal properties and different densities. Because of that, different performance of the pavement structures can occur in those areas during the freeze-thaw conditions. As frost is unlikely to penetrate through the LCC pavement due to its high porosity, reverse heaving of the transition occurs (Maher and Hagan, 2016). In order to mitigate this effect, granular transition tapers can be made in the transition areas. The commonly used is a 10/1 ratio of horizontal to vertical respectively.

Equipment

All the material brought to site must be transported in pre-cleaned equipment and machinery. The transporting equipment must be cleaned, rinsed and completely emptied of the concrete, aggregates, and any other materials that were previously transported (Maher and Hagan, 2016). This was a general consideration in the case studies that were using “dry” mix process; however, for the View Street and Victoria Street intersection, that used “wet” mix process, it was a significant consideration.

This study provides an overview of the current pavement condition of the five sections that were constructed using lightweight cellular concrete as subbase layer material. Results have shown that all five sections were in good pavement condition. However, in-depth pavement data collection has to be done in order to provide a comprehensive review of the performance of the sections with lightweight cellular concrete as subbase layer. Therefore, further investigation is recommended. This could be achieved by using pavement instrumentation such as asphalt gauges, earth pressure cells, and environmental equipment in the new pavement structures.

CHAPTER 4

4 PAVEMENT DESIGN AND ANALYSIS

This Chapter explains the procedure on how pavement design for LCC can be conducted. The predicted performance of the LCC road sections will be determined by failure criteria analysis. Comparison of LCC section to typical Granular material will also be conducted.

4.1 Introduction into Pavement Design

Structural design of pavements is a complex process. Several factors have to be considered when designing a road. These factors are traffic (axle or gear loads, repetitions), environment, available materials, desirable performance of the pavement, project cost, sustainability, and construction resources (TAC, 2013).

Traffic volume is usually described by Annual Average Daily Traffic (AADT), which shows the range of vehicles of various sizes, weights, and axle configurations. The 80 kN standard single axle is used for quantifying the traffic in pavement design. It allows transition of the cumulative damage from the range of vehicles into a number of Equivalent Single Axle Loads (ESALs) (ARA, 2015).

Climate is another factor that should be considered in pavement design. According to Applied Research Associates (2015), information about pavement surface temperatures expected for the south and east region of Ontario are summarized in Appendix II.

The above-stated factors and some others, that have significant influence on pavement performance, are implemented in several mechanistic pavement models. One of the commonly used ones is Mechanistic-Empirical Pavement Design Guide (MEPDG), which was developed to predict the deterioration of pavements and their associated expected service lives. The focus of this chapter is studying the pavement structure, although some approximate service life of the pavement without any maintenance was also estimated. The WESLEA software was used in this research - a linear elastic multi-layer program that enables analysis of a pavement structure, including the effects of complex load systems.

4.2 Pavement Design with Lightweight Cellular Concrete (LCC)

The structure of the typical pavement, with respect to the usage of LCC as a subbase, usually consists of LCC layer placed on the subgrade, followed by unbound Granular base material and the asphalt concrete layer as a top surface. Typical pavement structure with LCC is presented in Figure 4-1. Even though the LCC is different from traditional granular material and should be treated as a cement stabilized material, there are no calibration factors and performance models designed for the lightweight cellular concrete. In the MEPDG manual, it is noted that if

the cement stabilized base layer is beneath an unbound Granular base and hot-mix asphalt layer, the pavement design should treat it as an unbound layer with a constant layer modulus.

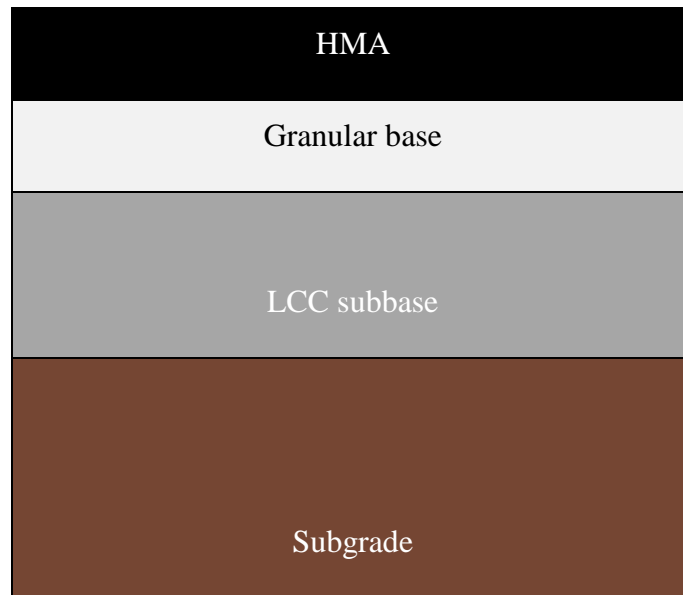


Figure 4-1: Pavement Structure with LCC

4.3 Analysis Method

Three roads in Ontario with installed LCC were chosen to be studied: Dixie Road, Highway 9 and Winston Churchill Boulevard. This Chapter aims to predict performance of the installed LCC sections in terms of fatigue cracking and rutting issues as well as to determine the bearing capacity of the road sections. These parameters were discussed as the failure criteria. Furthermore, the comparison between LCC and Granular B subbase materials that were installed on the same road sections was completed and discussed. The predicted service life of the pavements without any maintenance was determined.

The method for the failure criteria analysis consisted of the following approaches:

- Measuring the response of the pavement to different loadings. At this approach, the ability of the pavement to withstand various loads was studied by controlling stress values at the bottom and top of the subbase layer.
- Determining the allowable number of load repetitions on the pavement. The approach obtains the number of maximum load repetitions that can be withstand by the pavement.
- Identifying the maximum ESALs that road section can bear. Damages due to cumulative Equivalent Single Axle Loads were determined and presented in the graphs as potential fatigue cracking and rutting issues.

4.4 Failure Criteria Analysis

In order to understand the expected vertical stress and tensile stress that will occur in the pavement structure the failure criteria analysis was conducted using the WESLEA software. The pavement structure and material properties were taken from the existing projects in Canada. Some unknown values were assumed in this analysis based on engineering experience and recommended values (TAC, 2014). Modulus of elasticity for LCC was taken as 850 MPa as a result of the tests that were conducted by the author's colleagues in CPATT laboratory (for the LCC density of 475 kg/m³).

Two types of pavement structure using a different material for subbase layer were analyzed and compared, which are the Lightweight Cellular Concrete and the unbound Granular B subbase material. The pavement structure and material properties are provided in Table 4-1.

ESALs for Dixie Road were taken from the report completed by Griffiths and Popik (2013). The AADT information for Highway 9 was obtained from MTO (provincial highways traffic volumes 2016 report). The ESALs for Dixie Road and for Winston Churchill Boulevard were predicted to be 500,000 and 160,000 respectively (Table 4-2).

Table 4-1: WESLEA Settings for Dixie Road, Highway 9 and Winston Churchill Boulevard (Material Properties of the Pavement)

		Surfac	Base	Subbase		Subgrad
		HMA	Granular	Granular B	LC	Soil
Dixie Road	E (MPa)	3445	250	200	850	30
	Poisson's Ratio	0.35	0.4	0.35	0.2	0.45
	Thickness (mm)	140	150	650	650	-
Highway 9	E (MPa)	3445	250	200	850	30
	Poisson's Ratio	0.35	0.4	0.35	0.2	0.45
	Thickness (mm)	200	200	1100	1100	-
Winston Churchill Blvd	E (MPa)	3445	250	200	850	30
	Poisson's Ratio	0.35	0.4	0.35	0.2	0.45
	Thickness (mm)	120	240	550	550	-

Table 4-2: ESALs for Three Road Sections in Ontario

	Dixie Road	Highway 9	Winston Churchill Blvd
ESALs	500,000	1,500,000	160,000

LCC is a potential substitution of the granular material for the subbase in some projects. This chapter aimed to compare the predicted performance of the pavements with LCC with the same road but with granular material; thus the same steps for determining the stress values were taken for both pavements – LCC and granular subbase pavements.

4.4.1 First Approach

With the use of WESLEA software, the vertical stress and tensile stress happened on the top of the subbase layer and bottom of the subbase layer respectively at different loads is shown in Figure 4-2. To develop the graphs, the load range was varied from 20 kN to 120 kN of magnitude. The standard axle load number is usually considered to be 80 kN. Figure 4-2 presents the expected vertical stress that will be applied to the subbase layer.

The vertical stress applied to the LCC layer is higher than the one to the Granular B layer for every loading set for all three roads. However, the typical compressive strength of the LCC at low density ranges between 0.5 MPa to 1.0 MPa. Thus, the LCC layer is considered strong enough to support the pavement in the range of 20 kN to 120 kN of axle loads. The output of the WESLEA software is shown in Tables 4-3; 4-4; 4-5.

Table 4-3: Vertical and Tensile Stresses. Dixie Road

Dixie Road				
Load, kg	Vertical Stress at the Top of Granular B	Tensile Stress at the Bottom of Granular B	Vertical Stress at the Top of LCC layer	Tensile Stress at the Bottom
2000	55.53	-25.07	83.21	-45.68
4000	105.18	-49.63	156.01	-90.35
6000	150.34	-73.68	220.81	-134.04
8000	191.9	-97.24	279.2	-176.79
10,000	230.47	-120.32	332.28	-218.62
12,000	266.47	-142.93	380.84	-259.57

Table 4-4: Vertical and Tensile Stresses. Highway 9

Highway 9				
Load, kg	Vertical Stress at the Top of Granular layer	Tensile Stress at the Bottom of Granular Layer	Vertical Stress at the Top of LCC layer	Tensile Stress at the Bottom of LCC Layer
2000	34.27	-10.14	52.84	-18.68
4000	66.56	-20.19	102.11	-37.19
6000	97.12	-30.14	148.27	-55.51
8000	126.14	-40.01	191.67	-73.66
10,000	153.79	-49.78	232.57	-91.63
12,000	180.19	-59.47	272.2	-109.43

Table 4-5: Vertical and Tensile Stresses. Winston Churchill Blvd

Winston Churchill Boulevard				
Load, kg	Vertical Stress at the Top of Granular layer	Tensile Stress at the Bottom of Granular Layer	Vertical Stress at the Top of LCC layer	Tensile Stress at the Bottom of LCC Layer
2000	52.64	-0.92	74.72	-1.85
4000	101.26	-1.76	142.88	-3.56
6000	146.46	-2.51	205.46	-5.11
8000	188.7	-3.17	263.21	-6.53
10,000	228.31	-3.76	316.72	-7.82
12,000	265.58	-4.27	366.43	-8.97

The results of the tensile stress occurring at the bottom of the subbase layer are demonstrated in Figure 4-2. It is clear that the tensile stress happening at the LCC layer is higher than the tensile stress occurring at the Granular B layer. However, according to Narayanan and Ramamurthy (2000), the flexural strength of lightweight cellular concrete ranges from 15% to 35% of its compressive strength, which is between 0.075 to 0.35 MPa for the typical low-density lightweight cellular concrete. Predicted maximum value obtained from the WESLEA

software for tensile stress at the bottom of the LCC subbase layer (at 120 kN load magnitude) throughout all road sections was 0.26 MPa. The right part of Figure 4-2 displays that both of the subbase layers for all three roads are capable of resisting the tensile stress and protect the layer from damage.

Maximum vertical stresses that potentially could happen under 120 kN load magnitude at the top of LCC layer were 0.38 MPa, 0.27 MPa and 0.36 MPa for Dixie Road, Highway 9 and Winston Churchill Boulevard respectively. Those values are lower than typical compressive strength values for the Lightweight Cellular Concrete (0.5 to 1.5 MPa). Thus, LCC layer can potentially hold the vertical stress without being damaged (Figure 4-2).

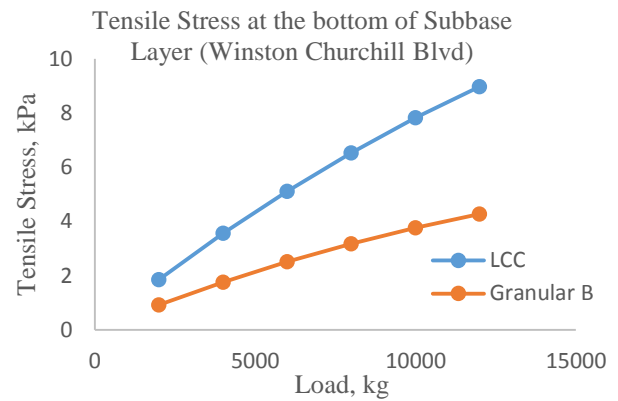
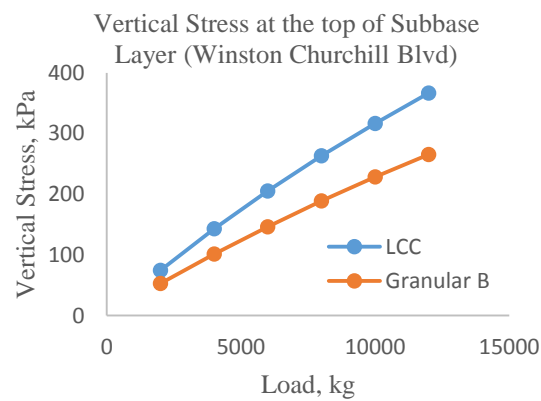
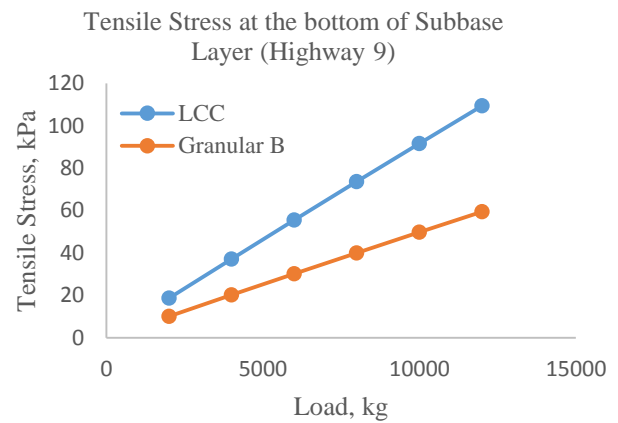
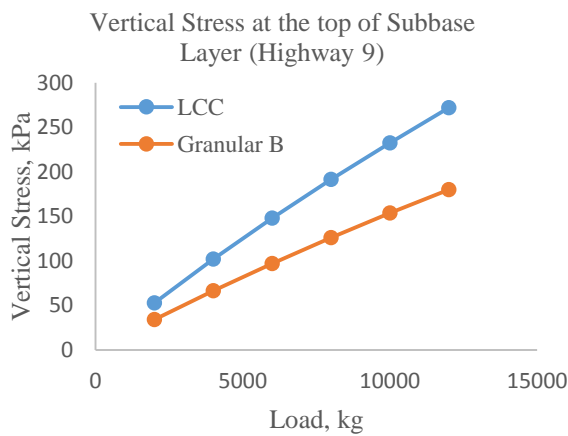
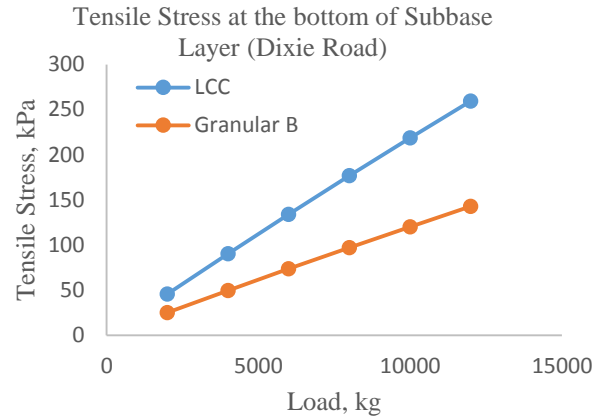
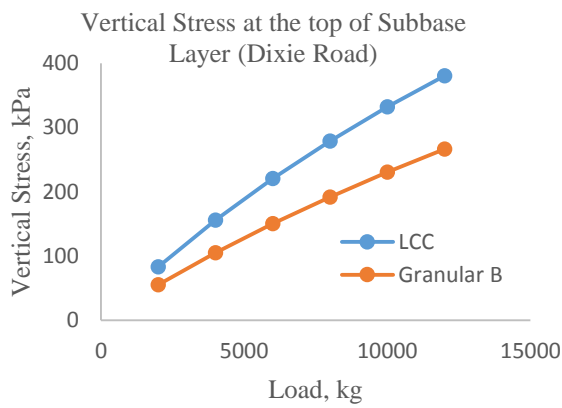


Figure 4-2: Vertical and Tensile Stresses. Comparison for Dixie Road, Highway 9 and Winston Churchill Blvd (WESLEA software, 2018)

4.4.2 Second Approach

The vertical stress value at the bottom of AC layer and tensile strength at the bottom of LCC layer were taken as the representatives of the fatigue and rutting measures respectively. By using the WESLEA software, damage analysis for fatigue cracking and permanent deformation was obtained. The equations that were used in the calculation of fatigue cracking and rutting in WESLEA software are presented below:

$$N_{fc} = 2.83 \times 10^{-6} \left(\frac{10^6}{\varepsilon_t} \right)^{3.148} \quad (1)$$

Where:

N_{fc} = Allowable number of load repetition before fatigue cracking

ε_t = Tensile strain at the bottom of surface layer

$$N_{fr} = 1.0 \times 10^{16} \left(\frac{1}{\varepsilon_v} \right)^{3.87} \quad (2)$$

Where:

N_{fr} = Allowable number of load repetition before rutting

ε_v = Compressive strain at the top of subgrade layer

The output of the WESLEA software of the predicted damage to the pavements is presented in Tables 4-6; 4-7; 4-8.

Table 4-6: Allowable Number of Load Repetition. Fatigue Cracking and Rutting for Dixie Road

Dixie Road				
Load, kg	Fatigue. Pavement with Granular B	Rutting. Pavement with Granular B	Fatigue.Pavement with LCC	Rutting.Pavement with LCC
2000	2,417,552	12,264,561	4,602,352	154,158,424
4000	451,514	870,860	1,005,395	10,962,335
6000	183,018	188,197	443,908	2,372,274
8000	107,632	64,135	287,635	809,479
10,000	76,547	28,049	227,081	354,437
12,000	60,720	14,631	200,912	181,681

It should be noted that the LCC layer could potentially carry more traffic loading than Granular B layer before fatigue cracking happens. This conclusion can be made due to the fact that the Total Allowable Number of Load Repetition (in terms of fatigue cracking) of LCC layer is 1.4 to 3.3 times higher than the Granular B layer depending on the project. Giving the example of the typical axle load of 80 kN for Dixie Road, the Total Allowable Number of Load Repetition with LCC is 287,635 whereas it is 107,632 with Granular B. The ratio comes to 2.67, meaning that pavement with LCC is superior in terms of resistance to fatigue cracking.

Table 4-7: Allowable Number of Load Repetition. Fatigue Cracking and Rutting for Highway 9

Highway 9				
Load, kg	Fatigue. Pavement with Granular B	Rutting. Pavement with Granular B	Fatigue. Pavement with LCC	Rutting. Pavement with LCC
2000	8,801,919	348,501,635	15,268,311	5,148,891,932
4000	1,335,740	24,233,438	2,433,609	358,295,756
6000	500,772	5,129,902	962,659	75,899,446
8000	269,727	1,712,909	548,875	25,360,318
10,000	175,802	734,178	379,512	10,876,822
12,000	128,467	368,512	294,602	5,462,865

Table 4-8: Allowable Number of Load Repetition. Fatigue Cracking and Rutting for Winston Churchill Boulevard

Winston Churchill Boulevard				
Load, kg	Fatigue. Pavement with Granular B	Rutting. Pavement with Granular B	Fatigue. Pavement with LCC	Rutting. Pavement with LCC
2000	1,605,741	8,847,648	2,279,127	90,925,930
4000	343,393	630,873	538,184	6,482,740
6000	145,964	136,897	241,716	1,406,532
8000	90,887	46,842	160,580	481,185
10,000	68,516	20,567	130,016	211,232
12,000	57,474	10,572	117,682	108,552

The results for predicted rutting performance show even stronger differentiation between values. The performance of the LCC based pavements in terms of rutting is from 10.2 to 14.8 times better than with Granular B. For Highway 9, under the typical axle load of 80 kN, the Total Allowable Number of Load Repetition with LCC and Granular B (in terms of rutting) is 25,360,318 and 1,712,909 respectively. Thus giving the ratio of 14.8. This is due to the fact that LCC material is stiffer itself and because rutting is a result of tensile stress at the bottom of the subbase layer, LCC-based pavements show lower rutting issues.

The results of the Allowable Number of Load Repetition under the various loadings are shown in Figure 4-3. It is clear that the pavement with LCC subbase is more durable than the pavement with Granular B layer at the same thickness since the allowable numbers of load repetitions for fatigue cracking and permanent deformation are higher.

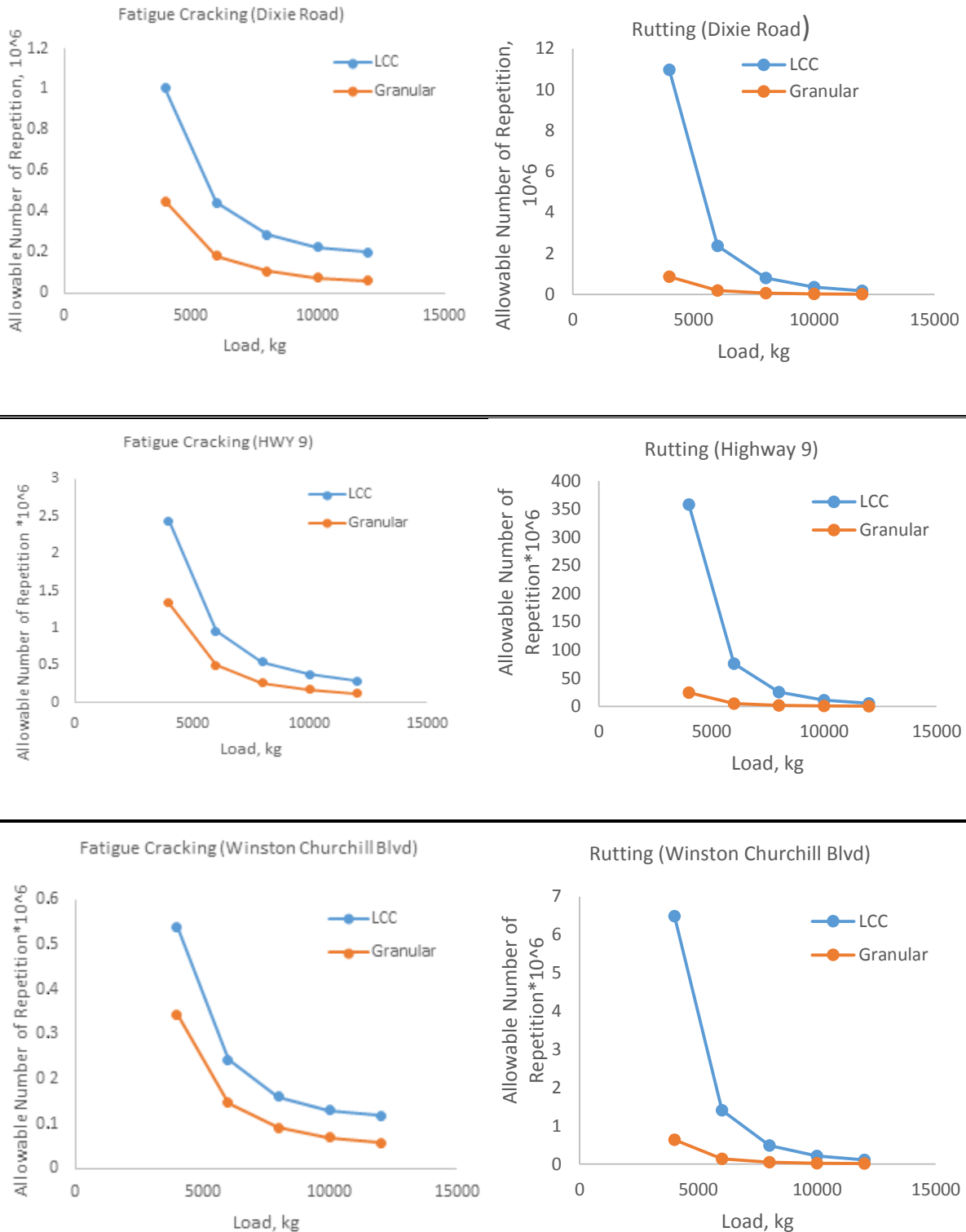


Figure 4-3: Allowable Number of Load Repetition. Fatigue Cracking and Rutting for Dixie Road, Highway 9 and Winston Churchill Blvd (WESLEA software, 2018)

4.4.3 Third Approach

In order to understand the approximate service life of the pavement without any maintenance, Allowable Number of Load Repetitions vs ESALs graphs were plotted on Figure 4-4. The maximum Allowable Number of Load Repetitions was calculated by WESLEA software and it was 107,632 for fatigue cracking and 64,135 for rutting (Dixie Road; Granular-based section). In comparison, for LCC-based section for the same road, those values were 287,635 and 809,479 for fatigue cracking and rutting respectively. Values for other sections are presented in Tables 4-11; 4-12; 4-13; 4-14.

The ratio between the range of ESALs and Allowable Number of Load Repetitions was calculated in order to predict the capacity of the particular section. If the damage ratio exceeds one, it indicates that a failure could happen on the pavement as traffic loading surpass the pavement's bearing capacity. Damage ratio under various ESALs for each road section were calculated to determine bearing capacity of the pavements under different traffic loading. Satisfactory result was considered when both rutting and fatigue cracking damage ratio were below one. For Dixie Road, Granular-based pavement, this number was 50,000 ESALs, whereas for the LCC-based it was 250,000 ESALs (Table 4-9; 4-10). The same trend was observed on two other roads – Highway 9 and Winston Churchill Boulevard. For Highway 9 (Tables 4-11; 4-12), both fatigue and rutting damage ratio were lower than one under the 100,000 ESALs (Granular layer) and 500,000 ESALs (LCC layer). For Winston Churchill Boulevard – 40,000 and 160,000 ESALs respectively (Tables 4-13; 4-14).

All three road sections installed with LCC as a subbase could potentially withstand higher ESALs than pavements with Granular material. This can lead to the conclusion that LCC-based pavements could be more durable in terms of fatigue cracking and rutting resistance.

The output from the WESLEA software of the predicted damage of the pavements is presented in Tables 4-9; 4-10; 4-11; 4-12; 4-13; 4-14.

Table 4-9: Predicted Damage (Fatigue Cracking and Rutting) of Pavement with Granular B Subbase. Dixie Road (WESLEA, 2018)

Granular B					
		Fatigue cracking. With Granular B		Rutting. With Granular B	
Load,kg	ESALs	Allowable	Damage	Allowable	Damage
80	500,000	107,632	4.65	64,135	7.80
80	450,000	107,632	4.18	64,135	7.02
80	400,000	107,632	3.72	64,135	6.24
80	350,000	107,632	3.25	64,135	5.46
80	300,000	107,632	2.79	64,135	4.68
80	250,000	107,632	2.32	64,135	3.90
80	200,000	107,632	1.86	64,135	3.12
80	150,000	107,632	1.39	64,135	2.34
80	100,000	107,632	0.93	64,135	1.56
80	50,000	107,632	0.46	64,135	0.78

Table 4-10: Predicted Damage (Fatigue Cracking and Rutting) of Pavement with LCC Subbase. Dixie Road (WESLEA, 2018)

LCC					
		Fatigue cracking. With LCC		Rutting. With LCC	
Load, kg	ESALs	Allowable	Damage	Allowable	Damage
80	500,000	287,635	1.74	809,479	0.62
80	450,000	287,635	1.56	809,479	0.56
80	400,000	287,635	1.39	809,479	0.49
80	350,000	287,635	1.22	809,479	0.43
80	300,000	287,635	1.04	809,479	0.37
80	250,000	287,635	0.87	809,479	0.31
80	200,000	287,635	0.70	809,479	0.25
80	150,000	287,635	0.52	809,479	0.19
80	100,000	287,635	0.35	809,479	0.12
80	50,000	287,635	0.17	809,479	0.06

Table 4-11: Predicted Damage (Fatigue Cracking and Rutting) of Pavement with Granular Subbase. Highway 9 (WESLEA, 2018)

Granular B					
		Fatigue cracking. With Granular B		Rutting. With Granular B	
Load, kg	ESALs	Allowable	Damage	Allowable	Damage
80	1,500,000	269,727	5.56	1,712,909	0.88
80	1,300,000	269,727	4.82	1,712,909	0.76
80	1,100,000	269,727	4.08	1,712,909	0.64
80	900,000	269,727	3.34	1,712,909	0.53
80	700,000	269,727	2.60	1,712,909	0.41
80	500,000	269,727	1.85	1,712,909	0.29
80	300,000	269,727	1.11	1,712,909	0.18
80	100,000	269,727	0.37	1,712,909	0.06

Table 4-12: Predicted Damage (Fatigue Cracking and Rutting) of Pavement with LCC Subbase. Highway 9 (WESLEA, 2018)

LCC					
		Fatigue cracking. With LCC		Rutting. With LCC	
Load, kg	ESALs	Allowable	Damage	Allowable	Damage
80	1,500,000	548,875	2.73	25,360,318	0.06
80	1,400,000	548,875	2.55	25,360,318	0.06
80	1,300,000	548,875	2.37	25,360,318	0.05
80	1,200,000	548,875	2.19	25,360,318	0.05
80	1,100,000	548,875	2.00	25,360,318	0.04
80	1,000,000	548,875	1.82	25,360,318	0.04
80	900,000	548,875	1.64	25,360,318	0.04
80	800,000	548,875	1.46	25,360,318	0.03
80	700,000	548,875	1.28	25,360,318	0.03
80	600,000	548,875	1.09	25,360,318	0.02
80	500,000	548,875	0.91	25,360,318	0.02

Table 4-13: Predicted Damage (Fatigue Cracking and Rutting) of Pavement with Granular Subbase. Winston Churchill Boulevard (WESLEA, 2018)

Granular B					
Input Parameters		Fatigue cracking. With Granular B		Rutting. With Granular B	
Load, kg	ESALs	Allowable	Damage	Allowable	Damage
80	160,000	90,887	1.76	46,842	3.42
80	145,000	90,887	1.60	46,842	3.10
80	130,000	90,887	1.43	46,842	2.78
80	115,000	90,887	1.27	46,842	2.46
80	100,000	90,887	1.10	46,842	2.13
80	85,000	90,887	0.94	46,842	1.81
80	70,000	90,887	0.77	46,842	1.49
80	55,000	90,887	0.61	46,842	1.17
80	40,000	90,887	0.44	46,842	0.85

Table 4-14: Predicted Damage (Fatigue Cracking and Rutting) of Pavement with LCC Subbase. Winston Churchill Boulevard (WESLEA, 2018)

LCC					
Input Parameters		Fatigue cracking. With LCC		Rutting. With LCC	
Load, kg	ESAL	Allowable	Damage	Allowable	Damage
80	220,000	160,580	1.37	481,185	0.6
80	200,000	160,580	1.25	481,185	0.42
80	180,000	160,580	1.12	481,185	0.37
80	160,000	160,580	1.00	481,185	0.33
80	140,000	160,580	0.87	481,185	0.29
80	120,000	160,580	0.75	481,185	0.25
80	100,000	160,580	0.62	481,185	0.21
80	80,000	160,580	0.50	481,185	0.17
80	60,000	160,580	0.37	481,185	0.12
80	40,000	160,580	0.25	481,185	0.08
80	20,000	160,580	0.12	481,185	0.04

Figure 4-4 shows the comparison between LCC and Granular materials in terms of performance. In all three roads, LCC-based pavements showed good performance in terms of fatigue cracking and rutting. In all cases, except for the fatigue cracking resistance on Dixie Road, pavements with LCC layer showed potential ability to resist the load. For Dixie Road, the ESALs of 500,000 was higher than one obtained from the WESLEA software of 250,000 ESALs, meaning that pavement cannot withstand this large number of ESALs without any maintenance. In terms of rutting, there was a significant margin in LCC-based pavements before they reached the allowable limit of load repetitions. By modeling different pavement structures (LCC and Granular B based) there is an opportunity to visually estimate the difference between the two performances. According to WESLEA output, LCC has performed better in all three projects in both fatigue cracking and rutting resistance. It should be noted that the difference in the performance of the sections was more significant in terms of rutting.

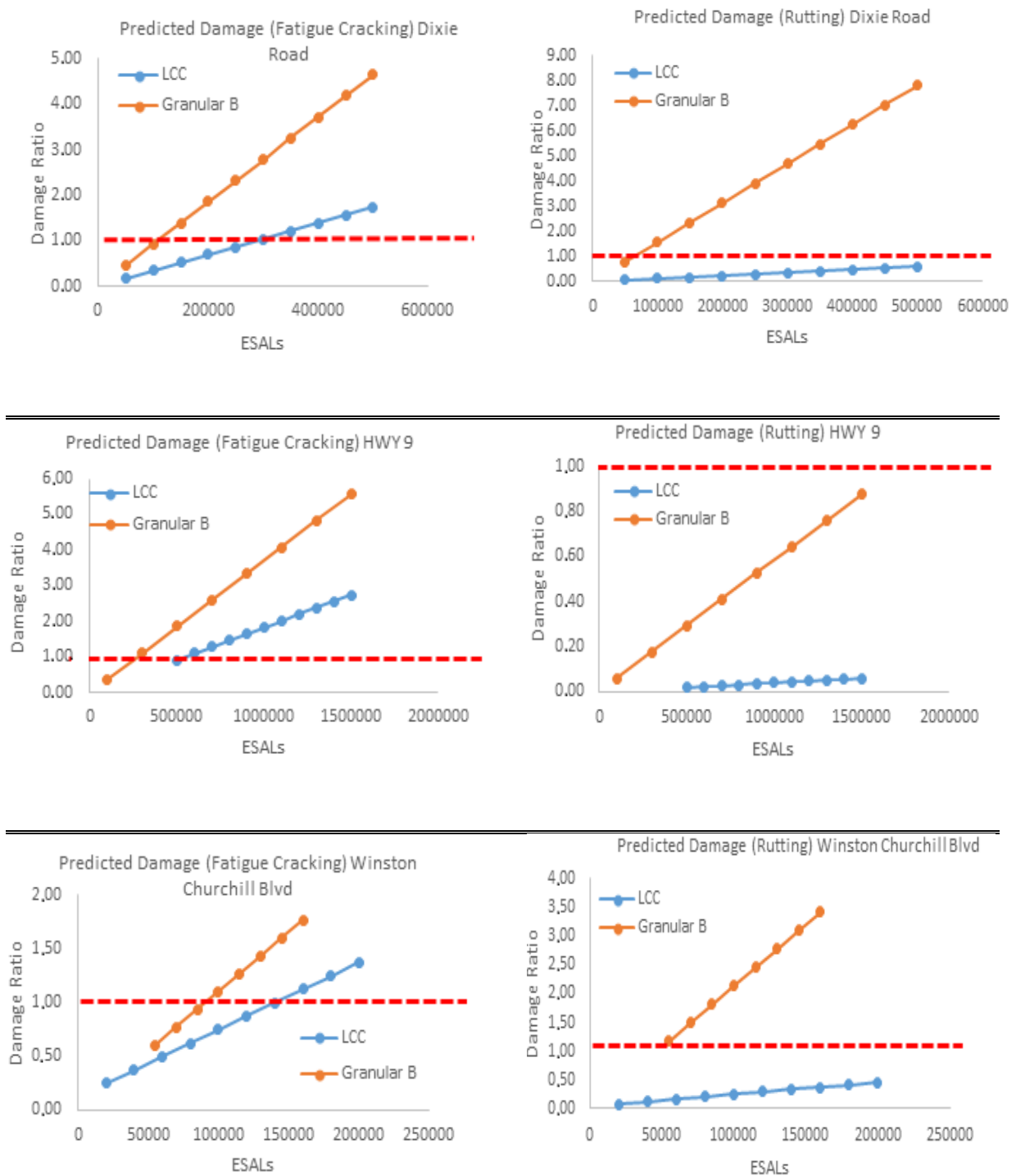


Figure 4-4: Predicted Damage. Fatigue Cracking and Rutting for Dixie Road, Highway 9 and Winston Churchill Blvd (WESLEA Software, 2018)

4.5 Summary

Three roads in Ontario were taken as examples of roads with settlement issues. All three sections were installed with the LCC layer as a subbase and prediction performance of those sections was determined by the criteria analysis.

The result of the failure criteria analysis indicated that the LCC layer is more durable compared to the conventional Granular B materials; thus, pavement thickness using LCC as a subbase material could be thinner than the conventional pavement structure, which may reduce the excavation depth during construction and save time and money. This also shows that using LCC as a subbase layer material could be effective. However, the software does not consider the environmental impact such as temperature and moisture. An in-situ field inspection is needed to evaluate the environmental effect on the pavement using LCC as a subbase layer. The results of the failure criteria analysis indicated that the usage of LCC as a subbase material is more durable than the conventional granular material with similar thickness. The findings demonstrate that LCC could be considered as a potential pavement subbase material in respect to mechanical properties. However, other durability and functional properties have to be assessed.

CHAPTER 5

5 TORONTO PROJECT

Mechanical properties of LCC samples, cast during constructing project will be studied in this Chapter. Results, obtained from the laboratory testing will be compared to the typical values for LCC in the literature.

All of the road sections described and studied in Chapters 3 and 4 were constructed prior to this research being carried out. In order to study the current state and condition of the sections installed with Lightweight Cellular Concrete (LCC) and, to predict the future performance of the pavement, laboratory tests on defining mechanical properties of LCC needed to be done. Some companies, such as CEMATRIX, have been running laboratory tests by using their own laboratories as well as using third-party companies. Typically, preparation of samples in laboratory conditions might not necessarily reflect actual site construction conditions. This could be due to a number of unforeseen circumstances that might occur during the construction process, including but not limited to weather conditions, challenges with equipment and human factor. As a result of this, it is important to assess the characteristics of the actual field-cast material. Therefore, this study obtained LCC samples from the actual site and tested them in the CPATT laboratory. Some of the most important mechanical properties such as Modulus of Elasticity, Poisson's ratio, and UCS were determined and compared to the typical values for the corresponding LCC densities.

5.1 Site Description

One of the ongoing projects Southern Ontario is a road section of Eglinton Avenue West, East of Black Creek Drive, Toronto, Ontario (Figure 5-1). The purpose of this project is to widen the road. This construction project consists of several measures including but not limited to constructing a retaining wall out of concrete and raising the surface of the road by approximately five meters. The latter was designed to be installed with lightweight material since the reduction in weight of this thick pavement layer was required.



Figure 5-1: Site Location (Google Maps, 2018)

5.2 Approach

The aim of this Chapter is to determine mechanical properties of the in-situ cast samples and to compare the obtained values to the typical values in literature. In addition, the relationship between the mechanical properties of LCC will be discussed.

Access to the construction site for collecting the fresh samples was provided by the company, which was conducting the Lightweight Cellular Concrete work (CEMATRIX). A total of 2521 m³ of LCC material was poured over a couple of weeks. As part of this project, cylindrical molds were prepared for casting the LCC samples by University of Waterloo team. Modulus of elasticity, unconfined compressive strength, and Poisson's ratio were determined by testing those samples.

5.3 Production and Placement

Lightweight Cellular Concrete with the 475 kg/m³ plastic density was used in this project. The “dry” mix process was utilized. The composition of the mix was cement (80%), slag (20%), w/c ratio of 0.5 and a foaming agent. The cement and slag were mixed together by a contractor before deliver to the site and after that, this dry mix was sucked into CEMATRIX “dry” mix equipment where it was blended with water. Figure 5-2 represents the construction process.



Figure 5-2: Construction Process. Toronto, May 2018

The target plastic density and the slurry temperature were controlled at this stage. Quality Control (QC) is one of the steps for checking the desirable features of the mix. Marsh cone test was conducted to ensure the mix met the desired requirement. According to industrial experience, it is found that 45 to 90 seconds in Marsh cone test could provide a stable and quality cement slurry.

After mixing the slurry, the mix is pumped to the site through a hose. At the same moment, the foaming agent is added to the mix and it is blended while moving inside the hose. In order to blend the LCC mix properly, a special device is installed in the beginning of the hose, which twists the torrent.

Plastic density was checked once per every 100 m^3 during the pouring to ensure the target plastic density was reached and maintained. No consolidating and vibrating during the placement process was carried out as it may harm the bubble structure of the material.

During the placement of the LCC mix, several buckets were filled with material. Shortly after that, all the prepared molds were cast from the above-mentioned buckets prefilled with LCC (Figure 5-3). The target density for LCC material was 475 kg/m^3 . According to Maher and Hagan, (2016) plastic density may vary in the range of $\pm 10\%$ of designed density. Thus, the range for the 475 kg/m^3 LCC mix is 427.5 to 522.5 kg/m^3 . During the mixing on site, Quality Control showed that the average plastic density of the mix was 454 kg/m^3 .



Figure 5-3: Samples, Collected on Site. 75*150 mm Molds for UCS test. 150*300 mm Molds for Modulus of Elasticity and Poisson's Ratio Tests

The following sections discuss the laboratory tests that were performed such as Unconfined Compressive Strength, Modulus of Elasticity and the Poisson's ratio. Samples for UCS test were collected in the amount of four samples per each test date. UCS testing was performed on 7, 14, 21 and 28th days. In addition, several samples were collected as spare samples for setting up the testing equipment. Modulus of elasticity and Poisson's Ratio test was conducted on 28th day only. Seven samples, including dummy ones, of 150 mm*300 mm were collected for testing modulus of elasticity and Poisson's ratio. The procedures followed for each test are described below.

5.4 Laboratory Tests

Laboratory tests were conducted at the University of Waterloo, at the Centre for Pavement Transportation and Technology (CPATT) laboratory from June 1, 2018 to June 22, 2018.

5.4.1 Unconfined Compressive Strength

This test was carried out in accordance with ASTM C495 and ASTM C796. Four cylinder specimens with dimensions 75 mm by 150 mm were tested. The samples were cast in-situ and in order to prevent them from being broken and to avoid compaction from vibration, samples were kept on site for three days. The ambient temperature on May 25th to May 27th, during the field work, is presented in Figure 5-4.

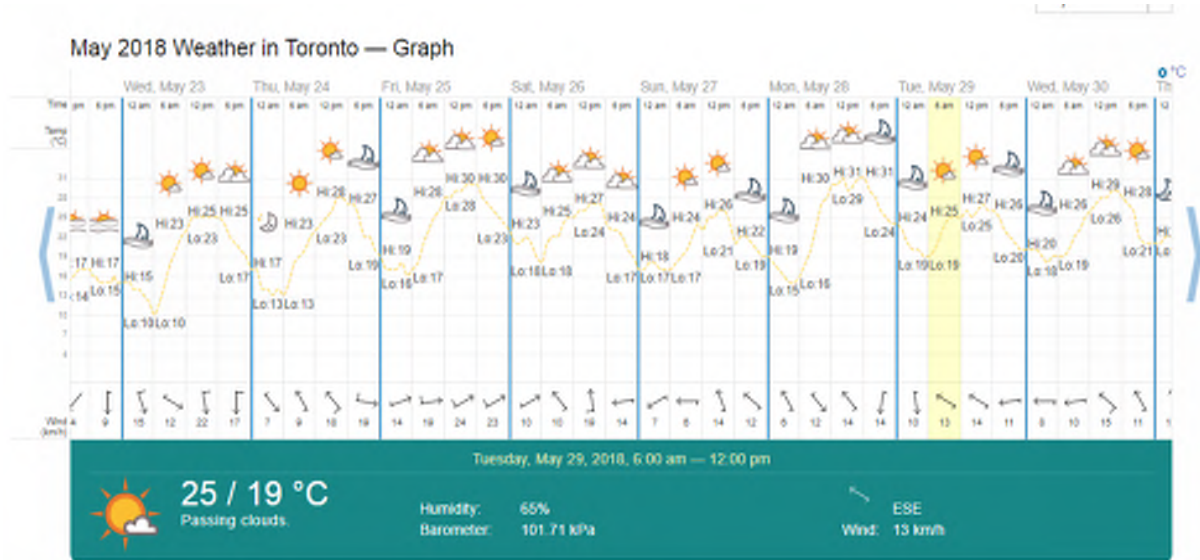


Figure 5-4: Weather Forecast during Construction and Casting the Samples
(<https://www.timeanddate.com/weather/canada/toronto/historic?month=5&year=2018>)

Later, samples were cured at room temperature $21 \pm 6^{\circ}\text{C}$ from day four to the testing day. Before testing the samples, they were demolded, grinded at the top and the bottom in order to have horizontal flat surfaces. Measurements of the samples were taken such as height, diameter, and weight. The average measured hardened state densities for the different batches of samples were reported as 416, 408, 410, 401 kg/m^3 . The actual density, which is known as a hardened state density, was observed to be lower than plastic density of material that was poured on site. The hardened state density of LCC is typically about 80 kg/m^3 less than its plastic density (Legatski, 1994). Thus, measured densities are within the expected range.

In addition, visual inspection was completed to reveal some possible structural cracks, apart from drying shrinkage, which can affect the test results. During the testing process, the load was applied at a constant rate and the maximum load was reached within considerable time. To calculate the compressive strength for each specimen, the following equation was used:

$$UCS = \frac{P}{A}$$

where:

UCS – Unconfined Compressive Strength, MPa

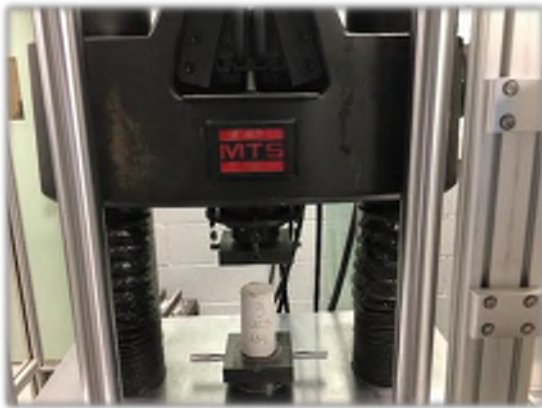
P – maximum load recorded, kN

A – the cross-section area of the specimen, mm²

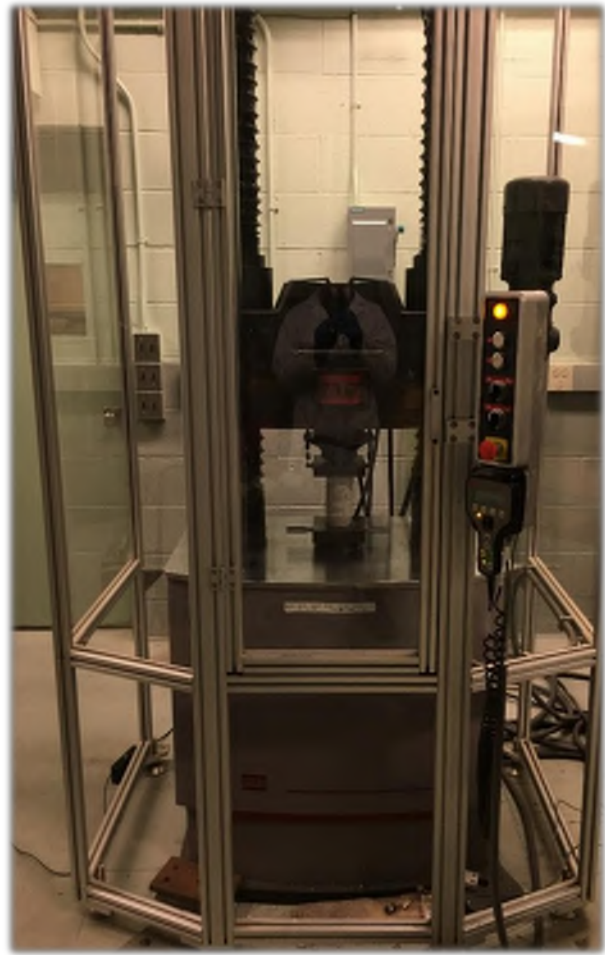
Figure 5-5 demonstrates test setup and frame of the UCS test in the CPATT lab.



(a)



(b)



(c)

Figure 5-5: Unconfined Compressive Strength. (a) - samples, ready to be tested; (b) and (c) - testing equipment

The UCS test was performed at 7, 14, 21, and 28 days at the CPATT laboratory. Figures 5-6 and 5-7 show the results from UCS test varies as low as 1.27 MPa to as high as 1.69 MPa. For 7 days and 28 days, the compressive strength was relatively consistent and stayed in the ranges of 1.37 to 1.61 MPa and 1.51 to 1.55 MPa respectively. One of the issues with the testing process was an insufficient number of samples for the 28 days UCS test – only two of them were correctly tested and results were obtained. Following the ASTM C495 procedure, four samples have to be tested in order to obtain reliable results. In addition, a few samples were needed for each testing day in order to calibrate the test frame. Also, a few samples were damaged during the curing period, while on site. Samples were left on site at the ambient temperature during the first three days and were discovered lying on the ground when it was time to pick the samples up from the site. Visually, cracks were observed later on the surface of some samples, but it was hard to say if those cracks were drying shrinkage cracks or some structural cracks. Those damaged samples were not tested to avoid confusion. Some of them were used as “dummy” samples, but overall number was already insufficient to have four good quality samples for 28 days UCS testing. UCS test results for 7, 14, 21 and 28 days are presented in Figure 5-6. The data for the testing are presented in Appendix III.

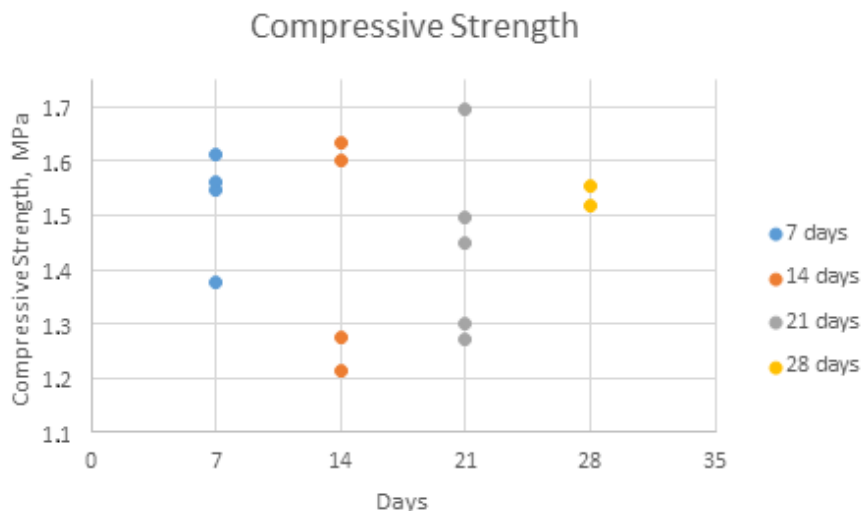


Figure 5-6: UCS Test Results

After calculating the average values for each sample age, 7, 14, 21 and 28 days, the compressive strength was determined to be within a small range throughout all the ages of the samples (Figure 5-7). The fluctuation of the results was from 1.44 MPa to 1.53 MPa, meaning no significant difference was observed between 7, 14, 21 and 28 days samples.

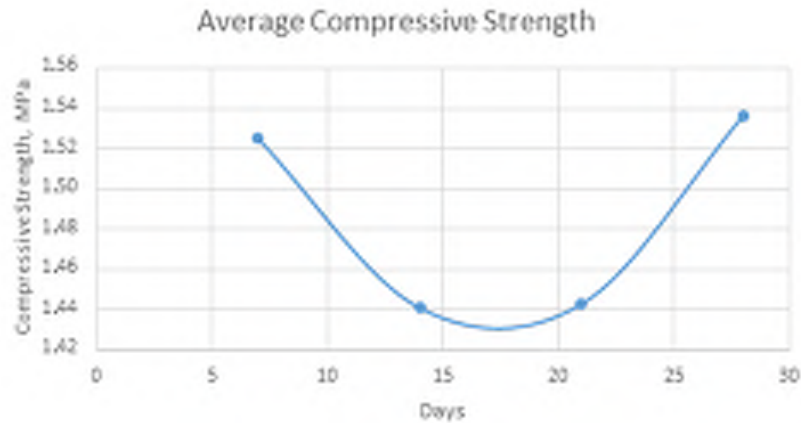


Figure 5-7: Average UCS Test Results

Table 5-1 presents typical values for Cellular Concrete. For the densities between 400 and 600 kg/m³, compressive strength ranges from 0.5 to 1.5 MPa. Those are the approximate values and the range for compressive strength is relatively large because it may include the cellular concrete with different mix compositions. The target density of the samples, taken from the site in Toronto, was 475 kg/m³. This means that the results were more than satisfied and material cast in-situ has gained relatively high compressive strength for its density.

Table 5-1: Typical Properties of Cellular Concrete Based on British Concrete Association (BCA 1994)

Dry Density (kg/m³)	Compressive Strength (MPa)	Drying Shrinkage (%)	Modulus of Elasticity (MPa)	Thermal Conductivity (W/mK)
400	0.5-1.0	0.30-0.35	800-1,000	0.10
600	1.0-1.5	0.22-0.25	1,000-1,500	0.11
800	1.5-2.0	0.20-0.22	2,000-2,500	0.17-0.23
1000	2.5-3.0	0.15-0.18	2,500-3,000	0.23-0.30
1200	4.5-5.5	0.09-0.11	3,500-4,000	0.38-0.42
1400	6.0-8.0	0.07-0.09	5,000-6,000	0.50-0.55
1600	7.5-10.0	0.06-0.07	10,000-12,000	0.62-0.66

5.4.2 Modulus of Elasticity and Poisson's Ratio

The testing method was completed in accordance with ASTM C469. The dimension of the specimen was 150 mm by 300 mm for the samples with targeted 475 kg/m³ density. Before testing the samples, they were grinded at the top and the bottom in order to have horizontal flat surfaces. Measurements of the samples were taken such as height, diameter, and weight. In addition, visual inspection was completed to reveal some possible structural cracks, apart from drying shrinkage, which can affect the test results. The same as for the compressive strength, actual density of the samples was calculated by dividing the weight of the sample to its volume. The average hardened state density appeared to be slightly higher than one in the smaller samples (for UCS test) and it was reported as 417 kg/m³ for this batch of samples.

The configuration of the test apparatus is shown in Figure 5-8. The calculation of the two parameters are described as follows:

- For Modulus of Elasticity:

$$E = \frac{(S_2 - S_1)}{(\varepsilon_2 - 0.000050)}$$

where:

E – modulus of elasticity, MPa

S₂ – stress corresponding to 40% of ultimate load, MPa

S₁ – stress corresponding to a longitudinal strain, ε_2 , of 50 million, MPa

ε_2 – longitudinal strain produced by stress S₂

- For Poisson's ratio:

$$\mu = \frac{(\varepsilon_{t2} - \varepsilon_{t1})}{(\varepsilon_2 - 0.000050)}$$

where:

μ - Poisson's ratio

ε_{t2} – transverse strain at midheight of the specimen produced by stress S₂

ε_{t1} – transverse strain at midheight of the specimen produced by stress S₁



Figure 5-8: Modulus of Elasticity and Poisson's Ratio Test Setup

Prior to the actual test, two specimens were tested to determine the compressive strength. The 40% of the maximum load was determined in this trial test, which then was used as the maximum load for the modulus of elasticity test. The compressometer and extensometer were used to measure the modulus of elasticity and Poisson's ratio as they provide readings for longitudinal strain and transverse strain. In accordance to ASTM C469, the sample should be loaded no less than three times and the first reading is not recorded as valid. During the test at the CPATT lab, each of the three samples was loaded six times, but the first reading was not taken into account since it is considered as a trial loading (according to the ASTM C469). Results are presented in Figure 5-9. Samples were tested at 28 days.

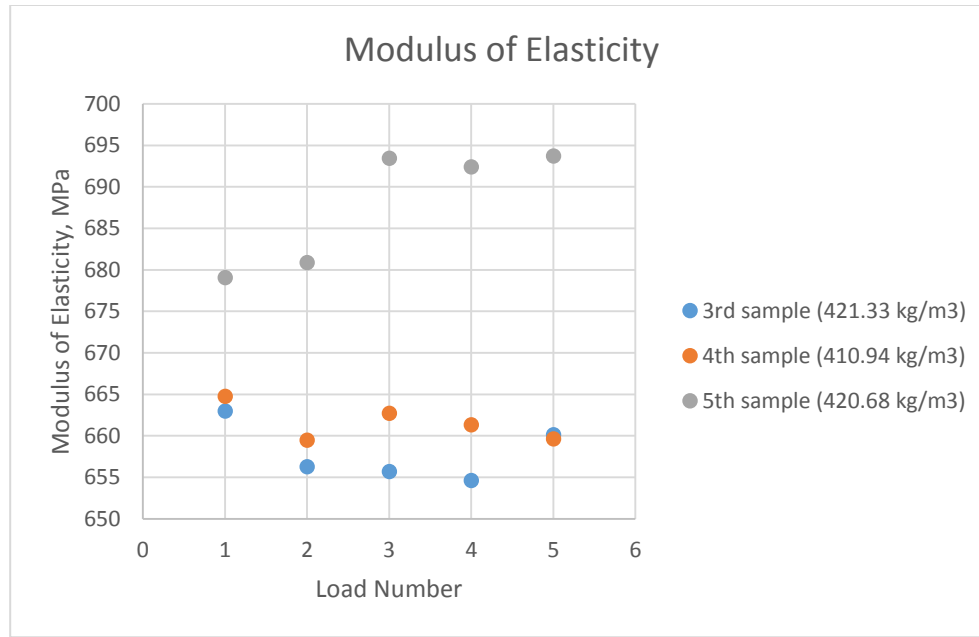


Figure 5-9: Modulus of Elasticity Test Results for 28 Days Samples

The average modulus of elasticity was determined as 657, 661 and 687 MPa for the 3rd, 4th, and 5th samples respectively. The result for modulus of elasticity for the 5th sample was obtained to be the highest, corresponding to the 420.68 kg/m³ density, whereas for the 3rd sample modulus of elasticity was determined as the lowest with the sample density at 421.33 kg/m³ (Figure 5-9). During the testing of the 5th sample, it was found that the reading increased from 680 to 693 MPa after the second cycle. This may be explained due to the fact that the test frame had some noise during testing and several adjustments were made to the longitudinal extensometer. According to Table 5-1, the lower limit for modulus of elasticity of the 400 kg/m³ density is approximately 800 MPa, whereas laboratory results observed it to be in the range of 657 to 687 MPa.

The Poisson's ratio was observed in the range of 0.24 to 0.30 (Appendix III), which is consistent to the past literature (BCA, 1994).

5.4.3 Relationship between Properties

Correlation between compressive strength and density is shown in Figure 5-10. The trend for 7 days samples was not typical because the lower density was observed, the higher compressive strength was, though 7 days samples had a good R^2 value of 0.96. For the 14 and 21 days samples with hardened state density of 404 to 414 kg/m³ the range of the compressive strength was relatively different, laying in the range of 1.2 to 1.69 MPa. For the 28 days samples, despite the expectations, compressive strength was observed to be at approximately same level as for other days samples (1.52 to 1.55MPa).

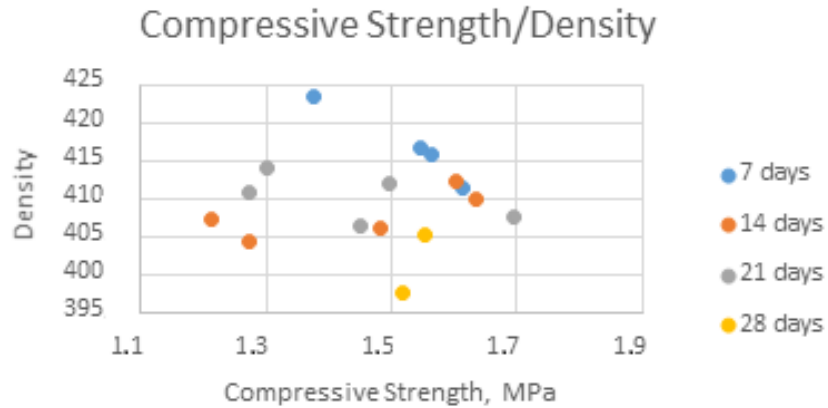


Figure 5-10: Correlation of Compressive Strength and Density

5.5 Summary

It is worth mentioning that one of the hypothesis of the thesis was that the mechanical properties of the site cast samples would be different from the typical values. As a result of the laboratory testing, some mechanical properties were different from the ones in the literature.

- The field cast samples usually have completely different curing procedure. Because of the high temperatures during the curing period, it is assumed that samples gained high strength in the first few days.
- Obtained results may be the reason of possibly damaged bubbled structure as none of the vibration should be done to the material although in order to test the samples they were transported to the laboratory on the 4th day. There is no specific requirement on after what day samples can be transported.
- For field cast samples correlation between compressive strength and modulus of elasticity was not found as strong. This could be studied more thoroughly by collecting more samples, thus having a greater data set.
- High compressive strength values, especially on early stages (before 28 days) may be the result of using good quality material in the field by CEMATRIX.

CHAPTER 6

6 CONCLUSIONS AND FUTURE RECOMMENDATIONS

6.1 Conclusions

Lightweight Cellular Concrete (LCC) is a lightweight product, consisting of Portland Cement, water, and foaming agent which contain air bubbles. LCC is relatively homogeneous compared to conventional concrete, as it does not contain coarse aggregate. It has constructive advantages such as low density with higher pound for pound strength compared with natural concrete and other fill materials. The properties of LCC depend on its microstructure and composition, methods of pore-formation and curing. Apart from being lightweight, LCC is a cost-effective and sustainable material and has superior thermal properties, freeze-thaw resistance, and good flowability. It can be used in a number of applications including but not limited to backfill, soil stabilization, embankment fills and pipe bedding, but this research was focused on studying of this material as an alternative construction material for reducing the weight of the subbase in pavement engineering, thereby mitigating excessive settlements and bearing failures.

In terms of insulation value, LCC also has energy absorbing, thermal insulating, and soundproofing properties. The air voids are homogeneously distributed within LCC and by utilizing the LCC within the roadway structure, pavement damage from frost heave and spring thaw softening are reduced.

This material is potentially cost-effective both in the short and long term. LCC typically replaces granular subbases two-to-three-times greater in thickness; therefore, less underlying soil needs to be excavated.

LCC also has environmental benefits, as it is inert and non-contaminating compared to other potential lightweight materials, and uses relatively easily available materials. It can also include industrial byproducts and waste materials such as fly ash. It is relatively inexpensive, easy to make, and easy to use. It is versatile in that it can be pumped into place and poured into complex forms.

With a greater emphasis on sustainability, materials such as LCC can minimize the generation of waste and deliver better performing pavements that require less maintenance.

The major conclusions drawn from this research are outlined in the following section:

- According to the report and visual inspection that were done at the Dixie Road, no significant transverse and longitudinal cracks were observed. Both, Winston Churchill Boulevard and Highway 9 sections are in good condition with no visual distresses. The

bus-lane in Calgary (the oldest section) is performing well. No recent data from the road section in British Columbia was collected.

- The inspections were done after the construction on the studied sections at different times. The results of the visual inspection, Falling Weight Deflectometer (FWD) as well as Benkelman Beam Test (for some cases) showed that the road sections are performing well and have some minor distresses on the surface (Dixie Road). FWD and Benkelman Beam Test are the most common tests for evaluating performance.
- However, in-depth pavement data collection must be complete to provide a comprehensive review of the performance of the sections with LCC as a subbase layer. Therefore, further investigation is recommended. This could be achieved by using pavement instrumentation such as asphalt gauges, earth pressure cells, and environmental equipment.
- In order to use LCC in a pavement structure as a subbase, certain activities have to be taken into consideration and implemented into the construction process. A number of general observations that are applicable to most LCC projects have been made from studying the road sections across Canada. These recommended construction activities include controlling the water table, constructing the proper drainage, transition areas between the sections and using quality equipment and professional personnel.
- It is clear from the failure criteria analysis that the pavement with LCC subbase is more durable than the pavement with Granular B layer at the same thicknesses.
- The result of the failure criteria analysis indicated that the pavement thickness using LCC as a subbase material could be thinner than the conventional pavement, which reduces the excavation depth during the construction and saves time and cost.
- The WESLEA software does not consider the environmental impact of temperature and moisture. In-situ field inspection is needed to evaluate the environmental effect on the pavement using LCC as a subbase layer.
- The mechanical properties of the site cast samples were found to be different from the typical values in the literature.
- For field cast samples correlation between the compressive strength and modulus of elasticity were not highly correlated. This could be studied more thoroughly by collecting more samples to obtain more data.
- The use of LCC as a pavement subbase layer could be practical and feasible in particular scenarios.

6.2 Future Recommendations

In terms of disadvantages of LCC, its high flowability means LCC must typically be placed into forms and cannot have a surface slope of more than 1 degree. Due to its low density, upward buoyancy forces must be taken into account if the concrete is expected to be submerged

in water. Its initial cost may be higher, depending on the density and composition. This area may also need clarification and analysis in the future

Based on this research, the following are recommended areas for future work:

- New road sections must be built to provide data collection opportunities for researchers regarding LCC performance.
- Those new pavements may be equipped with instrumentation such as earth pressure cell, horizontal strain gauge, and vertical strain gauge. This will help to quantitatively estimate pavement performance and will serve as a solid base for its evaluation.
- More in-depth study of the LCC properties is required.
- Correlation between laboratory and field cast samples could be determined in order to understand the effect of curing conditions and the quality of the material in general.
- LCC has many potential benefits in terms of sustainability in construction such as low ease of application, reduction in use of virgin materials, using by-products as a substitute to cement, for example. In order to evaluate and calculate those benefits, Life Cycle Cost Assessment and Life Cycle Cost Analysis must be performed, which was not accomplished in the past studies.

REFERENCES

- Aldridge, D. (2005). Introduction to foamed concrete: what, why, how? In Use of Foamed Concrete in Construction: Proceedings of the International Conference held at the University of Dundee, Scotland, UK on 5 July 2005 (pp. 1-14). *Thomas Telford Publishing*.
- American Society for Testing and Materials (ASTM) C796/C796M. (2012). Standard Test Method for Foaming Agents for Use in Producing Cellular Concrete Using Preformed Foam.
- American Society for Testing and Materials (ASTM) D4694-09 (2015). Standard Test Method for Deflections with a Falling-Weight-Type Impulse Load Device.
- American Society for Testing and Materials (ASTM) D4695-03 (2015). *Standard Guide for General Pavement Deflection Measurements*.
- American Society for Testing and Materials (ASTM) D6433 – 18 (2012). Standard Practice for Roads and Parking Lots Pavement Condition Index Surveys.
- Amran, Y. M., Farzadnia, N., and Ali, A. A. (2015). Properties and applications of foamed concrete; a review. *Construction and Building Materials*, 101, 990-1005.
- Applied Research Associates ARA (2015) Methodology for the Development of Equivalent Pavement Structural Design Matrix for Municipal Roadways.
- Arulrajah, A., Disfani, M. M., Maghoolpilehrood, F., Horpibulsuk, S., Udonchai, A., Imteaz, M., and Du, Y. J. (2015). Engineering and environmental properties of foamed recycled glass as a lightweight engineering material. *Journal of Cleaner Production*, 94, 369-375.
- Awang, H., Aljoumaily, Z. S., Noordin, N., & Al-Mulali, M. Z. (2014). The Mechanical Properties of Foamed Concrete containing Un-processed Blast Furnace Slag. *In MATEC Web of Conferences (Vol. 15, p. 01034). EDP Sciences*.
- British Cement Association (BCA) (1994). “*Foamed concrete - Composition and properties*”. *First published in 1991*, British Cement Association.
- Brady, K. C., Jones, M. R., & Watts, G. R. (2001). Specification for foamed concrete. TRL Limited.

- Byun, K. J., Song, H. W., Park, S. S., & Song, Y. C. (1998). Development of structural lightweight foamed concrete using polymer foam agent. *ICPIC-98*, 9.
- Darshan, M. (2016). Comparison on Auto Aerated Concrete to Normal Concrete. *GRD Journals, Global Research and Development Journal for Engineering*, 5.
- Dolton, B., Witchard, M., Luzzi, D., & Smith, T. J. (2016). Application of Lightweight Cellular Concrete to Reconstruction of Settlement Prone Roadways in Victoria. *GEOVancouver*.
- Dransfield, J. M. (2000, March). Foamed concrete: Introduction to the product and its properties. In One-day awareness seminar on Foamed Concrete: Properties, Applications and Potential, University of Dundee, Scotland (pp. 1-11).
- Friesen, J., Adedapo, D., Kenyon, R., & Eden, R. J. (2012). Bridge Embankment Stabilization in Deep Soft Lacustrine Clays Under High Artesian Pressures. *GEOManitoba*.
- Golder Associates (2008). Technical Memorandum. View Street and Vancouver Street, Victoria. Benkelman Beam Testing and Falling Weight Deflectometer Testing.
- Griffiths F. and Popik, M. (2013). Pavement Evaluation - CEMATRIX Site Dixie Road, Caledon, Ontario. Thurber Engineering Ltd. 2010 Winston Park Drive, Oakville, ON.
- Hoff Inge, Watn A, Oiseth E, EMDAL A., Amundsgard, K O., (2002). Light Weight Aggregate (LWA) Used In Road Pavements. Proceedings of the 6th international conference on the bearing capacity of roads and airfields, Lisbon, Portugal, 2, pp. 1013-22.
- Horpibulsuk, S., Suddeepong, A., Suksiripattanapong, C., Chinkulkijniwat, A., Arulrajah, A., & Disfani, M. M. (2014). Water-void to cement ratio identity of lightweight cellular-cemented material. *Journal of Materials in Civil Engineering*, 26(10), 06014021.
- Jones M.R., (2001). Foamed concrete for structural use. Proceedings of one-day seminar on foamed concrete: properties, applications, and latest technological developments. Loughborough University, pp. 27–60.
- Jones, M.R., & McCarthy, A. (2005). Utilising unprocessed low-lime coal fly ash in foamed concrete. *Fuel*, 84(11), 1398-1409.
- Jones, M.R., & McCarthy, A. (2005). Preliminary views on the potential of foamed concrete as a structural material. *Magazine of concrete research*, 57(1), 21-31.
- Jones, M.R., & McCarthy, A. (2006). Heat of hydration in foamed concrete: Effect of mix constituents and plastic density. *Cement and concrete research*, 36(6), 1032-1041.

- Jones, M.R., Zheng, L., Yerramala, A., Rao, K.S. (2012). Use of recycled and secondary aggregates in foamed concrete. *Magazine of Concrete Research*, 64(6), pp. 513-525.
- Jones, M.R., Ozlutas, K., & Zheng, L. (2016). Stability and instability of foamed concrete. *Magazine of Concrete Research*, 68(11), 542-549.
- Jones, M. R., Ozlutas, K., & Zheng, L. (2017). High-volume, ultra-low-density fly ash foamed concrete. *Magazine of Concrete Research*, 1-11.
- Kadela, M., Kozłowski, M., & Kukielka, A. (2017). Application of foamed concrete in road pavement–weak soil system. *Procedia Engineering*, 193, 439-446.
- Kearsley, E.P. (1996) The Use of Foamed Concrete for Affordable Development in Third World Countries. In *Appropriate Concrete Technology*; Dhir, R.K., McCarthy, M.J., Eds.; E & FN Spon: London, UK, pp. 233–243
- Kearsley E.P., Wainwright P.J. (2001). The effect of high fly ash content on the compressive strength of foamed concrete. *Cement Concrete Research*, 31, pp. 105–12.
- Kearsley E.P, Wainwright PJ (2002). Ash content for optimum strength of foamed concrete. *Cement Concrete Research*, 32, pp. 241–6
- Khayat, K. H., & Assaad, J. (2002). Air-void stability in self-consolidating concrete. *ACI Materials Journal*, 99(4), 408-416.
- Koudriashoff IT (1949). Manufacture of reinforced foam concrete roof slabs. *J Am Concr Inst*, 21(1), pp. 37–48.
- Lee, Y. L., Goh, K. S., Koh, H. B., & Bakar, I. (2009). Foamed aggregate pervious concrete—an option for road on peat.
- Legatski, L. A. (1994). Cellular concrete. In *Significance of Tests and Properties of Concrete and Concrete-Making Materials*. ASTM International. Loewen, E. B., Baril, M., & Eric, R. (2012). Rapid Design and Construction of an Integral Abutment Bridge with MSE Walls and Cellular Concrete Backfill. *Conference of the Transportation Association of Canada*.
- Maher, M. L., & Hagan, J. B. (2016). Constructability Benefits of Using Lightweight Foamed Concrete Fill in Pavement Applications. *CSCE Annual Conference, London*.

- McGovern, G. (2000, March). Manufacture and supply of ready-mix foamed concrete. In One Day Awareness Seminar on Foamed Concrete: Properties, Applications and Potential, University of Dundee, Scotland (pp. 12-25).
- Mohammad, M. (2011). Development of foamed concrete: enabling and supporting design (*Doctoral dissertation, School of Engineering, Physics and Mathematics*).
- Nambiar, E.K.K., Ramamurthy, K. (2006). 'Influence of filler type on the properties of foam concrete'. *Cement and concrete composites*, Vol.28, pp. 475-480.
- Narayanan, N., & Ramamurthy, K. (2000). Structure and properties of aerated concrete: a review. *Cement and Concrete Composites*, 22(5), 321-329.
- Neville, A. M. (2011). Properties of concrete. *5th edition, Pearson Education Ltd*.
- Oginni, F. A. (2015). Continental application of foamed concrete technology: Lessons for infrastructural development in Africa. *British Journal of Applied Science & Technology*, 5(4), 417.
- Ozlutas, K. (2015). Behavior of ultra-low density foamed concrete (*Doctoral dissertation, University of Dundee*).
- Ramamurthy, K., Nambiar, E. K., & Ranjani, G. I. S. (2009). A classification of studies on properties of foam concrete. *Cement and Concrete Composites*, 31(6), 388-396.
- Raphael, J. M. (1984, March). Tensile strength of concrete. In Journal Proceedings (Vol. 81, No. 2, pp. 158-165).
- Sabir, B. B., Wild, S., & O'farrell, M. (1998). A water sorptivity test for mortar and concrete. *Materials and Structures*, 31(8), 568.
- Sari, K. A. M., & Sani, A. R. M. (2017). Applications of Foamed Lightweight Concrete. In *MATEC Web of Conferences* (Vol. 97, p. 01097). *EDP Sciences*.
- Taylor, R., Eric, R., Wiebe, D., & Loewen, S. (2016). Waverly West Arterial Roads Project Kenaston Overpass. *Conference of the Transportation Association of Canada*.
- Tiwari, B. *et al.* (2017) 'Mechanical Properties of Lightweight Cellular Concrete for Geotechnical Applications', *Journal of Materials in Civil Engineering*, 29(7), p. 6017007. doi: 10.1061/(ASCE)MT.1943-5533.0001885.
- Transportation Association of Canada –TAC (2013). Transport Asset Design and Management Guide.

- Transportation Association of Canada TAC (2014) Default Parameters for AASHTOWare Pavement ME Design Canadian Guide.
- Valore, R. C. (1954b). Cellular concretes part 2 physical properties. *In Journal Proceedings* (Vol. 50, No. 6, pp. 817-836).
- Valore, R. C. (1954a). Cellular concretes Part 1 composition and methods of preparation. *In Journal Proceedings* (Vol. 50, No. 5, pp. 773-796).
- Van Deijk, S. (1919). Foam concrete. *Concrete*, 25(5).
- Wei, S., Yigiang, C., Yunsheng, Z., Jones, M.R. (2013). “Characterization and simulation of microstructure and thermal properties of foamed concrete”. *Construction and Building Materials*, 47, pp. 1278-1291.
- WCED, (1987).Our Common Future. *World Commission on Environment and Development*. Oxford University Press, Oxford.
- Yakovlev, G., Kerienė, J., Gailius, A., & Girnienė, I. (2006). Cement based foam concrete reinforced by carbon nanotubes. *Materials Science [Medžiagotyra]*, 12(2), 147-151.

APPENDIX I

FWD Dixie Road Data

Station (km)	Layer Thickness (mm)			ND (microns)	E_s (MPa)	M_R (MPa)	E_p (MPa)	SH _{ter} (mm)	LCC Structural Coefficient
	Asphalt	Base	Subbase						
Dole Road Northbound Lane									
10+280	137	150	400	201	200	66	690	154	
10+285	137	150	400	229	179	59	749	148	
10+290	137	150	400	248	197	65	650	141	
10+292	137	150	400	269	186	61	596	137	
10+294	137	150	400	303	203	67	495	129	
10+298	137	148	650	239	194	64	639	150	0.185
10+298	135	129	650	260	197	65	575	180	0.173
10+300	133	122	650	248	220	73	595	180	0.176
10+310	157	119	650	231	139	46	736	190	0.19
10+320	142	128	650	444	69	23	399	159	0.138
10+330	145	95	650	446	53	17	434	159	0.143
10+340	151	106	650	316	68	22	636	184	0.176
10+350	149	97	650	273	77	25	747	192	0.19
10+360	151	71	650	271	98	32	700	183	0.18
10+370	146	109	650	197	102	34	1055	218	0.229
10+380	159	97	650	205	98	32	1017	215	0.22
10+390	135	122	650	267	76	25	770	196	0.201
10+400	130	115	650	274	159	52	570	175	0.173
10+410	152	91	650	189	218	72	844	199	0.201
10+415	155	97	650	206	234	77	741	193	0.188
10+417	155	152	650	164	237	78	970	224	0.226
10+419	155	184	650	188	241	80	810	218	0.211
10+421	155	184	650	197	224	74	775	215	0.206
10+423	155	202	650	263	197	65	557	196	0.173
10+425	155	150	400	267	178	59	552	137	
10+430	155	150	400	277	227	75	536	135	
10+435	155	150	400	306	267	88	454	128	
NB Approach			Average	250	193	64	670	142	
			Std Dev.	39	10	3	140	10	
NB Cemetery Site			Average	257	152	50	714	193	
			Std Dev.	77	69	23	180	19	
NB Lease			Average	290	224	74	514	133	
			Std Dev.	15	45	15	52	5	

Station (km)	Layer Thickness (mm)			ND (microns)	E _s (MPa)	M _s (MPa)	E _p (MPa)	SH _{MR} (mm)	LCC Structural Coefficient
	Asphalt	Base	Subbase						
Dixie Road - Southbound Lane									
10+280	150	150	400	271	225	74	554	136	
10+285	150	150	400	290	205	68	521	133	
10+290	150	150	400	284	261	86	501	132	
10+292	150	150	400	313	249	82	451	127	
10+294	152	150	400	307	220	73	476	130	
10+296	157	111	650	229	225	74	649	166	0.177
10+298	157	117	650	201	219	72	771	200	0.195
10+300	155	111	650	194	225	74	805	201	0.199
10+310	149	111	650	205	199	66	774	198	0.195
10+320	141	132	650	276	168	36	632	167	0.181
10+330	138	128	650	385	56	19	514	174	0.163
10+340	144	131	650	226	68	29	907	212	0.217
10+350	143	103	650	248	115	38	725	190	0.19
10+360	149	99	650	206	128	42	887	204	0.208
10+370	150	69	650	196	115	36	994	210	0.218
10+380	140	100	650	206	115	36	942	206	0.217
10+390	130	143	650	227	112	37	818	204	0.211
10+400	164	109	650	235	99	33	817	204	0.198
10+410	132	197	650	208	171	56	779	213	0.214
10+415	131	195	650	236	185	61	650	200	0.195
10+417	138	203	650	214	214	71	705	208	0.203
10+419	145	220	650	220	192	63	696	213	0.201
10+421	160	212	650	195	202	67	796	224	0.212
10+423	168	224	650	236	188	62	633	212	0.196
10+425	175	150	400	253	183	60	639	148	
10+430	160	150	400	253	189	62	636	144	
10+435	150	150	400	316	179	59	495	130	
SB Approach			Average	251	188	62	638	171	
			Std Dev.	43	9	3	110	43	
SB Cemetery Site			Average	239	166	63	737	193	
			Std Dev.	49	58	19	151	25	
SB Leave			Average	282	230	76	526	134	
			Std Dev.	90	20	9	27	2	

APPENDIX II

**TYPICAL PAVEMENT SURFACE
TEMPERATURE IN SOUTHERN AND
EASTERN ONTARIO**

Month	1st Quintile (°C)	2nd Quintile (°C)	3rd Quintile (°C)	4th Quintile (°C)	5th Quintile (°C)	Mean Temp. (°C)	Std. Dev. (°C)
January	-13.0	-8.4	-5.5	-2.9	0.3	-5.9	4.8
February	-13.2	-8.7	-5.5	-2.7	1.4	-5.7	5.2
March	-7.9	-3.4	-0.6	2.3	7.3	-0.4	5.4
April	-1.1	3.3	6.7	10.7	17.4	7.4	6.7
May	5.2	10.4	14.1	18.4	26.0	14.8	7.4
June	11.9	16.9	20.7	25.2	32.4	21.4	7.3
July	14.6	19.6	23.4	27.8	34.4	23.9	7.1
August	13.3	17.9	21.3	25.6	32.1	22.1	6.7
September	8.3	13.1	16.6	20.3	26.7	17.0	6.6
October	2.8	6.8	9.9	13.3	19.2	10.4	5.9
November	-2.2	1.1	3.1	5.3	9.1	3.2	4.1
December	-9.3	-5.4	-3.1	-0.7	2.8	-3.1	4.3

APPENDIX III
DATA FOR
LABORATORY TESTING

7 days

Date cast	Date Tested	Code	Casted Density (kg/m ³)	Average Diameter (mm)	Average Height (mm)	volume (mm ³)	Weight of Specimen (g)	Applied Load (KN)	Surface Area (mm ²)	Comp. Strength (MPa)	Actual density (kg/m ³)
25-May-18	1-Jun-18	3	475	75,910	146,590	663425,574	276	7,072427	4525,722	1,563	416,023
		4		76,250	146,300	668057,592	283	6,286667	4566,354	1,377	423,616
		5		76,305	142,420	651278,672	268	7,375137	4572,944	1,613	411,498
		6		76,190	143,680	655061,609	273	7,052352	4559,170	1,547	416,755

14 days

25-May-18	8-Jun-18	1	475	76,325	144,595	661571,492	272,8	7,326274	4575,341	1,601	412,352
		2		76,435	150,085	688670,866	282,3	7,492442	4588,539	1,633	409,920
		3		76,520	146,995	675993,261	275,4	5,576168	4598,750	1,213	407,401
		4		76,320	145,860	667271,866	269,8	5,829073	4574,742	1,274	404,333
		5		76,425	144,245	661700,624	269,2		4587,338	0,000	406,831
		6		76,465	147,985	679568,068	276	6,810149	4592,142	1,483	406,140

21 days

25-May-18	15-Jun-18	1	475	77,14	76,840	151,020	151,280	701529,777	285,2	6,721827	4637,294	1,450	406,540
				76,54		151,540							
		2		77,05	76,645	150,490	150,575	694720,973	285,4	5,870159	4613,787	1,272	410,812
				76,24		150,660							
		3		76,96	76,615	149,610	149,615	689751,463	285,6	5,994846	4610,176	1,300	414,062
				76,27		149,620							
		4		77,44	76,825	147,850	147,605	684220,510	285,3	6,750173	4635,483	1,456	416,971
				76,21		147,360							
		5		76,25	76,170	151,290	151,280	689349,252	281	7,730247	4556,777	1,696	407,631
				76,09		151,270							
		6		76,72	76,220	151,340	151,000	688976,989	283,9	6,824816	4562,762	1,496	412,060
				75,720		150,660							

28 days

25-May-18	22-Jun-18	1	475	76,12	76,140	146,950	146,920	668954,448	271,2	7,073447	4553,188	1,554	405,409
				76,16		146,890							
		2		76,16	76,220	149,760	149,820	683592,931	271,9	6,932021	4562,762	1,519	397,751
				76,28		149,880							

	Height	average	Diameter	average	Weight	ultimate load	Cycle	E	P	S1	S2	ε_2	ε_{t2}	ε_{t1}	E	average of 3 samples	P	average of 3 samples			Density
3	300,36	300,24	150,97	151,51	2,280,7	9,00	1	642,519396	-0,2729921	0,049773	0,477093	0,00071507	-0,000179	2,614E-06	657,9486	669,1461	-0,28118	-0,26964	0,005413	2,281	421,33
	300,12		152,05				2	662,972431	-0,2711261	0,055746	0,47716	0,00068564	-0,000181	-8,325E-06						421,33	
							3	656,295094	-0,2962172	0,057138	0,478145	0,00069149	-0,000193	-3,44E-06						421,33	
							4	655,710551	-0,275486	0,056313	0,478632	0,00069406	-0,000191	-1,342E-05						421,33	
							5	654,634951	-0,2767729	0,055863	0,478132	0,00069505	-0,000169	9,632E-06						421,33	
							6	660,130068	-0,2862974	0,052951	0,479353	0,00069594	-0,0002	-1,493E-05						421,33	
4	301,08	301,43	153,28	153,37	2,288,4	9,00	1	615,43521	-0,241753	0,054	0,462443	0,00071367	-0,000159	0,000001	661,5838	669,1461	-0,24469	-0,26964	0,005569	2,288	410,94
	301,78		153,46				2	664,758994	-0,2373706	0,072788	0,466588	0,00064239	-0,000142	-1,359E-06						410,9365	
							3	659,488162	-0,2365564	0,061116	0,465074	0,00066253	-0,000151	-6,049E-06						410,9365	
							4	662,701418	-0,2536113	0,066985	0,455737	0,00063662	-0,000139	9,379E-06						410,9365	
							5	661,320369	-0,2409747	0,063958	0,455644	0,00064228	-0,000141	1,903E-06						410,9365	
							6	659,650138	-0,2578742	0,066265	0,45761	0,00064326	-0,000156	-2,719E-06						410,9365	
5	301,02	300,73	151,88	151,94	2,293,8	9,00	1	667,210312	-0,3033913	0,043022	0,459577	0,00067432	-0,000191	-1,989E-06	687,9059	669,1461	-0,28306	-0,26964	0,005453	2,294	420,68
	300,43		152,00				2	679,073003	-0,2991068	0,064895	0,475148	0,00065414	-0,000185	-4,322E-06						420,68	
							3	680,879413	-0,2735181	0,057177	0,472678	0,00066024	-0,000177	-9,604E-06						420,68	
							4	693,436836	-0,2587153	0,051636	0,476211	0,0006623	-0,0002	-3,77E-06						420,68	
							5	692,415536	-0,2766003	0,050982	0,474138	0,00066113	-0,000165	4,116E-06						420,68	
							6	693,724756	-0,2870394	0,058131	0,475953	0,00065229	-0,000177	-4,116E-06						420,68	

EXHIBIT F
Proposed Excavation and Backfill
Procedures for Lightweight Cellular
Concrete in Mission Rock Streets

(Exhibit by Mission Rock Partners)

**PROPOSED EXCAVATION AND BACKFILL PROCEDURE FOR
LIGHTWEIGHT CELLULAR CONCRETE**

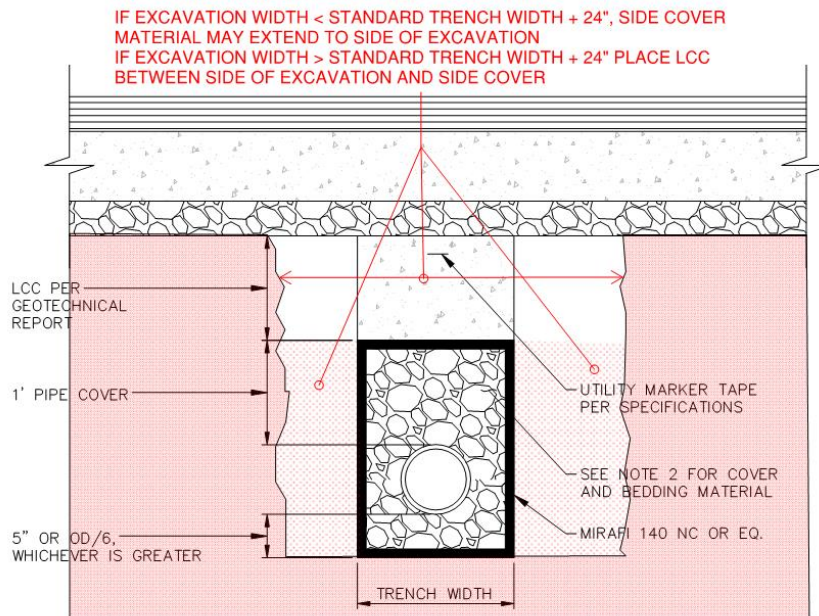
Revision 02

27 February 2020

1. **Purpose:** The purpose of this proposed procedure is describe utility excavation and backfill procedures in streets with Lightweight Cellular Concrete (LCC).
2. **Codes, Regulations:** Unless otherwise noted, DPW Order 187005 Section 10 Trench Backfill Requirements and all codes, regulations and standards referenced therein shall apply to excavation, trenching and backfill in LCC.
3. **Safety:** All trenching and excavation safety requirements required under Cal/OSHA CCR 1540 Article 6, Excavation shall be followed including, but not limited to
 - 3.1. Obtain DOSH Excavation Permit for all trenches deeper than 5'
 - 3.2. Trench shoring shall be installed and removed under the supervision of a Competent Person as defined by Cal/OSHA
4. **Control:** In order to ensure that excavation and trenching in Mission Rock streets, the following controls shall be implemented:
 - 4.1. Signs shall be posted prominently on street sign and/or street light poles with the following wording: "SUBGRADE IN MISSION ROCK STREETS IS LIGHTWEIGHT CELLULAR CONCRETE. EXCAVATION, TRENCHING AND BACKFILL ARE SUBJECT TO SPECIAL REQUIREMENTS. FOR MORE INFORMATION CONTACT SFPW AT (415) 554-5810 OR THE MISSION ROCK MASTER ASSOCIATION AT (415) NNN-NNN"
 - 4.2. All excavation and trenching in streets shall be performed under Excavation Permit. The Permit Section of SFPW shall be provided with a map showing the extend of LCC in Mission Rock Streets which shall be kept on file or recorded in the City Geographic Information System (GIS) and any other maps or other databases.
 - 4.3. When issuing Excavation Permits for street in in Mission Rock with LCC, SFPW shall require that this procedure be followed as a condition of the permit.
5. **Excavation:** LCC can be easily excavated using the same techniques and equipment as normal soil.
 - 5.1. Remove pavement per standard practice.
 - 5.2. Trenching can be done with standard back hoes, mini excavators and larger excavators with standard buckets as required for the particular trench width, depth and length. LCC can also be excavated by hand, or with the aid of small electric chipping hammers in tight places.
 - 5.3. LCC can also be excavated using a Vactor truck with a 2500-3000 psi water wand where it is necessary to excavate fill without damaging adjacent pipes.
 - 5.4. Standard Cal/OSHA shoring practices shall be followed. LCC in Mission Rock streets generally meets the criteria for Type A Soil having a compressive strength of > 1.5 tons/SF (typically the minimum compressive strength is >40 psi or 2.8 tons/SF).

6. Backfill:

- 6.1. In general the bedding, shading and backfill should be restored to its original condition after pipe repair. Trench widths, bedding and shading material and dimensions for new laterals or mains should follow standards for original utilities in Mission Rock—these are generally the same as standards for other City utilities with the following exceptions:
- 6.1.1. Filter fabric such as Mirafi 140NC or equal should be placed between bedding/shading and LCC to prevent fines from migrating into the LCC
- 6.1.2. Low Pressure Water (LPW) with standard depth of 44" for 12' mains shall be backfilled with clean, uniformly-graded sand up to the bottom of pavement basecourse.
- 6.2. Place bedding and shading around the pipe per applicable standards. In general, side cover should be the same as the original installation. If the excavation is up to 1' wider than the original width, sand or pea gravel shading may be placed up to 24" wider than the original trench for up to 20' where the added width is necessary for installing repair sleeves, valves or other appurtenances. However if excavation is > 24' wider than original standard trench or longer than 20', then space between side of excavation and side cover or shading shall be filled with LCC. (see figure below) The reason for this is to maintain the weight of the lightweight fill within the 10% safety margin of the design.



- 6.3. Backfill to top of subgrade (bottom of pavement basecourse) shall be LCC per the specification in Appendix A of this Procedure. LCC > 2-3' below top of subgrade shall have cast density of 26 PCF (+/- 2 PCF). LCC < 2-3' below top of subgrade shall have cast density of 30 PCF (+/- 2 PCF). NOTE: As an alternate, in case that permeable LCC is not available. non-permeable LCC may be used in repairs above Elevation 95 feet or in localized trenches that with a volume less than 10 cubic yards.

- 6.4. LCC shall be placed in 3' lifts. If multiple lifts are required, trench shall be covered with road plates or protected with barricades between lifts.
 - 6.5. Quality Control of LCC backfill shall be as described in the LCC Specifications
 - 6.6. Restore warning tape in backfill per applicable City standards.
 - 6.7. A list of approved LCC contractors can be found in Appendix B.
7. **Emergency backfill with other material:** In an emergency unplanned utility repair where the street must be restored immediately, it is permissible to temporarily use normal standard soil backfill, Class II AB or similar materials which have a higher density than LCC, as long as the temporary backfill is removed and replaced with LCC within three months or less, it is not expected to not cause differential settlement because a small amount of localized extra weight should not be enough to induce rapid settlement.
8. **Pavement Restoration:** Shall be per SFPW Standards. 4" of aggregate basecourse shall be placed on top of LCC below PCC pavement or concrete sidewalk.

Appendix A: LCC specification (see Exhibit H of TAP Comment and Response Exhibit. (Note: Final procedure will have same spec attached. It is omitted here to avoid redundancy.

Appendix B: List of approved LCC Contractors

Cell-Crete Corporation

995 Zephyr Ave,
Hayward, CA 94544
(800) 696-0433
<https://cell-crete.com/>

Throop Lightweight Fill

701 Hazelwood Drive
Walnut Creek, CA 94596
415-419-6876
<http://www.cellularconcrete.com>

Confoam (A Conco Company)

5141 Commercial Circle
Concord, CA 94520
925-685-6799
<https://www.conconow.com/commercial-concrete-contractors/confoam/>

Appendix C: Example calculation of non-permeable LCC Backfill

EXHIBIT G
Results of Long Term Test of LCC Cured
in Fresh Water and Salty/Brackish Water
Compared to Normal Dry Curing
Conditions

(Exhibit by Mission Rock Partners)

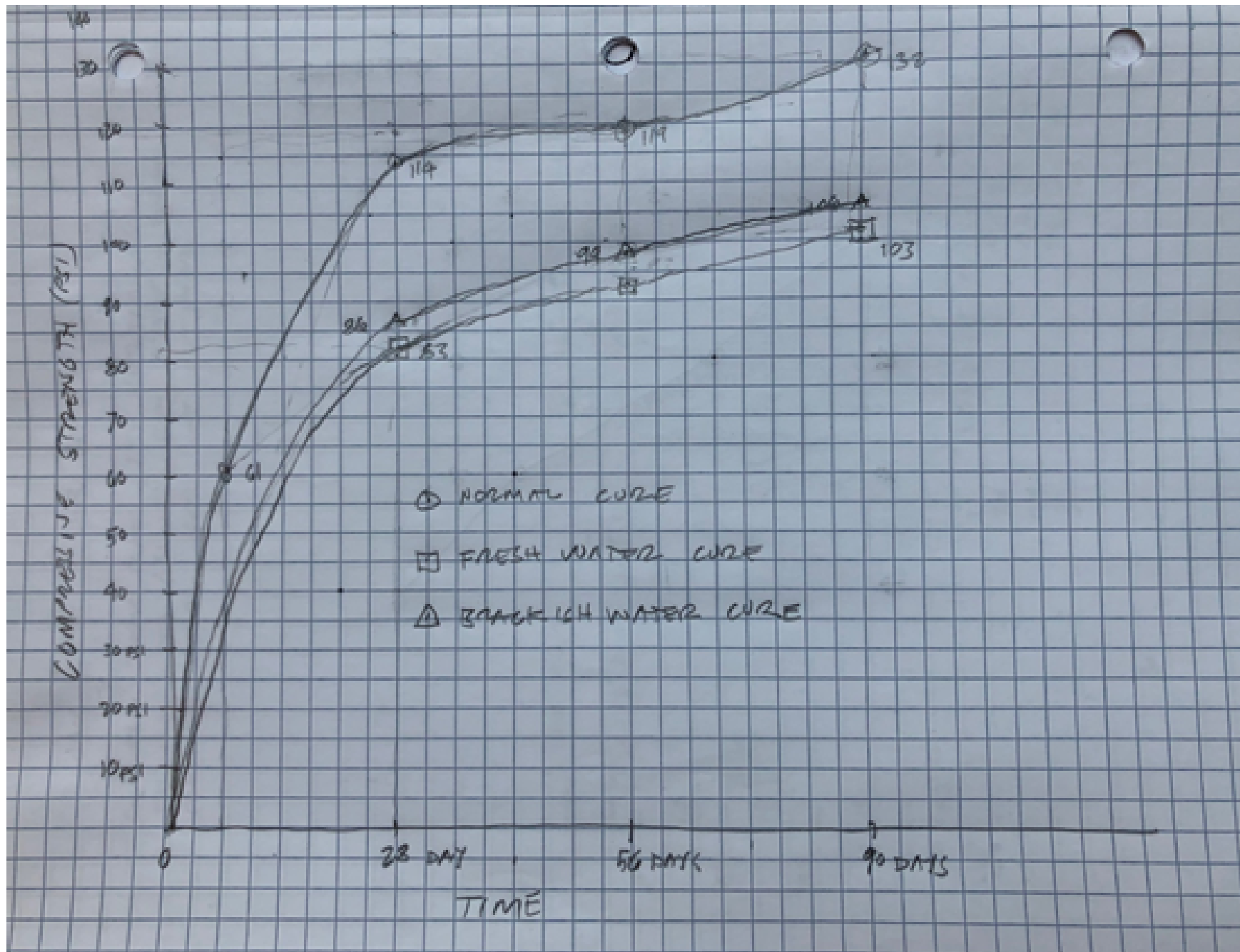
Summary of Effects of Fresh Water and Salty/Brackish Water Curing on LCC

Samples Cast 18 Oct 2019

			Sample ID: 19-562 A (Normal Curing Conditions)			Sample ID: 19-562 B (Cylinders Continue Curing in Fresh Water)			% of Normal	Sample ID: 19-562 C (Cylinders Continue Curing in Brackish Water)			% of Normal	% of FW
Date	No.	Age	Density	load	Strength	Density	load	Strength		Density	load	Strength		
25 Oct 2019	1	7 Days	23.3 pcf	412 lbs	58 psi									
	2	7 Days	23.3 pcf	434 lbs	61 psi									
				(Avg @ 28 days	= 60 psi)									
15 Nov 2019	3	28 Days	20.3 pcf	817 lbs	116 psi	40.3 pcf **	582 lbs	82 psi	71%	39.1 pcf **	601 lbs	85 psi	73%	104%
	4	28 Days	21.0 pcf	799 lbs	113 psi	40.7 pcf **	602 lbs	85 psi	75%	39.0 pcf **	613 lbs	87 psi	77%	102%
				(Avg @ 28 days	= 114 psi)		(Avg @ 28 days	= 83.5 psi)	73%		(Avg @ 28 days	= 86 psi)	75%	103%
13 Dec 2019	5	56 Days	21.5 pcf	843 lbs	119 psi	42.9 pcf	632 lbs	89 psi	75%	39.9 pcf	706 lbs	100 psi	84%	112%
	6	56 Days	21.6 pcf	802 lbs	114 psi	42.0 pcf	681 lbs	96 psi	84%	39.2 pcf	685 lbs	97 psi	85%	101%
				(Avg @ 28 days	= 117 psi)		(Avg @ 56 days	= 93 psi)	79%		(Avg @ 56 days	= 99 psi)	79%	106%
16 Jan 2020	7	90 Days	20.7 pcf	925 lbs	131 psi	42.6 pcf	711lbs	101psi	77%	39.7	706lbs	106psi	81%	105%
	8	90 Days	20.7 pcf	925 lps	133 psi	42.1 pcf	732lbs	104 psi	78%	41.1	745lbs	106psi	80%	102%
				(Avg @ 90 days	=132psi		(Avg @ 90 days	=103 psi	78%		(Avg @ 90 days	106psi	80%	103%
15 Apr 2020	9	180 Days												
	10	180 Days												
14 Jul 2020	11	270 Days												
	12	270 Days												
16 Oct 2020	13	364 Days												
	14	364 Days												

Mix Design 19-562 A

** These cylinders were allowed to drain absorbed water for 1-hour



SUMMARY OF AVERAGE COMPRESSIVE STRENGTH OVER TIME



Mix Design Laboratory Form

Date: 18 Oct 2019

Sample ID: 19-562 A (Normal Curing Conditions)

Client: Tishman Speyer

Application: Study Effects of Salt/Brackish Water on PLDCC for Mission Rock Project

Target Density: 27 pcf (Actual = 27.2 pcf)

Target Strength: To Be Determined

Date	No.	Age	Density	load	Strength
25 Oct 2019	1	7 Days	23.3 pcf	412 lbs	58 psi
	2	7 Days	23.3 pcf	434 lbs	61 psi
				(Avg @ 7 days	= 60 psi)
15 Nov 2019	3	28 Days	20.3 pcf	817 lbs	116 psi
	4	28 Days	21.0 pcf	799 lbs	113 psi
				(Avg @ 28 days	= 114 psi)
13 Dec 2019	5	56 Days	21.5 pcf	843 lbs	119 psi
	6	56 Days	21.6 pcf	802 lbs	114 psi
				(Avg @ 56 days	= 117 psi)
16 Jan 2020	7	90 Days	20.7 pcf	925 lbs	131 psi
	8	90 Days	20.7 pcf	943 lbs	133 psi
				(Avg @ 90 days	= 132 psi)
15 Apr 2020	9	180 Days			
	10	180 Days			
14 Jul 2020	11	270 Days			
	12	270 Days			
16 Oct 2020	13	364 Days			
	14	364 Days			

	Log No.	Lab Batch Weight	Unit
Cement	Quikrete Type I/II	40.0	lbs
Fly ash	N/A	N/A	g.
Sand	N/A	N/A	g.
Water	0.55 W/C Ratio	22.0	lbs
Chemical	Aquaerix	20	ml/L
Additive			
Base Density		111.5	pcf

This testing was conducted in accordance with ASTM C495 under laboratory conditions. Field testing is recommended to provide a comparison with the laboratory data, as field conditions do vary per project.

Foam Density = 2.2 pcf



Mix Design Laboratory Form

Date: 18 Oct 2019

Sample ID: 19-562 B (Cylinders Continue Curing in Fresh Water)

Client: Tishman Speyer

Application: Study Effects of Salt/Brackish Water on PLDCC for Mission Rock Project

Target Density: 27 pcf (Actual = 27.2 pcf)

Target Strength: To Be Determined

Date	No.	Age	Density	load	Strength
25 Oct 2019		7 Days **			
15 Nov 2019	1	28 Days	40.3 pcf **	582 lbs	82 psi
	2	28 Days	40.7 pcf **	602 lbs	85 psi
				(Avg @ 28 days	= 83.5 psi)
13 Dec 2019	3	56 Days	42.9 pcf	632 lbs	89 psi
	4	56 Days	42.0 pcf	681 lbs	96 psi
				(Avg @ 56 days	= 93 psi)
16 Jan 2020	5	90 Days	42.6 pcf	711 lbs	101 psi
	6	90 Days	42.1 pcf	732 lbs	104 psi
				(Avg @ 90 days	= 103 psi)
15 Apr 2020	7	180 Days			
	8	180 Days			
14 Jul 2020	9	270 Days			
	10	270 Days			
16 Oct 2020	11	364 Days			
	12	364 Days			

	Log No.	Lab Batch Weight	Unit
Cement	Quikrete Type I/II	40.0	lbs
Fly ash	N/A	N/A	g.
Sand	N/A	N/A	g.
Water	0.55 W/C Ratio	22.0	lbs
Chemical	Aquaerix	20	ml/L
Additive			
Base Density		111.5	pcf

This testing was conducted in accordance with ASTM C495 under laboratory conditions. Field testing is recommended to provide a comparison with the laboratory data, as field conditions do vary per project.

Foam Density = 2.2 pcf

** A total of twelve cylinders were demolded and placed in sealed 4" x 8" cylinder molds filled with fresh, potable water.

** These cylinders were allowed to drain absorbed water for 1 hour.



Mix Design Laboratory Form

Date: 18 Oct 2019

Sample ID: 19-562 C (Cylinders Continue Curing in Salty/Brackish Water)

Client: Tishman Speyer

Application: Study Effects of Salt/Brackish Water on PLDCC for Mission Rock Project

Target Density: 27 pcf (Actual = 27.2 pcf)

Target Strength: To Be Determined

Date	No.	Age	Density	load	Strength
25 Oct 2019		7 Days **			
15 Nov 2019	1	28 Days	39.1 pcf **	601 lbs	85 psi
	2	28 Days	39.0 pcf **	613 lbs	87 psi
				(Avg @ 28 days	= 86 psi)
13 Dec 2019	3	56 Days	39.9 pcf	706 lbs	100 psi
	4	56 Days	39.2 pcf	685 lbs	97 psi
				(Avg @ 56 days	= 99 psi)
16 Jan 2020	5	90 Days	39.7 pcf	746 lbs	106 psi
	6	90 Days	41.1 pcf	745 lbs	106 psi
				(Avg @ 90 days	= 106 psi)
15 Apr 2020	7	180 Days			
	8	180 Days			
14 Jul 2020	9	270 Days			
	10	270 Days			
16 Oct 2020	11	364 Days			
	12	364 Days			

	Log No.	Lab Batch Weight	Unit
Cement	Quikrete Type I/II	40.0	lbs
Fly ash	N/A	N/A	g.
Sand	N/A	N/A	g.
Water	0.55 W/C Ratio	22.0	lbs
Chemical	Aquaerix	20	ml/L
Additive			
Base Density		111.5	pcf

This testing was conducted in accordance with ASTM C495 under laboratory conditions. Field testing is recommended to provide a comparison with the laboratory data, as field conditions do vary per project.

Foam Density = 2.2 pcf

** A total of twelve cylinders were demolded and placed in sealed 4" x 8" cylinder molds filled with salty, brackish water.

** These cylinders were allowed to drain absorbed water for 1-hour.

EXHIBIT H
Draft Final LCC Specification including
QC/QA Testing and Inspection Schedule

**TECHNICAL SPECIFICATIONS
FOR
SEAWALL LOT 337 / MISSION ROCK PROJECT PHASE 1

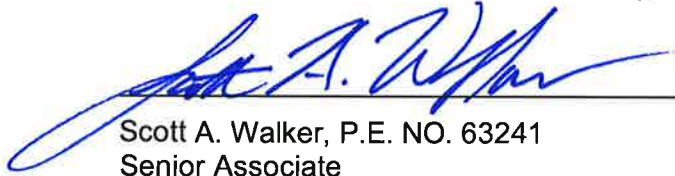
PERMEABLE / OPEN-CELL LIGHTWEIGHT CELLULAR
CONCRETE – PLLC (31-20-00)

CITY OF SAN FRANCISCO, SAN FRANCISCO COUNTY
CALIFORNIA**

Engineer's Attest:

The following Technical Specifications have been prepared under the supervision of the undersigned, who hereby certifies that he/she is registered in the State of California.

Geotechnical Specifications Prepared by:



Scott A. Walker, P.E. NO. 63241
Senior Associate
Langan Engineering and Environmental Services, Inc.

28 February 2020

Date



31 20 00
Permeable/Open-Cell Lightweight Cellular Concrete (P-LCC)

Geotechnical aspects of the specification were prepared by Langan Engineering and Environmental Services, Inc.

1. GENERAL

1.1. DESCRIPTION

- 1.1.1. Work Included: This work shall consist of batching, mixing, placing and testing P-LCC of the appropriate density as indicated by the specifications. A trained P-LCC installer shall furnish labor, material, equipment, and supervision for the installation of the P-LCC in accordance with the drawings and specifications.

1.2. QUALITY ASSURANCE

- 1.2.1. Use skilled labor that is thoroughly trained, experienced, and familiar with the specified requirements and the methods for proper performance of this work.
- 1.2.2. The P-LCC installer shall be approved in writing by Owner.

1.3. SUBMITTALS

- 1.3.1. The prime contractor shall list the product and qualified installer of the P-LCC and shall not employ any product or producer without the prior approval of the geotechnical engineer of record (GEOR).
- 1.3.2. Product data: within 30 calendar days after award of the contract, the prime contractor shall submit a mix design for approval by the GEOR and civil engineer of record (CEOR)
- 1.3.2.1. Manufacturer's specifications, catalog cut sheet, and other engineering data needed to demonstrate to the issuing authority compliance with the specified requirements.
- 1.3.3. Mix Design: Submit a mix design that will produce a cast density that complies with those listed in Section 2.2.1 of this specification at point of placement and a compressive strength within the range listed in Section 2.2.1. Include laboratory data using the mix design verifying un-foamed density, final foamed density, permeability (cm/sec) and compressive strengths. Mix design shall include water/cementitious ratio and foam solution dilution ratio, in accordance with manufacturer's recommendations. The mix design should also include Field Permeability Check Testing, by testing the percolation rate in modified 6" x 12" cylinder molds, filled half-way. The mix design should also include field saturation testing by the special inspector.
- 1.3.4. Work Plan: Submit a work plan before placement of P-LCC material. The plan shall include:
- 1.3.4.1. Proposed construction sequence and schedule
- 1.3.4.2. Type of equipment and tools to be used.
- 1.3.4.3. Material list of items and manufacturer's specifications
- 1.3.4.4. P-LCC lift thickness
- 1.3.4.5. P-LCC cure time and minimum strength prior to placing the next lift
- 1.3.4.6. QA/QC and testing items and protocols frequency.

2. PRODUCTS

2.1. MATERIALS

2.1.1. Foaming Agent: A foaming agent shall be used and shall comply with the standard specifications of ASTM C 869 when tested in accordance with ASTM C 796. Admixtures shall be tested by the foam concentrate manufacturer for compatibility with the foaming agent.

2.1.2. Cement: the Portland cement shall comply with ASTM C 150. Other supplemental cementitious material such as fly ash may be used when approved by the project engineer. Supplementary cementitious materials shall be tested prior to the start of the project for compatibility with the foaming agent.

2.1.3. Admixtures: admixtures for accelerating, water reducing, and other specific properties may be used when specifically approved by the GEOR. Admixtures shall be tested in mix design prior to the start of the project for compatibility with the foaming agent.

2.1.4. Water: use water that is potable and free from deleterious amounts of alkali, acid, and organic materials, which would adversely affect the setting or strength of the P-LCC.

2.1.5. Filter Fabric: Shall have permeability equal to or greater than that of the P-LCC. Filter fabric shall also have a maximum apparent opening size (AOS, ASTM D4751) of 0.212 mm (U.S. sieve size 70).

2.2. PROPERTIES

2.2.1. The P-LCC shall meet the following properties:

	Target	Maximum	Minimum
General Cast Density, pcf (ASTM C 796)	26	28	24
Cast Density for Upper Two Feet of LCC, pcf (ASTM C 796)	30	32	28
Compressive Strength at 28 Days, psi (ASTM C 495) for Upper Two feet	80	200	50
Compressive Strength at 28 Days, psi (ASTM C 495) balance of LCC	50	200	50
Coefficient of Permeability, cm/sec (ASTM D 2434 – modified)	0.1 (1E-1)	NA	0.005 (5E-3)
Saturated Density, pcf	55	68	45

3. EXECUTION

- 3.1. Subgrade: Subgrade to receive P-LCC material shall be free of all loose and extraneous material. Subgrade shall be uniformly moist, and any excess water standing on the surface shall be removed. The subgrade shall be approved by the GEOR before placing P-LCC material.
- 3.2. Curing: A minimum 12-hour curing period between lifts is required. Backfill or other usual loadings, including additional lifts of P-LCC, on the P-LCC shall not be permitted until the P-LCC has attained a compressive strength of at least 5 psi.
- 3.3. Weather Conditions: If ambient temperatures are anticipated to be below 40 degrees F within 24 hours after placement, the mixing water shall be heated when approved by the manufacturer of the foaming agent or placement shall be prohibited. Placement shall not be allowed on frozen ground.
- 3.4. Batching and Mixing: Cellular concrete shall be job site batched, mixed with the foaming agent and placed with specialized equipment certified by the manufacturer of the cellular concrete lightweight material. Cement and water may be premixed and delivered to the job site and the foaming agent added on site. Dilution ratio shall be adjusted as needed per manufacture's recommendation to achieve required end product.
- 3.5. Placement:
 - 3.5.1. Place P-LCC in lifts not to exceed 36 inches in thickness, unless otherwise recommended by the P-LCC manufacturer and approved by the GEOR.
 - 3.5.2. After curing for minimum of 12 hours, any crumbling area on the surface shall be removed before the next layer is placed. Surface stepping to achieve grade and super elevation shall not be less than 6 inches in thickness. Grades of up to 5 percent may be made by adding a thickening agent to the mix in conformance with the manufacturer's recommendation.
 - 3.5.3. Subgrade and P-LCC should be protected from water inundation until the P-LCC is sufficiently cured and has sufficient overlying weight so it does not become buoyant.
 - 3.5.4. Freshly placed P-LCC should be protected from rain until it has been sufficiently cured to prevent damage.
 - 3.5.5. Freshly placed P-LCC should be cured at least 3 hours before exposed to vibrations higher than a peak particle velocity 0.05 inches per second – such as those that may be generated during ground improvement activities.
- 3.6. Handling: Avoid excess handling of P-LCC according to industry standards.
- 3.7. Filter Fabric: Use filter fabric between P-LCC and adjacent soil and between P-LCC and shoring, where shoring will be removed after P-LCC placement.

4. QUALITY CONTROL TESTING BY CONTRACTOR AND OWNER

4.1. DENSITY CONTROL

- 4.1.1. During placement of the initial batches, check the un-foamed and foamed densities for each 100 cubic yards of P-LCC or as recommended per the GEOR and adjust the mix as required to obtain the specified cast density at the point of placement per ASTM.
- 4.1.2. Field saturated density test procedures developed and prepared by the special inspector shall be performed on one sample for each 100 cubic yards of P-LCC or as recommended per the GEOR. GEOR to review and approve test procedures prior to commencement of work.

4.2. COMPRESSIVE STRENGTH: The compressive strength shall be tested under ASTM C 495 except as follows:

- 4.2.1. Four (4) specimens (one 7-day and three 28-days) shall be taken for each 100 cubic yards of P-LCC or as recommended per the GEOR. Unless otherwise approved, the

- specimens shall be 3 x 6 inch cylinders. During molding, place the LCC in 2 equal layers and raise and drop the cylinders 1 inch, 3 times on a hard surface or lightly tap the side or bottom of the cylinder to close any accidental entrained air. No rodding is allowed.
- 4.2.2. Specimens must be covered and protected immediately after casting to prevent damage and loss of moisture. Specimens shall be moist cured in the molds for 7 days and air dry a minimum of 24 hours and minimum of 72 hours before the 7-day and 28-day compressive strength testing, respectively. Specimens shall not be oven dried.
- 4.2.3. Contractor should maintain process control "run" charts of un-foamed and foamed density, field percolation result, and compressive strength data, updated daily for review by Owner's representative, and distributed weekly to applicable project team members.
- 4.3. PERMEABILITY:
- 4.3.1. Proof of permeability (per ASTM D 2434 – Modified) of the proposed P-LCC mix design shall be provided in the mix design submittal. If there is any change to the mix design during production, additional permeability testing will be required. Two samples per week should be cast per ASTM D 2434 and shipped to Castle Rock Consulting for testing.
- 4.3.2. Field falling head permeability per procedures prepared by the special inspector performed on two samples per day. Falling Head permeability test procedures to be reviewed and approved by GEOR prior to commencement of work.
- 4.4. MOCK UP TEST SECTION: One mock up test section shall be installed prior to construction to prove out the contractor's construction methods.
- 4.5. Side-by-side sampling and testing by QC and QA staff should occur once daily during the LCC placement on the Pilot Project to identify any issues. At least one set of permeability samples should also be taken for saturation and drain down density and a permeability verification.
- 4.6. UNFOAMED SLURRY TESTING: Test unfoamed slurry density periodically during foaming to verify actual density (PCF) is +/- 1.5% of target. Target to be established in mix submittal.
- 4.7. QUALITY ASSURANCE INSPECTIONS & ACCEPTANCE TESTING BY OWNER'S AGENCY
- 4.7.1. Owner shall employ a qualified Special Inspector to observe LCC placement and test LCC as described below.
- 4.7.2. Daily Inspections should include review of previous day's density testing of un-foamed and foamed test data, field percolation test results, any 7-day & 28-day compressive strength data, and location of samples taken. Initially use mix design for 7-day to 28-day strength correlation, switching to project data when three sets are available to predict 28-day strengths.
- 4.7.3. Perform one side-by-side comparison test with Contractor every 1000 cubic yards, and verify saturation & drain-down densities and permeability (per ASTM D 2434) values every 1000 cubic yards placed, or whenever the field percolation rates are more than 20% lower than the mix design values.

Montez Group Inc.

Field Saturated Density of PLCC Test Procedure

Prepared: February 28, 2020

SUBMITTAL No.:
Field Saturated Density of PLCC Test Procedure

This submittal has been reviewed for the Geotechnical aspects of the design only. Contractor is responsible for all corrections indicated hereon, for dimensions quantities, fabrications, construction techniques, and coordination with other contractors, subcontractors and suppliers. This review does not authorize changes to the contract requirements unless stated in a separate letter or change order.

☒ NO EXCEPTIONS TAKEN ☐ AMEND & RESUBMIT
☐ EXCEPTIONS NOTED ☐ REJECTED-SEE COMMENTS

Checked By: P. Brady **Date:** 28 February 2020

LANGAN
135 Main Street
Suite 1500, S.F. CA 94105

Montez Group Inc.
249 Onondaga Avenue, San Francisco, CA 94112

Table of Contents

1.0	Equipment List	3
2.0	Significance and Use	3
3.0	Sampling Procedure	3
4.0	Testing Procedure	3
5.0	Appendix	5
1.	Sample – Test Results	5
2.	Sample – Table of Calculations	7

1.0 Equipment List

1. 4x8" Cylinder Mold
2. Bucket/Wheel Barrel for Taking Samples for 6x12" Molds
3. Unit Weight Air Pot (Used in ASTM C138)
4. 5-gallon Bucket of Water
5. Scale
6. Caliper
7. File or Scraper
8. Cylinder Stripping Tool or Box Cutter

2.0 Significance and Use

The Field Estimation of Saturated Density Test Procedure provides the Saturated Density of Permeable Lightweight Cellular Concrete (see appendix 2 for example of calculation).

3.0 Sampling Procedure

Sampling procedure for PLCC is like taking samples of compressive strengths of LCC (ASTM C39 except mold sizes used are 4x8".

1. Take and label 4x8" mold
2. Gather material in bucket or other container to transport material from placement location to sampling location
3. Use measuring cup, trowel or container to transfer material into 4x8" mold
4. Fill mold in 2 to 3 lifts up to top. Each lift should be consolidated by tapping the side of mold to release bubbles.
5. Place lid on sample
6. After samples are taken, handle carefully to location to allow to cure undisturbed for at least 24 hours

4.0 Testing Procedure

1. Sample will be cured for 3 days prior to testing
2. Carefully strip the PLCC sample from the cylinder mold using a cylinder stripping tool or box cutter without disturbing sample.
3. Use a file or scraper to remove about ¼" of material from the top and bottom ends of the cylinder to roughen the surface and expose the cellular structure while ensuring sample's corners are still squared. If larger amounts of material must be removed, a hand saw can be used, but be sure to square the ends as best

as possible with the file.

4. Measure the height of the PLCC cylinder. Measure to the nearest 1/8". Take the average of 3 to 4 heights around the circumference of the cylinder. Record this value (A).
5. Fully submerge the PLCC cylinder in a full 5-gallon bucket of water, upright and weighting the cylinder down to prevent floatation. Keep the cylinder fully submerged for at least 30 minutes. Multiple cylinders can be submerged simultaneously, provided they remain identified.
6. Weight a standard concrete air pot assembly, pot and cap, and record the tare weight (B).
7. Fill the air pot completely with water, with the cap on, fill and remove excess air through the petcocks as though for a concrete air test, close the petcocks when full.
8. Dry the air pot assembly off with a rag or cloth, weight the water filled assembly and record this value (C).
9. Remove the cap from the air pot and place it beside the bucket containing the submerged PLCC cylinder. The air pot should be full of water.
10. Quickly transfer the submerged PLCC cylinder from the water bucket to the air pot, submerging the cylinder completely.
11. Holding the PLCC cylinder under water with one hand, place the air pot cap on with the other and clamp it down.
12. Fill the air pot assembly completely with water through the petcocks, closing the petcocks when full.
13. Again dry the entire assembly off with a rag or cloth, weigh and record this value (D).
14. Calculate the Saturated Density
 - a. See Appendix Sample – Test Results & Table of Calculations

5.0 Appendix

1. Sample – Test Results

FIELD ESTIMATION OF SATURATED DENSITY OF PLCC
Test Method Provided by
CASTLE ROCK CONSULTING
TEST DATA SHEET

Project Name: Misson Rock -Lightweight Cellular Concrete Mock-up CEL # 10-37339PW
Sample Date: 12/17/2019 Sampled By: David Chin Lab # N/A
Sample Location/Source: Set 1
Material Description/Condition : Lightweight Cellular Concrete

Test Data

	Measure 1	Measure 2	Measure 3	Measure 4
Cylinder Heights, in	7.82	7.87	7.83	7.83

A. Average Cylinder Height (in) 7.84
B. Air pot assembly tare weight (pot + Cap), lb 17.70
C. Air pot assembly tare weight filled with water, lb 33.50
D. Air pot assembly with water + cylinder, lb 33.15
E. Cylinder Volume, $(12.57 \times A)/1728$, cf 0.0570
F. Displacement water weight, $62.4 \times E$, lb 3.56
G. Full pot water weight, C-B, lb 15.80
H. Balance Water weight, G-F, lb 12.24
I. Approximate Saturated Unit Weight, $(D-H-B)/E$ 56.26 pcf

Tested By: Y.Han
Date Tested: 12/31/2019

SAMPLE

2. Sample – Table of Calculations



Updated

Input Data

[illegible]

SAMPLE

Montez Group Inc.

Falling Head Field Permeability Test Procedure

Prepared: February 28, 2020

SUBMITTAL No.:

Falling Head Field Permeability Test Procedure

This submittal has been reviewed for the Geotechnical aspects of the design only. Contractor is responsible for all corrections indicated hereon, for dimensions quantities, fabrications, construction techniques, and coordination with other contractors, subcontractors and suppliers. This review does not authorize changes to the contract requirements unless stated in a separate letter or change order.

☒ NO EXCEPTIONS TAKEN ☐ AMEND & RESUBMIT

☐ EXCEPTIONS NOTED ☐ REJECTED-SEE COMMENTS

Checked By: P. Brady **Date:** 28 February 2020

LANGAN

135 Main Street
Suite 1500, S.F. CA 94105

Montez Group Inc.

249 Onondaga Avenue, San Francisco, CA 94112

Table of Contents

1.0	Equipment List	3
2.0	Significance and Use	3
3.0	Preparing 6x12" Modified Cylinder Molds.....	3
4.0	Sampling Procedure	4
5.0	Testing Procedure	4
6.0	Appendix	6
1.	Sample – Test Results	6
2.	Sample – Table of Calculations	8

1.0 Equipment List

1. Modified 6x12" Cylinder Mold
 - a. 6x12 Molds w/ Lids (Molds used for ASTM C31)
 - b. Scribing Tool
 - c. Tape
 - d. 100 grit sandpaper
2. Bucket/Wheel Barrel for Taking Samples for 6x12" Molds
3. 5 Gallon Bucket
4. Heavy Wire Screen or 12" Brass Sieve
5. Steel Ruler
6. Stopwatch
7. Water

2.0 Significance and Use

The Falling Head Field Permeability Test Procedure provides another method of calculating the Permeability Constant (K) while being able to perform in the field.

$$K = \frac{L}{T} \ln \frac{h_1}{h_2}$$

Where:

K = Coefficient of Permeability in cm/sec

L = Sample Length in cm

h_1 = Initial elevation of the water surface

h_2 = Final elevation of the water surface

T = Average time in seconds from h_1 to h_2 .

3.0 Preparing 6x12" Modified Cylinder Molds

1. Take a 6x12" cylinder mold and place open end upside down
2. Cut off the bottom of mold
3. Measure 6" from cut end of mold and mark a line on the inside with scribing tool
4. Use the 100 grit sandpaper and roughen the inside of the mold from 6" measurement to the cut end

5. Sand inside face of lid of cut end
6. Place lid on bottom (cut end) of mold
7. Tape lid on cylinder mold

4.0 Sampling Procedure

1. Take and label prepared modified 6x12" mold
2. Gather material in bucket or other container to transport material from placement location to sampling location
3. Use measuring cup, trowel or container to transfer material into modified 6x12" mold
4. Fill mold in 2 to 3 lifts up to pour line (approximately 6" mark). Each lift should be consolidated by tapping the side of mold to release bubbles.
5. After samples are taken, handle carefully to location to allow to cure undisturbed for at least 24 hours
6. Cover open tops of molds with another 6x12" lid or other suitable material to prevent moisture loss while curing

5.0 Testing Procedure

1. Sample will be cured for 3 days prior to testing
2. Place mold open side upside down and carefully remove tape and lid from bottom of mold. Ensure sides of mold will not break contact with samples.
3. Use scraper to scarify surface of bottom of sample and expose cellular structure
4. Turn mold upright and use scraper to scarify top surface and expose cellular structure and remove as little material as possible
5. With the cylinder mold with the open end up, press a ruler into the surface of the material to a depth of 1 inch, at the edge of the surface with the ruler oriented vertically. This is the depth scale for the falling head test. With one inch inserted, the next increment should be the 2" mark, corresponding to 1" of water above the surface, 3" will correspond to 2" of water, and so on
6. Fill a 5-gallon bucket completely with clean water
7. Place a heavy wire screen or 12" bass sieve on top of another, empty 5-gallon bucket. When the sample is removed from the water bucket, it will be transferred to the screen to allow it to drain freely
8. Submerge the mold, bottom surface first into the bucket of water, holding the top edges of the cylinder and pushing the sample down vertically, allowing water to infiltrate from the bottom and move upward through the cellular material
9. Keep mold submerged until water has infiltrated and covered the top surface of the material

10. Fully submerge the entire mold in the bucket, allowing the entire top half of the mold to fill with water
11. Holding the top edges of the mold, lift the entire mold vertically from the water and quickly transfer it to the screen over the empty bucket
12. The first run was to wash the water through to prime the sample. Once the sample is prime, it is not necessary to re-prime the sample in between tests.
13. Get a stopwatch ready to record time
14. Repeat steps 8 to 11
15. With the stopwatch ready, start timing when the water level reaches the 5" mark (4" above the material surface).
16. Continue timing until the water level reaches the 2" mark (1" above the surface), stop timing.
17. Record the time (T in seconds) where Trial 1 is T₁, Trial 2 is T₂ etc...
18. Repeat steps 15 to 17 two more times, recording the time for the water level to drop from the 5" mark to the 2" mark, for a total of three trials.
19. Calculate all T per trial and average for T to input into coefficient of permeability, K
20. The approximate permeability coefficient can now be calculated from the average of the three recorded times by the falling head formula as shown in section 2.0:

$$K = \frac{L}{T} \ln \frac{h_1}{h_2}$$

6.0 Appendix

1. Sample – Test Results

FALLING HEAD FIELD PERMEABILITY TEST
Test Method Provided by
CASTLE ROCK CONSULTING
TEST DATA SHEET

Project Name: Misson Rock -Lightweight Cellular Concrete Mock-up CEL # 10-37339PW
 Sample Date: 12/23/2019 Sampled By: David Chin Lab # N/A
 Sample Location/Source: _____
 Material Description/Condition : Lightweight Cellular Concrete

Test Data

Tested By: Y.Han Date Tested: 12/31/2019

Trial #		Initial	1	2	
L, Length of Sample, cm		15.24	15.24	15.24	
h1, Initial elevation of the water surface, in		4	4	4	
h2, Initial elevation of the water surface, in		1	1	1	
Average time from h1 to h2	Min.	54	34	37	
	Sec.	46.15	32.25	44.36	AVG
Average Time in Seconds, sec		3286.15	2072.25	2264.36	2540.92
K, Coefficient of Permeability, cm/sec $K=L/T*\ln(h1/h2)$					0.008315

SAMPLE

2. Sample – Table of Calculations



Falling Head Field Perm

Updated

Input Data

Item #	Location	Description	Cast Date	Date Tested	L (in Inches)	L (in cm)	h1 (Inches)	h2 (Inches)	Trial 1	Trial 2	Trial 3	T _{avg} (in Sec)	K (in cm/sec)	Comments
									T _A (in sec)	T _B (in sec)	T _C (in sec)			
10	Mission Rock Pilot Lift #4	Set1	12/31/2019	12/31/2019	6	15.24	4	1	3286.15	2072.25	2264.36	2540.92	8.31E-03	

- K Coefficient of Permeability in (cm/Sec)
- L Sample length in cm
- h1 Initial elevation of water surface
- h2 Final elevation of water surface
- T Average time in seconds from h1 to h2

$K=(L/T)\ln(h1/h2)$

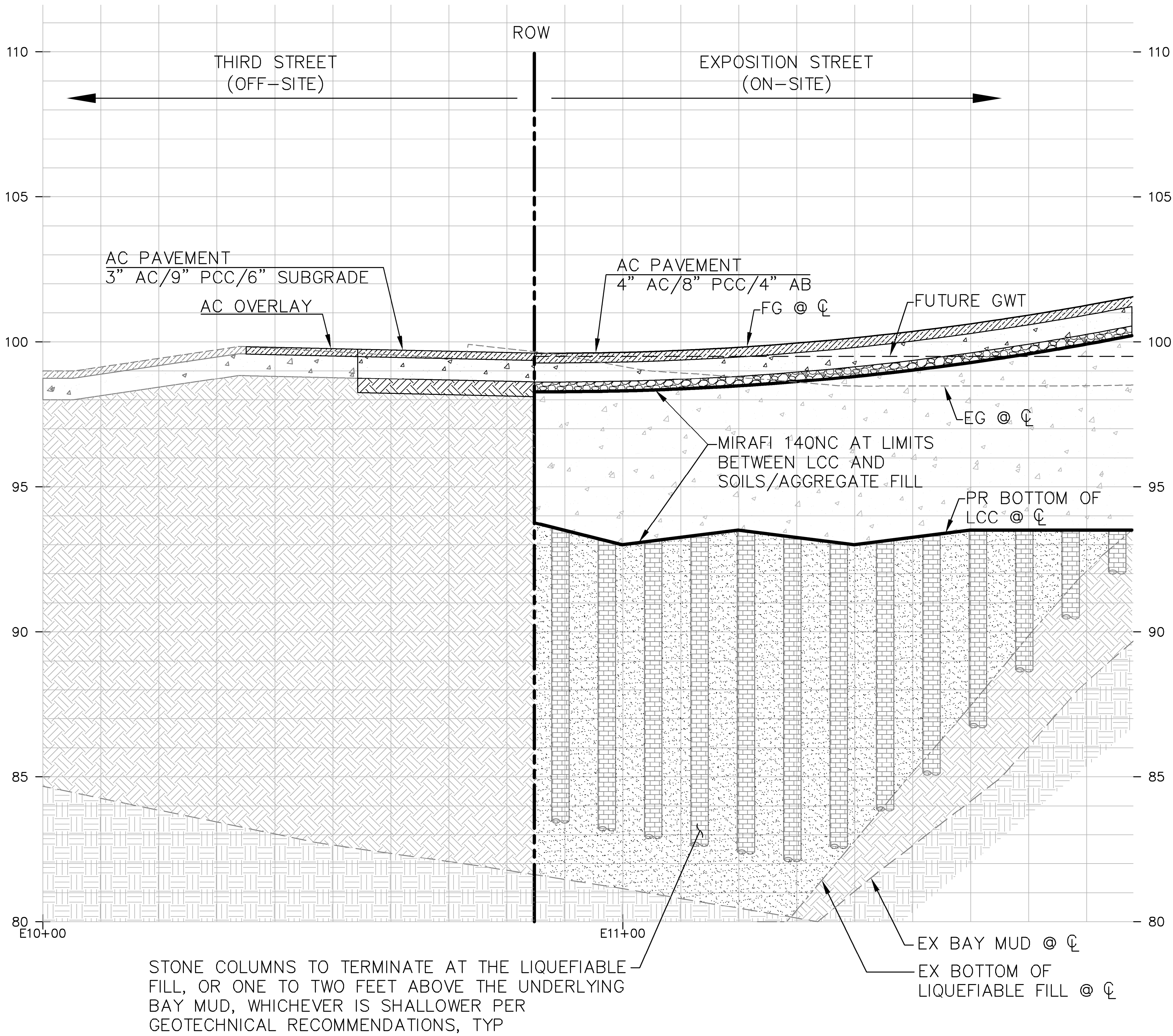
SAMPLE

EXHIBIT I

Typical Sections at LCC Interfaces

- Typical Interface with Existing Street
- Typical Interface with Vertical Parcel

DRAWING NAME: \\BKF-st\vol4\2008\080006 Mission Rock\ENG\Exhibits\20_0206 Expo Third Cross Section.dwg
PLOT DATE: 02-07-20 PLOTTED BY: mey



LEGEND:

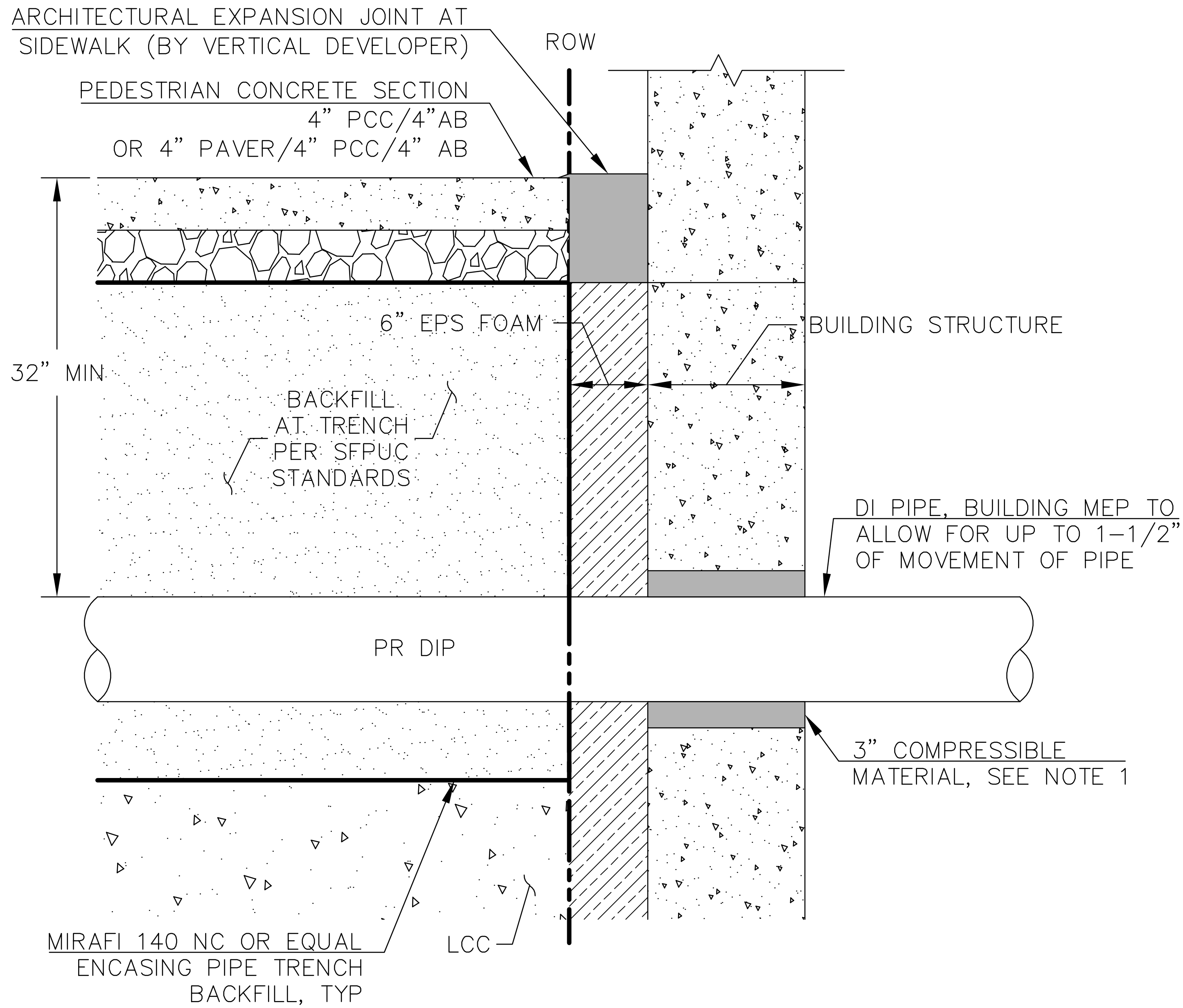
	AC
	PCC
	AB
	SUBGRADE
	LCC
	STONE COLUMNS
	DENSIFIED SOIL
	EX SOIL
	EX BAY MUD

ABBREVIATIONS:

AB	AGGREGATE BASE
AC	ASPHALT CONCRETE
CL	CENTERLINE
EG	EXISTING GRADE
EX	EXISTING
FG	FINISHED GRADE
LCC	LIGHTWEIGHT CELLULAR CONCRETE
PCC	PORTLAND CONCRETE CEMENT
PR	PROPOSED
ROW	RIGHT OF WAY
TYP	TYPICAL

THIRD STREET/EXPOSITION STREET CROSS-SECTION

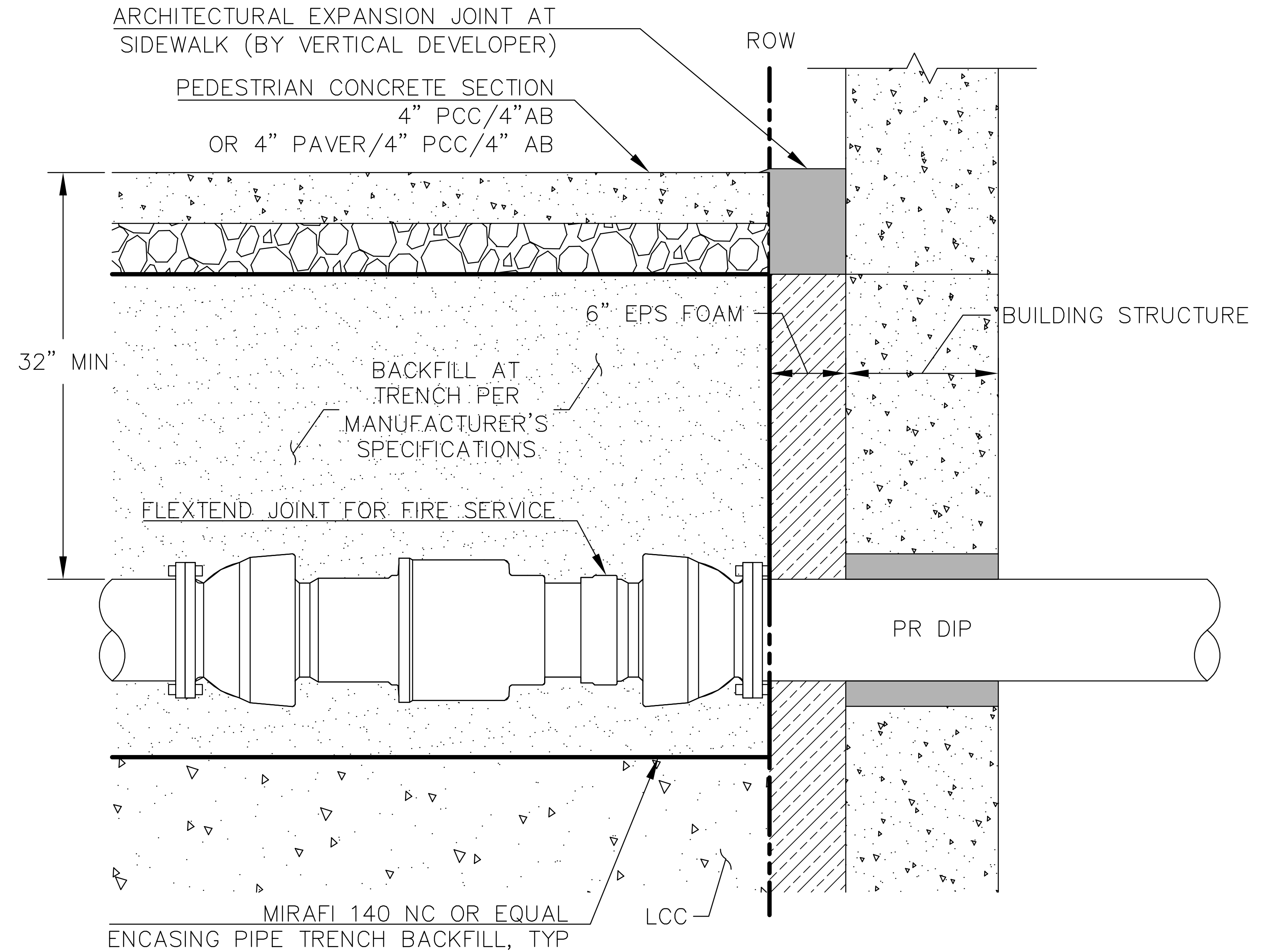
SCALE: 1"=10'



NOTES:

1. WATERPROOFER/MEP/STRUCTURAL ENGINEER TO COORDINATE AND SPECIFY WALL PENETRATION MATERIAL, WATERPROOFING DETAIL, ETC. COMPRESSIBLE MATERIAL TO ALLOW UP TO 1-1/2" OF MOVEMENT.
2. HDPE CONNECTIONS TO UTILIZE LINK-SEAL AND WATER STOPS IN LIEU OF COMPRESSIBLE MATERIAL.

DIP LPW/NPW WALL PENETRATION DETAIL
NTS



NOTES:

1. WATERPROOFER/MEP/STRUCTURAL ENGINEER TO COORDINATE AND SPECIFY WALL PENETRATION MATERIAL, WATERPROOFING DETAIL, ETC.

DIP FS WALL PENETRATION DETAIL
NTS

Revisions		No.	
Date 02/12/2020	Scale AS SHOWN		
	Design		
	Drawn		
	Approved		
	Job No 20080006		

EXHIBIT J
Permeability Based on Lag
Time

LANGAN TREADWELL ROLLO

SHEET _____ OF _____

JOB NO. 750604203

DATE 2-12-2020

PROJECT MISSION ROCK PHASE I HORIZ

COMPUTED BY CBR

SUBJECT LCC PERMEABILITY

CHECKED BY [Signature]

Goal: Calculate permeability based on "lag time" in arrival of water within the LCC compared to the water level outside the LCC.

$$Q = KIA \quad \text{where}$$

$$V = Q/A$$

K = hydraulic conductivity

$$L = \Delta h / V$$

$$\rightarrow K = \frac{VL}{\Delta h}$$

$$= \frac{L^2}{\Delta t \Delta h}$$

$$\Delta t = 9:10 - 9:30 \text{ AM} \rightarrow 20 \text{ min}$$

$$L = 97.5 - 96.55 \text{ ft}$$

$L = 0.95 \text{ ft}$ the distance traveled in vertical direction through LCC

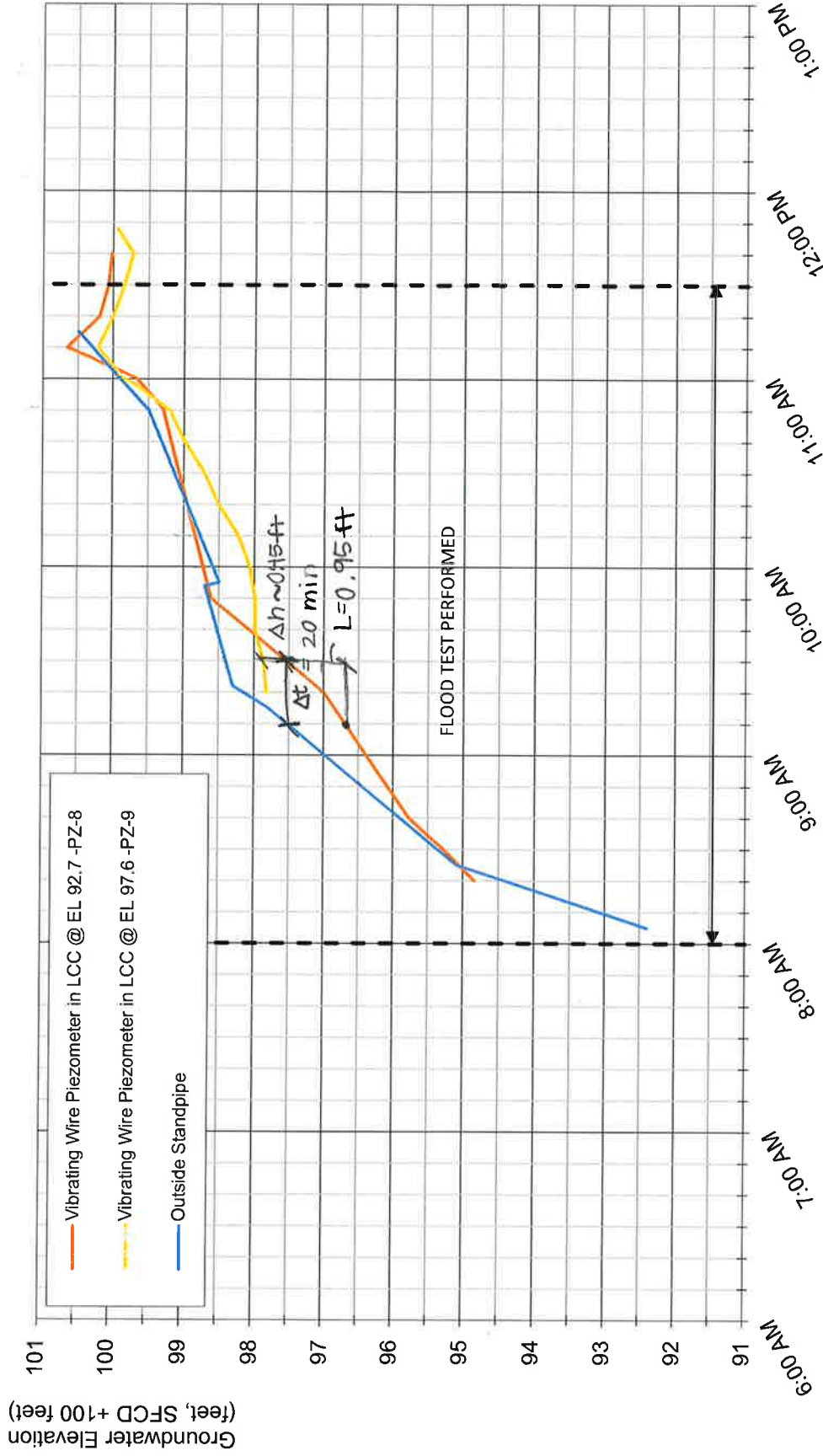
Δh = change in water elevation between piezometers inside + outside LCC

$$V = L / \Delta t = 0.95 \text{ ft} / \text{change in time } \Delta h \text{ occurs over}$$

$$K = \frac{(0.95 \text{ ft} \cdot 2.54 \text{ cm/in} \cdot 12 \text{ in}) (0.95 \text{ ft} \cdot 2.54 \cdot 12 \text{ in})}{(20 \text{ min} \cdot 60 \text{ s}) (0.95 \text{ ft} \cdot 12 \text{ in} \cdot 2.54)}$$

$$K = 0.05 \text{ cm/s}$$

Flood Test 2 1/15/2020



MISSION ROCK
- PHASE 1 HORIZONTAL DEVELOPMENT
San Francisco, California

LANGAN

FLOOD TEST PIEZOMETER DATA
PZ-8 and PZ-9

Project: 750604203

2/11/2020

Figure 6